Wavelet Based Numerical Techniques for Finding the Solution of Differential Equations

A Thesis

Submitted in the partial fulfillment of the requirements for the award of the degree of

DOCTOR OF PHILOSOPHY (Ph.D.)

in

(MATHEMATICS)

By

Ratesh Kumar

(Registration Number-41500074)

Supervised by

Dr. Geeta Arora

Assistant Professor

Lovely Professional University

Co-Supervised by

Dr. Harpreet Kaur

Assistant Professor

I.K. Gujral Punjab Technical University

LOVELY PROFESSIONAL UNIVERSITY

PUNJAB

2020

DECLARATION BY THE CANDIDATE

I declare that the thesis entitled "**Wavelet *Based Numerical Techniques for Finding the Solution of Differential Equations***" submitted for the award of the degree of Doctor of Philosophy in Mathematics, Lovely Professional University, Phagwara, is my own work conducted under the supervision of Dr. Geeta Arora (Supervisor), Assistant Professor, School of Chemical Engineering and Physical Sciences, Lovely Professional University, Chaheru, Punjab and Dr. Harpreet Kaur (Co-supervisor), Assistant Professor, Department of Mathematical Sciences, IKPTU, Jalandhar. I further declare that to the best of my knowledge the thesis does not contain any part of any work which has been submitted for the award of any degree in this University or in any other University/Deemed University without proper citation.

Signature of the Candidate
(Mr. Ratesh Kumar)

05/10/2020

Signature of the Supervisor
(Dr. Geeta Arora)

Signature of the Co-supervisor
(Dr. Harpreet Kaur)

CERTIFICATE

This is to certify that the work entitled "**Wavelet *Based Numerical Techniques for Finding the Solution of Differential Equations***" is a piece of research work done by Mr. Ratesh Kumar under my guidance and supervision for the degree of Doctor of Philosophy of Mathematics, Lovely Professional University, Phagwara (Punjab) India. To the best of my knowledge and belief the thesis:

1. Embodies the work of the candidate himself.

2. Has Duly been completed.

3. Fulfills the requirements of the ordinance related to the Ph.D. degree of the university

4. Is up to the standard both in respect of contents and language for being referred to the examiner.

05/10/2020

Signature of the Supervisor	Signature of the Co-Supervisor
(Dr. Geeta Arora)	(Dr. Harpreet Kaur)
Department of Mathematics	Department of Mathematical Sciences,
Lovely Professional University,	I.K. Gujral Punjab Technical
Phagwara, Punjab	University, Jalandhar

Dedicated

To God

and

My Family

ABSTRACT

Differential equations play a very crucial role in mathematical modeling of a variety of real-world problems. During the mathematical modeling of physical problems, most of the time modeled differential equation is not so easy to solve and it becomes more challenging when the mathematical model of phenomena carries the nonlinearities, variable coefficients or a greater number of variable (higher dimensional) in it. This results in the requirement of advanced numerical methods which can be regarded as a strong solver to get an accurate numerical solution for a big class of these types of differential equations. Researchers are putting continuous efforts for the improvement of existing methods and the development of new hybrid methods with the aim to develop a strong solver for these kinds of equations.

In the literature review, we came to know that the Taylor series can be used for the analysis of function locally. If we want to analyze the function globally, then the Taylor series fail, at that time, Fourier series come into literature. But Fourier series fail to analyze the function locally. In the last couple of years, a large number of numerical methods have been proposed to deal with the solution of different types of initial and boundary value problems locally and globally. Some of the well-known methods include the finite difference (FD) method and finite element (FE) method and finite volume (FV) methods. But these methods are low order, expensive and have some geometrical restrictions. These methods have very good spatial localization but are less accurate. Another class of numerical techniques is the spectral methods in which the solution is discretized by approximating it with a series of basis functions that are infinitely differentiable and nonvanishing on the whole domain (global support). Spectral methods are used in combination with the method of weighted residuals. These methods have an exponential rate of convergence if the expected solution is smooth in nature. But the spatial localization is not good when the expected solution is discontinuous and non-smooth in nature. Spectral methods are also less effective for the problems with more complex geometries but create less computationally cost as compare to FDM, FEM, and FVM. Also, the Spectral method works on global support

while FDM, FEM, and FVM work on compact (local) support. Spectral methods have poor spatial localization for complex problems and irregular geometry but these are more accurate and produce less error. On the other hand, FDM, FEM, and FVM are less accurate but have good spatial localization.

All the methods have their own advantages and limitations. Wavelet based techniques appear to be a solution for this situation where we can combine the benefits of all the approaches (good special-time localization as well as better solution accuracy) using wavelet bases in approximating the unknown solution. Because of the many advantages of wavelets which are orthonormal and having compact support like translation, and dilation using multiresolution analysis, highly compatible with the computer environment and localized in both space and time make it competent enough to deal with the various types of problems arises in the field of science and technology. Wavelet based methods can easily be extended to a higher dimension to deal with more complex problems. Wavelets are very compatible to make a connection with already established fast and highly accurate numerical technique.

Many wavelets with different characteristics are existing in the literature for the analysis of various types of data, signal, image, and solution analysis. But Haar wavelet is mathematically simplest, computationally cheap, conceptually simple, and memory-efficient oldest orthonormal wavelet with compact support existing in the literature. Haar Wavelets has the simplest rectangular pulse pair explicit expression which can integrate the desired number of times without any restriction. Special properties of Haar wavelets with the simple explicit expression motivated us to use Haar wavelet bases with spectral methods to solve various differential equations that arise in the field of science and technology. In wavelet techniques, the accuracy of the solution can be increased by increasing the dilation factor of the wavelet family. In literature, dyadic wavelets are in preponderance in which dilatation factor runs on the power of 2. In the thesis, novel Haar scale 3 (non-dyadic) wavelet-based numerical methods are developed in which the dilatation factor runs on the power of 3 to analyze linear and nonlinear differential equations of various types.

This thesis is dedicated to the development of Haar Scale 3 and Haar scale 2 Wavelets based algorithms in combination with the existing numerical techniques such as Collocation method, Quasilinearization process, and Gauss elimination method for solving the various important differential equations. Quasilinearization process is used for nonlinear problems along with Haar (scale 3 or scale 2) wavelets as described in chapters 2 to 8. The broad range of numerical problems arising in different fields like as higher-order linear and nonlinear boundary value problems, fractional Bagley-Torvik equations, coupled space-time fractional- Burgers' equation, hyperbolic Telegraph equations, NBBMB (non-linear Benjamin Bona Mahony Burgers) equation, linear and non-linear Sobolev equation are considered systematically. From the mathematical point of view, these problems represent the ordinary differential equation with associate boundary or initial conditions, higher-order linear and non-linear partial differential equations, linear ordinary fractional differential equations and nonlinear system of fractional partial differential equations which are treated in the mathematical framework of functional analysis, linear algebra and approximation theory.

The presented work in this thesis is organized into the following nine chapters, subsequently where the agenda for each of the chapters (with facts and details) is briefly illustrated.

Chapter 1-This chapter is regarding the introductory part of this thesis, the first two sections (1.1-1.2) of this chapter contains the introduction, mathematical preliminaries on differential equations and fractional calculus. Section 1.3 and section 1.4 include the motivation to use wavelets and mathematical preliminaries on wavelets. The next sections (1.5-1.6) include a brief introduction to the collocation method and quasilinearization techniques . Sections (1.7-1.9) contain the literature review, findings from the literature review, objectives, motivation, and scope. All these sections are essential for the next chapters. Lastly, it contains the plan of work.

Chapter 2- In this chapter, the Haar wavelet collocation mechanism (HWCM) is developed for obtaining the solution of higher-order linear and nonlinear boundary value problems. The mechanism is based on approximation of solution by Haar scale 2 wavelet family. To tackle the nonlinearity in the problems, the quasilinearization

technique is applied. Many examples are considered to prove the successful application of the mechanism developed for getting a highly accurate result. By using the HWCM, an approximate solution for higher-order boundary value problems (HOBVPs) are obtained and compared with exact and numerical solutions available in the literature.

Chapter 3 -The main focus of chapter 3 is to construct a compactly supported non-dyadic orthonormal wavelet family with scale factor 3. Orthonormal wavelet families are extremely helpful in solving the various problems arise in the field of science and technology. For the construction of the Haar scale 3 (non-dyadic) wavelet family, a multi-resolution analysis (MRA) technique is used on the trivial Haar scale 3 (non-dyadic) type function given by C.K Chui. Integrals of members of the Haar scale 3 (non-dyadic) wavelet family have been calculated for their use in the multiscale approximation of unknown function running in various types of differential or integral equations. Matrices of Haar Scale 3 wavelets and their integrals have been constructed for their use in solving the various types of differential and integral equations. Two numerical experiments have been considered to test the efficiency of the given wavelet family in approximating the unknown function.

Chapter 4 - In this chapter, a new Haar scale 3 wavelet-based hybrid method is developed for obtaining the solution of higher-order linear and nonlinear boundary value problems. The proposed method is based on approximation of solution by Haar scale 3 (non-dyadic) wavelets family with dilation factor 3. The discretization of the domain is done by the collocation method. The nonlinearities in boundary value problems are tackled by the quasi-linearization technique. Eleven linear and nonlinear boundary value problems with orders ranging from eighth to twelfth are considered to prove the successful application of the proposed method. Also, the obtained solutions are compared with exact and numerical solutions available in the literature to prove the efficiency of the method over other methods.

Chapter 5- The main agenda of this chapter is to develop a new hybrid method using the Haar scale 3 (non-dyadic) wavelets for the investigation of Bagley-Torvik Equation. From the mathematical point of view, it is an ordinary fractional differential equation. Haar Scale 3 (non-dyadic) wavelets are used to estimate the solution by series

approximation. To handle the fractional derivatives and integrals in the problem, Caputo's sense definition of derivatives and Riemann-Liouville definitions of integrals are used. A numerical solution has been produced for five different fractional Bagley-Torvik Equations to establish the competency of the proposed method.

Chapter 6- The focus of this chapter is to develop a hybrid method using Haar scale 3 (non-dyadic) wavelets for obtaining the solution of coupled space-time fractional Burgers' equation. Coupled space-time fractional Burgers' equations are mathematically represented by a system of fractional partial differential equations. Haar scale 3 (non-dyadic) wavelets are used to estimate the solution by series approximation. Caputo and Riemann-Liouville definitions are used to handle the fractional derivatives and integrals in the problem. A quasi-linearization technique is implemented to handle the nonlinearity in the problems. Two examples of coupled space-time fractional Burgers' equations are studied to analyze the performance of the proposed technique.

Chapter 7- The main focus of chapter 7 is to introduce a noval numerical technique based upon the two-dimensional Haar scale 3 (non-dyadic) wavelets for the solution of 1D- hyperbolic telegraph equation. It is a second order partial differential equation which involves the mixed partial derivatives w.r.t space and time variables. In this scheme, spatial discretization is done by two-dimensional Haar scale 3 (non-dyadic) wavelets. The collocation method is used with two-dimensional Haar scale 3 (non-dyadic) wavelets to convert 1D- hyperbolic telegraph equation into the system of algebraic equations which are further solved with the help of the Thomas algorithm. The proposed scheme is tested on four different equations of the above-said types to establish the competency of the proposed scheme.

Chapter 8 -The main objective of this chapter is to introduce a hybrid technique based upon the θ −weighted differencing and Haar scale 3 (non-dyadic) wavelets for the solution of (2+1)-dimensional partial differential equations such as Sobolev and BBMB (Benjamin–Bona–Mahony–Burgers) Equations etc. In this scheme, time discretization is done by θ −weighted finite differencing scheme and spatial discretization is done by Haar scale 3 (Non-dyadic) wavelets. The quasilinearization process is used wherever we encountered with the non-linearity in the equations.

The proposed scheme is tested on five different linear and nonlinear equations of the above said types to establish the competency of the proposed scheme.

Chapter 9- This chapter concludes the findings of the present research work and gives a discussion of the effects of method in dealing with different types of differential equations. Based on present study, conclusions are drawn and future research work in this direction is suggested.

During the study, nearly 210 reputed research publications, books, thesis, and notes have consulted and cited in the references. For numerical computation, MATLAB programs have developed.

List of Publications

1. Numerical solution by Haar wavelet collocation method for a class of higher-order linear and nonlinear boundary value problems. This paper has been published in the Scopus/UGC indexed American journal: AIP-Conference Proceedings with **SJR 0.19**.

Citation:

R. Kumar, H. Kaur, and G. Arora, "Numerical solution by Haar wavelet collocation method for a class of higher-order linear and nonlinear boundary value problems," *AIP Conf. Proc.*, vol. 1860, no. 1, pp. 020038–1–020038–12, 2017); DOI: 10.1063/1.4990337

View online: https://aip.scitation.org/doi/abs/10.1063/1.4990337
Published by the American Institute of Physics

2. A Novel Wavelet Based Hybrid Method for Finding the Solutions of Higher Order Boundary Value Problems. This paper has been published in the SCI/Scopus/UGC indexed Elsevier journal: Ain Shams Engineering Journal with **SJR 0.465** and **Impact factor 3.091** with manuscript no. ASEJ-D-17-00591.

Citation:

G. Arora, R. Kumar, and H. Kaur, "A novel wavelet based hybrid method for finding

the solutions of higher-order boundary value problems," *Ain Shams Eng. J.*, vol. 9, no. 4, pp. 3015–3031, Dec. 2018. https://doi.org/10.1016/j.asej.2017.12.006

View online: https://www.sciencedirect.com/science/article/pii/S2090447918300066
Published by Elsevier under the responsibility of Ain Shams University Cairo, Egypt

3. Non-Dyadic Wavelets Based Computational Technique for the investigation of Bagley-Torvik Equations.This paper has been published in the Scopus/UGC indexed journal: "International Journal on Emerging Technologies" with **SJR 0.12** (ISSN No. (Print): 0975-8364, (Online): 2249-3255).

Citation:

H. Kaur, R. Kumar, and G. Arora, "Non-dyadic wavelets based computational technique for the investigation of Bagley-Torvik equations," *Int. J. Emerg. Technol.*, vol. 10, no. 2, pp. 1–14, 2019.

View online: https://www.researchtrend.net/ijet/pdf/1%20IJET-MTH-00048.pdf

4. Scale-3 Haar wavelets and quasilinearization based hybrid technique for the solution of coupled space-time fractional-Burgers. This paper has been published ESCI/Scopus/UGC indexed journal with **SJR 0.16** (ISSN:0128-7680, e-ISSN:2231-8526).

Citation:

G. Arora, R. Kumar, and H. Kaur, "Scale-3 Haar wavelets and quasilinearization based hybrid technique for the solution of coupled space-time fractional-Burgers' equation," *Pertanika J. Sci. Technol.*, vol. 28, no. 2, pp. 579–607, 2020.
View online:
http://www.pertanika.upm.edu.my/Pertanika%20PAPERS/JST%20Vol.%2028%20(2)%20Apr.%202020/10%20JST-1776-2019.pdf

Published by the University Putra Malaysia

5. Haar Scale 3 Wavelet Based Solution of 1D- Hyperbolic Telegraph Equation. This paper has been published UGC indexed journal with ISSN:0971-1260.

Citation:

R. Kumar, “Haar Scale 3 Wavelet Based Solution of 1D- Hyperbolic Telegraph Equation,” *Think India J.*, vol. 22, no. 16, pp. 4030–4042, 2019.

Viewonline:
https://journals.eduindex.org/index.php/thinkindia/article/view/17683/12693

Published by Eduindex.

6. Historical Development in Haar Wavelets and Their Application - An Overview. This paper has been published UGC indexed journal with ISSN:2349-5162.

Citation:

R. Kumar, “Historical Development in Haar Wavelets and Their Application - An Overview,” *J. Emerg. Technol. Innov. Res.*, vol. 5, no. 11, pp. 1287–1296, 2018.

7. Construction of Non-Dyadic Wavelets Family and their Integral for Multiscale Approximation of Unknown Function. This paper has been published UGC indexed journal with ISSN:2349-5162.

Citation:

R. Kumar, “Construction of Non-Dyadic Wavelets Family and their Integral for Multiscale Approximation of Unknown Function,” *J. Emerg. Technol. Innov. Res.*, vol. 5, no. 12, pp. 1–29, 2018.

8. New Scheme for the Solution of (2 + 1)-Dimensional Non-Linear Partial Differential Equations Using 2D-Haar Scale 3 Wavelets and θ − Weighted Differencing. This paper has been published UGC indexed journal with ISSN:2349-5162.

Citation:

R. Kumar, “New Scheme for the Solution of (2 + 1) - Dimensional Non-Linear Partial Differential Equations Using 2D-Haar Scale 3 Wavelets and θ − Weighted Differencing,” *J. Emerg. Technol. Innov. Res.*, vol. 6, no. 1, pp. 194–203, 2019.

9. A Hybrid Scheme Based Upon Non-Dyadic Wavelets for the Solution of linear Sobolev Equations. This paper has been published UGC indexed journal with ISSN:2349-5162.

Citation:

R. Kumar, "A Hybrid Scheme Based Upon Non-Dyadic Wavelets for the Solution of linear Sobolev Equations," *J. Emerg. Technol. Innov. Res.*, vol. 6, no. 1, pp. 185–193, 2019.

International/National Conferences Attended

1. An international conference "Recent Advances in fundamental and Applied Science (RAFAS)" was attended on 25-26th November 2016 held at Lovely Professional University and a paper titled "Numerical solution by Haar wavelet collocation method for a class of higher-order linear and nonlinear boundary value problems" was presented (Details of the paper attached).

2. A national conference on "Recent Trends in Numerical Analysis and Computational Techniques" sponsored by DST-SERB, organized by Department of Applied Sciences, DAV Institute of Engineering and Technology, Jalandhar on March 28-29,2017 was attended and a paper titled "A Novel Wavelet-Based Hybrid Method for Finding the Solutions of Higher Order Boundary Value Problems" was presented (Details of the paper attached)

3. An international conference "International Conference on Functional Materials and Simulation Techniques (ICFMST)" jointly organized by the University of Mauritius, Concordia University and Chandigarh University was attended on 7th -8th June 2019 held at Chandigarh University Mohali and a paper titled "Non-Dyadic Wavelets Based Computational Technique for the investigation of Bagley-Torvik Equations" was presented (Details of the paper attached).

4. An international conference "Recent Advances in fundamental and Applied Science (RAFAS)" was attended on 05-06th November 2019 held at Lovely Professional University and a paper titled "Scale-3 Haar wavelets and quasilinearization based hybrid technique for the solution of coupled space-time fractional-Burgers." was presented (Details of the paper attached)

ACKNOWLEDGMENTS

I express my heartfelt gratitude to my thesis supervisor, ***Dr. Geeta Arora****, Assistant Professor, School of Chemical Engineering and Physical Sciences, Lovely Professional University, Chaheru, Punjab and my thesis co-supervisor,* ***Dr. Harpreet Kaur,*** *Assistant Professor, Department of Mathematical Sciences, IKPTU, Jalandhar for their interest, excellent rapport, untiring cooperation, invaluable advice and encouragement throughout my Ph.D. program. I feel highly obliged for their initial encouragement that led me to begin this work. Without their unfailing support and belief in me, this thesis would not have been possible. Their scholarly comments, thought, provoking discussions, and pointed criticism has saved me from numerous errors of omission and commissions. I am indeed feeling short of words to express my sense of gratitude towards them. Besides being a scholar par eminence, both are persons par excellence - a perfect embodiment of dedication, intelligence, and humility.*

I extend my sincere thanks and profound respect to Dr. Pankaj Kumar for his continuous support and motivation during my Ph.D. work. I acknowledge with pleasure the cooperation from Dr. Vikas Sharma, Mr. Gurpreet Singh Bhatia, Dr. Prince, and Dr. Kulwinder Gill for their enthusiastic help and encouragement throughout this research work.

Above all, I owe a great deal to my parents and feel very much obliged to my father Late Shri. Shori Lal Pushkarna and my mother Smt. Neelam Sharma, for what I have received from them in the form of inspiration, love, encouragement, and moral support. I also feel sorry to my daughters, Agrima Sharma (5yr) and Niyati Sharma (2.5yr) for missing their early childhood mischiefs because of my studies during this span of time. Last but not the least, I am highly grateful to my wife, Mrs. Munisha Sharma, without whom it would have really been impossible to carry out this task. She has supported me unconditionally and relentlessly over all these years.

Ratesh Kumar *Date: -*

TABLE OF CONTENTS

LIST OF TABLES

LIST OF FIGURES

Chapter 1
Introduction

1.1 Introduction

Differential equations play a very important role in predicting the world around us. These equations have a remarkable ability to study the characteristics of any phenomenon happening around us. The area of differential equations is not a unified topic; rather it is a union of numerous directions of research with a different source of problems, motivations, and goals. Differential equations act as a language with which one can commute with nature and natural phenomena. These equations have wide applications in the variety of disciplines like physics, medicine, biology, chemistry, economics, financial forecasting, image processing, environmental science, in almost all the branches of engineering and the list goes on. As a result, the study of finding solutions to these equations has attained huge importance in the field of science and technology. In the last few decades, many useful and interesting contributions have been made in this field. In general, the differential equations have been classified as Ordinary Differential Equations (ODEs), Partial Differential Equations (PDEs), and Fractional Differential Equations (FDEs). There are further classifications based upon their order (First order or Higher-order), type of linearity (Linear, Quasilinear, Semi-Linear, Non-linear), types of coefficients (constant or variable) they carry in the equation, Homogeneity (Homogeneous, Non- Homogeneous), degree, etc.

1.2 Basic Terminology Used for Differential Equations

1.2.1 Ordinary Differential Equations (ODEs)

The differential equations which contain only one independent variable, one dependent variable, and its derivative w.r.t an independent variable are known as ordinary differential equations. Some well -known examples of ordinary differential equations are exponential decay or growth population model, Prey-predator model, Rayleigh's

equation (has application in fluid dynamics), and Lane {Emden equation (has application in astrophysics), etc.

1.2.2 Partial Differential Equations (PDEs)

PDEs are the equations which involves more than one independent variables like $x_1, x_2, \dots, x_n$; a dependent variable y and its partial derivatives with respect to the independent variables such as

$$F\left(x_1, x_2, \dots, x_n, y, \frac{\partial y}{\partial x_1}, \frac{\partial y}{\partial x_2}, \dots, \frac{\partial y}{\partial x_n}, \frac{\partial^2 y}{\partial {x_1}^2}, \frac{\partial^2 y}{\partial {x_2}^2}, \dots, \frac{\partial^2 y}{\partial {x_n}^2}, \dots \frac{\partial^n y}{\partial {x_n}^n}\right) = 0$$

Some well -known examples of partial differential equations are Burgers' equation, Korteweg-de Vries equation, Klein–Gordon Equation, Blasius Equation, etc.

1.2.3 Fractional Differential Equations (FDEs)

FDEs are the equations which involve fractional derivatives (derivative of non-integer arbitrary order) of the dependent variable y with respect to one or more than one independent variable $x_1, x_2, \dots, x_n$.

$$F\left(x_1, x_2, \dots, x_n, y, \frac{\partial^{\alpha^1} y}{\partial {x_1}^{\alpha^1}}, \frac{\partial^{\alpha^1} y}{\partial {x_2}^{\alpha^1}}, \dots, \frac{\partial^{\alpha^1} y}{\partial {x_n}^{\alpha^1}}, \dots \frac{\partial^{\alpha^n} y}{\partial {x_n}^{\alpha^n}}\right) = 0$$

where $\lfloor \alpha^n \rfloor < \alpha^n < \lfloor \alpha^n \rfloor + 1 \ \forall \ n$

These equations are the generalizations of ODEs and PDEs. They have extensively attracted the scientific community because of their ability to model the rare complex phenomena. Some well -known examples of fractional differential equations are Fractional Bagley Torvik Equation, Coupled Burgers fractional Equation, Korteweg–de-Vries fractional equations, fractional Bergman's model

1.2.4 Order of Differential Equations

It is the order of the highest order derivative that occurs in an equation e.g. $\frac{d^3u}{dx^3} + u\frac{d^2u}{dx^2} = 0$ is an ODE of order 3, while $u_{tt} = c^2 u_{xxtt} = 0$ is PDE of order 4, where u_{tt} represents the second-order partial derivative with respect to t and u_{xxtt} is a fourth-order derivative with respect to x and t.

1.2.5 Degree of Differential Equation

It is the degree of the highest order derivative that occurs in the differential equation after making it free from radicals and fractions. E.g. Equation: $(u_x)^2 + \left(u_y\right)^2 = 1$ is the partial differential equation (PDE) of degree 2.

1.2.6 Linear Differential Equation (LDE)

A linear differential equation is that in which the dependent variable and its derivatives appear with first power only and there is no term containing the product of the dependent variable with its derivative or the product of any two derivatives of the dependent variable. Some well-known examples of linear differential equations are given below:

(i) $L\frac{d^2q}{dt^2} + R\frac{dq}{dt} + \frac{1}{C}q = \mathbb{V}(t)$ (L-C-R Circuit Equation)

(ii) $\frac{\partial \varphi}{\partial t} + V\frac{\partial \varphi}{\partial x} = 0$ (Transport Equation)

(iii) $\frac{\partial^2 \varphi}{\partial x^2} + \frac{\partial^2 \varphi}{\partial y^2} + \frac{\partial^2 \varphi}{\partial z^2} = 0$ (Laplace Equation)

1.2.7 Semi-Linear Differential Equation (SLDE)

A differential equation is said to be semilinear if the highest order derivative coefficient does not depend upon the dependent variable and its derivatives. Some of the well-known examples of semilinear differential equations are

(i) $\frac{d^2u}{dx^2} + \frac{1}{x}\frac{du}{dx} + u^2 = 0$ (Lane-Emden Equation)

(ii) $\frac{\partial \varphi}{\partial t} + \frac{\partial \varphi}{\partial x} + \varphi^2 = 0$ (Transport equation)

(iii) $\frac{\partial \varphi}{\partial t} + \frac{\partial \varphi}{\partial x} + \varphi\frac{\partial \varphi}{\partial x} - \frac{\partial^3 \varphi}{\partial x^3} = 0$ (Korteweg-de Vries equation)

1.2.8 Quasi-Linear Differential Equation (QLDE)

A differential equation of nth order which is not semilinear in nature is said to be quasi-linear if the nth order derivative coefficient may depend upon the independent variable(s), dependent variable and its derivatives of $(n-1)$th order but does not depend upon the n^{th} order derivative of the dependent variable. Some of the well-known examples of quasi-linear PDEs are:

(i) $\frac{\partial \varphi}{\partial t} + \varphi \frac{\partial \varphi}{\partial x} = 0$ (Inviscid Burgers' equation)

(ii) $2\frac{\partial^2 \varphi}{\partial t \partial x} + \frac{\partial \varphi}{\partial x}\frac{\partial^2 \varphi}{\partial x^2} - \frac{\partial^2 \varphi}{\partial y^2} = 0$ (Lin–Tsien equation)

1.2.9 Non-linear Differential Equation

A PDE is non-linear if the highest order derivative coefficient has non-linearity in the dependent variable. Some examples of non-linear partial differential equations are:

(i) $\left(\frac{\partial u}{\partial x}\right)^2 + \left(\frac{\partial u}{\partial y}\right)^2 = 1$ (Eikonal equation)

(ii) $div\left(\frac{\nabla \varphi}{\sqrt{1+|\nabla \varphi|^2}}\right) = 0$ (Minimal surface equation)

1.2.10 Solution of Differential Equation

The function φ is called the solution of the differential equation if the function φ is continuous and has continuous derivative up to the order of differential equations and satisfies the differential equation.

In each physical problem, the differential equations are to be solved within a given domain belongs to the space of independent variables with a specified value of the dependent variable given on the boundary ∂D of the domain D or at the given time t. Then the differential equations are get upgraded by some extra conditions, for example, initial and boundary conditions.

1.2.11 Initial Conditions (ICs)

If the independent variable is the time variable and condition to be satisfied by the required solution is given at the initial point, i.e. t = 0 then it is called initial condition. A problem that requires the solution of the differential equation based on initial conditions only is called initial value problem.

1.2.12 Boundary conditions (BCs)

If the conditions for the required solution are defined on the boundary ∂D of the domain D then, these conditions are called boundary conditions. The differential equation in which conditions for the required solution are given on the boundary is said

to be a boundary value problem. There are mainly three types of boundary conditions:

1.2.12.1 Dirichlet Boundary Conditions (DBCs)

If the conditions for the required solution are prescribed on dependent variable along the boundary ∂D of the domain D in the space of independent variables, then these conditions are said to be a Dirichlet boundary conditions. For example: Consider the following BVP

$$\frac{\partial^2 \varphi}{\partial t^2} - c^2 \nabla^2 \varphi = 0\,, \qquad x, y \in \mathbb{R}, t > 0 \tag{1.1}$$

With the boundary condition $\varphi(x, y, t) = f(x, y, t)\ on\ \partial$D. If $\varphi = 0\ on\ \partial$D then it is called homogeneous Dirichlet boundary condition otherwise non-homogeneous. Dirichlet boundary condition

1.2.12.2 Neumann Boundary Conditions (NBCs)

If the conditions for the required solution are specified on derivative of the dependent variable on the boundary ∂D of the domain D, then the conditions are said to be a Neumann boundary condition. For example: if in the problem (1.1), the boundary conditions are of the form $\frac{\partial \varphi}{\partial n}(x, y, t) = f(x, y, t)\ on\ \partial$D (Neumann condition) where $\frac{\partial \varphi}{\partial n}$ directional derivative in the direction of n. If $\frac{\partial \varphi}{\partial n} = 0\ on\ \partial$D then it is called homogeneous Neumann boundary Condition otherwise non-homogeneous Neumann boundary Condition.

1.2.12.3 Robin boundary condition (RBCs)

If the conditions for the required solution are prescribed on linear combination of the dependent variable and its derivative on the boundary ∂D of the domain D, then the conditions are said to be a Robin boundary condition or mixed boundary conditions. For example: if in problem (1.1), the boundary condition is of the form $k\frac{\partial \varphi}{\partial x} + h\varphi = f(x, y, t)\ on\ \partial$D (Robin condition). If $k\frac{\partial \varphi}{\partial x} + h\varphi = 0\ on\ \partial$D then it is called homogeneous Robin boundary condition otherwise non-homogeneous Robin boundary Condition.

1.3 Fractional Calculus

Fractional calculus emerged as a great tool in explaining the physical and chemical phenomenon with alienate kinetics having microscopic complex behavior. The fractional calculus is as old as traditional calculus, however, it has gained significant importance amid the previous few decades, because of its immense importance in various assorted fields of science and engineering which include fluid flow, viscoelasticity, solid mechanics, signal processing, probability, statistics, etc. The number of works managing dynamical frameworks portrayed by fractional-order equations that include derivative and integral of arbitrary order as they delineate the memory and innate properties of various substances. In 1695, L'Hopital wrote a letter to Leibnitz in which he used to get some information about a particular notation he published for the nth-order derivative of the linear function. He made an inquiry to Leibniz, what may the result be if n is half. Leibniz responded by saying that it is an obvious conundrum, which will result in significant outcomes one day. So, it was the first time when fractional derivative came into the picture. There are fractional differential models which have a non-differentiable but continuous solution such as Weierstrass type functions[1]. These kinds of characteristics are not possible to explain with the help of ordinary or partial differential models. Earlier the field of fractional calculus was purely mathematical without any visible application but in these days, fractional calculus has gained huge importance in the field of science and technology because of its application in the various field like theory of thermo-elasticity[2], viscoelastic fluids[3], dynamics of earthquakes[4], fluid dynamics[5], etc. In one of the experiments of Bagley and Torvik in which they studied the motion of a rigid plate immersed into the Newtonian fluid. It was found in the experiment that retarding force is proportional to the fractional derivative of the displacement instead of the velocity. It has been observed during the experiment also that the fractional model is superior to the integer-order model for the prediction of characteristics of the same material. It has also been observed experimentally and from the real-time observation that there are many complex systems in the real world like relaxation in viscoelastic material, pollution diffusion in the surrounding, charge transport in amorphous semiconductors, and many more which show anomalous dynamics. This capability of fractional

differential equations of explaining the abnormal dynamic of the system with more efficiency and accuracy has gained huge attention from the scientific community. Many of the important classical differential equations with integer-order has got extensions to the generalized fraction differential equation with an arbitrary order for in-depth study of the corresponding physical model

1.3.1 Some Basic Definitions of Fractional Calculus

Many researchers are utilizing their definitions and notations to present the idea of fractional order derivative and integral. The definitions which have been advanced in the realm of the fractional derivative are the Caputo, Grunwald-Letnikov, and Riemann-Liouville. The Riemann-Liouville definition is most utilized part yet but this methodology isn't appropriate for all physical problems and real-world problems. Caputo introduced the definition in which the initial conditions are defined at the integral order dissimilar to the Riemann-Liouville at which the initial conditions are defined at fractional order. The Grunwald - Letnikov method proceeds towards the problem from the definition of the derivative. This method is used exclusively in numerical algorithms. Grunwald-Letnikov's definition is the extension of the definition of derivative for fractional order.

1.3.1.1 Mittag-Leffler Function

It is an extension of exponential function which has huge importance in the field of fractional calculus. It has two forms of expression as given below

i. *One Parameter Mittag-Leffler Function* [6] for a set of complex numbers and any positive real no α is defined as

$$E_{\alpha} = \sum_{m=0}^{\infty} \frac{z^m}{\Gamma(\alpha m+1)} \, , \alpha > 0, \alpha \epsilon \mathbb{R} \, , z \in \mathbb{C} \tag{1.2}$$

ii. *Two-Parameter Mittag-Leffler Function* [6] for a set of complex numbers and positive real no's $\alpha \, , \beta$ is defined as

$$E_{\alpha,\beta} = \sum_{m=0}^{\infty} \frac{z^m}{\Gamma(\alpha m+\beta)} \, , \alpha \, , \beta > 0, \alpha, \beta \epsilon \mathbb{R}, z \in \mathbb{C} \tag{1.3}$$

1.3.1.2 Riemann-Liouville Fractional Integral Operator [6]

The fractional integral operator defined by the mathematician Riemann-Liouville for the positive real nos. α, a, t over the interval $[a, b]$ is given by

$$ {}_{RL}J_a^{\alpha} f(t) = \frac{1}{\Gamma(\alpha)} \int_a^t f(z)(t-z)^{\alpha-1} dz \tag{1.4} $$

where α denotes the order of derivative and $t \epsilon [a, b]$.

1.3.1.3 Riemann-Liouville Fractional Differential Operator [6]

The fractional differential operator defined by the mathematician Riemann-Liouville for the positive real nos. α, a, t over the interval $[a, b]$ is given by

$$ {}_{RL}D_a^{\alpha} f(t) = \begin{cases} \frac{1}{\Gamma(m-\alpha)} \frac{d^m}{dt^m} \int_a^t \frac{f(z)}{(t-z)^{\alpha-m+1}} dz & , m-1 < \alpha < m \in \mathbb{N} \\ \frac{d^m}{dt^m} f(t) & , \quad \alpha = m \in \mathbb{N} \end{cases} \tag{1.5} $$

where α denotes the order of derivative and $t \epsilon [a, b]$.

1.3.1.4 Caputo Fractional Differential Operator [6]

The fractional differential operator defined by the Italian mathematician Caputo for the positive real nos. α, a, t is

$$ {}_{c}D_a^{\alpha} f(t) = \begin{cases} \frac{1}{\Gamma(m-\alpha)} \int_a^t \frac{f^m(z)}{(t-z)^{\alpha-m+1}} dz & , m-1 < \alpha < m \in \mathbb{N} \\ \frac{d^m}{dt^m} f(t) & , \quad \alpha = m \in \mathbb{N} \end{cases} \tag{1.6} $$

where α denotes the order of derivative and $t \epsilon [a, b]$.

1.3.1.5 Grunwald-Letnikov Fractional Derivative[7]

Grunwald-Letnikov fractional derivative of order $\alpha > 0$ for $f(t)$ with respect to t and with a terminal value a is given by

$$ f_h^{\alpha}(t) = \lim_{\substack{h \to 0 \\ nh = t-a}} \frac{1}{h^{\alpha}} \sum_{k=0}^{n} (-1)^k \frac{\Gamma(\alpha+1)}{\mathrm{k}!\, \Gamma(\alpha-k+1)} f(t-kh) \tag{1.7} $$

1.4 Motivation for Using Wavelets

During the mathematical modeling of physical problems, most of the time modeled differential equation is not so easy to solve and it becomes more challenging when the mathematical model of phenomena carries nonlinearities, variable coefficients or a greater number of variable (higher dimensional) in it. Most of the real-time phenomena of motion, reaction, diffusion, equilibrium, conservation, etc, are governed by these types of differential equations. Yet, analytical theories provide only limited methods for the investigation and analysis of these types' equations. There are many differential equations for which current mathematics fails to give any closed-form solution as more advances are yet to come. However, we still desire some sort of solution for these equations. There is a big class of ODEs, PDEs, FDEs models that cannot be solved analytically. This results in the requirement of advanced numerical methods which can be regarded as a strong solver to get an accurate numerical solution for these types of equations. Researchers are putting continuous efforts for the improvement of existing methods and the development of new hybrid methods with the aim to develop a strong solver for these kinds of equations.

In the last couple of years, a large number of numerical methods are proposed for the solution of initial and boundary value problems. Some of the well-known methods include the finite difference (FD) method and finite element (FE) method and finite volume (FV) methods. But these methods are low order, expensive and have some geometrical restrictions. These methods have very good in their spatial localization but are less accurate. Another approach of the Semi analytic technique gives us the result in the form of a series solution but the biggest problem in the series solution is the convergence of the series solution and the solution is not valid if series does not converge and some of these are very sensitive to the initial guess. Another class of numerical techniques is the spectral methods in which the solution is discretized by approximating it with a series of basis functions which are infinitely differentiable and nonvanishing on the whole domain (global support). Spectral methods are used in combination with the method of weighted residuals. Spectral methods have an exponential rate of convergence if the expected solution is smooth in nature. But the spatial localization is not good when the expected solution is discontinuous and non-

smooth in nature. Spectral methods are also less effective for the problems with more complex geometries but create less computationally cost as compare to FDM, FEM, and FVM. The spectral method works on global support while FDM, FEM, and FVM work on compact (local) support. Spectral methods have poor spatial localization for complex problems and irregular geometry but these are more accurate and produce less error. On the other hand, FDM, FEM, and FVM are less accurate but have good spatial localization. All methods have their own advantages and limitations.

Wavelet-based techniques appear to be a solution for this situation where we can combine the benefits of all the approaches (good special-time localization as well as better solution accuracy) using wavelet bases in approximating the unknown solution. Because of many advantages of wavelets which are orthonormal and having compact support like translation, and dilation using multiresolution analysis, highly compatible with the computer environment and localized in both space and time make it competent enough to deal with the various types of problems arise in the field of science and technology. Wavelet-based methods can easily be extended to a higher dimension to deal with more complex problems. Wavelets are very compatible to make a connection with the established fast and highly accurate numerical technique.

Many wavelets with different characteristics are existing in the literature for the analysis of various types of data, signal, image, and solution analysis. But Haar wavelet is mathematically simplest, computationally cheap, conceptually simple, and memory-efficient oldest orthonormal wavelet with compact support existing in the literature. Haar Wavelets has a simplest rectangular pulse pair explicit expression which can integrate the desired number of times without any restriction. Special properties of wavelets with the simple explicit expression of Haar wavelets motivated us to use Haar wavelet bases with spectral methods to solve various differential equations that arise in the field of science and technology.

For discretization of the approximate solution of problem using the Haar wavelet series, some of the weighted residual scheme is required. The collocation method is one of the popular discretization schemes for the solution of differential equations. This will be used for dealing with a variety of numerical problems to get the solution of different linear and nonlinear differential equations. It includes fulfilling a differential equation to some resilience at some chosen limited number of points, called collocation points.

Differential equations are broadly examined by many researchers in a previous couple of years due to an indispensable utilization of these equations in different fields of research by the collocation method.

1.5 Basic Definition and Concepts of Wavelets

Orthonormal wavelets are one of the modernistic functions which have the capability of dilation and translation. Because of these properties, numerical techniques that involve wavelet bases are showing the qualitative improvement in contrast with other methods. Some basic definitions for the understanding of wavelets are given below:

1.5.1 Definition (The Space $L^2(R)$)

Space $L^2(R)$ is vector space of square integral functions i.e. $L^2(R) = \{f: R \to C : \int_{-\infty}^{\infty} |f(t)|^2 dt < \infty\}$.For getting the finite value of unknown coefficients it is very much required that vector space should be a space of square integral function.

1.5.2 Definition (Inner Product)

The inner product of two functions $f, g \in L^2(R)$ is defined by $\langle f, g \rangle = \int_{-\infty}^{\infty} f(t)g(t)dt$, in particular, the norm of function f is defined by $\|f\|_2 = \langle f, f \rangle^{\frac{1}{2}} = \left(\int_{-\infty}^{\infty} |f(t)|^2 dt\right)^{\frac{1}{2}}$

1.5.3 Definition (Orthonormal functions)

Two functions $f, g \in L^2(R)$ are said to be orthonormal if

$$\langle f, g \rangle = \begin{cases} 0, if\ f \neq g \\ 1, if\ f = g \end{cases}$$

This means that information carried by one function is independent of information carried by any other function. There is no redundancy in the representation. This is good because it means that neither computing cycles nor storage is wasted because of coefficient redundancy.

1.5.4 Definition (Dilation and Translation operator in $L^2(\mathbb{R})$)

For any square-integrable function $f(t) \in L^2(\mathbb{R})$ dilation operator D_a and the translation operator T_b are respectively defined as

(i) $D_a f(t) = a^{\frac{1}{2}} f(at)$ for any real a > 0.

(ii) $T_b f(t) = f(t-b)$ for any real $b \in \mathbb{R}$.

Where translation means shifting in a location of function by b units and dilation means spread or compression in function. For $a > 1$, $D_a f(t)$ becomes the narrow down version of $f(t)$, that is, D_a compressed the function $f(t)$. If $0 < a < 1$, then $D_a f(t)$ is spread out version of $f(t)$,that is, D_a stretched the function $f(t)$.

1.5.5 Definition (Wavelets)

The family of the translated and dilated version of function $\psi(t) \in L^2(R)$,

$$\psi_{b,a}(t) = \frac{1}{\sqrt{|a|}}\, \psi\left(\overline{\frac{t-b}{a}}\right), \qquad a > 0\,, b \in \mathbb{R} \tag{1.8}$$

where ψ satisfies the "admissibility condition" given by

$$C_\psi = \int_{-\infty}^{\infty} \frac{\left|\hat{\psi}(\omega)\right|^2}{|\omega|} d\omega < \infty, \tag{1.9}$$

is called a wavelet family. If we fix function ψ (by taking $a = 1$ and $b = 0$), it is often called mother wavelet.

1.5.6 Definition (Wavelet Transformation)

Relative to every basic wavelet ψ, the integral wavelet transforms (IWT) on $L^2(\mathbb{R})$ is defined by

$$W_\psi f(a,b) = \frac{1}{\sqrt{|a|}} \int_{-\infty}^{\infty} f(t)\, \psi\left(\overline{\frac{t-b}{a}}\right) dt\,, \qquad f(t) \in L^2(\mathbb{R}) \tag{1.10}$$

which represents how much amount of scaled and translated component of wavelet is superimposed with the function $f\ (t)$.It can also be written as

$$W_\psi f(a,b) = \langle f\ , \psi_{b,a} \rangle \tag{1.11}$$

1.5.7 Definition (Wavelet Series)

A function $\psi(t)\ \epsilon\, L^2(R)$ is called an orthonormal wavelet if the family $\{\psi_{b,a}(t)\}_{b,a}$ of wavelet ψ given in Equation (1.8), forms an orthonormal basis of $L^2(\mathbb{R})$ i.e

$$\langle \psi_{b,a}\ , \psi_{d,c} \rangle = \delta_{b,d}\,.\,\delta_{a,c} \tag{1.12}$$

where $\delta_{b,a}$ is the Kronecker delta symbol given by

$$\delta_{b,a} = \begin{cases} 0, & if\ a \neq b \\ 1, & if\ a = b \end{cases} \tag{1.13}$$

and series representation of every function $f(t) \in L^2(\mathbb{R})$ by the orthonormal wavelet family $\{\psi_{b,a}(t)\}_{b,a}$ is called a wavelet series as given below

$$f(t) = \sum_{b,a=0}^{\infty} C_{b,a}\, \psi_{b,a}(t) \tag{1.14}$$

where the wavelet coefficients $C_{b,a}$ are given below

$$C_{b,a} = \langle f\, , \psi_{b,a} \rangle \tag{1.15}$$

To solve a mathematical model with wavelet transforms, it is desirable from a mathematical point of view to use a space where the inner product of a function with itself is related to the size (norm) of the function. For this reason, we will work in the space $L^2(R)$. The simplest wavelet satisfying the admissibility condition is the Haar wavelet which forms an orthonormal family with compact support and it is defined as

1.5.8 Definition (Haar Scale 2 Function)

$$\phi(t) = \begin{cases} 1 & for \quad 0 \leq t < 1\,; \\ 0 & otherwise \end{cases} \tag{1.16}$$

1.5.9 Definition (Haar Scale 2 Wavelet)

$$\psi(t) = \begin{cases} 1\,, & for \quad 0 \leq t < \dfrac{1}{2}\,; \\ -1\,, & for \quad \dfrac{1}{2} \leq t < 1; \\ 0\,, & otherwise \end{cases} \tag{1.17}$$

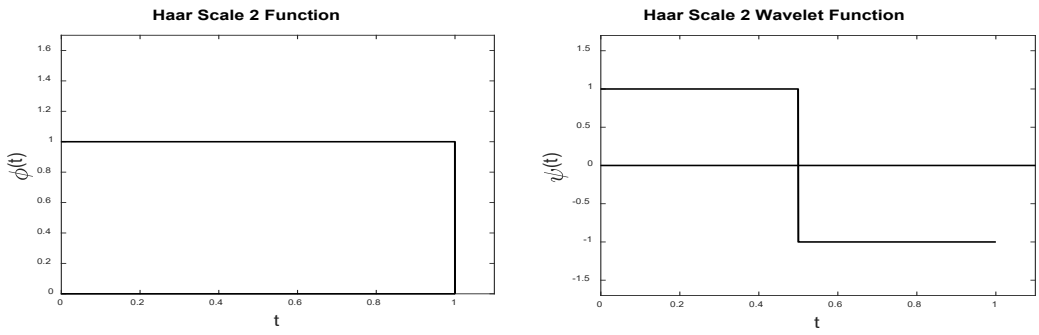

Haar scale 2 Function **Haar scale 2 Wavelet function**

Figure 1.1 Haar scale 2 Function and Haar scale 2 Wavelet function

1.5.10 Construction of wavelets family with multiresolution analysis

The concept of multiresolution analysis (MRA), formulated by Y. Meyer and S. Mallat is crucial to the theory of wavelets. A multiresolution analysis (MRA) is a sequence of closed subspaces $\{V_j\ ,\ j \in \mathbb{Z}\ \}$ of $L^2(\mathbb{R})$ satisfying the following properties:

(i) $\cdots V_{-1} \subset V_0\ \subset V_1\ \cdots$

(ii) $\text{clos}_{L^2}\left(\bigcup_{j\in\mathbb{Z}} V_j\right) = L^2(\mathbb{R})$,

(iii) $\bigcap_{j\in\mathbb{Z}} V_j = \{0\}$,

(iv) If $f(x) \in V_j$ if and only if $f\left(2^{-j}x\right) \in V_{0,}$ i.e. the spaces are the scaled versions of the central space V_0.

(v) $f(x) \in V_0$ if and only if $f(x-m) \in V_{0,}$ for all $m \in \mathbb{Z}$

(vi) There exists a function $\phi \in V_0$ called the scaling function s.t set $\{\phi(x-m)\}_{m\in\mathbb{Z}}$ forms the orthonormal basis in V_0 which is also known as a Riesz Basis in V_0.

Condition (i) to (iii) means that every function in $L^2(\mathbb{R})$can be uniquely approximated by elements of the subspaces V_j, and as j approaches ∞, the precision of approximation increases. Conditions (iv) and (v) express the invariance of the system of subspaces $\{V_j\}$ with respect to the translation and dilation operators. For a given MRA $\{V_j\}$ in $L^2(\mathbb{R})$ with scaling function ϕ, a wavelet is obtained by a new subspace W_j of $L^2(\mathbb{R})$ is defined which satisfies the following conditions

a) $V_{j+1} = V_j\ + W_j\ ,\ V_j\ \perp W_j$ for all j i.e $V_{j+1} = V_j \oplus\ W_j$

b) $\cdots W_{-1}\ \perp W_0\ \perp W_1\ \cdots$

c) $V_j = V_0\ \oplus \sum_{i=0}^{j-1} W_j$ which implies $L^2(\mathbb{R}) = V_0\ \oplus \sum_{i=0}^{j-1} W_j$ as $j \to \infty$

Hence every square-integrable function can be expressible in terms of Haar wavelet series expansion and it can be used to solve numerical problems. Using Multi-resolution

analysis (MRA) which is also known as a multiscale approximation (MSA), Haar wavelet family with Scale 2 is obtained as follows:

1.5.11 Definition (Haar Scale 2 wavelet family)

Haar wavelet family is defined as

$$h_i(t) = \psi\left(2^j t - k\right) = \begin{cases} 1 & \varkappa_1(i) \le t \le \varkappa_2(i) \\ -1 & \varkappa_2(i) \le t < \varkappa_3(i), \\ 0 & elsewhere \end{cases} \tag{1.18}$$

$$i = 1,2,3, \dots \dots 2p$$

where $\varkappa$

$\varkappa_1(i) = \frac{k}{p}$, $\varkappa_2(i) = \frac{2k+1}{2p}$, $\varkappa_3(i) = \frac{(k+1)}{p}$, $p = 2^j$, $j = 0,1,2, \dots, k = 0,1,2, \dots, p-1.$

j is dilation parameter, k is the translation parameter and i is the wavelet number which is calculated from the relation $i - 1 = p + k$. The function $h_1(t)$ is called father wavelet,$h_2(t)$ mother wavelet and all other functions $h_3(t), h_4(t)$ ... are generated from the translation and dilation of the mother wavelet. In chapter 3 of the thesis, scale 3 Haar wavelet family is constructed which is an improved version of Haar scale 2 wavelets.

So, this research aims to investigate the execution of collocation method with Haar scale 2 and Haar scale 3 wavelets basis functions for the numerical solutions of some important linear and nonlinear differential equations.

1.6 Collocation method

Considerable work has been accounted in the literature utilizing the Haar wavelet collocation strategy for investigating and understanding the various physical phenomena governed by the differential equations. The collocation method is one of the popular discretization schemes for the solution of differential equations and it belongs to the method of weighted residuals. It was first proposed by Kantorovich [Kan] in 1934 and three years later, it was again proposed by Frazer R. A, et.al in 1937 for the same purposes. In the collocation method, weighted truncated series expansion of the basis functions are used to approximate the solution function at the different points of the domain which are also known as collocation points. The weight functions

are used to ensure that the differential equation is satisfied as closely as possible by the truncated series expansion of basis functions. Thus, the suitable values of the weight functions are essential to achieving a good approximate solution to the differential equations with minimum residual. The basic idea behind the use of the collocation method in our thesis work is to find the most suitable weight such that the residual is zero at the collocation points. In this method, we approximate the unknown solution function by the truncated series of Haar wavelet basis functions and weight function are used as a coefficient of Haar wavelets which will be evaluated in the process of Haar wavelet collocation method. The brief description of the Haar wavelet collocation method is as follows

Consider the one-dimensional boundary value problem

$$\mathcal{L}\,\xi(\tau) = \psi(\tau), \qquad \forall \quad \mathfrak{a} \le \tau \le \mathfrak{b} \tag{1.19}$$

with boundary constraints

$$\xi(\mathfrak{a}) = \alpha\,, \qquad \xi(\mathfrak{b}) = \beta \tag{1.20}$$

where $\mathcal{L}$ is the linear differential operator (maybe a constant coefficient or a variable coefficient differential operator) and ψ is a real-valued continuous function of τ on $[\,\mathfrak{a}, \mathfrak{b}]$. Consider the set of Haar wavelet family $\{h_i\}_i$. It is well known that the Haar wavelets family form a complete orthonormal basis in $l_2([\,\mathfrak{a},\ \mathfrak{b}])$. Then, there will exist some finite set Δ such that

$$l_2([\,\mathfrak{a}, \mathfrak{b}]) = span\{h_i\ :i\ \in \Delta\} \tag{1.21}$$

Let H be any subspace of $l_2([\,\mathfrak{a}, \mathfrak{b}])$ in which we wish to represent the solution to the given problem. Then for any finite set Δ_1

$$H = span\{h_i\ :i\ \in \Delta_1\} \tag{1.22}$$

Now approximate the unknown solution function using Haar wavelet family as

$$\xi(\tau) = \sum_{i=1}^{n} a_i h_i(\tau), \qquad \forall \quad \mathfrak{a} \le \tau \le \mathfrak{b} \tag{1.23}$$

These $a_i's$ are the wavelet coefficients which are to be determined in the process.

Also, $\mathcal{L}$ is the linear differential operator by assumption, then by applying $\mathcal{L}$ on above equation we get

$$\mathcal{L}\,\xi(\tau) = \sum_{i=1}^{n} a_i \mathcal{L}\, h_i(\tau), \qquad \forall \quad \mathfrak{a} \le \tau \le \mathfrak{b} \tag{1.24}$$

Boundary conditions will be used in applying the linear differential operator $\mathcal{L}$. Now after using the Equation (1.23) and the boundary conditions, Equation (1.24) becomes

$$\sum_{i=1}^{n} a_i \mathcal{L}\, h_i(\tau) = \psi(\tau) \qquad \forall \quad \mathfrak{a} \le \tau \le \mathfrak{b} \tag{1.25}$$

Discretize the above equation using the n collocation points $\{\tau_i\}_{i=1}^{n}$. To avoid the singular system of algebraic equations one has to be very careful while selecting the collocation points. Haar wavelets are discontinuous in nature. Therefore, to avoid the collocation point at the point of discontinuity, following strategy is adopted

Firstly, the grid points on the curve or surface are selected using the formula $\overline{\tau_l} = \frac{l}{n}$, where $l = 0,1,2,\dots n,\ n = 2^j$ or 3^j , $j = 0,1,2,\dots$ then the Collocation points are calculated by using the expression given below

$$\tau_l = \frac{\overline{\tau_{l-1}} + \overline{\tau_l}}{2}, \qquad l = 0,1,2,\dots,n \tag{1.26}$$

Now, Equation (1.25) becomes

$$\sum_{i=1}^{n} a_i \mathcal{L}\, h_i(\tau_l) = \psi(\tau_l), \qquad l = 0,1,2,\dots,n \tag{1.27}$$

The above system of n equations can easily be put into the matrix form.

$$\begin{bmatrix} \mathcal{L}\,h_1(\tau_1) & \mathcal{L}\,h_2(\tau_1) & \cdots & \mathcal{L}\,h_{n-1}(\tau_1) & \mathcal{L}\,h_n(\tau_1) \\ \mathcal{L}\,h_1(\tau_2) & \mathcal{L}\,h_2(\tau_2) & \cdots & \mathcal{L}\,h_{n-1}(\tau_2) & \mathcal{L}\,h_n(\tau_2) \\ \mathcal{L}\,h_1(\tau_3) & \mathcal{L}\,h_2(\tau_3) & \cdots & \mathcal{L}\,h_{n-1}(\tau_3) & \mathcal{L}\,h_n(\tau_3) \\ \vdots & \vdots & & \vdots & \vdots \\ \mathcal{L}\,h_1(\tau_{n-2}) & \mathcal{L}\,h_2(\tau_{n-2}) & \cdots & \mathcal{L}\,h_{n-1}(\tau_{n-2}) & \mathcal{L}\,h_n(\tau_{n-2}) \\ \mathcal{L}\,h_1(\tau_{n-1}) & \mathcal{L}\,h_2(\tau_{n-1}) & \cdots & \mathcal{L}\,h_{n-1}(\tau_{n-1}) & \mathcal{L}\,h_n(\tau_{n-1}). \\ \mathcal{L}\,h_1(\tau_n) & \mathcal{L}\,h_2(\tau_n) & \cdots & \mathcal{L}\,h_{n-1}(\tau_n) & \mathcal{L}\,h_n(\tau_n) \end{bmatrix} \begin{bmatrix} a_1 \\ a_2 \\ a_3 \\ \vdots \\ a_{n-2} \\ a_{n-1} \\ a_n \end{bmatrix} = \begin{bmatrix} \psi(\tau_1) \\ \psi(\tau_2) \\ \psi(\tau_3) \\ \vdots \\ \psi(\tau_{n-2}) \\ \psi(\tau_{n-1}) \\ \psi(\tau_n) \end{bmatrix} \tag{1.28}$$

Solving the above system of equations, wavelet coefficients $a_i's$ can easily be calculated. Substituting the wavelet coefficients $a_i's$ in the equation (1.23), one can represent an approximate solution of equation 1 uniquely in solution space H as

$$\xi(\tau) = \sum_{i=1}^{n} a_i h_i(\tau), \qquad \forall \quad \mathfrak{a} \le \tau \le \mathfrak{b} \tag{1.29}$$

1.7 Quasilinearization

In 1965, Bellman and Kalaba introduced the concept of quasilinearization method to solve nonlinear equations. Quasilinearization technique has its origin in the Taylor series approximation and Newton-Raphson method. Because of its features and working, it is also known as the generalization of the Newton-Raphson method. The quasilinearization technique helps in linearize the non-linear terms in the functional equation and gives a sequence of functions that generally converges to exact solution of parent non-linear functional equation. Quasilinearization technique transformed the non-linear differential equation into a sequence of linear differential equations which can be further solved recursively with less effort. The main idea to use this technique is based upon the fact there is no analytic method to solve many non-linear functional equations but the solution of these equations is the demand of the society. So, this technique will help in converting the given nonlinear system into the equivalent sequence of linear functional equations which can be further solve using the existing techniques. In our thesis, we used this technique in combination with Haar scale 2 and Haar scale 3 wavelets to solve various types of functional equations like ODEs, FDEs, PDEs governing the various physical phenomena. In order to make the explanation of the process involved in the technique simple and easy to understand, we considere a non-linear 2nd order differential equation of the form

$$\xi''(\tau) = \psi(\xi(\tau), \tau) \qquad \forall \quad \mathfrak{a} \leq \tau \leq \mathfrak{b} \tag{1.30}$$

with boundary constraints

$$\xi(\alpha) = \mathfrak{a}\,, \qquad \xi(\beta) = \mathfrak{b} \tag{1.31}$$

where ψ is a non-linear function of τ and ξ.

Choose an initial approximation for $\xi(\tau)$ as $\xi_0(\tau) = \xi(\alpha) = \mathfrak{a}$ and approximate $\psi(\xi(\tau), \tau)$ using Taylor series expansion about $\xi_0(\tau)$ up to first two terms as

$$\psi(\xi(\tau), \tau) \approx \psi(\xi_0(\tau), \tau) + (\xi(\tau) - \xi_0(\tau))\ \psi_\xi(\xi_0(\tau), \tau) \tag{1.32}$$

From Equations (1.31-1.33), we have

$$\xi''(\tau) \approx \psi(\xi_0(\tau), \tau) + (\xi(\tau) - \xi_0(\tau))\ \psi_\xi(\xi_0(\tau), \tau) \tag{1.33}$$

Solving the above equation for $\xi(\tau)$, we will get the next approximation for $\xi(\tau)$ as $\xi_1(\tau)$. Now again expand $\psi(\xi(\tau),\tau)$ about $\xi_1(\tau)$ using Taylor series as explained above, we get

$$\xi''(\tau) \approx \psi(\xi_1(\tau),\tau) + (\xi(\tau) - \xi_1(\tau))\ \psi_{\xi}(\xi_1(\tau),\tau) \tag{1.34}$$

Solving the above equation again for $\xi(\tau)$, we will get the next approximation for $\xi(\tau)$ as $\xi_2(\tau)$. To attain the required accuracy, continue the above process by using the following recurrence relation as a generalization of the above process

$$\xi''_{k+1}(\tau) \approx \psi(\xi_k(\tau),\tau) + (\xi_{k+1}(\tau) - \xi_k(\tau))\ \psi_{\xi}(\xi_k(\tau),\tau) \tag{1.35}$$

with boundary constraints

$$\xi_k(\alpha) = \mathfrak{a}\,, \qquad \xi_k(\beta) = \mathfrak{b} \tag{1.36}$$

Now, considering the non-linear 2nd order differential equation of the following form

$$\xi''(\tau) = \psi(\xi'(\tau),\xi(\tau),\tau) \qquad \forall \quad \mathfrak{a} \le \tau \le \mathfrak{b} \tag{1.37}$$

where ψ is a non-linear function of τ , ξ and ξ' . Repeating the above process following recurrence relation is obtained.

$$\begin{aligned}\xi''_{k+1}(\tau) \approx \psi(\xi'_k(\tau),\xi_k(\tau),\tau) + \left(\xi_{k+1}(\tau) - \xi_k(\tau)\right)\psi_{\xi}(\xi'_k(\tau),\xi_k(\tau),\tau) \\ + (\xi'_{k+1}(\tau) - \xi'_k(\tau))\ \psi_{\xi'}(\xi'_k(\tau),\xi_k(\tau),\tau)\end{aligned} \tag{1.38}$$

Generalizing the process of quasilinearization to the higher-order non-linear functional equation following recurrence relation is obtained

$$\begin{aligned}&\mathcal{L}^{\mathfrak{n}}\xi_{k+1}(\tau) \approx \psi(\xi_k^{n-1}(\tau),\xi_k^{n-2}(\tau),\cdots,\xi'_k(\tau),\xi_k(\tau),\tau) + \textstyle\sum_{j=0}^{n-1}\left(\xi_{k+1}^{j}(\tau) - \right.\\ &\left.\xi_k^{j}(\tau)\right)\ \psi_{\xi^j}\left(\xi_k^{n-1}(\tau),\xi_k^{n-2}(\tau),\cdots,\xi'_k(\tau),\xi_k(\tau),\tau\right)\end{aligned} \tag{1.39}$$

Where $\mathcal{L}^{\mathfrak{n}}$ is the linear differential operator of order n and ψ is a non-linear function of $\xi_k^{n-1}(\tau),\xi_k^{n-2}(\tau),\cdots,\xi'_k(\tau),\xi_k(\tau)$ and $\tau.\,\xi_k(\tau)$ will be a known value at each step which will be used to calculateξ_{k+1}.The process will be started with $\xi_0(\tau)$ is a rough initial approximation at the first stage and it will lead to the solution of the actual non-linear differential equation through a sequence of convergent functions. These sequences of functions are the solution of corresponding Linear differential equations represented by Equation (1.40).

1.8 Literature Review

First time the wavelets appeared in the thesis of Hungarian mathematician Alfred Haar [8] in 1909. The Haar wavelet is a piecewise constant function and the main property of this wavelet is compact support of wavelet. Unfortunately, it is not continuously differentiable therefore it was not studied much at that time because of this limitation. In the 1980s multiresolution analysis invented by S. Mallat [9] and Y. Meyer [10] has given the most prosperity to the field of wavelet analysis. The main advantage of multiresolution analysis was that it has provided scope for other researchers to develop mathematically their own family of wavelets. Using work on multiresolution analysis Y. Meyer developed his wavelets and these wavelets were continuously differentiable but they do not have compact support. After a few years, Ingrid Daubechies [11], [12] took the idea from Mallat and Meyer 's work to create a new set of wavelet basis, which were orthonormal and have compact support. These wavelets became the foundation of wavelet application. Right from the beginning, the wavelets were considered as scientific curiosity but because of huge research in the development of wavelets, it has turned to an influential scientific mathematical tool, which can be used for many applications. Within the Daubechies family of wavelets, wavelets were generally classified by the number of vanishing moments. After applying the condition of vanishing movements, a set of linear and non-linear simultaneous algebraic equations on coefficients were obtained.Solving these equations, numerical values for the coefficients were obtained. This straight forward approach has fulfilled the need of researchers for understanding the construction of wavelets and became very popular in the construction of wavelets. As a result, a new set of wavelets families came into existence like coiflet wavelets, symlets wavelets, etc. These wavelets were continuous, differentiable, and had compact support. These were extensively used in signal processing, image processing and there were some applications in the numerical analysis also. With the attractable properties of these wavelets, there was a big limitation of these wavelets that they did not possess any explicit form of expression and could not be used comfortably for discretization. One had to construct the wavelets with the help of filter coefficients and because of this analytical differentiation or integration for these wavelets became impossible. This made the process very

complicated when the integrals of some nonlinear functions were required in an application. Then a new concept of connection coefficients developed to calculate these kinds of integrals but the process of calculation of these connection coefficients was very complicated and had to perform separately for each such integral. Other than that, the method was applicable only for some simple types of nonlinearities in the equations (quadratic). Mishra and Sabina[13]also solved the differential equations using the connection coefficients in the Galerkin method. Now because of this complexity in obtaining the solutions by wavelets induced some pessimistic estimates. It was considered that solving the mathematical problems by the wavelet method had no advantage over the conventional methods. Strang and Nguyen [14](1996, p. 394) wrote "The competition with other methods is severe. We do not necessarily predict that wavelets will win". It gave a new impulse to look for other possibilities to come out of this deadlock. Again researchers started thinking about all the wavelets family developed till that time.In 1997 Chen and Hsiao [15] had overcome the disadvantage of the Haar wavelet of not being differentiable at the point of discontinuity. They approximated the highest order derivative present in the problem with the Haar wavelet series instead of approximating the solution function by the Haar wavelet series. The rest all derivatives and solution function itself were founded by integrating the highest order derivative. This technique has been proved very faithful and researchers are using this technique in solving the mathematical models governed by differential, integral and intro-differential equation. In 2001 Ülo Lepik [16] took the idea of Chen and Hsiao [15] and used the wavelet transformations to analyze the linear vibration of single and two degrees of freedom. He used the three type of wavelets transforms and found that, in the case of single degree of freedom vibrations, all three wavelets were given the same qualitative results but for the second degree of freedom of motion two wavelets i.e. Mexican hat and Haar wavelets have given qualitatively different results are from third wavelet i.e. Morlet wavelet. In 2004 Ülo Lepik and Enn Tamme[17] used Haar wavelet to investigate the behavior of solution for linear integral equations. Different kinds of integral equations (Fredholm and Volterra equations, integrodifferential equations, etc) were considered. He found that the solution obtained by using Haar wavelets was more effective than conventional solutions with the same step size and in the case of Fredholm and Volterra equations the convergence rate was O(M^{-2}). In

2005 U¨.Lepik [18] developed a new technique based upon Haar wavelet to investigate the solution of different types of ODEs and PDEs and compared Chen and Hsiao method (CHM) with the method of segmentation and approximation by piecewise constant approximation. He found that Chen and Hsiao wavelet method is mathematically very simple because the wavelet matrices *H* and the matrices of their integrals became more and more sparse which made the process very fast. But its instability for approximating the higher-order derivatives became a disadvantage. In 2007 U. Lepik [19] applied the Haar wavelet method to solve the nonlinear evolution equation. The method was tested on Burgers and Sine Gordon equations and found that the method is in full competition with the other existing classical methods. The method found was very economical as far as the computational cost and simplicity was concerned. The method was found to be very suitable for the boundary value problem as it automatically takes care of the boundary condition in the process of solution. In 2007, a little survey on the use of the Haar wavelet transform was given by the U. Lepik [20] in which he discussed some different types of integral and differential equations. In 2007 Ülo Lepik and Enn Tamme[21] applied the Haar wavelet transform technique to test the applicability of the method on nonlinear Fredholm integral equations and the results obtained were very promising. In 2008 U. Lepik [22] developed a new technique of non-uniform Haar wavelets for solving the integral and differential equations and proved that the Haar wavelet method with non-uniform mesh was suitable in the case of problems where abrupt or rapid changes in the solution took place. In 2008 Phang Chang, Phang Piau [23] developed the operational Matrices for Haar Wavelets to solve the ODEs and performed all the calculations with the matrix representation of wavelets and all of its integrals which reduced the complexity of the process. In 2009 Ü. Lepik [24] developed the algorithm based upon Haar wavelets to solve the various fractional integral equations. It was found that the method is very simple and fast to solve these kind of fraction equations In 2009 E. Babolian and A.Shahsavaran[25] has proved the convergence of the Haar wavelets method by doing the error analysis which was a big question at that time and also handle the non- linearity in his process to solve nonlinear Fredholm integral equations. In 2010 G. Hariharan, K. Kannan[26] had extended the utility of the Haar wavelet technique to solve some nonlinear parabolic partial differential equations using the Haar wavelet method where he considered very well

know nonlinear PDEs for testing the performance of the method. He proved that the proposed scheme was working better and had a good ability to handle the non-linearity in the process and it could be used to a big group of nonlinear PDEs. In 2010 G.Hariharan [27] solved a physical model of deflection in a beam of finite length which is governed by a fourth-order ODE with the associated boundary and initial conditions using the Haar wavelets method. In the method a generalized operation matrix and the matrices of their integrals were developed to solve this model and results were compared with the exact solution available in the literature. It was shown in the results that Haar wavelet method took smaller time on CPU and was able to give better results for less degree of freedom as compare to the other methods. In 2011, G. Hariharan [28] extended the use of Haar wavelet Method to solve the Klein-Gordon and the Sine-Gordon Equations with modification in approximation. He found that the results were closer to the exact real values for a very small no of collocation points and the accuracy can further be improved by increasing the number of collocation points. In 2011 , Ülo Lepik[29] applied the Haar wavelet method on the physical model of buckling of elastic beams in which he produced the solution for the different situation in buckling of elastic beams like crack simulation, beam vibrations on an elastic foundation, beams having flexible cross-section etc. In this application of Haar wavelets, author revealed many advantageous features of the Haar wavelet method like high accuracy for small number of grid points, use of common subprograms for solving the different problems, treatment of singularities in intermediate boundary condition and simplicity for implementation etc. Author proved that the method could also be applied to more complicated problems by taking the different examples. In 2011 V. Mishra, H. Kaur, and R.C. Mittal [30] developed an algorithm by using Haar wavelet with collocation method for solving various types of ODEs ,IDEs and integral equations .Numerical experiment were performed to prove the reliability and efficiency of the algorithm developed and found that wavelet-collocation algorithm was less time consuming, less complicated as compare to the wavelet-Galerkin procedure for solving the similar types of problems. In 2011 Ü. Lepik[31] solved partial differential equations with the aid of two-dimensional Haar wavelets which could be used for solving the higher-dimensional equation with less complexity. In 2012 Naresh Berwal, Dinesh Panchal and C. L. Parihar [32] solved the Wave-Like Equation by using the Haar wavelet technique. In

2013 Hariharan [33] developed a Haar wavelet algorithm for Fractional Klein-Gordon Equations in which the author developed the wavelet operational matrices and the operational matrices of their fractional integrals. A group of algebraic equations were obtained by using these operational matrices on fractional Klein–Gordon equations. Further, the group of algebraic equations was transformed into a matrix system and solved for getting the unknown coefficients of the Haar wavelet series approximation of the solution. The author claimed that method was very effective, simple, fast, and flexible for other differential and integral systems. Also, the complexity of calculating the correction coefficients could also be avoided in comparison with Daubechies wavelets. In 2013 S. Sekar [34] has solved the Integro-Differential Equations using single term Haar Wavelet and compare the results with Local Polynomial Regression (LPR) method and proved the efficiency of the Haar wavelet method. In 2013 Naresh Berwal and Dinesh Panchal[35] proved the efficiency of Haar wavelet method by applying it onto L−C−R equation and comparing the results with exact solution. In 2013 Harpreet Kaur, et.al [36] Author have applied a quasi-linearization technique along with the Haar wavelet bases to solve the nonlinear Blasius equation at uniform collocation points. Blasius equation is very important equation of fluid mechanics and needed some promising solution. Author claimed that in applying the quasi-linearization technique along with Haar wavelet approximation did not require any iteration on the selected collocation points which made the quasilinearization process of handling non linearity very easy. In 2014 Umer Saeed and Mujeeb Ur Rehman[37] extended the utility of the method of approximation of solution using Haar wavelet series for the fractional-order nonlinear oscillation equations and found that solutions on large intervals were in agreement with fourth-order Runge-Kutta method. In 2014 Umer Saeed and Mujeeb ur Rehman[38] applied the Haar wavelet-Quasilinearization technique on Heat Convection-Radiation Equations for getting the approximate solution. In which the author first linearized the nonlinear heat transfer equation using quasilinearization technique. Then the linear system was solved by approximating the dependent variable and their derivatives by the truncated convergent series of Haar wavelet bases which results into a matrix system after using the collocation points in the resultant algebraic equations. Two special case of nonlinear heat transfer equation i.e distribution of temperature in lumped system of slab made of variable thermal conductivity material

and lumper system cooling profile were studied by using the proposed scheme. Author in the manuscript claimed that Haar wavelet-quasilinearization technique was roughly coincide with exact solution and gave better results as compare to the other methods. In 2014 R.C. Mittal, Harpreet Kaur, and Vinod Mishra [39] developed Haar wavelet-based algorithm to investigate the phenomena governed by the nonlinear coupled Burgers' equation. After applying the Haar wavelets with Collocation method the system of nonlinear coupled Burgers' partial differential equations transformed in the new system of ODEs. Resultant system of ODEs then solved by the Runge Kutta technique. Author established the stability analysis of this hybrid scheme also. The method was tested on some test problems and author claimed that it was giving the quite satisfactory results and the method could be extended to solve other higher order differential system of equation. In 2014 Asmita C. Patel & V. H. Pradhan [40] applied the Wavelet Galerkin scheme for solving the nonlinear partial differential Equations. They used Daubecheis wavelet with Galerkin method to solve the nonlinear partial differential equations. In 2014 Sangeeta Arora , Yadwinder Singh Brar and Sheo Kumar[41] implemented the Haar Wavelet Matrices techniques for finding the Numerical Solutions of Differential Equations . In 2014 Osama H. M., Fadhel S. F and Zaid A. M [42] applied Haar wavelet method to solve fractional Variational problems. In 2014 Santanu Saha Ray[43] did a comparison of two most promising schemes for solving the Fractional differential equations.In his work, he compared the performance of the Haar wavelet method with the Optimal Homotopy Asymptotic method on Fractional Fisher type equations. The author claimed that both methods were appropriate and reliable for solving these kinds of equations. But optimal Homotopy Asymptotic method provided better results as compared to the Haar wavelet method for a certain number of grid points. On the other hand, the accuracy of the Haar wavelet method could be improved by increasing the number of grid points. In 2015 Ö. Oruç, F. Bulut, A. Esen [44] developed a new hybrid technique for the investigation of the solution of modified Burgers Equation. In the algorithm temporal part was discretized and handled by finite differencing, spatial part was discretized by Haar wavelets whereas the non-linearities in the equation were handled by quasi-linearization technique. Author tested the method developed on three test problems and claimed that method is fully consistent, fast, and very much economical in terms of computational

cost. In 2015 Manoj Kumar and sapna pandit[45]solved the Fokker Plank Equations with constant and variable coefficients by using an algorithm based on the Haar wavelet method. In 2015 S. C. Shiralashetti and A. B. Deshi[46] addressed the multi-term FDEs by using collocation method with Haar wavelet bases and found that HWCM equally competent and easy to implement in comparison with other existing methods. It was very effective, was easy to implement and able to approximate the solution accurately compared to existing methods. In 2015 M. Fallahpour, M. Khodabin, and K. Maleknejad [47] developed Haar wavelet-based method to tackle more variables in two-dimensional linear Stochastic Volterra integral equation and difficulty of finding solution because of the randomness. After testing the method on the test examples author claimed that method is reliable, efficient, and fast but could be improved to be more accurate by using other numerical methods. In 2015 S.C. Shiralashetti et.al [48] extended the applicability of Haar wavelet collocation method for the investigation of models governed by singular initial value problems . Authors of the manuscript showed that HWCM was a powerful numerical method for the solution of the linear and non-linear singular initial value Problems as compared to other methods like Adomian decomposition Method (ADM) &Variational iteration method (VIM) etc. In 2015 Inderdeep Singh, Sangeeta Arora, Sheo Kumar [49] solved the wave equation by using Haar wavelet and proved that the method was better than other method . In 2016 S. C. Shiralashetti, M. H. Kantli and A. B. Deshi[50] developed Haar wavelet based collocation method to address the nonlinear ODEs emerging in the field of fluid dynamics with different boundary conditions. After testing the method on different problems of fluid dynamics with different boundary conditions the author claimed that HWCM established a solid foundation for its use in solving these kinds of problems because of their simplicity and fast convergence. In 2016 S. C. Shiralashetti et.al [51] solved the Klein–Gordon equations by using the Haar wavelet method and showed that it worked better than classical numerical methods like finite difference method. In 2016 Firdous A. Shah et.al [52] developed an explicit form of operational matrix of Haar wavelets for solving the various linear and non-linear fractional differential equations.Many standard benchmark problems were tested and claimed the superiority of the method by giving numerical evidence in terms of fast convergence and better accuracy. In 2016 A. C. Patel and V. H. Pradhan[53] implemented the Haar wavelet

method on the advection-dispersion equation representing one-dimensional contaminant transport through a porous medium. In 2016 O. Oruc, F. Bulut, and A. Esen [54] developed the Haar wavelet-based hybrid technique for the investigation of the phenomena governed by Regularized Long Wave Equation. Time derivatives were discretized by using finite differencing and space derivatives were approximated by truncated Haar wavelet series. Various test problems related to solitary wave motion had been analysed and claimed that method was working well to analyze these kinds of problems. In 2016 Harpreet Kaur, Shin Min Kang [55] developed the time discretization of Haar wavelet Series approximations with Quasilinearization technique for solving well known nonlinear PDEs .Quasilinearization was used to tackle the nonlinearity in nonlinear PDEs .Haar wavelet method with collocation method was used to convert the given PDEs into a linear system of equations which were further solved by Thomas algorithm. In 2017 S. C. Shiralashetti, et.al [56] used adaptive grid by adding the more grid points which were actually the midpoints of the regular uniform grid points in the regular uniform grid of Haar Wavelets. The new adaptive grid Haar wavelet technique was applied to solve the parabolic type of PDEs along with collocation method and showed that the new technique gives better accuracy in comparison to regular HWCM and FDM. In 2017 Saedeh Foadian et.al [57]claimed that the system of equations obtained after applying the Haar wavelets along with the quasilinearization and collocation technique on the coupled nonlinear Reaction-Diffusion Equations (RDEs) was very sensitive to the wavelets coefficients and the matrix on the right-hand side of the equation. They used Tikhonov Regularization (TR) method to stabilize this ill-conditioned system of linear equation to obtain a stable numerical approximation for RDEs with suitable initial and boundary conditions. Further Author claimed that proposed methods was faster, stable and was giving the better results as compared to finite difference method (FDM) and radial basis function (RBF) method. In 2017 Bijil Prakash et.al [58] extended the application of Haar wavelets for the solution of SEIR epidemic model governed by nonlinear fractional differential equation. The model carried the non-constant population which was very cumbersome, sometime not possible to solve analytically. It became more difficult when the corresponding model is fractional and non-linear in nature. In this article Author claimed that the method was working very well to address these kinds of

biological mathematical models of various infectious diseases. In 2017 M. Erfanian et.al [59] developed the method for integro-differential equations of mixed Volterra–Fredholm type using the rationalized Haar wavelet bases to avoid the numerical integration involved in the process. It was claimed by the author in the manuscript that proposed method reduced the computational cost and increased the efficiency by avoiding the step of converting Integro-Differential Equation into a difference equation. In 2017 , Somayeh Arbabi et.al [60] applied the two-dimensional Haar wavelets method for solving the systems of partial differential equations. Convergence and stability of the method was proved. Method was tested on the test problems and claimed that results obtained were in a very good coincidence with the exact solution. In 2017 Firdous A. Shah and R. Abass[61] extended the application of Haar wavelet method to one-dimensional singularly perturbed boundary-value problems. In their work they converted the given singularly perturbed boundary-value problems in the system of difference equations with the help of Haar Wavelet series approximation and then by using the collocation approach a system of linear equations was obtained. In this manuscript author tested the given method on five benchmark problems and claimed that the proposed method was easy to implement on computer, giving better results as compare to other existing methods and could be implemented to more challenging and more complex problems of singularly perturbed equation. In 2017 Umer Saeed [62] developed an algorithm for the solution of fractional Lane-Emden type equations. In this algorithm, he approximated the unknown solution, nonlinear term in the differential equation by using the Adomian decomposition method and reduced the given non-linear equation into the system of linear FDEs. Then linear FDEs were then solved with the help of the Haar wavelet collocation method and back substituting these solutions in the Adomian series the series solution is obtained. The author compared the results obtained by the present method with the other methods available in the literature and claimed that the method was giving an excellent result as compared to the other methods. The author also claimed that the method was competent enough to handle different types of nonlinearities in the various types of the differential equations. In 2017 S. C. Shiralashetti, et.al [63] extended the application of the Haar wavelet collocation method to solve the nonlinear Volterra-Fredholm-Hammerstein integral equations. In the manuscript, nonlinear Volterra-Fredholm-Hammerstein integral

equations were first converted in the corresponding differential equations by differentiating the given integral equations using Leibnitz rule and then solved with the help of Haar wavelet collocation method. The results were compared with the exact solution and found satisfactory with error of order 10^{-13} . In 2017 Ravikiran A. Mundewadi, et.al [64] applied the same procedure of Haar wavelet collocation method to solve the various integro-differential and integral equations. In 2017 Imran Aziz, et.al [65] developed a new algorithm by using the three-dimensional Haar wavelets to solve the mathematical model governed by the three-dimensional partial differential equations with Dirichlet boundary conditions which are elliptic in nature. Many benchmark problems were tested by the author to prove the exactness and diverse applicability of the method. In 2017 Zakieh Avazzadeh [66] extended the application of 2D Haar wavelet method to solve the nonlinear age structured population model governed by the non-classical partial differential equation with boundary constraint as integral equations. In this manuscripts author reduced the given problem into an algebraic system which lead to a sparse matrix system and increased the computational efficiency. In 2017 Umer Saeed [67] used the Haar wavelet quasilinearization technique for finding the solution of the system of fractional nonlinear differential equations and compared the results with other existing methods like variational iteration method (VIT), Homotopy perturbation method (HPM) and found that present method is a numerical accuracy enhancement over the existing methods. In 2017 Ram Jiwari, et.al [68] developed the technique to investigate the MHD Falkner-Skan flow over permeable. In this technique, authors used a Lie algebra of infinitesimal generators to transform the given system of 2D partial differential equations into a system of linear and nonlinear ordinary differential equations which are further solved by the Haar wavelet quasilinearization technique. In 2017 Randhir Singh, et.al [69] extended the application of the Haar wavelet quasilinearization technique for getting the solution of doubly singular boundary value problems. The method was tested on different physical models governed by the doubly singular differential equation and it was claimed by the author that the proposed method is giving the results better than other methods. In 2017 Sapna Pandit, et.al [70] extended the application of the 2D Haar wavelet method finding the solution of well-known linear and non-linear hyperbolic type wave equations and claimed that the method was reliable and it could be expanded to explore more

biological, physical and chemical phenomena. In 2017 Somayeh Arbabi, et.al[60] extended the application of the 2D Haar wavelet method for finding the solution of systems of nonlinear partial differential equations in higher dimensions. The author also discussed the convergence and stability of the 2D Haar wavelet method. The method was tested on some 2D and 3D PDEs and found that it was working better and giving better results as compared to other methods. In 2017 R. C. Mittal, et.al [71] developed a new technique based upon a Haar scale 3 wavelets. It was improved and hybrid version Haar Scale 2 wavelets. The New technique was used for the Sensitivity Analysis of Shock Wave in planar and non-planar Burgers Equations. Forward finite difference scheme was used for time discretization, scale 3 wavelets were used for space discretization of the derivatives and quasilinearization technique was used to tackled the non-linearities in the equation. Proposed Technique was tested on six problems. Author claimed that the method performed was superior in contrast to other classical methods and could be applied to a vast class of integral equations, PDEs, ODEs. In 2017 Sapna Pandit, et.al[72] applied the Scale-2 Haar wavelets technique for the sensitivity analysis of shock wave in planar and non-planar Burgers Equations. Author claimed that the proposed method was fully capable of capturing the shock wave behaviour for small values of viscosity where most of the numerical methods failed. In 2018 Sirajul Haq, et.al [73]used two dimensional Haar scale 2 wavelets for finding the solutions of Sobolev Equations and BBMB equations in higher dimensions where the discretization of temporal part was done by finite differencing scheme and spatial part was discretize by 2D Haar Wavelets collocation scheme. Method was tested on Sobolev and BBMB equations and results were compared modified weak Galerkin finite element method. Author claimed that present method gave better results in comparison with modified weak Galerkin finite element method. In 2018 Muhammad Ahsan, et.al [74]used two types of Haar wavelet collocation schemes to solve the unsteady inverse heat problems. In the first scheme (HWCM1), author used a transformation to convert a non-homogeneous PDE into a homogeneous form and in the second scheme (HWCM2) author used the traditional Haar wavelet collocation scheme. Both schemes were tested on unsteady inverse heat problems and found that HWCM1 was working better than HWCM2. Further author claimed that HWCM1 could be applied to a huge class of nonlinear inverse PDEs as well. In 2018 Maarjus Kris, et.al[75] used FDM-

finite difference method, HWM -Haar wavelet method, DQM-differential quadrature method for the investigation of functionally graded material beam in terms of free vibration analysis. All three methods were evaluated on the bases of their performance. It was concluded that HWM outperformed over FDM but the accuracy of the DQM was more than the HWM and FDM. Also, HWM could be more efficient for the analysis of nanostructures because of its properties. In 2018 Inderdeep Singh, et.al [76] used one and two dimensional Haar wavelets for finding the solution of BBMB, Harry Dym (HD), higher dimensional Diffusion Equations and the results were compared with other existing methods (ADM,HPM,HAM,FDM,QTBS).It was concluded by the author that the presented method was working better than the other methods. In 2018 J. Majak, et.al [77] developed a new higher order Haar wavelet method for finding the solution of integro-differential and differential equations. The method was tested on some integro-differential and differential equations as an application to FGM Structures. It was found that new method had improved order of convergence and less order of error and it could be utilized with minor adaption for a vast class of integro-differential and differential equations. In 2018 R.C. Mittal, et.al [78] developed a Haar Scale-3 wavelet-based technique for finding the solution of ordinary fractional dynamical systems. The method was tested with some test problem and compared with scale 2 Haar wavelets. It was found that Haar Scale-3 wavelet-based method converged faster than Haar Scale-2 wavelet-based method. In 2019 Omid Baghani [79] made a correction on the convergence analysis of Rationalized Haar wavelet method .He tested the claim for order of convergence on three examples and verified by the theoretical and numerical evidence that order of convergence for rationalized Haar wavelet method is $O(iq^i)$,not $O(q^i)$ where $q = \frac{M}{|\lambda|}$. In 2019 Sidra Saleem, et.al [80]used two dimensional Haar wavelet for finding the solution of higher dimensional nonlinear parabolic partial differential equations. After converting the differential system into a 4D array system, Kronecker tensor product was used to find the unknown coefficients. These coefficients were used to write the final solution. The method was tested on five different problems and concluded that it was efficient enough to handle these kinds of equations in higher dimensions. In 2019 Ömer Oruç, et.al [81] extended the use of two dimensional Haar wavelet along with the finite difference method for finding the

solution of time fractional reaction–sub diffusion equation. The proposed method was tested on two different equations and compared with alternating direction implicit method and meshless-based method. As a conclusion, author claimed that method is equally competent , extremely simple and easy to use as compare to other methods. In 2019 Muhammad Ahsan, et.al [82] applied Haar wavelet-finite difference method along with the quasilinearization technique to investigate linear and nonlinear Schrodinger equation and concluded that the method successfully simulates the physical behaviour of the phenomena governed by the Schrodinger equation. It can be extended for the higher dimensional Schrodinger equation with high computational cost. But one has to take on irregular domain with some supporting technique. In 2019 Amir Mohammadi, et.al [83] applied Haar wavelet collocation–Picard method for the investigation of fractional Emden–Fowler equations and the results were compared with the Adomian decomposition method and Homotopy perturbation method introduced. It was concluded by the author that proposed method was easy and effective in handling the singular and nonlinear fractional partial differential equations as compare to HPM and ADM. In 2019 Aditya Kaushik, et.al [84] used Rationalized Haar functions along with the collocation method to solve the various types of differential and integral equations and claimed that the method was effective, highly accurate, highly competitive and caused less computational cost. In 2019 R. C. Mittal, et.al [85] developed a New Scale-3 Haar wavelet-based technique to solve the second order ODEs with singular coefficient and nonlinearity. The new technique was tested on some benchmark problems and it was claimed by the author that the proposed scheme gave better results as compared to the cubic spline method, quadratic spline method, and scale-2 Haar wavelet method. It was shown that the scale-3 Haar wavelet method had a faster rate of convergence as compare to scale-2 Haar wavelet method. In 2020 Irfan Awana, et.al [86] extended the application of Haar wavelet-based collocation technique for the investigation of Pennes bioheat transfer model. The results were compared with exact solution of Pennes bioheat transfer model available in literature and found that present technique was working well for these kinds of problems also. In 2020 Mart Ratas, et.al[87] have extended the application of Higher Order Haar Wavelet Method (HOHWM) for the investigation of mathematical models governed nonlinear evolution equations. The given method was compared with Haar wavelet method (HWM) and

concluded that both the methods are equally capable of handling these kinds of problems. If higher accuracy was required then HOHWM was suggested and less computational cost was required then HWM was suggested. In 2020 Nosheen Pervaiz, et.al [88] extended the application of Haar Wavelet Method for the investigation of nonlinear Schrodinger equations with Dirichlet boundary conditions. Crank-Nicolson scheme was used for time discretization and Haar wavelet collocation scheme was used for space discretization. The method was tested on some nonlinear Schrodinger equations with different initial and boundary conditions and found that method was working well with these kind of problems. In 2020 Arun Kumar, et.al [89] extended the application of Haar wavelet Method to the field of electromagnetic problems. Author tested the Haar wavelet method on four electromagnetic problems related to transmission line, uniform plane wave in lossy dielectric, EM waves travelling in different media and telegrapher's equation. It was concluded by the author after the comparative analysis that Haar wavelet methods were expressively faster as compared to standard analytic solutions. In 2020 Ghader Ahmadnezhad, et.al [90] extended the application of Haar wavelet method for the investigation of fractional Fisher equation the field. In the proposed method ,Iteration Picard technique was used to handle the non-linearity in the fractional fisher's equation. The Haar wavelets were used to convert the resultant differential system into the system of difference equation which were further solved by matrix method. The results then compared with the other methods like HPM, MVIM with exact solution.It was concluded that obtained results coincide with exact solution. In 2020 Randhir Singh, et.al [91] extended the application of Haar wavelet quasilinearization Method for the investigation of Emden-Fowler Type Equations with different boundary conditions which were nonlinear doubly singular boundary value problem. It was concluded that obtained results were in good agreement with the exact solution and method was working better than finite difference method and cubic spline method. In 2020 Saedeh Foadian, et.al [92] used the Haar wavelet method along with the Tikhonov regularization method for getting the solution of time-delayed Burgers-Fisher equation. It was concluded by the author that method was easy to implement on computer environmental with less computational cost and less storage.

A literature review of about 100 papers shows that the Haar wavelet-based methods are very accurate, powerful, and efficient methods for solving the problems of science and technology. During the literature review, besides the immense application and great utility of Haar wavelets in the field of science and technology, the scope for new findings has been observed which is given below.

1.9 Finding from the literature review

1. There are many shreds of evidence for the existence of non-dyadic (Scale 3) wavelets in electronics engineering but a very few algorithm was developed till date in mathematics for non-dyadic(Scale 3) wavelets.
2. Though some hybrid methods in the literature have been seen, still there is a huge possibility of a new hybrid method where wavelets can also be combined with any of the Variational techniques, approximation techniques, semi-analytic techniques to create a hybrid method.
3. There is no algorithm developed for finding the solution of higher-order ordinary differential equations by the wavelet method.
4. There is a huge scope for finding the solution of Fractional differential equations by the wavelet method.
5. There is no algorithm developed to solve the system of nonlinear ordinary differential equations by wavelet methods.
6. There is no algorithm developed to solve the system of nonlinear partial differential equations in more than two variables by the wavelet method.

1.10 Objectives

Wavelet methods have become popular for their simplicity of implementation, small computation costs resulting from the sparsity, very high accuracy for small number of grid points, etc. The thesis presented will be used to find the solution of differential equations using wavelet methods in various fields like physics, medicine, biology, chemistry, economics, financial forecasting, image processing, Environmental science, etc.

The objectives of the proposed study are

1. To explore the possibility of coupling the Wavelet method with other legacy methods or by changing the dilation factor to frame hybrid method.
2. To investigate the applicability of the wavelet method in solving the differential equations used in various fields.
3. To implement the method developed for solving the Physical models which have significance in the field of science and engineering.
4. To analyze the solution obtained for the concerning problems with the analytical or numerical solution available in the literature.

This thesis is dedicated to the development of Haar Scale 3 and Haar scale 2 Wavelets based algorithms for solving the linear-nonlinear differential equations. The broad range of numerical problems arising in different fields like as higher-order linear and nonlinear boundary value problems, fractional Bagley-Torvik equations, coupled space-time fractional- Burgers' equation, hyperbolic Telegraph equations, NBBMB (non-linear Benjamin Bona Mahony Burgers) equation, linear and non-linear Sobolev equation are considered systematically. From the mathematical point of view, these problems represent the ordinary differential equation with associate boundary or initial conditions, Higher-order Linear and non-linear partial differential equations, Linear ordinary Fractional differential equations and Nonlinear system of fractional partial differential equations which are treated in the mathematical framework of functional analysis, linear algebra, and approximation theory. All the calculations have been performed using MATLAB 7 software installed on system with 4gb ram and intel core i3 processor .

Chapter 2

Numerical Solution by Haar Scale 2 Wavelet Collocation Method for a Class of Higher Order Linear and Nonlinear Boundary Value Problems

2.1 Introduction

Higher order boundary value problems (HOBVPs) are getting huge attention from researchers because of the fact that many physical phenomena like hydrodynamic and hydromagnetic stability [93], induction motor with two rotor circuits [94], viscoelastic flows in fluid dynamics, etc. are governed by the higher-order boundary value problems. Therefore, to find an accurate, efficient, and simple solution to these problems have achieved great significance during the last decades. The existence and uniqueness of the solution of HOBVPs have been proved by Agarwal in his book [95]. General analytical solution for these kinds of problems has not yet been established. Therefore, researchers are using numerical techniques to find the solutions of HOBVPs. Many numerical mechanisms have been developed in the literature to solve these problems such as Variational Iteration Decomposition Method (VIDM) [96], Optimal Homotopy Asymptotic Method (OHAM) [97], Galerkin Method with Quintic B-splines (GMQBS) [98], Legendre Galerkin Method (LGM) [99], Reproducing Kernel Space Method (RKSM) [100], Variational Iteration Method (VIM) [101], Modified Variational Iteration Method (MVID) [102], Sextic B-splines Collocation Method (SBSCM) [103], Petrov-Galerkin Method (PGM)[104], etc. But many of these methods involve cumbersome calculation process which slows down the rate of convergence and some of these methods are also very sensitive to the initial guess and can fall in the process of infinite iteration for the wrong initial guess and hence can increase the computational cost. In the past decade, the wavelet-based numerical method has become predominant because of its simple applicability and high accuracy. Wavelet is

a small wave that can be manipulated in two ways; one way is the translation which means shifting of all points of wavelet in the same direction and for the same distance and other is scaling or dilatation which means stretching or shrinking of original wavelet.

Mathematically wavelet can be represented by Equation (2.1)

$$\psi_{a,b} = \frac{1}{\sqrt{|a|}}\psi\left(\frac{t-b}{a}\right) \tag{2.1}$$

Here a is the dilation parameter and b is the translation parameter.

Wavelet transformation of any function $x(t)$is defined by Equation (2.2)

$$w(a,b) = \int_t x(t)\frac{1}{\sqrt{|a|}}\psi\left(\frac{t-b}{a}\right)dt \tag{2.2}$$

which gives us an information that at $t = \frac{b}{a}$, how much the scaled function is similar to the given solution function $x\ (t)$.

Many wavelets have been developed and used by the researchers for finding the numerical solutions of differential equations. Out of which Haar wavelet family is the simplest wavelet family having explicit mathematical expression as given by the Equation (2.3) and (2.4)

$$\text{Haar Scaling Function } \varphi(t) = \begin{cases} 1 & 0 \le t < 1 \\ 0 & elsewhere \end{cases} \tag{2.3}$$

$$\text{Haar Wavelet function } \psi(t) = \begin{cases} 1 & 0 \le t < \frac{1}{2} \\ -1 & \frac{1}{2} \le t < 1 \\ 0 & elsewhere \end{cases} \tag{2.4}$$

Haar wavelet family has very useful characteristics, such as localization in frequency and time, orthogonality of family members, compact support, simple applicability, high accuracy for a smaller number of collocation points, and time efficiency for a large system with more variable quantities, etc. In the past two decades, many researchers have worked on finding the solution of HOBVPs by HWCM. Siraj-ul-Islam et al.[105] have obtained the solution of second-order BVPs by HWCM. Fazal-i-Haq et al. [106]–[108] have obtained solutions of Third, fourth, sixth-order BVPs by HWCM. A.P.Reddy et al. [109], [110] have obtained a solution of fifth and seventh order BVPs by HWCM. So far, more than seventh order BVPs have not been solved by Haar Wavelet Collocation Method (HWCM).

This inspires us to use the collocation method with Haar wavelets as a basis function to solve HOBVPs of the type given below in Equation no.(2.5).

The main objective of our work is to establish and apply the Haar wavelet collocation method for the numerical solutions of linear and nonlinear HOBVPs emerging in many physical phenomena. To test the efficiency and accuracy of the method, we consider the general HOBVPs (Equation (2.5)) of the type

$$x^n(t) = f(t, x, x', x'', \cdots, x^{n-1}), \qquad a \le t \le b \tag{2.5}$$

with the following types of constraints on the solution at the boundary points given by Equation (2.6) and (2.7)

$$\begin{aligned} x(a) = \nu_1, x(b) = \sigma_1, x'(a) = \nu_2, x'(b) = \sigma_2, \cdots\cdots, x^{\left(\frac{n}{2}-1\right)}(a) \\ = \nu_{\frac{n}{2}}, x^{\left(\frac{n}{2}-1\right)}(b) = \sigma_{\frac{n}{2}} \ , \qquad \text{if n is even integer} \end{aligned} \tag{2.6}$$

$$\begin{aligned} x(a) = \gamma_1, x(b) = \delta_1, x'(a) = \gamma_2, x'(b) = \delta_2, \cdots\cdots, \ x^{\left(\frac{n-1}{2}-1\right)}(a) \\ = \gamma_{\frac{n-1}{2}}, x^{\left(\frac{n-1}{2}\right)}(b) = \delta_{\frac{n+1}{2}}, \qquad \text{if n is an odd integer} \end{aligned} \tag{2.7}$$

2.2 Haar Wavelet and Its Integrals

In generalized form, Haar wavelet family [10] is represented by the Equation (2.8)

$$h_i(t) = \psi\left(2^j t - k\right) = \begin{cases} 1 & \varkappa_1(i) \le t < \varkappa_2(i) \\ -1 & \varkappa_2(i) \le t < \varkappa_3(i), \\ 0 & elsewhere \end{cases} \quad i = 1,2,3, \ldots 2p \tag{2.8}$$

Where

$\varkappa_1(i) = \frac{k}{p}$, $\varkappa_2(i) = \frac{2k+1}{2p}$, $\varkappa_3(i) = \frac{(k+1)}{p}$, $p = 2^j$, $j = 0,1,2, \cdots, k = ,1,2, \ldots, p-1$

, i represents wavelet number calculated from the relation $i - 1 = p + k$, j represents the level of dilation/resolution of the wavelet (as we increase the value of j support of wavelet decreases) and k represents the translation parameters of the wavelet. The function $h_1(t)$ is called father wavelet,$h_2(t)$ are mother wavelet and all other functions $h_2(t)$, $h_3(t), h_4(t)$ ... are generated from the translation and dilation of the mother wavelet.

Using the explicit mathematical expression of Haar wavelet family, we can integrate Equation (2.3) and (2.8) over the interval [0,1) as many time as required by using the formula given in Equation (2.9)

$$q_{m,i}(t) = \int_0^t \int_0^t \int_0^t \cdots\cdots m\ times \cdots\cdots \int_0^t h_i(x)(dx)^m$$

$$= \frac{1}{(m-1)!}\int_0^t (t-x)^{m-1} h_i(x)dx \qquad (2.9)$$

$$\forall\ m = 1,2,3 \ldots\ldots\ ,\quad i = 1,2,3, \ldots\ldots 2p$$

After evaluating the above integrals for Equation (2.3) and (2.8), we get Equation (2.10) and (2.11)

$$q_{\beta,i}(t) = \frac{t^{\beta}}{\beta!} \quad for \quad i = 1 \qquad (2.10)$$

$$q_{\beta,i}(t) = \begin{cases} 0 & t < \varkappa_1(i) \\ \frac{1}{\beta!}\left(t-\varkappa_1(i)\right)^{\beta} & \varkappa_1(i) \le t \le \varkappa_2(i) \\ \frac{1}{\beta!}\left[\left(t-\varkappa_1(i)\right)^{\beta} - 2\left(t-\varkappa_2(i)\right)^{\beta}\right] & \varkappa_1(i) \le t \le \varkappa_3(i) \\ \frac{1}{\beta!}\left[\left(t-\varkappa_1(i)\right)^{\beta} - 2\left(t-\varkappa_2(i)\right)^{\beta} + \left(t-\varkappa_3(i)\right)^{\beta}\right] & t > \varkappa_3(i) \end{cases} \qquad (2.11)$$

$$for \quad i \ge 2$$

2.3 Approximation of Function by Haar Wavelets

From the properties, one can observe that the members of a family of Haar wavelet are orthogonal to each other, thus any square-integrable function $x(t)$ over the interval [0,1) can be expressed an infinite series of scale 3 Haar bases as given in Equation (2.12)

$$x(t) = \sum_{i=0}^{\infty} a_i h_i(t) \qquad (2.12)$$

Here $a_i's$ are Haar wavelet coefficients whose values can be calculated as $a_i = \int_0^1 x(t)\, h_i(t)dt$,$i = 1,2,3, \ldots$ .But in practice, only the finite number of terms of the above equation are considered. We are considering only the first $2p$ terms where $p = 2^j$, $j = 0,1,2, \ldots$ of series to approximate the function $x(t)$ as given in Equation (2.13)

$$x(t) \approx x_{2p} = \sum_{i=0}^{2p} a_i h_i(t) \qquad (2.13)$$

2.4 Haar Wavelet Mechanism for Boundary Value Problems

Case 1: Consider the linear higher-order boundary value problems as given in Equation (2.14)

$$a_0(t)x^n(t) + a_1(t)x^{n-1}(t) + a_2(t)x^{n-2}(t) + \cdots + a_n(t)x(t) = f(t), \quad \forall\, t\epsilon(a,b) \tag{2.14}$$

with the constraints on the solution at the boundary points given in Equation(2.6) and (2.7).$a_0(t), a_1(t), a_2(t) \ldots\ldots a_n(t)$ and $f(t)$ as continuous functions of variable t defined on the interval [a, b].

The step-wise mechanism for obtaining the solution of HOBVPs by applying the Haar wavelet collocation method can be defined as follows:

Step 1: Approximate the highest order derivative present in the equation as $x^n(t) = \sum_{i=1}^{2p} a_i h_i(t)$ where $h_i(t)$ are members of Haar wavelet family and $a_i's$ are the wavelet coefficients which are to be determined in the process.

Step 2: Now integrate $x^n(t) = \sum_{i=1}^{2p} a_i h_i(t)$ from 0 to t as many times as desired in the application. If we integrate $n - m$ number of times we get the following expression

$$x^m(t) = \sum_{i=1}^{2p} a_i q_{n-m,i}(t) + \sum_{\nu=0}^{n-m-1} \frac{t^\nu}{\nu!} x^{m+\nu}(0) \tag{2.15}$$

$$\forall\, m = 1,2,3,\cdots,n-1$$

Where the values of $q_{n-m,i}$'s can be calculated using the formulas given in Equations (2.10) and (2.11)

Now we introduce the following notation

$$B_{i,1=} \int_0^1 h_i(x)dx \qquad i = 1,2,3,\ldots 2p \tag{2.16}$$

Step 3: Convert the given boundary value problem into the initial value problem to get the matrix system given in Equation (2.17)

$$\begin{bmatrix} 1 & n-1 & (n-1)(n-2) & \cdots & (n-1)(n-2)(n-3)(n-4)\cdots\cdots(n-(s-1)) \\ 1 & n-2 & (n-2)(n-3) & \cdots & (n-2)(n-3)(n-4)(n-5)\cdots\cdots\cdots\cdots(n-s) \\ 1 & n-3 & (n-3)(n-4) & \cdots & (n-3)(n-4)(n-5)(n-6)\cdots\cdots(n-(s+1)) \\ \vdots & \vdots & \vdots & \cdots & \vdots \\ 1 & n-(s-1) & n-(s-1) & \cdots & (n-(p-1))(n-(p-2))\cdots\cdots(n-(2s-3)) \\ 1 & n-s & (n-s)(n-(s+1)) & \cdots & (n-p)(n-(p+1))(n-(p+2)\cdots\cdots(n-(2s-2)) \end{bmatrix} \begin{bmatrix} x^{n-1}(0) \\ x^{n-2}(0) \\ x^{n-3}(0) \\ \vdots \\ x^{n-(s-1)}(0) \\ x^{n-s}(0) \end{bmatrix} = \begin{bmatrix} (n-1)!A_1 \\ (n-2)!A_2 \\ (n-3)!A_3 \\ \vdots \\ (n-(s-1))!A_{s-1} \\ (n-s)!A_s \end{bmatrix} \quad (2.17)$$

where $A_s = x^{s-1}(1) - \left(\sum_{s-1}^{\frac{n}{2}-1} \frac{x^m(0)}{m!}\right) - \sum_{i=1}^{2p} a_i B_{n+1-s,i}$, $s = \begin{cases} \frac{n}{2}, & if\ n\ is\ even \\ \frac{n-1}{2}, & if\ n\ is\ odd \end{cases}$

by solving the above system, we get the values of $x^{n-1}(0), x^{n-2}(0), x^{n-3}(0), \cdots,$

$x^{n-(s-1)}(0), x^{n-s}(0)$ in terms of a_i, $B_{n+1-s,i}$.

Step 4: Substitute the value of $x(t)$ and its derivatives $x'(t), x''(t), x'''(t) \cdots x^m(t)$ as obtained in the Step1 and Step 2 in the linear differential equation (2.14)

Step 5: Find the grid points for the curve or surface using $\bar{t_l} = \frac{l}{2p}$, where $l = 0,1,2, \ldots 2p$, $p = 2^j, j = 0,1,2, \ldots$ then the Collocation points are calculated by using the expression in Equation (2.18)

$$t_l = \frac{\overline{t_{l-1}} + \bar{t_l}}{2} \quad l = 0,1,2, \ldots, 2p \quad (2.18)$$

Step 6: Discretize the equations obtained in step 4 by using the collocation points Given in Equation (2.18) and the initial conditions obtained in step 3. Then we can easily put the result into the matrix form.

Step 7: Solve this system obtained in step 6 for the values of wavelet coefficients $a_i's$. Substitute these coefficients in the equation obtained for $x(t)$ and obtain the Haar wavelet collocation method-based solution of given differential equation.

Case 2: For Nonlinear higher-order boundary value problems

$$x^n(t) = f(t, x, x', x'', \cdots, x^{n-1}), \qquad a \le t \le b \quad (2.19)$$

with the constraints on the solution at the boundary points given in Equations (2.6)-(2.7)

Step1: Apply Quasilinearization technique [111], [112]on nonlinear HOBVPs to obtain the sequence of Linear HOBVPs by using the following recurrence relation

$$x_{r+1}^{n}(t) = f(t, x_r(t), x_r'(t), x_r''(t), \cdots, x_r^{n-1}(t)) + \sum_{u=0}^{n-1} (x_{r+1}^{u} - x_r^{u}) f_{x^u}(t, x_r(t), x_r'(t), x_r''(t), \cdots, x_r^{n-1}(t)) \quad (2.20)$$

$x_r(t)$ is the initial guess for the approximated solution which is used to find the next refined approximated solution $x_{r+1}(t)$ and the constraints on the solution at the boundary points are now transformed as

$x_{r+1}(a) = \nu_1,\ x_{r+1}(b) = \sigma_1,\ x_{r+1}'(a) = \nu_2,\ x_{r+1}'(b) = \sigma_2,\ \cdots, x_{r+1}^{\left(\frac{n}{2}-1\right)}(b) = \nu_{\frac{n}{2}}$,

$x_{r+1}^{\left(\frac{n}{2}-1\right)}(b) = \sigma_{\frac{n}{2}}$, if n is even

$x_{r+1}(a) = \gamma_1,\ x_{r+1}(b) = \delta_1,\ x_{r+1}'(a) = \gamma_2,\ \ldots,\ x_{r+1}^{\left(\frac{n-1}{2}-1\right)}(b) = \delta_{\frac{n-1}{2}}, x_{r+1}^{\left(\frac{n-1}{2}\right)}(a) = \gamma_{\frac{n+1}{2}}$, if n is an odd integer

$\nu_1, \nu_2 \cdots \nu_{\frac{n}{2}}, \sigma_1, \sigma_2, \cdots, \sigma_{\frac{n}{2}}, \gamma_1, \gamma_2, \ldots \ldots, \gamma_{\frac{n+1}{2}}, \delta_1, \delta_2, \cdots \cdots, \delta_{\frac{n-1}{2}}$ are the real constants.

Step 2: After applying Step 1 of Case 2 for nonlinear HOBVPs, apply all the steps given under case 1 for linear HOBVPs from Step 1 to Step 7.

2.5 Convergence Analysis

It has been proved by the Babolian and Shahsavaran [113] if $x(t)$is any differentiable function such that $|x'(t)| \leq M\ \forall\ t \in (0,1)$ for some positive real constant M and x(t) is approximated by haar wavelet family as given in Equation (2.21)

$$x_{2p}(t) = \sum_{i=0}^{2p} a_i h_i(t) \quad (2.21)$$

Then the error bound calculated for Haar wavelet approximation of function $x(t)$ by L_2-norm is given by Equation (2.22)

$$\left\|x(t) - x_{2p}(t)\right\|^2 \leq \frac{M^2}{12p^2} \quad \Rightarrow \quad \left\|x(t) - x_{2p}(t)\right\| = O\left(\frac{1}{p}\right) \quad (2.22)$$

which means if we know the exact value of M then we can get the exact error bound for the approximation. Also, with the increase in the level of resolution (the value of j or p=2^j) error decreased which proves the convergence for approximate solutions to the exact solution. This same is shown in the Numerical Experiments performed below.

2.6 Numerical Experiments and Error Analysis

To describe the applicability and effectiveness of the proposed mechanism, some Numerical Experiments on "eighth and ninth order linear and nonlinear boundary value problems" have been performed with the given mechanism as the given below. L_2 ,L_∞ and absolute errors are calculated to check the efficiency of the proposed method.L_2 ,L_∞ and absolute errors are defined as

$$\text{Absolute error} = |u_{exact}(t_l) - u_{num}(t_l)| \tag{2.23}$$

$$L_\infty = \max_l |u_{exact}(t_l) - u_{num}(t)| \tag{2.24}$$

$$L_2 = \frac{\sqrt{\sum_{l=1}^{2p} |u_{exact}(t_l) - u_{num}(t)|^2}}{\sqrt{\sum_{l=1}^{2p} |u_{exact}(t_l)|^2}} \tag{2.25}$$

Numerical Experiment No. 2.1: - Eighth order linear differential equation is considered for the numerical solution as given in Equation (2.26)

$$\frac{d^8x(t)}{dt^8} - x(t) = -8e^t \quad , \quad 0 \le t \le 1 \tag{2.26}$$

with the following types of constraints on the solution as given in Equation (2.27)

$$x(0) = 1, x'(0) = 0, x''(0) = -1, x'''(0) = -2, x(1) = 0, x'(1) = -e\,, \quad x''(1) = -2e\,, x'''(1) = -3e \tag{2.27}$$

Exact solution of numerical experiment no. 2.1 is given in the literature as

$$x(t) = (1-t)e^t.$$

By applying the mechanism of solution explained above for the linear differential equation, we get the HWCM solution for numerical experiment no. 2.1. Table 2.1 and Figure 2.1 shows the comparison between the exact and HWCM solution for j=2 which explains the high accuracy obtained by HWCM for a small number of grid points (in this case only 8 Grid pts). L_2 and L_∞ errors at j=2 are 7.08E-10, 9.45E-10 respectively. It has been observed from the Table 2.2 and Figure 2.2 that with the increase in the level of resolution j, the errors between the exact solution and HWCM solution decreases which ensures the convergence of HWCM solution to exact solution. The performance of HWCM is compared with the other method in Table 2.3 and it has been found that HWCM is working better than the other methods [96], [97]

Table 2.1: Exact and Approximated solution by HWCM for j=2 for Numerical Experiment No. 2.1

$x(t)$	Exact Solution	Solution by HWCM
0.0625	0.997963555235493	0.997963555232622
0.1875	0.980062077654547	0.980062077521416
0.3125	0.939701084556985	0.939701084023347
0.4375	0.871217042981700	0.871217042050077
0.5625	0.767836412420131	0.767836411475210
0.6875	0.621480459244466	0.621480458687880
0.8125	0.422537772602477	0.422537772459936
0.9375	0.159599341128933	0.159599341125753

Table 2.2: L_2 and L_∞ errors at different level of resolution for Numerical Experiment No. 2.1

Level of Resolution (j)	p=2^j	Number of Grid Points(2p)	L_2-error	L_∞-error
0	1	2	1.33E-08	1.36E-08
1	2	4	2.79E-09	3.06E-09
2	4	8	7.08E-10	9.45E-10
3	8	16	1.77E-10	2.47E-10
4	16	32	4.43E-11	6.25E-11
5	32	64	1.11E-11	1.56E-11
6	64	128	2.77E-12	3.91E-12
7	128	256	6.93E-13	9.78E-13
8	256	512	1.73E-13	2.45E-13

Table 2.3: Comparision of absolute errors obtained by different methods in Numerical Experiment No. 2.1

x(t)	Exact Solution	HWCM Solution	HWCM(E^*)	VIDM(E^*) [96]	OHAM(E^*) [97]
0.1	0.994653826268083	0.994653826297070	2.90E-11	6.71E-06	2.55E-09
0.2	0.977122206528136	0.977122206759530	2.31E-10	1.27E-07	2.84E-09
0.3	0.944901165303202	0.944901165717264	4.14E-10	1.75E-07	3.12E-09
0.4	0.895094818584762	0.895094818707398	1.23E-10	2.06E-07	3.40E-09
0.5	0.824360635350064	0.824360634815975	5.34E-10	2.18E-07	3.67E-09
0.6	0.728847520156204	0.728847519355493	8.01E-10	2.08E-07	3.94E-09
0.7	0.604125812241143	0.604125811877154	3.64E-10	1.78E-07	4.20E-09
0.8	0.445108185698494	0.445108185798495	1.00E-10	1.29E-07	4.45E--09

E^* (Absolute Error) =Exact Solution-Approximate Solution

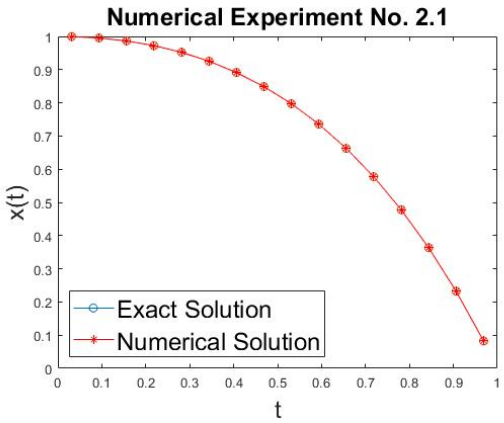

Figure 2.1: Exact and Numerical solution of eighth order linear BVP in Numerical Experiment No. 2.1

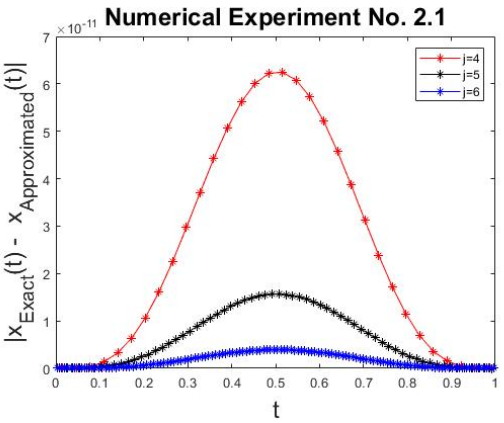

Figure 2.2: Absolute Error at different level of resolution in Numerical Experiment No. 2.1

Numerical Experiment No. 2.2: - Eighth order linear differential equation is considered for the numerical solution as given in Equation (2.28)

$$\frac{d^8x(t)}{dt^8}+\frac{d^7x(t)}{dt^7}+\frac{d^6x(t)}{dt^6}+\frac{d^5x(t)}{dt^5}+\frac{d^4x(t)}{dt^4}+\frac{d^3x(t)}{dt^3}+\frac{d^2x(t)}{dt^2}+\frac{dx(t)}{dt}+x(t)=14\cos t-16\sin t-4tsint\ ,0\le t\le 1 \tag{2.28}$$

with the constraints on the solution at the boundary points as given in Equation (2.29)

$$x(0)=0,x'(0)=-1,x''(0)=0,x'''(0)=7,x(1)=0,x'(1)=2sin1$$
$$x''(1)=4\cos 1+2\sin 1,x'''(1)=6\cos 1-6\sin 1 \tag{2.29}$$

Exact solution of numerical experiment no. 2.2 is given in the literature as

$$x(t)=(t^2-1)\sin t\ .$$

By applying the mechanism of solution explained above for linear differential equation we get the HWCM solution for numerical experiment no. 2.2. Table 2.4 and Figure 2.3 shows the comparison between the exact and HWCM solution for j=2 which explains the high accuracy obtained by HWCM for a small number of grid points (in this case only 8 Grid pts). L_2 and L_∞ errors at j=2 are 1.47E-08, 6.60E-09 respectively. Table 2.5 and Figure 2.4 ensures the convergence of the HWCM solution to the exact solution. The performance of HWCM is compared with the other method in Table 2.6 and it has been found that HWCM is working better than the other methods [99], [114].

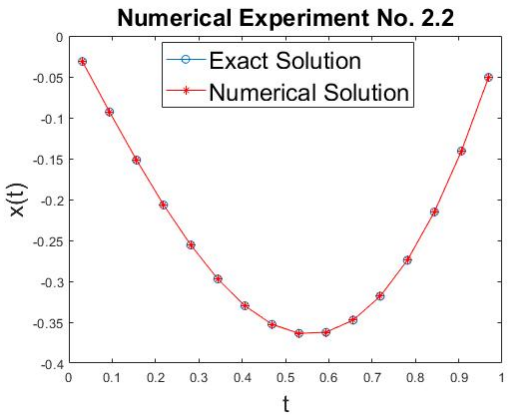

Figure 2.3: Exact and Numerical solution of of eighth order linear BVP given in Numerical Experiment No. 2.2

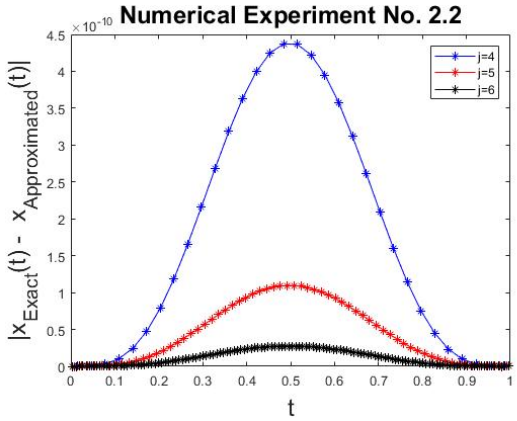

Figure 2.4: Absolute Error at different level of resolution in Numerical Experiment No. 2.2

Table 2.4: Exact and Approximated solution by HWCM for j=2 for Numerical Experiment No. 2.2

$x(t)$	Exact Solution	Approximated Solution by HWCM
0.0625	-0.0622153361320580	-0.0622153361104450
0.1875	-0.1798500558604710	-0.1798500548792540
0.3125	-0.2774152221408910	-0.2774152182804620
0.4375	-0.3425819735984970	-0.3425819669995290
0.5625	-0.3645623744875140	-0.3645623679434340
0.6875	-0.3346560773518020	-0.3346560735861070
0.8125	-0.2467295039362580	-0.2467295029938770
0.9375	-0.0976113842034430	-0.0976113841830550

Table 2.5: L_2 and L_∞ errors at different level of resolution for Numerical Experiment No. 2.2

Level of Resolution (j)	$p=2^j$	Number of Grid Points	L_2-error	L_∞-error
0	1	2	2.00E-07	6.89E-08
1	2	4	5.79E-08	2.14E-08
2	4	8	1.47E-08	6.60E-09
3	8	16	3.67E-09	1.73E-09
4	16	32	9.19E-10	4.37E-10
5	32	64	2.30E-10	1.10E-10
6	64	128	5.74E-11	2.74E-11
7	128	256	1.44E-11	6.85E-12
8	256	512	1.08E-14	2.60E-14

Table 2.6: Comparision of Numerical results in terms of Absolute error obtained by different methods

x(t)	Exact Solution	HWCM Solution	HWCM (E^*)	GMQBS(E^*) [114]	LGM(E^*) [99]
0.1	-0.098835082480360	-0.098835081782372	6.98E-10	3.80E-07	5.04E-08
0.2	-0.190722557563259	-0.190722550744819	6.82E-09	2.15E-06	5.14E-07
0.3	-0.268923388061819	-0.268923368938548	1.91E-08	5.63E-06	1.56E-10
0.4	-0.327111407539266	-0.327111377683842	2.99E-08	9.75E-06	2.71E-06
0.5	-0.359569153953152	-0.359569122469850	3.15E-08	1.14E-05	3.26E-06
0.6	-0.361371182972823	-0.361371158840556	2.41E-08	1.01E-05	2.82E-06
0.7	-0.328551020491222	-0.328551006968581	1.35E-08	7.27E-06	1.68E-06
0.8	-0.258248192723828	-0.258248187818473	4.91E-09	3.87E-06	5.78E-07

E^* (Absolute Error) = Exact Solution-Approximate Solution

Numerical Experiment No. 2.3: - For Eighth Order Non-linear differential equation as given in Equation (2.30)

$$\frac{d^8y(t)}{dt^8} = (y(t))^2e^{-t} \quad , 0 \le t \le 1 \tag{2.30}$$

with the following types of constraints on the solution as given in Equation (2.31)

$$x(0) = 1, x'(0) = 1, x''(0) = 1, x'''(0) = 1, x(1) = e\,, x'(1) = e\,, \\ x''(1) = e\,, x'''(1) = e \tag{2.31}$$

Exact solution of numerical experiment no. 2.3 is given in the literature as

$$x(t) = e^t.$$

By applying the mechanism of solution explained above for non-linear differential equations, we get the HWCM solution for a given numerical experiment no. 2.3. Table 2.7 and Figure 2.5 shows the comparison between the exact and HWCM solution for j=2 which explains the high accuracy obtained by HWCM for a small number of grid points (in this case only 8 Grid pts). L_2 and L_∞ errors at j=2 are 3.22E-11, 9.92E-11 respectively. Figure 2.6 and Table 2.8 ensure the convergence of the HWCM solution to the exact solution. The performance of HWCM is compared with the other methods in Table 2.9 and it has been found that HWCM is working better than the other methods [100], [101].

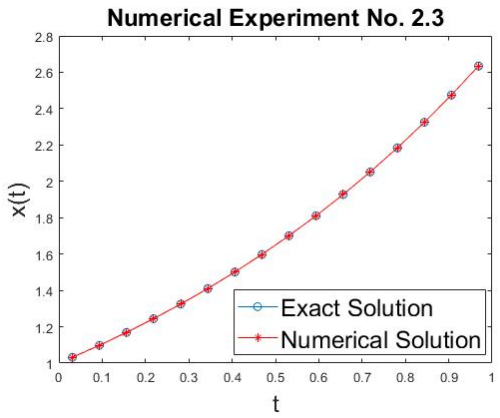

Figure 2.5: Exact and Numerical solution of eighth order Non-linear BVP given in Numerical Experiment No. 2.3

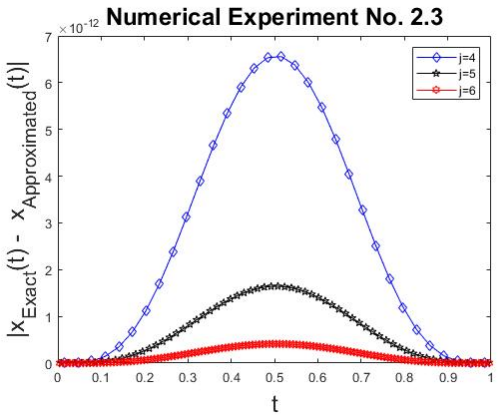

Figure 2.6: Absolute Error at a different level of resolution in Numerical Experiment No. 2.3

Table 2.7: Exact and Approximated solution by HWCM for j=2 for Numerical Experiment No. 2.3

$x(t)$	Exact Solution	Approximated Solution by HWCM
0.0625	1.064494458917860	1.064494458916330
0.1875	1.206230249420980	1.206230249344930
0.3125	1.366837941173790	1.366837940844480
0.4375	1.548830298634130	1.548830298011330
0.5625	1.755054656960290	1.755054656273750
0.6875	1.988737469582290	1.988737469141240
0.8125	2.253534787213200	2.253534787089520
0.9375	2.553589458062920	2.553589458059910

Table 2.8: L_2 and L_∞ errors at different level of resolution for Numerical Experiment No. 2.3

Level of Resolution (j)	p=2^j	Number of Grid Points(2p)	L_2-error	L_∞-error
0	1	2	6.31E-10	1.48E-09
1	2	4	1.27E-10	3.20E-10
2	4	8	3.22E-11	9.92E-11
3	8	16	8.05E-12	2.60E-11
4	16	32	2.01E-12	6.56E-12
5	32	64	5.03E-13	1.64E-12
6	64	128	1.26E-13	4.11E-13
7	128	256	3.15E-14	1.03E-13
8	256	512	1.73E-13	2.45E-13

Table 2.9: Comparision of Numerical results in terms of Absolute error obtained by different methods

x(t)	Exact Solution	HWCM Solution	HWCM(E^*)	Reproducing Kernel(E^*) [100]	VIT(E^*) [101]
0.1	1.105170918075640	1.105170918071520	4.13E-12	1.61E-08	1.91E-07
0.2	1.221402758160170	1.221402758125510	3.47E-11	3.07E-08	1.25E-07
0.3	1.349858807576000	1.349858807504780	7.12E-11	4.227E-08	7.25E-08
0.4	1.491824697641270	1.491824697588310	5.30E-11	4.972E-08	4.85E-08
0.5	1.648721270700120	1.648721270718270	1.81E-11	5.231E-08	2.91E-07
0.6	1.822118800390500	1.822118800448210	5.77E-11	4.978E-08	7.80E-08
0.7	2.013752707470470	2.013752707493520	2.30E-11	4.237E-08	1.11E-07
0.8	2.225540928492460	2.225540928475000	1.75E-11	3.08E-08	1.71E-07

E^* (Absolute Error) =Exact Solution-Approximate Solution

Numerical Experiment No. 2.4: - Ninth order linear differential equation is considered for the numerical solution as given in Equation (2.32)

$$\frac{d^9x(t)}{dt^9} = x(t) - 9e^t, \qquad 0 \le t \le 1 \tag{2.32}$$

with the following types of constraints on the solution as given in Equation (2.32)

$$x(0) = 1, x'(0) = 0, x''(0) = -1, x'''(0) = -2, x^{iv}(0) = -3, x(1) = 0, x'(1) = -e \ , x''(1) = -2e \ , x'''(1) = -3e \tag{2.33}$$

Exact solution of numerical experiment no. 2.4 as given in the literature is

$$x(t) = (1-t)e^t$$

By applying the mechanism of solution explained above for linear differential equation we get the HWCM solution for numerical experiment no. 2.4. Table 2.10 and Figure 2.7 shows the comparison between the exact and HWCM solution for j=2 which explains the high accuracy obtained by HWCM for a small number of grid points (in this case only 8 Grid pts). $L_2$and L_∞ errors at j=2 are 4.26E-11, 6.20E-11 respectively. Figure 2.8 and Table 2.11 ensure the convergence of HWCM solution to the exact solution. The performance of HWCM is compared with the other methods in Table 2.12 and it has been found that HWCM is working better than the other methods [102], [103].

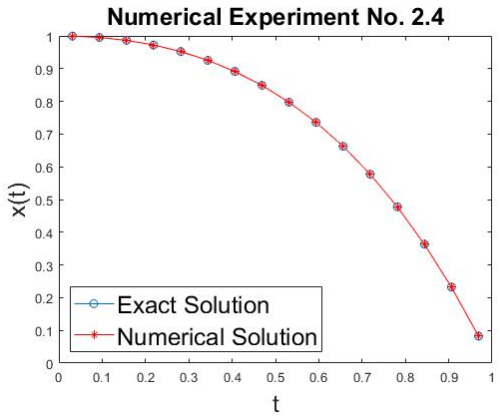

Figure 2.7: Exact and Numerical solution of ninth order linear BVP given in Numerical Experiment No. 2.4

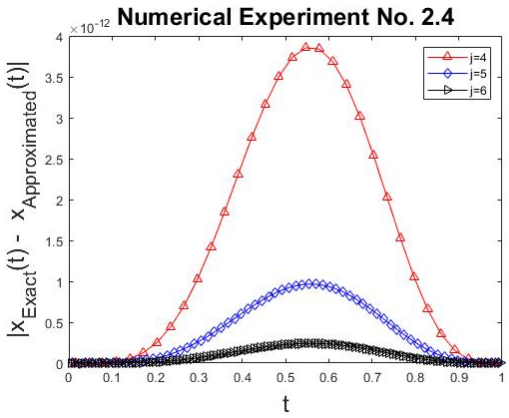

Figure 2.8: Absolute Error at different level of resolution in Numerical Experiment No. 2.4

Table 2.10: Exact and Approximated solution by HWCM for j=2 for Numerical Experiment No. 2.4

$x(t)$	Exact Solution	Approximated Solution by HWCM
0.0625	0.997963555235493	0.997963199230146
0.1875	0.980062077654547	0.980005763297981
0.3125	0.939701084556985	0.939262340817424
0.4375	0.871217042981700	0.869924631962752
0.5625	0.767836412420131	0.765699977494341
0.6875	0.621480459244466	0.619356938393400
0.8125	0.422537772602477	0.421480313163833
0.9375	0.159599341128933	0.159519239821921

Table 2.11: L_2 and L_∞ errors at different level of resolution for Numerical Experiment No. 2.4

Level of Resolution (j)	p=2^j	Number of Grid Points	L_2-error	L_∞-error
0	1	2	5.32E-10	5.82E-10
1	2	4	1.73E-10	2.29E-10
2	4	8	4.26E-11	6.20E-11
3	8	16	1.06E-11	1.53E-11
4	16	32	2.65E-12	3.86E-12
5	32	64	6.64E-13	9.66E-13
6	64	128	1.66E-13	2.41E-13
7	128	256	4.15E-14	6.04E-14
8	256	512	1.03E-14	1.52E-14

Table 2.12: Comparision of Numerical results in terms of Absolute error obtained by different methods

x(t)	Exact Solution	HWCM Solution	HWCM(E^*)	MVIM(E^*) [102]	SBSCM(E^*) [103]
0.1	0.9946538262680830	0.9946538262688390	7.56E-13	2.00E-10	1.08E-06
0.2	0.9771222065281360	0.9771222065427060	1.46E-10	2.00E-10	5.19E-06
0.3	0.9449011653032020	0.9449011653609080	5.77E-10	2.00E-10	6.13E-06
0.4	0.8950948185847620	0.8950948186884760	1.04E-10	2.00E-10	1.23E-05
0.5	0.8243606353500640	0.8243606354476210	9.76E-11	2.00E-10	1.07E-05
0.6	0.7288475201562040	0.7288475201913140	3.51E-11	6.00E-10	4.91E-06
0.7	0.6041258122411430	0.6041258122230930	1.80E-11	1.00E-09	9.95E-06
0.8	0.4451081856984940	0.4451081856796940	1.88E-11	2.00E-09	1.65E-06

E^* (Absolute Error) =Exact Solution-Approximate Solution

Numerical Experiment No. 2.5 : - For Ninth order non- linear differential equation as given in Equation (2.34)

$$\frac{d^9x(t)}{dt^9} - \left(x(t)\right)^2 \frac{dx(t)}{dt} = cos^3 t \ , \ \ 0 \leq t \leq 1 \tag{2.34}$$

with the following types of constraints on the solution as given in Equation (2.35)

$$x(0) = 0, x'(0) = 1, x''(0) = 0, x'''(0) = -1, x'^{v}(0) = 0, x(1) = \sin 1 \ , x'(1) = \cos 1 \, , x''(1) = -\sin 1 \ , x'''(1) = -\cos 1 \tag{2.35}$$

Exact solution of numerical experiment no. 2.5 is given in the literature as

$$x(t) = \sin t.$$

By applying the mechanism of solution explained above for the non-linear differential equation we get the HWCM solution for numerical experiment no. 2.5. Table 2.13 and Figure 2.9 shows the comparison between the exact and HWCM solution for j=2 which explains the high accuracy obtained by HWCM for a small number of grid points (in this case only 8 Grid pts). L_2 and L_∞ errors at j=2 are 3.37E-11, 9.99E-11 respectively. Figure 2.10 and Table 2.14 ensure the convergence of HWCM solution to the exact solution. The performance of HWCM is compared with the other methods in Table 2.15 and it has been found that HWCM is working better than the other methods [103], [104].

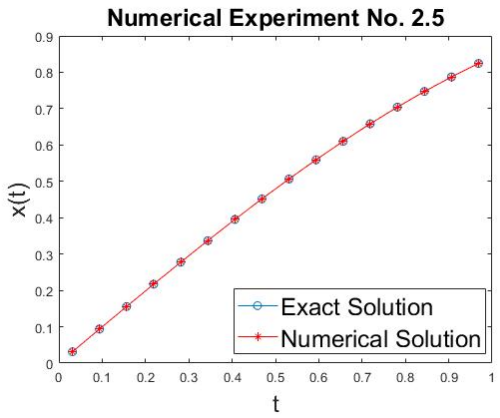

Figure 2.9: Exact and Numerical solution of ninth order Non-linear BVP given in Numerical Experiment.No. 2.5

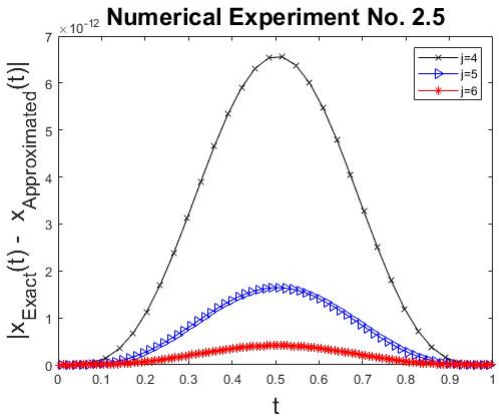

Figure 2.10: Absolute Error at different level of resolution in Numerical Experiment.No. 2.5

Table 2.13: Exact and Approximated solution by HWCM for j=2 for Numerical Experiment No 2.5

$x(t)$	Exact Solution	Approximated Solution by HWCM
0.0625	0.0624593178423800	0.0624593178422206
0.1875	0.1864032967622700	0.1864032967589660
0.3125	0.3074385145803810	0.3074385145651280
0.4375	0.4236762572039380	0.4236762571679480
0.5625	0.5333026735360200	0.5333026734810870
0.6875	0.6346070800152690	0.6346070799572420
0.8125	0.7260086552607130	0.7260086552196350
0.9375	0.8060811082606930	0.8060811082443460

Table 2.14: L_2 and L_∞ errors at different level of resolution for Numerical Experiment No. 2.5

Level of Resolution (j)	p=2^j	Number of Grid Points	L_2-error	L_∞-error
0	1	2	6.41E-10	1.68E-09
1	2	4	1.47E-10	3.40E-10
2	4	8	3.37E-11	9.99E-11
3	8	16	8.25E-12	2.85E-11
4	16	32	2.01E-12	6.56E-12
5	32	64	5.03E-13	1.64E-12
6	64	128	1.26E-13	4.11E-13
7	128	256	3.25E-14	1.23E-13
8	256	512	1.93E-13	2.60E-13

Table 2.15: Comparision of Absolute error obtained by different methods

x(t)	Exact Solution	HWCM Solution	HWCM(E^*)	PGM(E^*) [104]	SBSCM(E^*)[103]
0.1	0.099833416646828	0.099833416646669	1.59E-13	1.86E-07	2.85E-06
0.2	0.198669330795061	0.198669330791757	3.30E-12	7.30E-07	1.35E-06
0.3	0.295520206661340	0.295520206646087	1.53E-11	9.83E-07	4.09E-06
0.4	0.389418342308651	0.389418342272661	3.60E-11	1.22E-06	1.05E-06
0.5	0.479425538604203	0.479425538549270	5.49E-11	8.34E-07	3.45E-05
0.6	0.564642473395035	0.564642473337008	5.80E-11	3.87E-06	3.46E-05
0.7	0.644217687237691	0.644217687196613	4.11E-11	5.66E-06	2.09E-05
0.8	0.717356090899523	0.717356090883176	1.63E-11	4.89E-06	2.01E-05

E^* (Absolute Error) =Exact Solution-Approximate Solution

2.7 Conclusion

We have applied the Haar Wavelet Collocation Method (HWCM) to find the numerical solution of linear and nonlinear HOBVPs.Some numerical experiments are performed by considering the linear and nonlinear HOBVPs.L_2 ,L_∞ and absolute errors are calculated for each numerical experiments. It has been observed that as we increase the level of resolution L_2 ,L_∞ , absolute errors decreases which prove the convergence of HWCM solution to the exact solution. High level of accuracy obtained by the proposed method for few grid points (In Numerical Experiment No.5 for two grid points, level of accuracy obtained is of 10^{-10}) proves the reliability of this mechanism. The proposed method is equally effective for both linear and nonlinear HOBVPs. The accurateness of the solution is up to the level of 10^{-14} and can be increased by increasing the level of resolution. The performance of HWCM is compared with the other methods like Variational Iteration Decomposition Method (VIDM) [96], Optimal Homotopy Asymptotic Method (OHAM) [97], Galerkin Method with Quintic B-splines (GMQBS) [98], Legendre Galerkin Method (LGM) [99], Reproducing Kernel Space Method (RKSM) [100], Variational Iteration Method (VIM) [101], Modified Variational Iteration Method (MVID) [102], Sextic B-splines Collocation Method (SBSCM) [103], Petrov-Galerkin Method (PGM)[104] and it is found that HWCM is working better than these methods . The rapid convergence and high accuracy obtained from the proposed method provides a strong base to extend the application of HWCM to solve a big class of physical problems governed by ODEs, PDEs, and Integral equations. Computational work is fully supportive and compatible with the proposed algorithm.

Chapter 3

Haar Scale 3 Wavelets and Related Integral

3.1 Haar Scale 3 Wavelets Family

Let us Consider any two arbitrary integers $\mathcal{A}, \mathcal{B}$ such that $\mathcal{B} > \mathcal{A}$. let J be the maximum level of resolution to be considered for phenomena under study. Define new quantities $M, j, k.p$ such that $M = 3^J$, $p = 3^j$, $j = 0,1,2, \dots J$, $k = 0,1,2, \dots, p-1$, where j denotes the level of resolution and k the translation in wavelets. Now divide the interval $[\mathcal{A}, \mathcal{B})$ into $3M$ uniform subinterval of equal length $\Delta t = \frac{\mathcal{B}-\mathcal{A}}{3M}$. When J=0, $\mathcal{A} = 0$ and $\mathcal{B} = 1$ then we have the following members in Haar Scale 3 wavelet family [115] represented by the Equations (3.1)-(3.3)

$$h_1(t) = \psi^0(t) = \begin{cases} 1 & 0 \le t < 1 \\ 0 & elsewhere \end{cases} \quad (3.1)$$

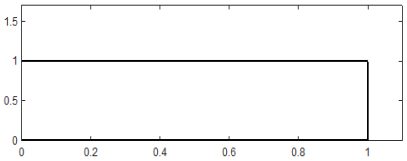

Figure 3.1: Haar scale 3 Function

$$h_2(t) = \psi^1(t) = \frac{1}{\sqrt{2}} \begin{cases} -1 & 0 \le t < \frac{1}{3} \\ 2 & \frac{1}{3} \le t < \frac{2}{3} \\ -1 & \frac{2}{3} \le t < 1 \\ 0 & elsewhere \end{cases} \quad (3.2)$$

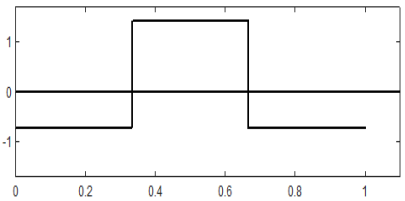

Figure 3.2: Haar wavelet $\boldsymbol{\psi^1(t)}$ with dilation 3

$$h_3(t) = \psi^2(t) = \sqrt{\frac{3}{2}} \begin{cases} 1 & 0 \le t < \frac{1}{3} \\ 0 & \frac{1}{3} \le t < \frac{2}{3} \\ -1 & \frac{2}{3} \le t < 1 \\ 0 & elsewhere \end{cases} \quad (3.3)$$

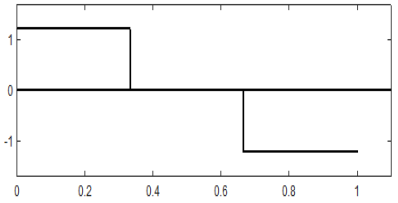

Figure 3.3: Haar wavelet $\boldsymbol{\psi^2(t)}$ with dilation 3

where the function $h_1(t)$ is called father wavelet, $h_2(t)$, $h_3(t)$ are called mother wavelets.

3.1.1 Construction of Orthonormal Function Spaces [10]

Consider $t \in [0,1)$,then we get

$$\int_{-\infty}^{\infty} \psi^0(t)\psi^0(t)dt = \int_0^1 1.1\, dt = 1 \tag{3.4}$$

$$\int_{-\infty}^{\infty} \psi^0(t)\psi^0(t-1)dt = \int_0^1 1.0\, dt + \int_1^2 0.1\, dt = 0 + 0 = 0 \tag{3.5}$$

It follows from Equations (3.4)-(3.5) and the geometric structure of Haar function that translations of Haar functions are orthonormal but the scaled translations are only orthogonal, not orthonormal (Equation (3.6)-(3.7)) $i.e$

$$\int_{-\infty}^{\infty} \psi^0(t-k_1)\psi^0(t-k_2)dt = \delta_{m-n} = \begin{cases} 1 & k_1 = k_2 \\ 0 & k_1 \neq k_2 \end{cases}. \tag{3.6}$$

$$\int_{-\infty}^{\infty} \psi^0(3^j t-k_1)\psi^0(3^j t-k_2)dt = \begin{cases} \frac{1}{3^j} & k_1 = k_2 \\ 0 & k_1 \neq k_2 \end{cases} \tag{3.7}$$

where $\psi^0(3^j t-k) = \begin{cases} 1 & \frac{k}{3^j} \leq t < \frac{k+1}{3^j} \\ 0 & elsewhere \end{cases}$ for any integer j and k

But the orthogonal scaled translations can be normalized using the way given in Equation (3.8)

$$\int_{-\infty}^{\infty} \left(3^{\frac{j}{2}}\psi^0(3^j t-k_1)\right)\left(3^{\frac{j}{2}}\psi^0(3^j t-k_2)\right)dt = \begin{cases} 1 & k_1 = k_2 \\ 0 & k_1 \neq k_2 \end{cases} \tag{3.8}$$

Let V_0 be space spanned by the set $\{\psi^0(t), \psi^0(t-1), \psi^0(t-2) \dots,\}$ which will act as a bases for V_0 .Therefore

$$V_0 = span\{\psi^0(t-k): k\epsilon\mathbb{Z}\} \tag{3.9}$$

Let V_1 be space spanned by the set $\{\sqrt{3}\,\psi^0(3t), \sqrt{3}\,\psi^0(3t-1),\ \sqrt{3}\,\psi^0(3t-2), \dots,\}$ which will act as a bases for V_1 and we denote it as

$$V_1 = span\left\{3^{\frac{1}{2}}\psi^0(3t-k): k\epsilon\mathbb{Z}\right\} \tag{3.10}$$

Similarly

$$V_2 = span\left\{3^{\frac{2}{2}}\psi^0(3^2t-k): k\epsilon\mathbb{Z}\right\} \tag{3.11}$$

$$V_3 = span\left\{3^{\frac{3}{2}}\psi^0(3^3t-k): k\epsilon\mathbb{Z}\right\} \tag{3.12}$$

$$\vdots$$

$$\vdots$$

$$\vdots$$

$$V_j = span\left\{3^{\frac{j}{2}}\psi^0\left(3^jt-k\right): k\epsilon\mathbb{Z}\right\} = \psi^0_{j,k}(\mathrm{t}) \tag{3.13}$$

It is always possible to write the bases of V_0 (Equation (3.9)) itself as a linear combination of bases of V_1(Equation (3.10))

$$\psi^0(t) = \frac{1}{\sqrt{3}}\left(\sqrt{3}\,\psi^0(3t) + \sqrt{3}\,\psi^0(3t-1) + \sqrt{3}\,\psi^0(3t-2)\right) \tag{3.14}$$

$$\psi^0(t-1) = \frac{1}{\sqrt{3}}\left(\sqrt{3}\,\psi^0(3t-3) + \sqrt{3}\,\psi^0(3t-4) + \sqrt{3}\,\psi^0(3t-5)\right) \tag{3.15}$$

$$\psi^0(t-2) = \frac{1}{\sqrt{3}}\left(\sqrt{3}\,\psi^0(3t-6) + \sqrt{3}\,\psi^0(3t-7) + \sqrt{3}\,\psi^0(3t-8)\right) \tag{3.16}$$

Also, the bases of V_1 (Equation (3.10)) itself as a linear combination of bases of V_2 (Equation(3.11))

$$\sqrt{3}\,\psi^0(3t) = \frac{1}{\sqrt{3}}\left(3\psi^0(9t) + 3\psi^0(9t-1) + 3\psi^0(9t-2)\right) \tag{3.17}$$

$$\sqrt{3}\,\psi^0(3t-1) = \frac{1}{\sqrt{3}}\left(3\psi^0(9t-3) + 3\psi^0(9t-4) + 3\psi^0(9t-5)\right) \tag{3.18}$$

$$\sqrt{3}\,\psi^0(3t-2) = \frac{1}{\sqrt{3}}\left(3\psi^0(9t-6) + 3\psi^0(9t-7) + 3\psi^0(9t-8)\right) \tag{3.19}$$

and so, on

Therefore, we can write

$$\ldots V_{-1} \subset V_0 \subset V_1 \subset V_2 \ldots \subset V_\infty \tag{3.20}$$

Where

$$\psi^0(3^j t-k)=\begin{cases}1 & \frac{k}{3^j}\le t<\frac{k+1}{3^j}\\ 0 & elsewhere\end{cases} \tag{3.21}$$

Now we will test the orthonormality of mother wavelets $\psi^1(t)$, $\psi^2(t)$ represented by the Equation (3.22)

$$\psi^1(t)=\frac{1}{\sqrt{2}}\begin{cases}-1 & t\in\left[0,\frac{1}{3}\right)\\ 2 & t\in\left[\frac{1}{3},\frac{2}{3}\right)\\ -1 & t\in\left[\frac{2}{3},1\right)\\ 0 & elsewhere\end{cases},\quad \psi^2(t)=\sqrt{\frac{3}{2}}\begin{cases}1 & t\in\left[0,\frac{1}{3}\right)\\ 0 & t\in\left[\frac{1}{3},\frac{2}{3}\right)\\ -1 & t\in\left[\frac{2}{3},1\right)\\ 0 & elsewhere\end{cases} \tag{3.22}$$

Consider $t\in[0,1)$,then

$$\int_{-\infty}^{\infty}\psi^1(t)\psi^1(t)dt=$$

$$\int_0^{\frac{1}{3}}\left(\frac{-1}{\sqrt{2}}\right)\left(\frac{-1}{\sqrt{2}}\right)dt+\int_{\frac{1}{3}}^{\frac{2}{3}}\left(\frac{2}{\sqrt{2}}\right)\left(\frac{2}{\sqrt{2}}\right)dt+\int_{\frac{2}{3}}^{1}\left(\frac{-1}{\sqrt{2}}\right)\left(\frac{-1}{\sqrt{2}}\right)dt \tag{3.23}$$

$$=\frac{1}{3}\left(\frac{1}{2}+\frac{4}{2}+\frac{1}{2}\right)=1$$

$$\int_{-\infty}^{\infty}\psi^2(t)\psi^2(t)dt=$$

$$\int_0^{\frac{1}{3}}\left(\sqrt{\frac{3}{2}}\right)\left(\sqrt{\frac{3}{2}}\right)dt+\int_{\frac{1}{3}}^{\frac{2}{3}}(0)(0)\,dt+\int_{\frac{2}{3}}^{1}\left(-\sqrt{\frac{3}{2}}\right)\left(-\sqrt{\frac{3}{2}}\right)dt \tag{3.24}$$

$$=\frac{1}{3}\left(\frac{3}{2}+0+\frac{3}{2}\right)=1$$

$$\int_{-\infty}^{\infty}\psi^1(t)\psi^2(t)dt=$$

$$\int_0^{\frac{1}{3}}\left(\frac{-1}{\sqrt{2}}\right)\left(\sqrt{\frac{3}{2}}\right)dt+\int_{\frac{1}{3}}^{\frac{2}{3}}\left(\frac{2}{\sqrt{2}}\right)(0)\,dt+\int_{\frac{2}{3}}^{1}\left(\frac{-1}{\sqrt{2}}\right)\left(-\sqrt{\frac{3}{2}}\right)dt \tag{3.25}$$

$$=\frac{1}{3}\left(-\frac{\sqrt{3}}{2}+0+\frac{\sqrt{3}}{2}\right)=0$$

It follows from Equations (3.23)-(3.25) and the geometric structure of the wavelets that Set $\{\psi^1(t-k_1),\psi^2(t-k_2):k_1,k_2\epsilon\mathbb{Z}\}$ is orthonormal. Let W_0 be space spanned by the set of bases $\{\psi^1(t),\psi^2(t),\psi^1(t-1),\psi^2(t-2),\dots\}$.

$$\int_{-\infty}^{\infty}\psi^1(3t)\psi^1(3t)dt=$$

$$\int_0^{\frac{1}{9}}\left(\frac{-1}{\sqrt{2}}\right)\left(\frac{-1}{\sqrt{2}}\right)\,dt+\int_{\frac{1}{9}}^{\frac{2}{9}}\left(\frac{2}{\sqrt{2}}\right)\left(\frac{2}{\sqrt{2}}\right)\,dt+\int_{\frac{2}{9}}^{\frac{3}{9}}\left(\frac{-1}{\sqrt{2}}\right)\left(\frac{-1}{\sqrt{2}}\right)\,dt=\frac{1}{9}\left(\frac{1}{2}+\frac{4}{2}+\frac{1}{2}\right)=\frac{1}{3}$$

$$\Rightarrow \quad \int_{-\infty}^{\infty}\sqrt{3}\,\psi^1(3t)\,\sqrt{3}\,\psi^1(3t)dt=1 \tag{3.26}$$

$\int_{-\infty}^{\infty}\psi^2(3t)\psi^2(3t)dt=$

$$\int_0^{\frac{1}{9}}\left(\sqrt{\frac{3}{2}}\right)\left(\sqrt{\frac{3}{2}}\right)\,dt+\int_{\frac{1}{9}}^{\frac{2}{9}}(0)(0)\,dt+\int_{\frac{2}{9}}^{\frac{3}{9}}\left(-\sqrt{\frac{3}{2}}\right)\left(-\sqrt{\frac{3}{2}}\right)\,dt=\frac{1}{9}\left(\frac{3}{2}+0+\frac{3}{2}\right)=\frac{1}{3}$$

$$\Rightarrow \quad \int_{-\infty}^{\infty}\sqrt{3}\,\psi^2(3t)\,\sqrt{3}\,\psi^2(3t)dt=1 \tag{3.27}$$

$\int_{-\infty}^{\infty}\psi^1(3t)\psi^2(3t)dt=$

$$\int_0^{\frac{1}{9}}\left(\frac{-1}{\sqrt{2}}\right)\left(\sqrt{\frac{3}{2}}\right)\,dt+\int_{\frac{1}{9}}^{\frac{2}{9}}\left(\frac{2}{\sqrt{2}}\right)(0)\,dt+\int_{\frac{2}{9}}^{\frac{3}{9}}\left(\frac{-1}{\sqrt{2}}\right)\left(-\sqrt{\frac{3}{2}}\right)\,dt$$

$$=\frac{1}{9}\left(-\frac{\sqrt{3}}{2}+0+\frac{\sqrt{3}}{2}\right)=0$$

$$\Rightarrow \quad \int_{-\infty}^{\infty}\sqrt{3}\,\psi^1(3t)\,\sqrt{3}\,\psi^2(3t)dt=0 \tag{3.28}$$

From Equations (3.26)-(3.28) one can generalized that the Set $\{\sqrt{3}\,\psi^1(3t-k_1),\sqrt{3}\,\psi^2(3t-k_2):k_1\,,k_2\epsilon\mathbb{Z}\}$ is orthonormal. Let W_1 be space spanned by the set of bases $\{\sqrt{3}\,\psi^1(3t),\sqrt{3}\,\psi^2(3t),\sqrt{3}\,\psi^1(3t-1),\sqrt{3}\,\psi^2(3t-1),\dots\}$.

From the geometric properties, it has been verified that the linear combinations of the elements of W_1 are not able to create W_0. i.e W_0 is not a subset of W_1 .But

$\int_{-\infty}^{\infty}\psi^1(t)\psi^1(3t)dt=$

$$\int_0^{\frac{1}{9}}\left(\frac{-1}{\sqrt{2}}\right)\left(\frac{-1}{\sqrt{2}}\right)\,dt+\int_{\frac{1}{9}}^{\frac{2}{9}}\left(\frac{-1}{\sqrt{2}}\right)\left(\frac{2}{\sqrt{2}}\right)\,dt+\int_{\frac{2}{9}}^{\frac{3}{9}}\left(\frac{-1}{\sqrt{2}}\right)\left(\frac{-1}{\sqrt{2}}\right)\,dt \tag{3.29}$$

$$=\frac{1}{9}\left(\frac{1}{2}-\frac{2}{2}+\frac{1}{2}\right)=0$$

$$\int_{-\infty}^{\infty} \psi^2(t)\psi^2(3t)dt =$$

$$\int_0^{\frac{1}{9}} \left(\sqrt{\frac{3}{2}}\right)\left(\sqrt{\frac{3}{2}}\right) dt + \int_{\frac{1}{9}}^{\frac{2}{9}} \left(\sqrt{\frac{3}{2}}\right)(0)\, dt + \int_{\frac{2}{9}}^{\frac{3}{9}} \left(\sqrt{\frac{3}{2}}\right)\left(-\sqrt{\frac{3}{2}}\right) dt \tag{3.30}$$

$$= \frac{1}{9}\left(\frac{3}{2} + 0 - \frac{3}{2}\right) = 0$$

$$\int_{-\infty}^{\infty} \psi^1(t)\psi^2(3t)dt =$$

$$\int_0^{\frac{1}{9}} \left(\frac{-1}{\sqrt{2}}\right)\left(\sqrt{\frac{3}{2}}\right) dt + \int_{\frac{1}{9}}^{\frac{2}{9}} \left(\frac{-1}{\sqrt{2}}\right)(0)\, dt + \int_{\frac{2}{9}}^{\frac{3}{9}} \left(\frac{-1}{\sqrt{2}}\right)\left(-\sqrt{\frac{3}{2}}\right) dt \tag{3.31}$$

$$= \frac{1}{9}\left(-\frac{\sqrt{3}}{2} - 0 + \frac{\sqrt{3}}{2}\right) = 0$$

$$\int_{-\infty}^{\infty} \psi^2(t)\psi^1(3t)dt =$$

$$\int_0^{\frac{1}{9}} \left(\sqrt{\frac{3}{2}}\right)\left(\frac{-1}{\sqrt{2}}\right) dt + \int_{\frac{1}{9}}^{\frac{2}{9}} \left(\sqrt{\frac{3}{2}}\right)\left(\frac{2}{\sqrt{2}}\right) dt + \int_{\frac{2}{9}}^{\frac{3}{9}} \left(\sqrt{\frac{3}{2}}\right)\left(\frac{-1}{\sqrt{2}}\right) dt \tag{3.32}$$

$$= \frac{1}{9}\left(-\frac{\sqrt{3}}{2} + \frac{2\sqrt{3}}{2} - \frac{\sqrt{3}}{2}\right) = 0$$

Therefore from Equation (3.29)-(3.32), we can conclude $W_0 \perp W_1$.

Similarly, if

$$W_2 = span\{3\,\psi^1(3^2t - k_1), 3\,\psi^2(3^2t - k_2) : k_1, k_2 \epsilon \mathbb{Z}\} \tag{3.33}$$

$$W_3 = span\left\{3^{\frac{3}{2}}\psi^1(3^3t - k_1), 3^{\frac{3}{2}}\psi^2(3^3t - k_2) : k_1, k_2 \epsilon \mathbb{Z}\right\} \tag{3.34}$$

$$\vdots$$

$$\vdots$$

$$\vdots$$

$$W_j = span\left\{3^{\frac{j}{2}}\psi^1\left(3^jt - k_1\right), 3^{\frac{j}{2}}\psi^2\left(3^jt - k_2\right) : k_1, k_2 \epsilon \mathbb{Z}\right\} \tag{3.35}$$

Then, it can easily be proved

$$\cdots W_{-2} \perp W_{-1} \perp W_0 \perp W_1 \perp W_2 \cdots \tag{3.36}$$

Also

$$W_j = span\left\{3^{\frac{j}{2}}\psi^1(3^j t - k_1), k_1 \epsilon \mathbb{Z}\right\} \oplus \left\{3^{\frac{j}{2}}\psi^2(3^j t - k_2):, k_2 \epsilon \mathbb{Z}\right\} = W_j^1 \oplus W_j^2$$

$$W_j = W_j^1 \oplus W_j^2 \tag{3.37}$$

Where

$$W_j^1 = span\left\{3^{\frac{j}{2}}\psi^1(3^j t - k_1), k_1 \epsilon \mathbb{Z}\right\}, W_j^2 = span\left\{3^{\frac{j}{2}}\psi^2(3^j t - k_2):, k_2 \epsilon \mathbb{Z}\right\}$$

$$\psi^1(3^j t - k_1) = \frac{1}{\sqrt{2}} \begin{cases} -1 & \frac{k_1}{3^j} \le t < \frac{3k_1+1}{3^{j+1}} \\ 2 & \frac{3k_1+1}{3^{j+1}} \le t < \frac{3k_1+2}{3^{j+1}} \\ -1 & \frac{3k_1+2}{3^{j+1}} \le t < \frac{3k_1+3}{3^{j+1}} \\ 0 & elsewhere \end{cases} \tag{3.38}$$

$$\psi^2(3^j t - k_2) = \sqrt{\frac{3}{2}} \begin{cases} 1 & \frac{k_2}{3^j} \le t < \frac{3k_2+1}{3^{j+1}} \\ 0 & \frac{3k_2+1}{3^{j+1}} \le t < \frac{3k_2+2}{3^{j+1}} \\ -1 & \frac{3k_2+2}{3^{j+1}} \le t < \frac{3k_2+3}{3^{j+1}} \\ 0 & elsewhere \end{cases} \tag{3.39}$$

As $V_0 \subset V_1$ then what is missing in V_0 in comparison with V_1 .Now we will investigate it with the help of the following function graph. Consider the arbitrary function $f(t)$

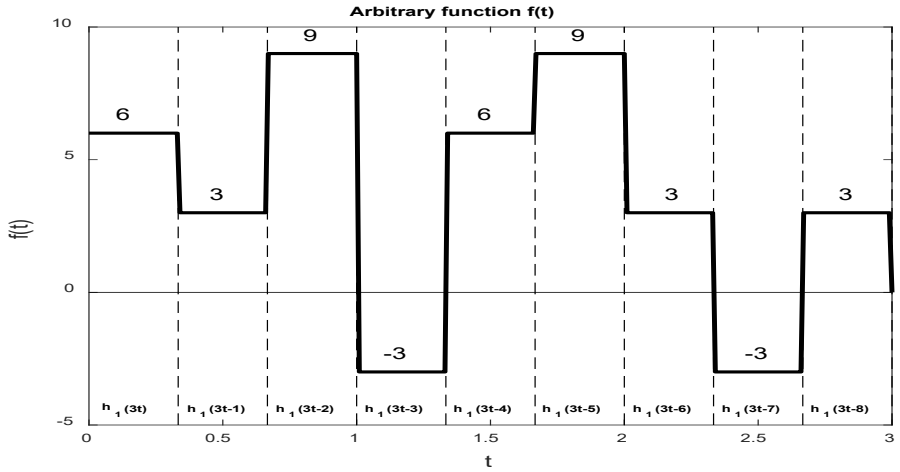

Figure 3.4: Arbitrary Function in 2D

Now we will express $f(t)$ in terms of the bases of V_1 as follows

$$f(t) = 6\psi^0(3t) + 3\psi^0(3t-1) + 9\psi^0(3t-2) - 3\psi^0(3t-3) + 6\psi^0(3t-4) + 9\psi^0(3t-3) + 3\psi^0(3t-3) - 3\psi^0(3t-3) + 3\psi^0(3t-3) \quad (3.40)$$

It can be seen from the function graph that terms of the above function in the different unit intervals can be expressible in terms of the bases of V_0, W_0^1, W_0^2 as follows

$$6\psi^0(3t) + 3\psi^0(3t-1) + 9\psi^0(3t-2) = 6\psi^0(t) - \frac{3\sqrt{2}}{2}\psi^1(t) - \sqrt{\frac{3}{2}}\psi^2(t) \quad (3.41)$$

$$9\psi^0(3t-5) + 6\psi^0(3t-4) - 3\psi^0(3t-3) = 4\psi^0(t-1) + \sqrt{2}\psi^1(t-1) - 2\sqrt{6}\psi^2(t-1) \quad (3.42)$$

$$3\psi^0(3t-6) - 3\psi^0(3t-7) + 3\psi^0(3t-8) = \psi^0(t-2) - 2\sqrt{2}\psi^1(t-2) - 0\,\psi^2(t-2) \quad (3.43)$$

Using Equations (3.41)-(3.43) ,Equation (3.40) becomes

$$f(t) = 6\psi^0(t) - \tfrac{3\sqrt{2}}{2}\psi^1(t) - \sqrt{\tfrac{3}{2}}\psi^2(t) + 4\psi^0(t-1) + \sqrt{2}\psi^1(t-1) - \sqrt{6}\psi^2(t-1) + \psi^0(t-2) - 2\sqrt{2}\psi^1(t-2) - 0\,\psi^2(t-2) \quad (3.44)$$

Now $f(t)$ (Equation (3.45)) has been completely expressed in terms of the bases of V_0, W_0^1, W_0^2.Similar way it can easily be proved that V_0 is also orthogonal to W_0^1, W_0^2. Therefore, any function in V_1 can be expressed in terms of the bases of V_0 and W_0 where $W_0 = W_0^1 \oplus W_0^2$.

Mathematically one can say

$$V_1 = V_0 \oplus W_0 = V_0 \oplus W_0^1 \oplus W_0^2 \quad (3.45)$$

Similarly, using similar arguments we can prove

$$V_2 = V_1 \oplus W_1 = V_0 \oplus W_1^1 \oplus W_1^2 \quad (3.46)$$

$$V_3 = V_2 \oplus W_2 = V_2 \oplus W_2^1 \oplus W_2^2 \quad (3.47)$$

$$\vdots$$

$$V_{j-1} = V_{j-2} \oplus W_{j-2} = V_{j-2} \oplus W_{j-2}^1 \oplus W_{j-2}^2 \quad (3.48)$$

$$V_j = V_{j-1} \oplus W_{j-1} = V_{j-1} \oplus W_{j-1}^1 \oplus W_{j-1}^2 \quad (3.49)$$

$$V_j = V_0 \oplus W_0^1 \oplus W_0^2 \oplus \cdots\cdots\cdots \oplus W_{j-2}^1 \oplus W_{j-2}^2 \oplus W_{j-1}^1 \oplus W_{j-1}^2 \quad (3.50)$$

which mean each square-integrable function $f(t)$ can be expressible in terms of the bases of V_0 , W_j^1, W_j^2 $j = 01,2,3$ ... ...

3.1.2 Multi-resolution analysis (MRA)

Now it clear from the above discussion (Equation (3.4) - (3.50)) that the sequence of closed subspaces of $W_j , V_j \subset L_2(R), j \in \mathbb{Z}$ of $L_2(R)$ space satisfies the following properties

a) $\psi^0(t) \in V_0 \implies \psi^0(3^j t) \in V_j$

b) $\psi^0(t) \in V_0 \implies \psi^0(3^j t - k) \in V_j$

c) $\psi^i(t) \in W_0^i ,\ i = 1,2 \implies \psi^i(3^j t) \in W_j^i$

d) $\psi^i(t) \in W_0^i ,\ i = 1,2 \implies \psi^i(3^j t - k) \in W_j^i$

e) $W_J = W_j^1 \oplus W_j^2 = \oplus W_j^i \ , i = 1,2$

f) $\cdots \subset V_0 \subset V_1 \subset V_2 \subset V_3 \subset V_4 \subset \cdots$

g) $\cdots \perp W_0 \perp W_1 \perp W_2 \perp W_3 \perp W_4 \perp \cdots$

h) $V_j = V_0 \oplus \sum_{i=0}^{j-1} W_j^1 \oplus \sum_{i=0}^{j-1} W_j^2$

i) $\psi^0(t) \in V_0 \implies \psi^0(\mathrm{t-k}) \in V_0; k \in \mathbb{Z}$ is a Riesz Basis in V_0

Process of designing the orthonormal wavelet family using the sequence of closed subspace $W_j , V_j , j \in \mathbb{Z}$ of $L_2(R)$, which satisfies the above set of properties is also known as Multi-resolution analysis (MRA)[9]. The approximation of arbitrary function using the members of these orthonormal wavelet families is known as a multiscale approximation (MSA). The multiscale approximation is one of the modern numerical frameworks to find the solution of various types of differential and integral equation arises in the field of science and technology.

Now using the above-described process, Haar Scale 3 wavelet family is obtained as follows:

$For\ i = 1$

$$h_i(t) = \varphi(t) = \begin{cases} 1 & 0 \le t < 1 \\ 0 & elsewhere \end{cases} \tag{3.51}$$

$For \quad i = 2,4, \dots 3p - 1$

$$h_i(t) = \psi^1(3^j t - k) = \frac{1}{\sqrt{2}} \begin{cases} -1 & \varkappa_1(i) \le t < \varkappa_2(i) \\ 2 & \varkappa_2(i) \le t < \varkappa_3(i) \\ -1 & \varkappa_3(i) \le t < \varkappa_4(i) \\ 0 & elsewhere \end{cases} \tag{3.52}$$

$For \quad i = 3,5,7 \dots 3p$

$$h_i(t) = \psi^2(3^j t - k) = \sqrt{\frac{3}{2}} \begin{cases} 1 & \varkappa_1(i) \le t < \varkappa_2(i) \\ 0 & \varkappa_2(i) \le t < \varkappa_3(i) \\ -1 & \varkappa_3(i) \le t < \varkappa_4(i) \\ 0 & elsewhere \end{cases} \tag{3.53}$$

where $\varkappa_1(i) = \frac{k}{p}$, $\varkappa_2(i) = \frac{3k+1}{3p}$, $\varkappa_3(i) = \frac{(3k+2)}{3p}$, $\varkappa_4(i) = \frac{k+1}{p}$, $p = 3^j$, $j = 0,1,2, \dots$, $k = 0,1,2, \dots, p-1$.

Table 3.1: Relationship between the wavelet number i ,dilation parameter j and translation parameter k for even members of wavelet family

i	2	4	6	8	10	12	14	16	18	20	22	24	26
j	0	1	1	1	2	2	2	2	2	2	2	2	2
k	0	0	1	2	0	1	2	3	4	5	6	7	8
m	1	3	3	3	9	9	9	9	9	9	9	9	9

Table 3.2: Relationship between the wavelet number i ,dilation parameter j and translation parameter k for odd members of wavelet family

i	1	3	5	7	9	11	13	15	17	19	21	23	25	27
j	0	0	1	1	1	2	2	2	2	2	2	2	2	2
k	0	0	0	1	2	0	1	2	3	4	5	6	7	8
m	1	1	3	3	3	9	9	9	9	9	9	9	9	9

The wavelet number $i > 1$ is calculated from the relation $i = p + 2k + 2$ (for even index) and $i = p + 2k + 1$(for odd index). j represents the level of dilation of the and k represents the translation parameters of the wavelet. The function $h_1(t)$ is called father wavelet, $h_2(t)$, $h_3(t)$ mother wavelet and all other functions $h_4(t)$, $h_5(t), h_6(t)$ ... ... are generated from the translation and dilation of the mother wavelet. For even index $i, \psi^1(t)$ will be considered and for odd index $i, \psi^2(t)$ will be considered.

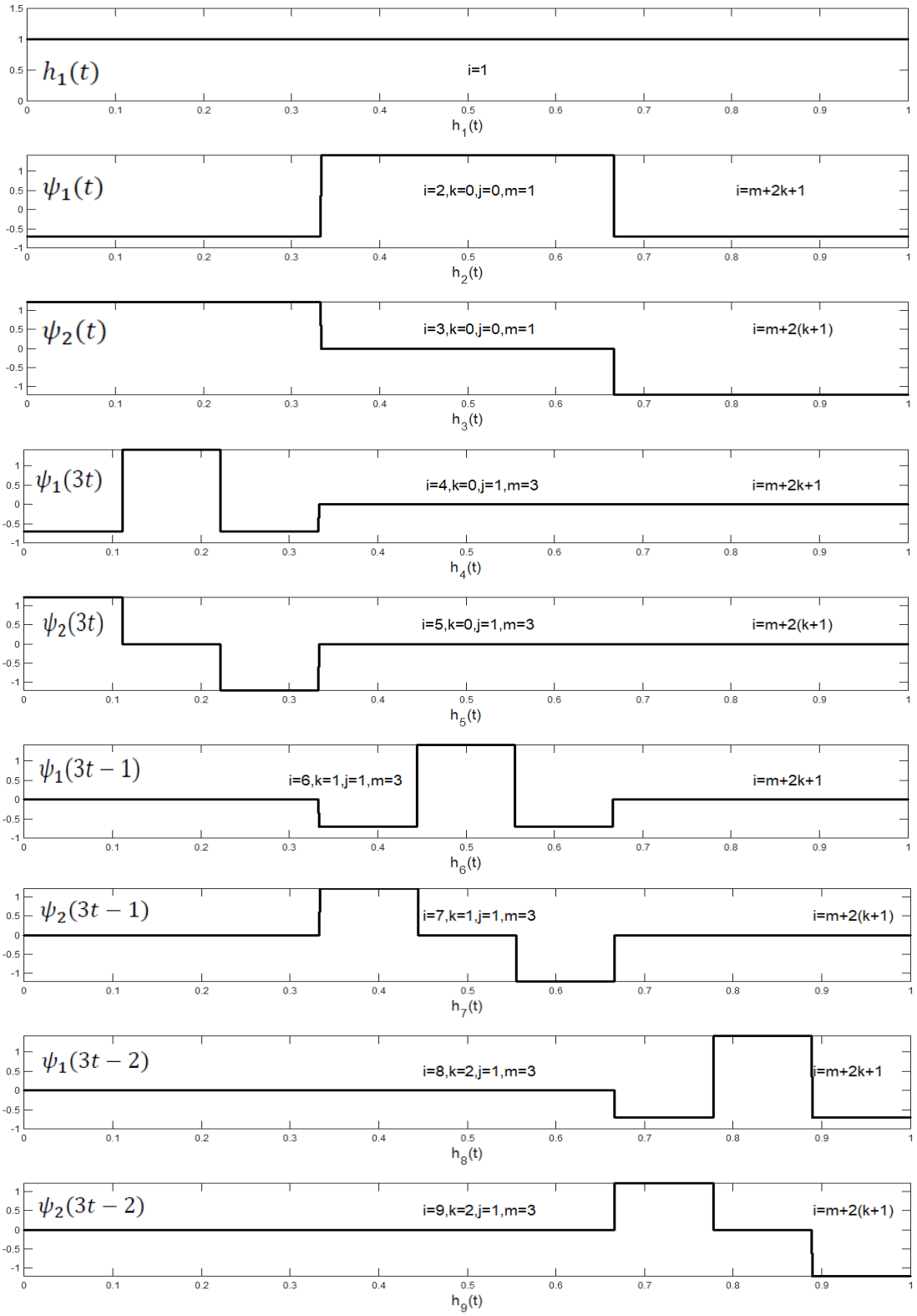

Figure 3.5: Members of the Haar Scale 3 wavelet family ($h_1(t) - h_9(t)$) at $J = 0$ and $J = 1$

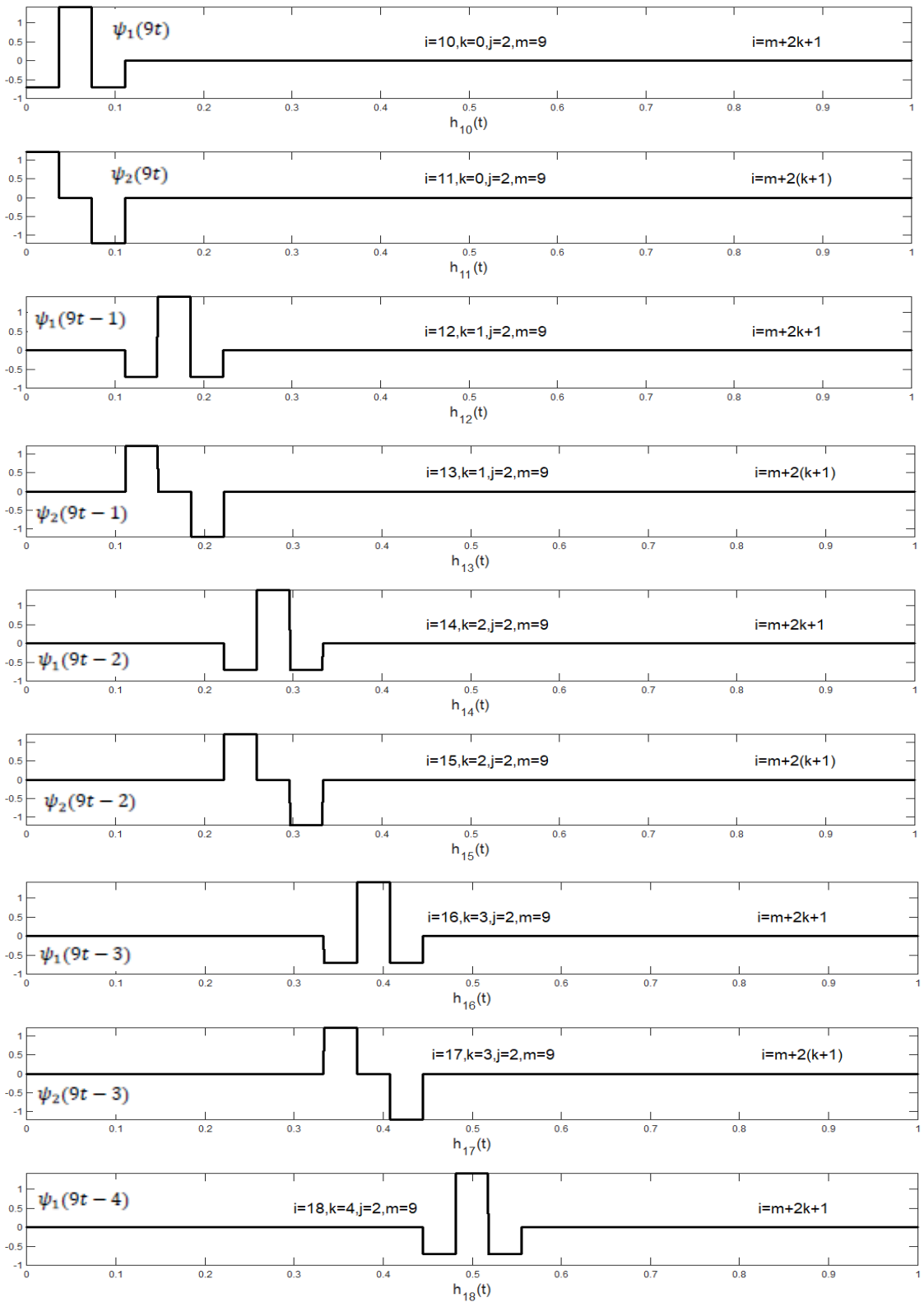

Figure 3.6: Members of the Haar Scale 3 wavelet family ($h_{10}(t) - h_{18}(t)$) at third level of resolution $J = 2$

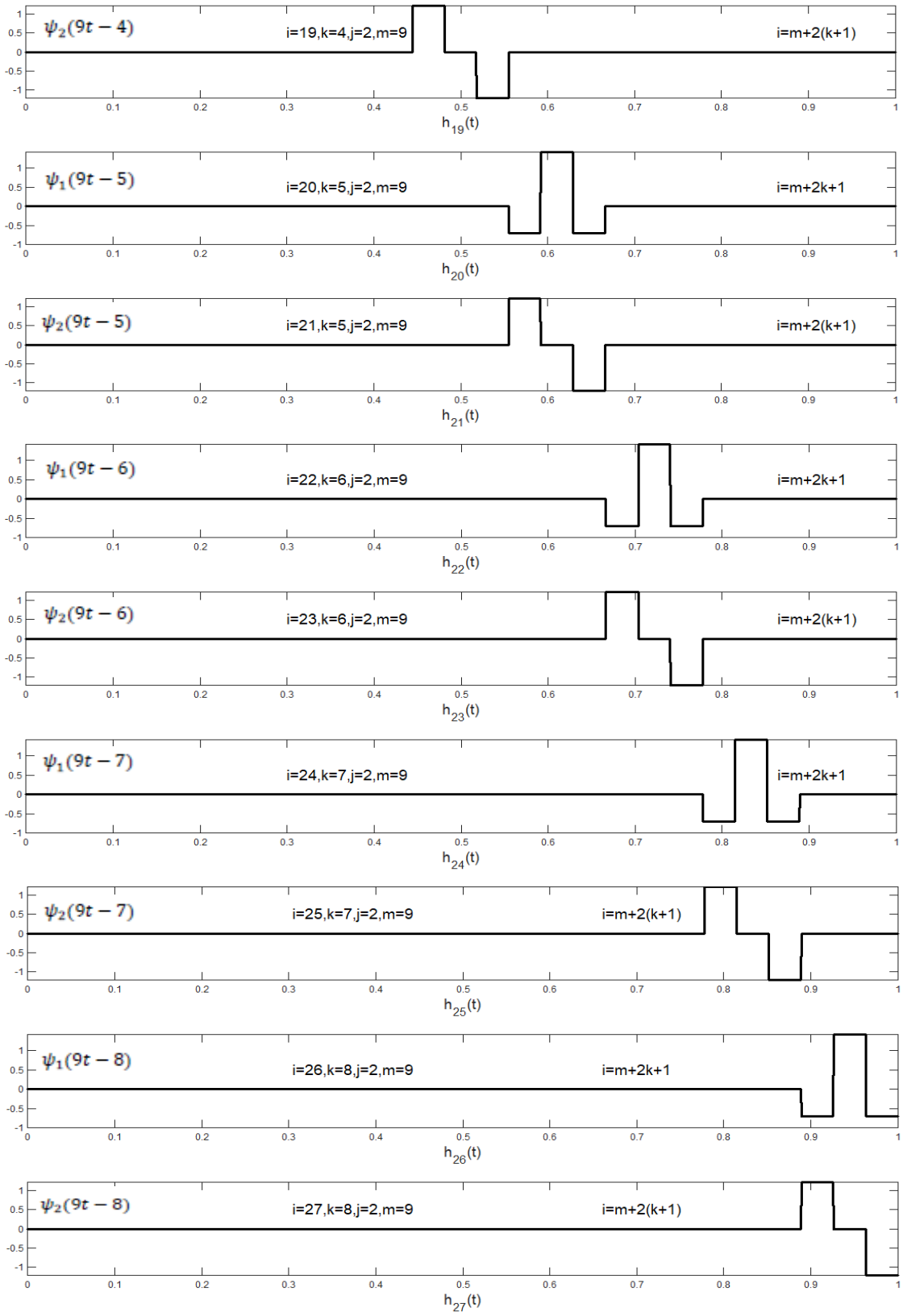

Figure 3.7: Members of Haar Scale 3 wavelet family ($h_{19}(t) - h_{27}(t)$) at the third level of resolution $J = 2$

3.2 Integrals of Haar Scale 3 Wavelet Family

we can integrate Equations (3.51)-(3.53) over the interval [A, B) as many times as required by using the formula given in Equation (3.54)

$q_{\beta,i}(t) = \int_A^t \int_A^t \int_A^t \cdots\cdots\cdots \beta\ times \cdots\cdots\cdots \int_A^t h_i(x)(dx)^\beta$

$$q_{\beta,i}(t) = \frac{1}{(\beta-1)!}\int_A^t (t-x)^{\beta-1} h_i(x)dx \qquad \forall\ \beta = 1,2,3\ldots\ldots\ ,\quad i = 1,2,3,\ldots\ldots 3p \tag{3.54}$$

For $i = 1$ the value of $h_i(t) = \begin{cases} 1 & A \le t < B \\ 0 & elsewhere \end{cases}$

Therefore

$$q_{1,1}(t) = \frac{1}{(1-1)!}\int_A^t (t-x)^{1-1} h_1(x)dx = \int_A^t 1\ dx = (t-A)$$

$$q_{2,1}(t) = \frac{1}{(2-1)!}\int_A^t (t-x)^{2-1} h_1(x)dx = \int_A^t (t-x)\ dx = \frac{1}{2!}\ (t-A)^2$$

$$q_{3,1}(t) = \frac{1}{(3-1)!}\int_A^t (t-x)^{3-1} h_1(x)dx = \frac{1}{2}\int_A^t (t-x)^2\ dx = \frac{1}{3!}\ (t-A)^3$$

$$\begin{array}{cccc} \vdots & \vdots & \vdots & \vdots \\ \vdots & \vdots & \vdots & \vdots \\ \vdots & \vdots & \vdots & \vdots \end{array}$$

$q_{\beta,1}(t) = \frac{1}{(\beta-1)!}\int_A^t (t-x)^{\beta-1} h_i(x)dx = \frac{1}{(\beta-1)!}\int_A^t (t-x)^{\beta-1}dx\ =$

$\frac{1}{\beta!}(t-A)^\beta \qquad \forall\ \beta = 1,2,3\ldots\ldots$ (3.55)

For an even integer $i = 2,4,6,8,\cdots,3p-1$

$$h_i(t) = \psi^1\left(3^j t - k\right) = \frac{1}{\sqrt{2}}\begin{cases} -1 & \varkappa_1(i) \le t < \varkappa_2(i) \\ 2 & \varkappa_2(i) \le t < \varkappa_3(i) \\ -1 & \varkappa_3(i) \le t < \varkappa_4(i) \\ 0 & elsewhere \end{cases}$$

$q_{1,i}(t) = \frac{1}{(1-1)!}\int_A^t (t-x)^{1-1} h_i(x)dx\ =\ \int_A^t h_i(x)\ dx$

$$\forall\ i = 2,4,6,8,\cdots,3p-1 \tag{3.56}$$

When $t \in [A, \varkappa_1(i))$ then $q_{1,i}(t) = \int_A^t h_i(x)\ dx = \int_A^t 0\ dx = 0$

When $t \in \left[\varkappa_1(i),\ \varkappa_2(i)\right)$ then

$$q_{1,i}(t) = \int_A^{\varkappa_1(i),} h_i(x)\,dx + \int_{\varkappa_1(i),}^{t} h_i(x)\,dx$$

$$= \int_A^{\varkappa_1(i),} 0\,dx + \int_{\varkappa_1(i)}^{t} \frac{-1}{\sqrt{2}}\,dx = \frac{-1}{\sqrt{2}}\frac{(t-\varkappa_1(i))}{1!}$$

When $t \in [\varkappa_2(i),\ \varkappa_3(i))$ then

$$q_{1,i}(t) = \int_A^{\varkappa_1(i),} h_i(x)\,dx + \int_{\varkappa_1(i),}^{\varkappa_2(i)} h_i(x)\,dx + \int_{\varkappa_2(i),}^{t} h_i(x)\,dx$$

$$= \int_A^{\varkappa_1(i),} 0\,dx + \int_{\varkappa_1(i),}^{\varkappa_2(i)} \frac{-1}{\sqrt{2}}\,dx + \int_{\varkappa_2(i),}^{t} \frac{2}{\sqrt{2}}\,dx$$

$$= -\frac{1}{\sqrt{2}}\big(\varkappa_2(i) - \varkappa_1(i)\big) + \frac{2}{\sqrt{2}}\big(t - \varkappa_2(i)\big) = \frac{1}{\sqrt{2}}(2t - 3\varkappa_2(i) + \varkappa_1(i)$$

$$= \frac{1}{\sqrt{2}}\Big(-\big(t - \varkappa_1(i)\big)^1 + 3\big(t - \varkappa_2(i)\big)^1\Big)$$

When $t \in [\varkappa_3(i), \varkappa_4(i))$ then

$$q_{1,i}(t) = \int_A^{\varkappa_1(i)} h_i(x)\,dx + \int_{\varkappa_1(i)}^{\varkappa_2(i)} h_i(x)\,dx + \int_{\varkappa_2(i)}^{\varkappa_3(i)} h_i(x)\,dx + \int_{\varkappa_3(i)}^{t} h_i(x)\,dx$$

$$= \frac{1}{\sqrt{2}}\Big(\int_A^{\varkappa_1(i)} 0\,dx + \int_{\varkappa_1(i)}^{\varkappa_2(i)} -1\,dx + \int_{\varkappa_2(i)}^{\varkappa_3(i)} 2\,dx + \int_{\varkappa_3(i)}^{t} -1\,dx\Big)$$

$$= \frac{1}{\sqrt{2}}\big(0 - \big(\varkappa_2(i) - \varkappa_1(i)\big) + 2\big(\varkappa_3(i) - \varkappa_2(i)\big) - (t - \varkappa_3(i))\big)$$

$$= \frac{1}{\sqrt{2}}\big(-t + \varkappa_1(i) - 3\varkappa_2(i) + 3\varkappa_3(i)\big) = \frac{1}{\sqrt{2}}\big(-t + \varkappa_1(i) - 3\varkappa_2(i) + 3\varkappa_3(i)\big)$$

$$= \frac{1}{\sqrt{2}}\Big(-\big(t - \varkappa_1(i)\big)^1 + 3\big(t - \varkappa_2(i)\big)^1 - 3\big(t - \varkappa_3(i)\big)^1\Big)$$

When $t \in [\varkappa_4(i), B)$ then

$$q_{1,i}(t) = \int_A^{\varkappa_1(i)} h_i(x)\,dx + \int_{\varkappa_1(i)}^{\varkappa_2(i)} h_i(x)\,dx + \int_{\varkappa_2(i)}^{\varkappa_3(i)} h_i(x)\,dx + \int_{\varkappa_3(i)}^{\varkappa_4(i)} h_i(x)\,dx + \int_{\varkappa_4(i)}^{t} h_i(x)\,dx$$

$$= \frac{1}{\sqrt{2}}\left(\int_A^{\varkappa_1(i)} 0\,dx + \int_{\varkappa_1(i)}^{\varkappa_2(i)} -1\,dx + \int_{\varkappa_2(i)}^{\varkappa_3(i)} 2\,dx + \int_{\varkappa_3(i)}^{\varkappa_4(i)} -1\,dx + \int_{\varkappa_4(i)}^{t} 0\,dx\right)$$

$$= \frac{1}{\sqrt{2}}\left(0 - \left(\varkappa_2(i) - \varkappa_1(i)\right) + 2\left(\varkappa_3(i) - \varkappa_2(i)\right) - \left(\varkappa_4(i) - \varkappa_3(i)\right) + 0\right)$$

$$= \frac{1}{\sqrt{2}}\left(\varkappa_1(i) - 3\varkappa_2(i) + 3\varkappa_3(i) - \varkappa_4(i)\right)$$

$$= \frac{1}{\sqrt{2}}\left(-\left(t - \varkappa_1(i)\right)^1 + 3\left(t - \varkappa_2(i)\right)^1 - 3\left(t - \varkappa_3(i)\right)^1 + \left(t - \varkappa_4(i)\right)^1\right)$$

Therefore, the first integral of the even members' of Haar Scale 3 wavelets family is represented by the Equation (3.57)

$$q_{1,i}(t) = \frac{1}{\sqrt{2}}\begin{cases} 0 & for \quad 0 \le t \le \varkappa_1(i) \\ \frac{-1}{1!}\left(t - \varkappa_1(i)\right)^1 & for \quad \varkappa_1(i) \le t \le \varkappa_2(i) \\ \frac{1}{1!}\left[-\left(t - \varkappa_1(i)\right)^1 + 3\left(t - \varkappa_2(i)\right)^1\right] & for \quad \varkappa_2(i) \le t \le \varkappa_3(i) \\ \frac{1}{1!}\left[-\left(t - \varkappa_1(i)\right)^1 + 3\left(t - \varkappa_2(i)\right)^1 - 3\left(t - \varkappa_3(i)\right)^1\right] & for\ \varkappa_3(i) \le t \le \varkappa_4(i) \\ \frac{1}{1!}\left[-\left(t - \varkappa_1(i)\right)^1 + 3\left(t - \varkappa_2(i)\right)^1 - 3\left(t - \varkappa_3(i)\right)^1 + \left(t - \varkappa_4(i)\right)^1\right] & for\ \varkappa_4(i) \le t \le 1 \end{cases} \tag{3.57}$$

Now second integrals take $\beta = 2$

$$q_{2,i}(t) = \frac{1}{(2-1)!}\int_A^t (t-x)^{2-1} h_i(x)dx = \int_A^t (t-x)h_i(x)dx \tag{3.58}$$

$$\forall\ i = 2,4,6,8,\cdots,3p-1$$

When $t \in [A, \varkappa_1(i))$ then

$$q_{2,i}(t) = \int_A^t (t-x)h_i(x)dx = \int_A^t (t-x)\,0\,dx = 0$$

When $t \in \left[\varkappa_1(i),\ \varkappa_2(i)\right)$ then

$$q_{2,i}(t) = \int_A^{\varkappa_1(i)} (t-x)h_i(x)\,dx + \int_{\varkappa_1(i)}^{t} (t-x)h_i(x)\,dx$$

$$= \int_A^{\varkappa_1(i)} (t-x)\ 0\,dx + \int_{\varkappa_1(i)}^{t} \frac{-1}{\sqrt{2}}(t-x)\,dx = \frac{-1}{\sqrt{2}}\frac{\left(t-\varkappa_1(i)\right)^2}{2!}$$

When $t \in [\varkappa_2(i),\ \varkappa_3(i))$ then

$$q_{2,i}(t) = \int_A^{\varkappa_1(i)} (t-x)\ h_i(x)\,dx + \int_{\varkappa_1(i)}^{\varkappa_2(i)} (t-x)\ h_i(x)\,dx + \int_{\varkappa_2(i)}^{t} (t-x)\ h_i(x)\,dx$$

$$= \int_A^{\varkappa_1(i),} 0\ (t-x)\,dx + \int_{\varkappa_1(i),\ \sqrt{2}}^{\varkappa_2(i)} \frac{-1}{\sqrt{2}}(t-x)\,dx + \int_{\varkappa_2(i),\ \sqrt{2}}^{t} \frac{2}{\sqrt{2}}(t-x)\,dx$$

$$= -\frac{1}{\sqrt{2}}\frac{\left(\left(t-\varkappa_2(i)\right)^2-\left(t-\varkappa_1(i)\right)^2\right)}{2!} + \frac{2}{\sqrt{2}}\frac{\left(t-\varkappa_2(i)\right)^2}{2!}$$

$$= \frac{1}{\sqrt{2}} \times \frac{1}{2!}\left(-\left(t-\varkappa_1(i)\right)^2 + 3\left(t-\varkappa_2(i)\right)^2\right)$$

When $t \in [\varkappa_3(i), \varkappa_4(i))$ then

$$q_{2,i}(t) = \int_A^{\varkappa_1(i)} (t-x)h_i(x)\,dx + \int_{\varkappa_1(i)}^{\varkappa_2(i)} (t-x)h_i(x)\,dx + \int_{\varkappa_2(i)}^{\varkappa_3(i)} (t-x)h_i(x)\,dx + \int_{\varkappa_3(i)}^{t} (t-x)\ h_i(x)\,dx$$

$$= \frac{1}{\sqrt{2}}\left(\int_A^{\varkappa_1(i)}\ 0\,dx + \int_{\varkappa_1(i)}^{\varkappa_2(i)} -(t-x)\,dx + \int_{\varkappa_2(i)}^{\varkappa_3(i)} 2(t-x)\,dx + \int_{\varkappa_3(i)}^{t} -(t-x)\,dx\right)$$

$$= \frac{1}{\sqrt{2}}\left(0 + \frac{\left(\left(t-\varkappa_2(i)\right)^2-\left(t-\varkappa_1(i)\right)^2\right)}{2!} - 2\,\frac{\left(\left(t-\varkappa_3(i)\right)^2-\left(t-\varkappa_2(i)\right)^2\right)}{2!} - \frac{(t-\varkappa_3(i))^2}{2!}\right)$$

$$= \frac{1}{\sqrt{2}} \times \frac{1}{2!}\left(-\left(t-\varkappa_1(i)\right)^2 + 3\left(t-\varkappa_2(i)\right)^2 - 3\left(t-\varkappa_3(i)\right)^2\right)$$

When $t \in [\varkappa_4(i), B)$ then

$$q_{2,i}(t) = \int_A^{\varkappa_1(i)} (t-x)h_i(x)\,dx + \int_{\varkappa_1(i)}^{\varkappa_2(i)} (t-x)h_i(x)\,dx + \int_{\varkappa_2(i)}^{\varkappa_3(i)} (t-x)h_i(x)\,dx + \int_{\varkappa_3(i)}^{\varkappa_4(i)} (t-x)h_i(x)\,dx + \int_{\varkappa_4(i)}^{t} (t-x)h_i(x)\,dx$$

$$= \frac{1}{\sqrt{2}}\left(\int_A^{\varkappa_1(i)} 0\;dx + \int_{\varkappa_1(i)}^{\varkappa_2(i)} -(t-x)\,dx + \int_{\varkappa_2(i)}^{\varkappa_3(i)} 2(t-x)\,dx + \int_{\varkappa_3(i)}^{\varkappa_4(i)} -(t-x)\,dx + \int_{\varkappa_4(i)}^{t} 0\,dx\right)$$

$$= \frac{1}{\sqrt{2}}\left(0 + \frac{\left((t-\varkappa_2(i))^2 - (t-\varkappa_1(i))^2\right)}{2!} - 2\frac{\left((t-\varkappa_3(i))^2 - (t-\varkappa_2(i))^2\right)}{2!} + \frac{(t-\varkappa_4(i))^2 - (t-\varkappa_3(i))^2}{2!} + 0\right)$$

$$= \frac{1}{\sqrt{2}} \times \frac{1}{2!}\left(-\left(t-\varkappa_1(i)\right)^2 + 3\left(t-\varkappa_2(i)\right)^2 - 3\left(t-\varkappa_3(i)\right)^2 + (t-\varkappa_4(i))^2\right)$$

Therefore, the second integral of the even members of Haar Scale 3 wavelets family is given by Equation (3.59)

$$q_{2,i}(t) =$$

$$\frac{1}{\sqrt{2}}\begin{cases} 0 & for \quad 0 \le t \le \varkappa_1(i) \\ \frac{-1}{2!}\left(t-\varkappa_1(i)\right)^2 & for \;\; \varkappa_1(i) \le t \le \varkappa_2(i) \\ \frac{1}{2!}\left[-\left(t-\varkappa_1(i)\right)^2 + 3\left(t-\varkappa_2(i)\right)^2\right] & for \quad \varkappa_2(i) \le t \le \varkappa_3(i) \\ \frac{1}{2!}\left[-\left(t-\varkappa_1(i)\right)^2 + 3\left(t-\varkappa_2(i)\right)^2 - 3\left(t-\varkappa_3(i)\right)^2\right] & for\; \varkappa_3(i) \le t \le \varkappa_4(i) \\ \frac{1}{2!}\left[-\left(t-\varkappa_1(i)\right)^2 + 3\left(t-\varkappa_2(i)\right)^2 - 3\left(t-\varkappa_3(i)\right)^2 + \left(t-\varkappa_4(i)\right)^2\right] & for\; \varkappa_4(i) \le t \le 1 \end{cases} \tag{3.59}$$

Proceeding in this way, integral of any order β for the even members of Haar scale 3 wavelet family are given by Equation (3.60)

$q_{\beta,i}(t)'s \;\; for \;\; i = 2,4,6,8,\cdots,3p-1$ are given below

$$q_{\beta,i}(t) =$$

$$\frac{1}{\sqrt{2}}\begin{cases} 0 & for \quad 0 \le t \le \varkappa_1(i) \\ \frac{-1}{\beta!}\left(t-\varkappa_1(i)\right)^{\beta} & for \;\; \varkappa_1(i) \le t \le \varkappa_2(i) \\ \frac{1}{\beta!}\left[-\left(t-\varkappa_1(i)\right)^{\beta} + 3\left(t-\varkappa_2(i)\right)^{\beta}\right] & for \quad \varkappa_2(i) \le t \le \varkappa_3(i) \\ \frac{1}{\beta!}\left[-\left(t-\varkappa_1(i)\right)^{\beta} + 3\left(t-\varkappa_2(i)\right)^{\beta} - 3\left(t-\varkappa_3(i)\right)^{\beta}\right] & for\; \varkappa_3(i) \le t \le \varkappa_4(i) \\ \frac{1}{\beta!}\left[-\left(t-\varkappa_1(i)\right)^{\beta} + 3\left(t-\varkappa_2(i)\right)^{\beta} - 3\left(t-\varkappa_3(i)\right)^{\beta} + \left(t-\varkappa_4(i)\right)^{\beta}\right] & for\; \varkappa_4(i) \le t \le 1 \end{cases} \tag{3.60}$$

For odd integers $i = 3,5,7 \ldots 3p$

$$h_i(t) = \psi^2\left(3^j t - k\right) = \sqrt{\frac{3}{2}}\begin{cases} 1 & \varkappa_1(i) \le t < \varkappa_2(i) \\ 0 & \varkappa_2(i) \le t < \varkappa_3(i) \\ -1 & \varkappa_3(i) \le t < \varkappa_4(i) \\ 0 & elsewhere \end{cases}$$

$$q_{1,i}(t) = \frac{1}{(1-1)!}\int_A^t (t-x)^{1-1} h_i(x)dx \;=\; \int_A^t h_i(x)\,dx \quad \forall \; i = 3,5,7 \ldots 3p \tag{3.61}$$

When $t \in [A, \varkappa_1(i))$ then

$$q_{1,i}(t) = \int_A^t h_i(x)\,dx = \int_A^t 0\,dx = 0$$

When $t \in \left[\varkappa_1(i),\ \varkappa_2(i)\right)$ then

$$q_{1,i}(t) = \int_A^{\varkappa_1(i),} h_i(x)\,dx + \int_{\varkappa_1(i),}^t h_i(x)\,dx$$

$$= \int_A^{\varkappa_1(i),} 0\,dx + \int_{\varkappa_1(i)}^t \sqrt{\frac{3}{2}}\,dx = \sqrt{\frac{3}{2}}\,\frac{(t-\varkappa_1(i))}{1!}$$

When $t \in [\varkappa_2(i),\ \varkappa_3(i))$ then

$$q_{1,i}(t) = \int_A^{\varkappa_1(i),} h_i(x)\,dx + \int_{\varkappa_1(i),}^{\varkappa_2(i)} h_i(x)\,dx + \int_{\varkappa_2(i),}^t h_i(x)\,dx$$

$$= \int_A^{\varkappa_1(i)} 0\,dx + \int_{\varkappa_1(i)}^{\varkappa_2(i)} \sqrt{\frac{3}{2}}\,dx + \int_{\varkappa_2(i)}^t 0\,dx$$

$$= 0 + \sqrt{\frac{3}{2}}\left(\varkappa_2(i) - \varkappa_1(i)\right) + 0 = \sqrt{\frac{3}{2}}\left(\frac{(t-\varkappa_1(i))^1 - (t-\varkappa_2(i))^1}{1!}\right)$$

When $t \in [\varkappa_3(i), \varkappa_4(i))$ then

$$q_{1,i}(t) = \int_A^{\varkappa_1(i)} h_i(x)\,dx + \int_{\varkappa_1(i)}^{\varkappa_2(i)} h_i(x)\,dx + \int_{\varkappa_2(i)}^{\varkappa_3(i)} h_i(x)\,dx + \int_{\varkappa_3(i)}^t h_i(x)\,dx$$

$$= \sqrt{\frac{3}{2}}\left(\int_A^{\varkappa_1(i)} 0\,dx + \int_{\varkappa_1(i)}^{\varkappa_2(i)} 1\,dx + \int_{\varkappa_2(i)}^{\varkappa_3(i)} 0\,dx + \int_{\varkappa_3(i)}^{t} -1\,dx\right)$$

$$= \sqrt{\frac{3}{2}}\left(0 + \left(\varkappa_2(i) - \varkappa_1(i)\right) + 0 - \left(t - \varkappa_3(i)\right)\right) = \sqrt{\frac{3}{2}}\left(-t - \varkappa_1(i) + \varkappa_2(i) + \varkappa_3(i)\right)$$

$$= \sqrt{\frac{3}{2}}\left(\frac{\left(t-\varkappa_1(i)\right)^1 - \left(t-\varkappa_2(i)\right)^1 - \left(t-\varkappa_3(i)\right)^1}{1!}\right)$$

When $t \in [\varkappa_4(i), B)$ then

$q_{1,i}(t) = \int_A^{\varkappa_1(i)} h_i(x)\,dx + \int_{\varkappa_1(i)}^{\varkappa_2(i)} h_i(x)\,dx + \int_{\varkappa_2(i)}^{\varkappa_3(i)} h_i(x)\,dx + \int_{\varkappa_3(i)}^{\varkappa_4(i)} h_i(x)\,dx +$

$\int_{\varkappa_4(i)}^{t} h_i(x)\,dx = \sqrt{\frac{3}{2}}\left(\int_A^{\varkappa_1(i)} 0\,dx + \int_{\varkappa_1(i)}^{\varkappa_2(i)} dx + \int_{\varkappa_2(i)}^{\varkappa_3(i)} 0\,dx + \int_{\varkappa_3(i)}^{\varkappa_4(i)} -1\,dx +\right.$

$\left.\int_{\varkappa_4(i)}^{t} 0\,dx\right)$

$$= \sqrt{\frac{3}{2}}\left(0 + \left(\varkappa_2(i) - \varkappa_1(i)\right) + 0 - \left(\varkappa_4(i) - \varkappa_3(i)\right) + 0\right)$$

$$= \sqrt{\frac{3}{2}}\left(-\varkappa_1(i) + \varkappa_2(i) + \varkappa_3(i) - \varkappa_4(i)\right)$$

$$= \sqrt{\frac{3}{2}}\left(\left(t - \varkappa_1(i)\right)^1 - \left(t - \varkappa_2(i)\right)^1 - \left(t - \varkappa_3(i)\right)^1 + \left(t - \varkappa_4(i)\right)^1\right)$$

Therefore, the first integral of the odd members of the Haar Scale 3 wavelets family is given by Equation (3.62)

$$q_{1,i}(t) = \sqrt{\frac{3}{2}}\begin{cases} 0 & for \quad 0 \le t \le \varkappa_1(i) \\ \frac{1}{1!}\left(t - \varkappa_1(i)\right)^1 & for \quad \varkappa_1(i) \le t \le \varkappa_2(i) \\ \frac{1}{1!}\left[\left(t - \varkappa_1(i)\right)^1 - \left(t - \varkappa_2(i)\right)^1\right] & for \quad \varkappa_2(i) \le t \le \varkappa_3(i) \\ \frac{1}{1!}\left[\left(t - \varkappa_1(i)\right)^1 - \left(t - \varkappa_2(i)\right)^1 - \left(t - \varkappa_3(i)\right)^1\right] & for \quad \varkappa_3(i) \le t \le \varkappa_4(i) \\ \frac{1}{1!}\left[\left(t - \varkappa_1(i)\right)^1 - \left(t - \varkappa_2(i)\right)^1 - \left(t - \varkappa_3(i)\right)^1 + \left(t - \varkappa_4(i)\right)^1\right] & for\ \varkappa_4(i) \le t \le 1 \end{cases} \tag{3.62}$$

Now for second integrals take $\beta = 2$

$$q_{2,i}(t) = \frac{1}{(2-1)!}\int_A^t (t-x)^{2-1} h_i(x)dx \;=\; \int_A^t (t-x)h_i(x)dx \qquad \forall\; i = 2,4,6,8,\cdots,3p-1 \tag{3.63}$$

When $t \in [A, \varkappa_1(i))$ then

$$q_{2,i}(t) = \int_A^t (t-x)h_i(x)dx = \int_A^t (t-x)\,0\,dx = 0$$

When $t \in \left[\varkappa_1(i),\ \varkappa_2(i)\right)$ then

$$q_{1,i}(t) = \int_A^{\varkappa_1(i)} (t-x)h_i(x)\,dx + \int_{\varkappa_1(i)}^t (t-x)h_i(x)\,dx$$

$$= \int_A^{\varkappa_1(i)} (t-x)\,0\,dx + \int_{\varkappa_1(i)}^t \sqrt{\frac{3}{2}}(t-x)\,dx = \sqrt{\frac{3}{2}}\;\frac{\left(t-\varkappa_1(i)\right)^2}{2!}$$

When $t \in [\varkappa_2(i),\ \varkappa_3(i))$ then

$$q_{1,i}(t) = \int_A^{\varkappa_1(i)} (t-x)\,h_i(x)\,dx + \int_{\varkappa_1(i)}^{\varkappa_2(i)} (t-x)\,h_i(x)\,dx + \int_{\varkappa_2(i)}^t (t-x)\,h_i(x)\,dx$$

$$= \int_A^{\varkappa_1(i),} 0\,(t-x)\,dx + \int_{\varkappa_1(i),}^{\varkappa_2(i)} \sqrt{\frac{3}{2}}(t-x)\,dx + \int_{\varkappa_2(i),}^t 0\,(t-x)\,dx$$

$$= 0 - \sqrt{\frac{3}{2}}\;\frac{\left(\left(t-\varkappa_2(i)\right)^2 - \left(t-\varkappa_1(i)\right)^2\right)}{2!} + 0 = \sqrt{\frac{3}{2}} \times \frac{1}{2!}\left(\left(t-\varkappa_1(i)\right)^2 - \left(t-\varkappa_2(i)\right)^2\right)$$

When $t \in [\varkappa_3(i), \varkappa_4(i))$ then

$$q_{1,i}(t) = \int_A^{\varkappa_1(i)} (t-x)h_i(x)\,dx + \int_{\varkappa_1(i)}^{\varkappa_2(i)} (t-x)h_i(x)\,dx + \int_{\varkappa_2(i)}^{\varkappa_3(i)} (t-x)h_i(x)\,dx + \int_{\varkappa_3(i)}^t (t-x)\,h_i(x)\,dx$$

$$= \sqrt{\frac{3}{2}}\left(\int_A^{\varkappa_1(i)} 0\,dx + \int_{\varkappa_1(i)}^{\varkappa_2(i)} (t-x)\,dx + \int_{\varkappa_2(i)}^{\varkappa_3(i)} 0\,dx + \int_{\varkappa_3(i)}^{t} -(t-x)\,dx\right)$$

$$= \sqrt{\frac{3}{2}}\left(0 - \frac{\left((t-\varkappa_2(i))^2 - (t-\varkappa_1(i))^2\right)}{2!} - 0 - \frac{(t-\varkappa_3(i))^2}{2!}\right)$$

$$= \sqrt{\frac{3}{2}} \times \frac{1}{2!}\left(\left(t-\varkappa_1(i)\right)^2 - \left(t-\varkappa_2(i)\right)^2 - \left(t-\varkappa_3(i)\right)^2\right)$$

When $t \in [\varkappa_4(i), B)$ then

$q_{1,i}(t) = \int_A^{\varkappa_1(i)} (t-x)h_i(x)\,dx + \int_{\varkappa_1(i)}^{\varkappa_2(i)} (t-x)h_i(x)\,dx + \int_{\varkappa_2(i)}^{\varkappa_3(i)} (t-x)h_i(x)\,dx +$

$\int_{\varkappa_3(i)}^{\varkappa_4(i)} (t-x)h_i(x)\,dx + \int_{\varkappa_4(i)}^{t} (t-x)h_i(x)\,dx = \sqrt{\frac{3}{2}}\left(\int_A^{\varkappa_1(i)} 0\,dx + \int_{\varkappa_1(i)}^{\varkappa_2(i)} (t-\right.$

$\left. x)\,dx + \int_{\varkappa_2(i)}^{\varkappa_3(i)} 0\,dx + \int_{\varkappa_3(i)}^{\varkappa_4(i)} -(t-x)\,dx + \int_{\varkappa_4(i)}^{t} 0\,dx\right)$

$$= \sqrt{\frac{3}{2}}\left(0 - \frac{\left((t-\varkappa_2(i))^2 - (t-\varkappa_1(i))^2\right)}{2!} - 0 + \frac{\left(t-\varkappa_4(i)\right)^2 - \left(t-\varkappa_3(i)\right)^2}{2!} + 0\right)$$

$$= \sqrt{\frac{3}{2}} \times \frac{1}{2!}\left(\left(t-\varkappa_1(i)\right)^2 - \left(t-\varkappa_2(i)\right)^2 - \left(t-\varkappa_3(i)\right)^2 + (t-\varkappa_4(i))^2\right)$$

Proceeding in this way, integral of any order β for the odd members of Haar scale 3wavelet family are given by Equation (3.64)

$q_{\beta,i}(t)'s \quad for \quad i = 3,5,7,9,\cdots,3p$ are given below

$q_{\beta,i}(t) =$

$$\sqrt{\frac{3}{2}}\begin{cases} 0 & for \quad 0 \le t \le \varkappa_1(i) \\ \frac{1}{\beta!}\left(t-\varkappa_1(i)\right)^{\beta} & for \quad \varkappa_1(i) \le t \le \varkappa_2(i) \\ \frac{1}{\beta!}\left[\left(t-\varkappa_1(i)\right)^{\beta} - \left(t-\varkappa_2(i)\right)^{\beta}\right] & for \quad \varkappa_2(i) \le t \le \varkappa_3(i) \\ \frac{1}{\beta!}\left[\left(t-\varkappa_1(i)\right)^{\beta} - \left(t-\varkappa_2(i)\right)^{\beta} - \left(t-\varkappa_3(i)\right)^{\beta}\right] & for \quad \varkappa_3(i) \le t \le \varkappa_4(i) \\ \frac{1}{\beta!}\left[\left(t-\varkappa_1(i)\right)^{\beta} - \left(t-\varkappa_2(i)\right)^{\beta} - \left(t-\varkappa_3(i)\right)^{\beta} + \left(t-\varkappa_4(i)\right)^{\beta}\right] & for\ \varkappa_4(i) \le t \le 1 \end{cases} \tag{3.64}$$

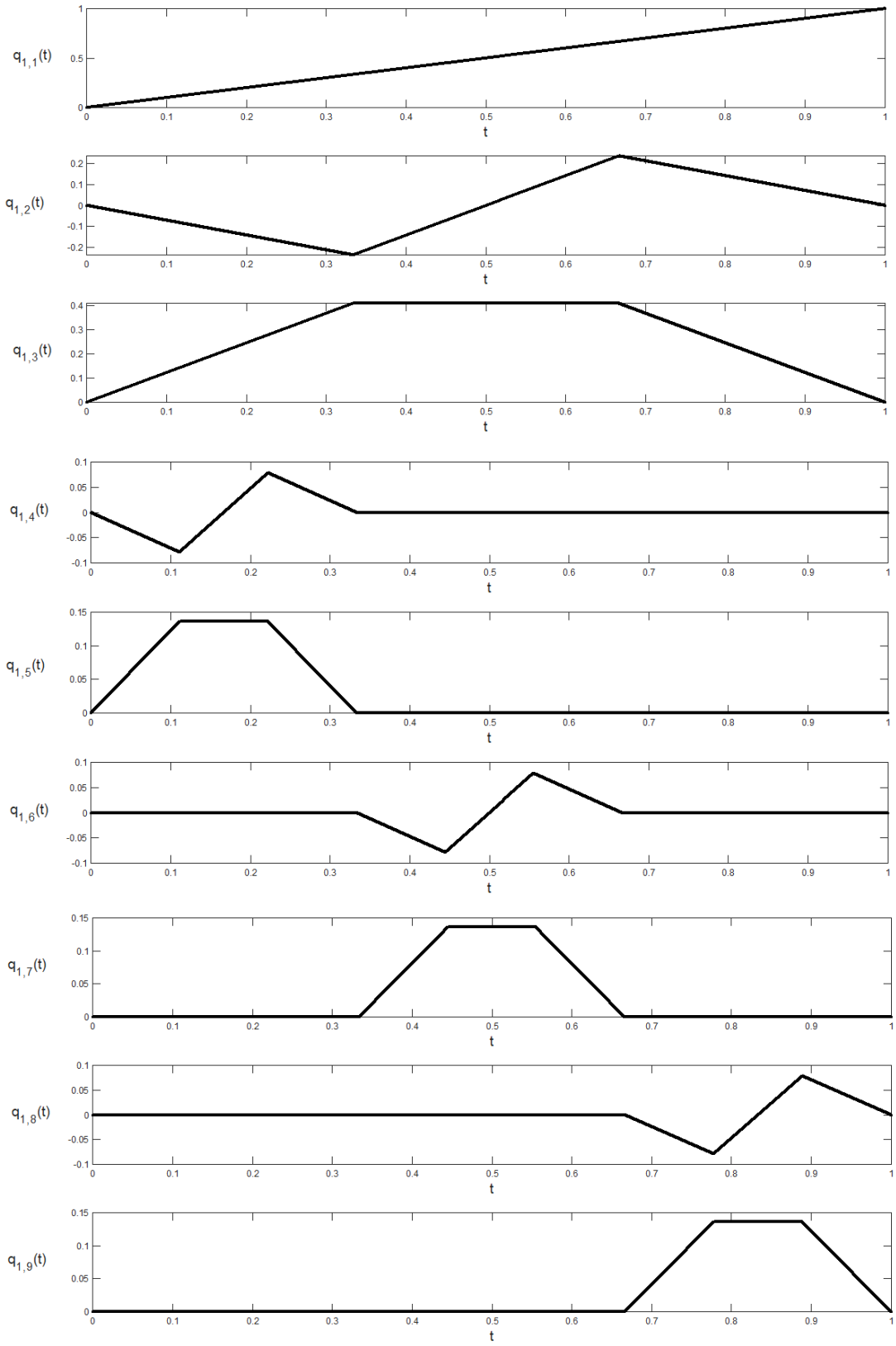

Figure 3.8: First integral of the first nine members of the Haar Scale 3 wavelet family

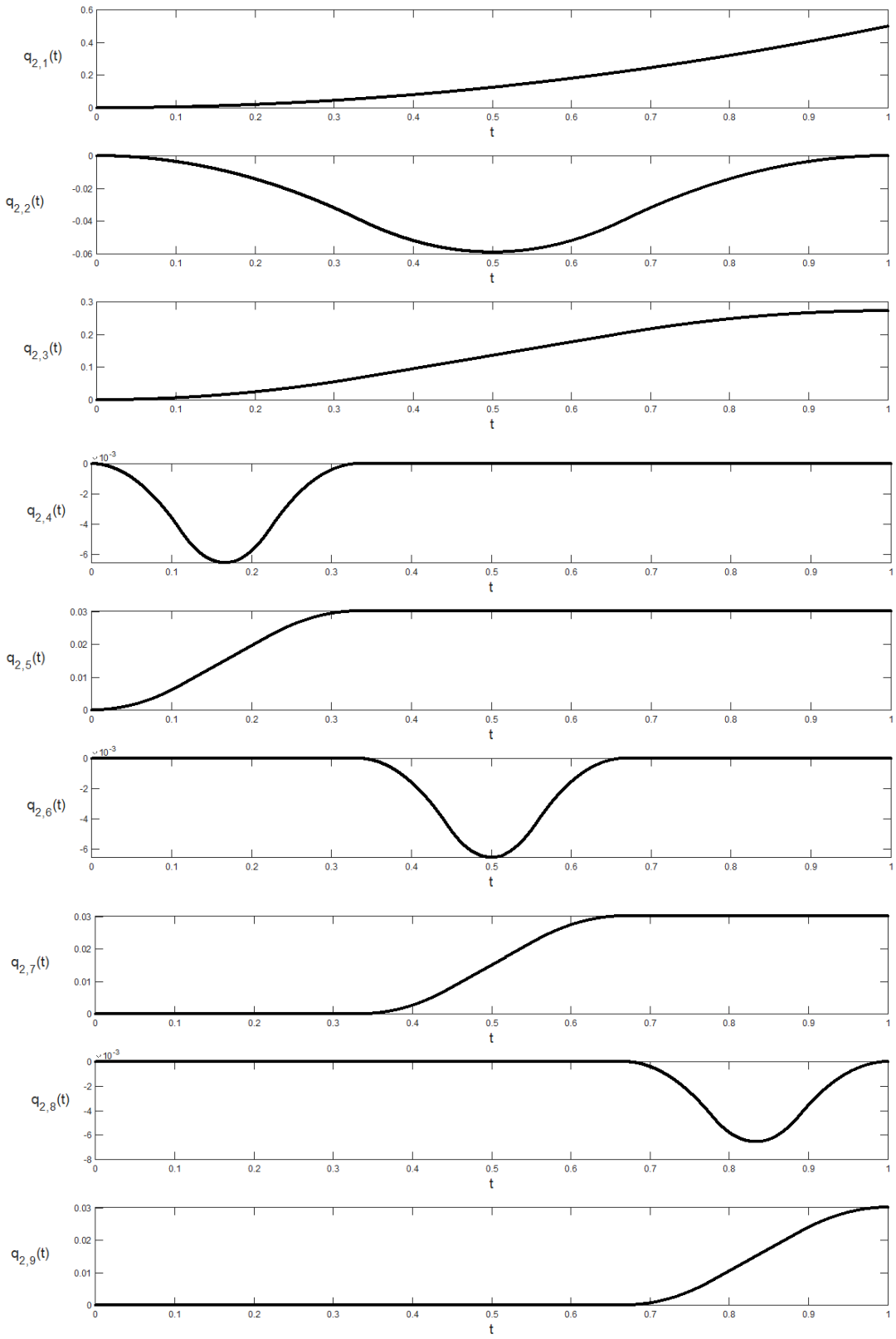

Figure 3.9: Second integral of the first nine members of the Haar Scale 3 wavelet family

3.3 Matrices of Haar Scale 3 Wavelets and their Integrals

To find the numerical solution of differential equations using Haar scale 3 wavelets, a discrete form of the Haar scale 3 wavelets series is required. There are many techniques to do this but we are restricting ourselves to the collocation method. Haar scale 3 wavelets are discontinuous in nature. Therefore, to avoid the collocation point at the point of discontinuity approach given in Equations (3.65)-(3.66) is applied for the selection of collocation points t_l.

$$t_l = \frac{(T_{l-1} + T_l)}{2} \quad , \quad l = 1,2,3 \cdots 3p, \qquad p = 3^j \tag{3.65}$$

Where

$$T_l = A + \frac{(B-A)}{3p} * l \quad , \quad l = 1,2,3 \cdots 3p \, , \qquad p = 3^j \tag{3.66}$$

Now replacing t with t_l in the above equations, a discrete form of wavelet can be obtained which can easily expressible in the matrix form. Now for $A = 0, B = 1$ and $J = 0$, we have the following Haar scale 3 matrix H and Matrices Q_1 , Q_2 of their first and second integrals.

$$A = 0, B = 1, j = 0 \Rightarrow T_0 = \frac{1}{3} \qquad T_2 = \frac{2}{6} \quad T_3 = \frac{5}{6} \qquad T_4 = \frac{5}{6}$$

Haar Scale 3 Wavelet matrix for the initial level of resolution $(j = 0)$

Collocation points $\Rightarrow$ $t_1 = \frac{1}{6}$ $t_2 = \frac{3}{6}$ $t_3 = \frac{5}{6}$

$$\text{H=} \begin{bmatrix} 1 & 1 & 1 \\ -0.70711 & 1.414214 & 0.70711 \\ 1.224745 & 0 & 1.224745 \end{bmatrix} \begin{matrix} \leftarrow h_1 \\ \leftarrow h_2 \\ \leftarrow h_3 \end{matrix}$$

First integral matrix Q_1 of Haar Scale 3 Wavelet matrix for the initial level of resolution $(j = 0)$

Collocation points $\Rightarrow$ $t_1 = \frac{1}{6}$ $t_2 = \frac{3}{6}$ $t_3 = \frac{5}{6}$

$$Q_1 = \begin{bmatrix} 0.167666666666667 & 0.500000000000000 & 0.833333333333333 \\ -0.117851130197758 & 0 & 0.117851130197758 \\ 0.204124145231931 & 0.408248290463863 & 0.204124145231932 \end{bmatrix} \begin{matrix} \leftarrow q_{1,1} \\ \leftarrow q_{1,2} \\ \leftarrow q_{1,3} \end{matrix}$$

Second integral matrix Q_2 of Haar Scale 3 Wavelet matrix for the initial level of resolution $(j = 0)$

Collocation points $\Rightarrow$ $t_1 = \frac{1}{6}$ $t_2 = \frac{3}{6}$ $t_3 = \frac{5}{6}$

$$Q_2 = \begin{bmatrix} 0.167666666666667 & 0.500000000000000 & 0.833333333333333 \\ -0.117851130197758 & 0 & 0.117851130197758 \\ 0.204124145231931 & 0.408248290463863 & 0.204124145231932 \end{bmatrix} \begin{matrix} \leftarrow q_{2,1} \\ \leftarrow q_{2,2} \\ \leftarrow q_{2,3} \end{matrix}$$

Haar Scale 3 Wavelet matrix for the next level of resolution ($j = 1$)

Coll. pts $\Rightarrow$ $t_1 = \frac{1}{18}$ $t_2 = \frac{3}{18}$ $t_3 = \frac{5}{18}$ $t_4 = \frac{7}{18}$ $t_5 = \frac{9}{18}$ $t_6 = \frac{11}{18}$ $t_7 = \frac{13}{18}$ $t_8 = \frac{15}{18}$ $t_9 = \frac{17}{18}$

$$H = \begin{bmatrix} 1 & 1 & 1 & 1 & 1 & 1 & 1 & 1 & 1 \\ -0.707 & -0.707 & -0.707 & 1.414 & 1.414 & 1.414 & -0.707 & -0.707 & -0.707 \\ 1.225 & 1.225 & 1.225 & 0 & 0 & 0 & -1.225 & -1.225 & -1.225 \\ -0.707 & 1.414 & -0.707 & 0 & 0 & 0 & 0 & 0 & 0 \\ 1.225 & 0 & -1.225 & 0 & 0 & 0 & 0 & 0 & 0 \\ 0 & 0 & 0 & -0.707 & 1.414 & -0.707 & 0 & 0 & 0 \\ 0 & 0 & 0 & 1.225 & 0 & -1.225 & 0 & 0 & 0 \\ 0 & 0 & 0 & 0 & 0 & 0 & -0.707 & 1.414 & -0.707 \\ 0 & 0 & 0 & 0 & 0 & 0 & 1.225 & 0 & -1.225 \end{bmatrix} \begin{matrix} \leftarrow h_1 \\ \leftarrow h_2 \\ \leftarrow h_3 \\ \leftarrow h_4 \\ \leftarrow h_5 \\ \leftarrow h_6 \\ \leftarrow h_7 \\ \leftarrow h_8 \\ \leftarrow h_9 \end{matrix}$$

First integral matrix Q_1 of Haar Scale 3 Wavelet matrix for the initial level of resolution ($j = 1$)

Coll. Pts $\Rightarrow$ $t_1 = \frac{1}{18}$ $t_2 = \frac{3}{18}$ $t_3 = \frac{5}{18}$ $t_4 = \frac{7}{18}$ $t_5 = \frac{9}{18}$ $t_6 = \frac{11}{18}$ $t_7 = \frac{13}{18}$ $t_8 = \frac{15}{18}$ $t_9 = \frac{17}{18}$

$$Q_1 = \begin{bmatrix} 0.056 & 0.167 & 0.278 & 0.389 & 0.500 & 0.611 & 0.722 & 0.833 & 0.944 \\ -0.039 & -0.118 & -0.196 & -0.157 & 0.000 & 0.157 & 0.196 & 0.118 & 0.039 \\ 0.068 & 0.204 & 0.340 & 0.408 & 0.408 & 0.408 & 0.340 & 0.204 & 0.068 \\ -0.039 & 0 & 0.039 & 0 & 0 & 0 & 0 & 0 & 0 \\ 0.068 & 0.136 & 0.068 & 0 & 0 & 0 & 0 & 0 & 0 \\ 0 & 0 & 0 & -0.039 & 0 & 0.039 & 0 & 0 & 0 \\ 0 & 0 & 0 & 0.068 & 0.136 & 0.068 & 0 & 0 & 0 \\ 0 & 0 & 0 & 0 & 0 & 0 & -0.039 & 0 & 0.039 \\ 0 & 0 & 0 & 0 & 0 & 0 & 0.068 & 0.136 & 0.068 \end{bmatrix} \begin{matrix} \leftarrow q_{1,1} \\ \leftarrow q_{1,2} \\ \leftarrow q_{1,3} \\ \leftarrow q_{1,4} \\ \leftarrow q_{1,5} \\ \leftarrow q_{1,6} \\ \leftarrow q_{1,7} \\ \leftarrow q_{1,8} \\ \leftarrow q_{1,9} \end{matrix}$$

Second integral matrix Q_2 of Haar Scale 3 Wavelet matrix for the initial level of resolution ($j = 1$)

Coll. Pts $\Rightarrow$ $t_1 = \frac{1}{18}$ $t_2 = \frac{3}{18}$ $t_3 = \frac{5}{18}$ $t_4 = \frac{7}{18}$ $t_5 = \frac{9}{18}$ $t_6 = \frac{11}{18}$ $t_7 = \frac{13}{18}$ $t_8 = \frac{15}{18}$ $t_9 = \frac{17}{18}$

$$Q_2 = \begin{bmatrix} 0.002 & 0.014 & 0.039 & 0.076 & 0.125 & 0.187 & 0.261 & 0.347 & 0.446 \\ -0.001 & -0.010 & -0.027 & -0.050 & -0.059 & -0.050 & -0.027 & -0.010 & -0.001 \\ 0.002 & 0.017 & 0.047 & 0.091 & 0.136 & 0.181 & 0.225 & 0.255 & 0.270 \\ -0.001 & -0.007 & -0.001 & 0 & 0 & 0 & 0 & 0 & 0 \\ 0.002 & 0.015 & 0.028 & 0.030 & 0.030 & 0.030 & 0.030 & 0.030 & 0.030 \\ 0 & 0 & 0 & -0.001 & -0.007 & -0.001 & 0 & 0 & 0 \\ 0 & 0 & 0 & 0.002 & 0.015 & 0.028 & 0.030 & 0.030 & 0.030 \\ 0 & 0 & 0 & 0 & 0 & 0 & -0.001 & -0.007 & -0.001 \\ 0 & 0 & 0 & 0 & 0 & 0 & 0.002 & 0.015 & 0.028 \end{bmatrix} \begin{matrix} \leftarrow q_{2,1} \\ \leftarrow q_{2,2} \\ \leftarrow q_{2,3} \\ \leftarrow q_{2,4} \\ \leftarrow q_{2,5} \\ \leftarrow q_{2,6} \\ \leftarrow q_{2,7} \\ \leftarrow q_{2,8} \\ \leftarrow q_{2,9} \end{matrix}$$

3.4 Approximation of Function Using Haar Scale 3 Wavelet Series

Consider any square-integrable function $f(t)$ over the interval $[A, B)$. Now to approximate $f(t)$ using Haar scale 3 wavelet family, $f(t)$ can be written as an infinite series of Haar scale three wavelet family as given in Equation (3.67)

$$f(t) = \sum_{i=0}^{\infty} a_i h_i(t) \\ = a_1 h_1(t) + \sum_{even\ i} a_i \psi^1(3^j t - k) + \sum_{odd\ i>1} a_i \psi^2(3^j t - k) \tag{3.67}$$

Here $a_i's$ are the wavelet coefficients and their values are to be determined by the proposed method. But for computational purposes, one can consider a finite number of terms. By considering the first $3p$ terms to approximate the function $f(t)$ we get Equation (3.68)

$$f(t) \approx f_{3p}(t) = \sum_{i=0}^{3p} a_i h_i(t) \quad , \quad p = 3^j \ , \ j = 0,1,2, \ldots \tag{3.68}$$

using the collocation points t_l , $l = 1,2,3\cdots$ in Equation (3.68), it takes the discrete form as given in Equation (3.69)

$$f(t_l) \approx f_{3p}(t) = \sum_{i=0}^{3p} a_i h_i(t_l) \quad , l = 1,2,3\cdots \tag{3.69}$$

The above equation can easily be expressible into the matrix form as

$$F = AH$$

Where H is the Haar matrix of order $3p \times 3p$ and F, A are the row matrices of order $1 \times 3p$.H and F are known matrices and the value of A can be evaluated by solving the above matrix system as

$$A = FH^{-1}$$

Then by substituting the values of unknown coefficients a_i's from the matrix $A = [a_i]_{1\times 3p}$ in the above equation, wavelet approximation of $f(t)$ at the desired level of resolution can be obtained. To test order of accuracy of approximation a well-defined L_2 ,L_∞ and absolute errors can be calculated which are defined as

$$\text{Absolute error} = |u_{exact}(t_l) - u_{num}(t_l)|$$

$$L_\infty = \max_l |u_{exact}(t_l) - u_{num}(t_l)|$$

$$L_2 = \frac{\sqrt{\sum_{l=1}^{3p} |u_{exact}(t_l) - u_{num}(t_l)|^2}}{\sqrt{\sum_{l=1}^{3p} |u_{exact}(t_l)|^2}}$$

where t_l represents the collocation points of the domain.

3.5 Numerical Experiments

Numerical Experiment No. 3.1: Consider a function $f(t) = t^2$ over the interval $(0,1)$.Now approximate the function $f(t)$ using the Haar scale 3 wavelet series at $J = 1$ as

$$f(t) = \sum_{i=0}^{3p} a_i h_i(t) \quad , \quad p = 3^1$$

using the collocation points $t_1 = \frac{1}{18}$ $t_2 = \frac{3}{18}$ $t_3 = \frac{5}{18}$ $t_4 = \frac{7}{18}$ $t_5 = \frac{9}{18}$ $t_6 = \frac{11}{18}$ $t_7 = \frac{13}{18}$ $t_8 = \frac{15}{18}$ $t_9 = \frac{17}{18}$ above equation transforms to a system of simultaneous linear equations which can be further be put in the matrix system as

$$AH = F$$

$$\begin{bmatrix} a_1 \\ a_2 \\ a_3 \\ a_4 \\ a_5 \\ a_6 \\ a_7 \\ a_8 \\ a_9 \end{bmatrix}^T \begin{bmatrix} 1 & 1 & 1 & 1 & 1 & 1 & 1 & 1 & 1 \\ -0.707 & -0.707 & -0.707 & 1.414 & 1.414 & 1.414 & -0.707 & -0.707 & -0.707 \\ 1.225 & 1.225 & 1.225 & 0 & 0 & 0 & -1.225 & -1.225 & -1.225 \\ -0.707 & 1.414 & -0.707 & 0 & 0 & 0 & 0 & 0 & 0 \\ 1.225 & 0 & -1.225 & 0 & 0 & 0 & 0 & 0 & 0 \\ 0 & 0 & 0 & -0.707 & 1.414 & -0.707 & 0 & 0 & 0 \\ 0 & 0 & 0 & 1.225 & 0 & -1.225 & 0 & 0 & 0 \\ 0 & 0 & 0 & 0 & 0 & 0 & -0.707 & 1.414 & -0.707 \\ 0 & 0 & 0 & 0 & 0 & 0 & 1.225 & 0 & -1.225 \end{bmatrix} = \begin{bmatrix} 0.0031 \\ 0.0278 \\ 0.0772 \\ 0.1512 \\ 0.2500 \\ 0.3735 \\ 0.5216 \\ 0.6944 \\ 0.8920 \end{bmatrix}$$

Solving the above matrix system using MATLAB software, following of Haar scale 3 coefficients are obtained

$a_1 = 0.3323$, $a_2 = -0.0524$, $a_3 = -0.2722$, $a_4 = -0.0058$, $a_5 = -0.0302$, $a_6 = -0.0058$ $a_7 = -0.0907$, $a_8 = -0.0058$, $a_9 = -0.1512$

By using these values of wavelet coefficients f(t) is approximated as follows

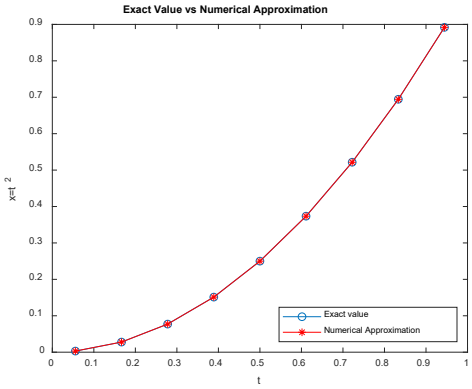

Fig.3.10a

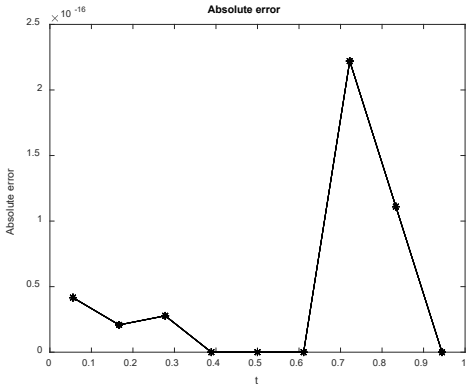

Fig.3.10b

Figure 3.10: Graph of approximation of function $f(t) = t^2$ in comparison with exact values at the different collocation points (Fig.3.10a) and absolute error(Fig.3.10b) in the approximation of a function by Haar scale 3 wavelets at $J = 1$.

Table 3.3: Comparison of the exact and approximated solution by Haar scale 3 Wavelets for Numerical Experiment No. 3.1

t	Exact Value (t^2)	Approximated value (t^2)	Absolute Error
0.0555555555555556	0.0030864197530864	0.0030864197530864	4.16E-17
0.1666666666666670	0.0277777777777778	0.0277777777777778	2.08E-17
0.2777777777777780	0.0771604938271605	0.0771604938271605	2.78E-17
0.3888888888888890	0.1512345679012350	0.1512345679012350	0.00E+00
0.5000000000000000	0.2500000000000000	0.2500000000000000	0.00E+00
0.6111111111111110	0.3734567901234570	0.3734567901234570	0.00E+00
0.7222222222222220	0.5216049382716050	0.5216049382716050	2.22E-16
0.8333333333333330	0.6944444444444440	0.6944444444444440	1.11E-16
0.9444444444444440	0.8919753086419750	0.8919753086419750	0.00E+00

Numerical Experiment No. 3.2 : Consider a function $f(t) = \sin t$ over the interval $(0,1)$.Now approximate the function $f(t)$ using the Haar scale 3 wavelet series at $J = 1$ as

$$f(t) = \sum_{i=0}^{3p} a_i h_i(t) \quad , \quad p = 3^1$$

using the collocation points $t_1 = \frac{1}{18}$ $t_2 = \frac{3}{18}$ $t_3 = \frac{5}{18}$ $t_4 = \frac{7}{18}$ $t_5 = \frac{9}{18}$ $t_6 = \frac{11}{18}$ $t_7 = \frac{13}{18}$ $t_8 = \frac{15}{18}$ $t_9 = \frac{17}{18}$ above equation transforms to a system of simultaneous linear equations which can be further be put in the matrix system as

$$\begin{bmatrix} a_1 \\ a_2 \\ a_3 \\ a_4 \\ a_5 \\ a_6 \\ a_7 \\ a_8 \\ a_9 \end{bmatrix}^T \begin{bmatrix} 1 & 1 & 1 & 1 & 1 & 1 & 1 & 1 & 1 \\ -0.707 & -0.707 & -0.707 & 1.414 & 1.414 & 1.414 & -0.707 & -0.707 & -0.707 \\ 1.225 & 1.225 & 1.225 & 0 & 0 & 0 & -1.225 & -1.225 & -1.225 \\ -0.707 & 1.414 & -0.707 & 0 & 0 & 0 & 0 & 0 & 0 \\ 1.225 & 0 & -1.225 & 0 & 0 & 0 & 0 & 0 & 0 \\ 0 & 0 & 0 & -0.707 & 1.414 & -0.707 & 0 & 0 & 0 \\ 0 & 0 & 0 & 1.225 & 0 & -1.225 & 0 & 0 & 0 \\ 0 & 0 & 0 & 0 & 0 & 0 & -0.707 & 1.414 & -0.707 \\ 0 & 0 & 0 & 0 & 0 & 0 & 1.225 & 0 & -1.225 \end{bmatrix} = \begin{bmatrix} 0.0555 \\ 0.1659 \\ 0.2742 \\ 0.3792 \\ 0.4794 \\ 0.5738 \\ 0.6611 \\ 0.7402 \\ 0.8102 \end{bmatrix}$$

Solving the above matrix system using MATLAB software, following of Haar scale 3 coefficients are obtained

a_1 =0.4599 , $a_2 = 0.0124$, $a_3 = -0.2335$, $a_4 = 0.0005$, $a_5 = -0.0893$, $a_6 = 0.0014$,a_7 =-0.0795, $a_8 = 0.0022$, $a_9 = -0.0609$

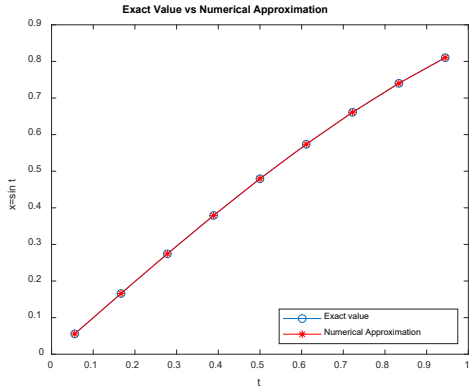

Fig.3.11a

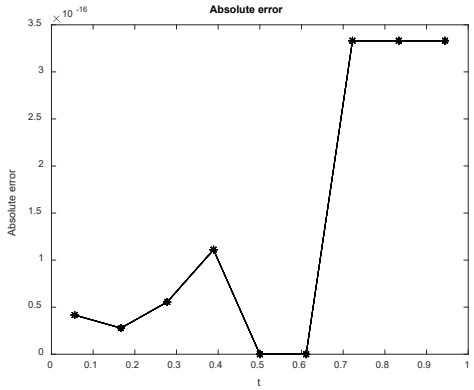

Fig.3.11b

Figure 3.11: Graph of approximation of function $f(t) = Sin\ t$ in comparison with exact values at the different collocation points (Fig.3.11a) and absolute error(Fig.3.11b) in the approximation of a function by Haar scale 3 wavelets at $J = 1$.

Table 3.4: Comparison of the exact and approximated solution by Haar scale 3 wavelets for Numerical Experiment No. 3.2

t	Exact Value ($Sin\ t$)	Approximated value ($Sin\ t$)	Absolute Error
0.0555555555555556	0.0555269820047339	0.0555269820047339	4.16E-17
0.1666666666666670	0.1658961326934150	0.1658961326934150	2.78E-17
0.2777777777777780	0.2742192892107270	0.2742192892107270	5.55E-17
0.3888888888888890	0.3791605039172600	0.3791605039172600	1.11E-16
0.5000000000000000	0.4794255386042030	0.4794255386042030	0.00E+00
0.6111111111111110	0.5737778263110660	0.5737778263110660	0.00E+00
0.7222222222222220	0.6610537218848880	0.6610537218848880	3.33E-16
0.8333333333333330	0.7401768531960370	0.7401768531960370	3.33E-16
0.9444444444444440	0.8101713960172990	0.8101713960172990	3.33E-16

3.6 Conclusion

Construction scheme introduced by Charles K. Chui, Jian-ao Lian has been followed to construct the compactly supported orthonormal Haar scale 3 nondyadic wavelet family. Haar Scale 3 function and their corresponding compactly supported symmetric and anti-symmetric wavelets are used and their general Integrals of nth order have been calculated by integrating then n-time. Matrices of Haar Scale 3 Wavelets and their Integrals have been calculated for the approximation of arbitrary function using the members of Haar scale 3 orthonormal wavelet families which will also be used to solve the various types of integral and differential equations in the subsequent chapters. Two functions of different types have been approximated using the Haar scale 3 wavelet families at the first level of resolution $J = 1$ and errors have been analyzed. It is found that error is of the order 10^{-16} which is the default precision level of MATLAB 7 software. In the next chapters, we will extend the application of the method to solve the various types of Differential equations (ODEs, PDEs, FDEs). The proposed Technique is well-suited and very much helpful with the computer environment. Common programs can be used to solve various types of problems.

Chapter 4

A Novel Haar Scale 3 Wavelet Based Hybrid Method for Finding the Solutions of Higher Order Boundary Value Problems

4.1 Introduction

Many physical phenomena like hydrodynamic and hydromagnetic stability [93], induction motor with two rotor circuits [116], viscoelastic flows in fluid dynamics, etc. are governed by the higher-order boundary value problems. Higher-order boundary value problems (HOBVPs) have been a major concern for the researchers, especially when these are nonlinear or higher-order linear ODE with variable coefficients. The existence and uniqueness of the solution for HOBVPs have already been established by Agarwal in his book [95]. But general closed-form solution for these kinds of problems has yet not been established. Therefore, researchers are using numerical techniques to find the solutions of HOBVPs. Many numerical mechanisms have been developed by the researchers to solve these problems such as Variational Iteration Decomposition Method (VIDM) [96], Optimal Homotopy Asymptotic Method (OHAM) [97], Galerkin Method with Quintic B-splines (GMQBS) [117], Legendre Galerkin Method (LGM) [99], Reproducing Kernel Space Method (RKSM) [100], Variational Iteration Method (VIM) [101] , Modified Variational Iteration Method (MVID) [102], Sextic B-splines Collocation Method (SBSCM) [103], Petrov-Galerkin Method (PGM)[104], Homotopy Perturbation Method (HPM) [118] , Quintic B-Spline Collocation Method (QBSCM) [119] , Haar Wavelet Collocation Method (HWCM) [120] with dilation factor 2, Modified Adomian Decomposition Method (MADM) [121] etc.

Wavelet-based numerical techniques are one of the latest techniques in the mathematical theory of approximation which are in considerable qualitative progress in comparison with other methods. The majority of the work has been done by using

Scale 2 dilation (dyadic) wavelets. Till date, no literature is available for the use of Haar scale 3 (non-dyadic) wavelets in finding the solution of higher-order boundary value problems. The existence of Haar scale 3 wavelets has been proved by Chui and Lian [115] in 1995 in the study of the construction of wavelets. This motivates and inspires us to use the Haar scale 3 wavelets with a collocation method for the solution of HOBVPs. In the present study, a new wavelet-based hybrid method is developed by using the Haar scale 3 wavelets with the collocation method.

The main objective of our work is to establish a Haar scale 3 wavelet-based collocation technique for the numerical solution of linear and nonlinear HOBVPs emerging in many physical phenomena. To test the efficiency and accuracy of the method, we consider the general HOBVPs of the type given in Equation (4.1)

$$x^n(t) = f(t, x, x', x'' \cdots \cdots \cdots x^{n-1}) \qquad a \le t \le b \tag{4.1}$$

with the constraints on the solution at the boundary points given in Equations (4.2)-(4.3)

$$\begin{aligned} x(a) = \nu_1, x(b) = \sigma_1, x'(a) = \nu_2, x'(b) = \sigma_2, \cdots \cdots, x^{\left(\frac{n}{2}-1\right)}(a) \\ = \nu_{\frac{n}{2}}, x^{\left(\frac{n}{2}-1\right)}(b) = \sigma_{\frac{n}{2}}, \qquad \text{if n is even integer} \end{aligned} \tag{4.2}$$

$$\begin{aligned} x(a) = \gamma_1, x(b) = \delta_1, x'(a) = \gamma_2, x'(b) = \delta_2, \cdots \cdots, \ x^{\left(\frac{n-1}{2}-1\right)}(a) \\ = \gamma_{\frac{n-1}{2}}, x^{\left(\frac{n-1}{2}\right)}(b) = \delta_{\frac{n+1}{2}}, \qquad \text{if n is an odd integer} \end{aligned} \tag{4.3}$$

where $\nu_1, \nu_2 \cdots \nu_{\frac{n}{2}}, \sigma_1, \sigma_2, \cdots, \sigma_{\frac{n}{2}}, \gamma_1, \gamma_2, \ldots \ldots, \gamma_{\frac{n+1}{2}}, \delta_1, \delta_2, \cdots \cdots, \delta_{\frac{n-1}{2}}$ are the real constants

This chapter is prearranged into the sections as follows. In section 2, the Haar scale 3 wavelet and its integrals are briefly described. In this section, the wavelet family has also been generated with the help of a multiresolution analysis. The approximation of solution by Haar scale 3 wavelets is briefly described in section 3. The convergence of the method is given in section 4. To validate the proposed method, eleven non-linear and linear higher-order boundary value problems are considered in section 5. In this section performance of the proposed method is compared with other methods to demonstrate the efficiency and accuracy of the method. Error analysis and convergence

of the proposed method have also been discussed for each of the examples at different levels of resolution in section 5. In the last section, conclusions are drawn from the results of Numerical Experiments and ideas for future research is given.

4.2 Haar Scale 3 wavelets and their integrals

The explicit mathematical expressions of Haar scale 3 function and mother wavelets for Haar scale 3 wavelet family with dilation factor three [71], [115] are given in the Equations (4.4)-(4.6)

$$\text{Haar scaling function } \varphi(t) = \begin{cases} 1 & 0 \le t < 1 \\ 0 & elsewhere \end{cases} \tag{4.4}$$

$$\text{Haar symmetric wavelet } \psi_1(t) = \frac{1}{\sqrt{2}} \begin{cases} -1 & 0 \le t < \frac{1}{3} \\ 2 & \frac{1}{3} \le t < \frac{2}{3} \\ -1 & \frac{2}{3} \le t < 1 \\ 0 & elsewhere \end{cases} \tag{4.5}$$

$$\text{Haar antisymmetric wavelet } \psi_2(t) = \sqrt{\frac{3}{2}} \begin{cases} 1 & 0 \le t < \frac{1}{3} \\ 0 & \frac{1}{3} \le t < \frac{2}{3} \\ -1 & \frac{2}{3} \le t < 1 \\ 0 & elsewhere \end{cases} \tag{4.6}$$

The main difference between the Haar scale 2 and Haar scale 3 wavelet family is that, in the construction of Haar scale 2 wavelet family, we get only one mother wavelet to generate whole wavelet family, but in the case of Haar scale 3 wavelet family, we get more than one mother wavelets to generate whole wavelet family, which increases the rate of convergence of the solution. In the case of dilation factor 3, two wavelets represented by Equations (4.5) and (4.6) are obtained to generate the whole wavelet family. The construction of the Haar scale 3 wavelet family is done by using the properties of Multi-resolution analysis which are described below.

4.2.1 Multi-resolution Analysis (MRA)

A multi-resolution analysis(MRA) of $L_2(R)$ is defined as a sequence of closed subspace $W_j, V_j \subset L_2(R), j \in \mathbb{Z}$ with the following properties (where $L_2(R)$ is vector space of square integral functions)

a) $\phi(t) \in V_0 \implies \phi(3^j t) \in V_j,$

b) $\phi(t) \in V_0 \implies \varphi(3^j t - k) \in V_j$

c) $\psi^i(t) \in W_0^i,\ i = 1,2 \implies \psi^i(3^j t) \in W_j^i$

d) $\psi^i(t) \in W_0^i,\ i = 1,2 \implies \psi^i(3^j t - k) \in W_j^i$

e) $W_J = W_j^1 \oplus W_j^2 = \oplus W_j^i\ , i = 1,2$

f) $\cdots \subset V_0 \subset V_1 \subset V_2 \subset V_3 \subset V_4 \subset \cdots$

g) $\cdots \perp W_0 \perp W_1 \perp W_2 \perp W_3 \perp W_4 \perp \cdots$

h) $V_j = V_0 + \sum_{i=0}^{j-1} W_j^1 + \sum_{i=0}^{j-1} W_j^2$

i) $\phi(t) \in V_0 \implies \phi(\mathrm{t} - \mathrm{k}) \in V_0; k \in \mathbb{Z}$ is a Riesz Basis in V_0

Now by applying MRA, generalized form of Haar scale 3 wavelet family is obtained and is represented by the Equations (4.7)-(4.9)

$$h_i(t) = \varphi(t) = \begin{cases} 1 & 0 \le t < 1 \\ 0 & elsewhere \end{cases} \qquad \text{for } i = 1 \tag{4.7}$$

$$h_i(t) = \psi^1(3^j t - k) = \frac{1}{\sqrt{2}} \begin{cases} -1 & \varkappa_1(i) \le t < \varkappa_2(i) \\ 2 & \varkappa_2(i) \le t < \varkappa_3(i) \\ -1 & \varkappa_3(i) \le t < \varkappa_4(i) \\ 0 & elsewhere \end{cases}, \quad for \quad i = 2,4, \ldots 3p - 1 \tag{4.8}$$

$$h_i(t) = \psi^2(3^j t - k) = \sqrt{\frac{3}{2}} \begin{cases} 1 & \varkappa_1(i) \le t < \varkappa_2(i) \\ 0 & \varkappa_2(i) \le t < \varkappa_3(i) \\ -1 & \varkappa_3(i) \le t < \varkappa_4(i) \\ 0 & elsewhere \end{cases}, \quad for \quad i = 3,6, \ldots 3p \tag{4.9}$$

where $\varkappa_1(i) = \frac{k}{p}$, $\varkappa_2(i) = \frac{3k+1}{3p}$, $\varkappa_3(i) = \frac{(3k+2)}{3p}$, $\varkappa_4(i) = \frac{k+1}{p}$, $p = 3^j$, $j = 0,1,2, \ldots$, $k = 0,1,2, \ldots, p-1$. Here $i > 1$ represents wavelet number calculated from the relations $i - 1 = p + 2k$ (for even i) and $i - 2 = p + 2k$ (for odd i), j represents the level of dilation/resolution of the wavelet (as we increase the value of j support of wavelet decreases) and k represents the translation parameters of the wavelet. The function $h_1(t)$ is called father wavelet, $h_2(t)$ and $h_3(t)$ are mother wavelets and all other

functions $h_4(t), h_5(t), h_6(t), \ldots$ are generated from translation and dilation of the mother wavelets are called daughter wavelets.

Using the explicit mathematical expression of Haar scale 3 wavelet family given in Equations (4.4)-(4.9), we can integrate over the interval [0,1) as many time as required by using the formula given in Equation (4.10)

$$q_{m,i}(t) = \int_0^t \int_0^t \int_0^t \cdots\cdots m\ times \cdots\cdots \int_0^t h_i(x)(dx)^m = \frac{1}{(m-1)!}\int_0^t (t-x)^{m-1} h_i(x)dx\ ,\quad m = 1,2,3 \ldots\ldots\ldots\ ,\ i = 1,2,3, \ldots\ldots\ldots 3p \tag{4.10}$$

After evaluating the above integrals for Equation (4.7), we get Equation (4.11)

$$q_{\beta,i}(t) = \frac{t^m}{m!} \quad for \quad i = 1 \tag{4.11}$$

Using Equation (4.10) on Equation (4.8), we get the values of $q_{m,i}(t)'s \quad for \quad i = 2,4,6,8,\cdots, 3p-1$ which are given by Equation (4.12)

$$q_{m,i}(t) = \frac{1}{\sqrt{2}}\begin{cases} 0 & for \quad 0 \le t \le \varkappa_1(i) \\ \frac{-1}{m!}\left(t-\varkappa_1(i)\right)^m & for \quad \varkappa_1(i) \le t \le \varkappa_2(i) \\ \frac{1}{m!}\left[-\left(t-\varkappa_1(i)\right)^m + 3\left(t-\varkappa_2(i)\right)^m\right] & for \quad \varkappa_2(i) \le t \le \varkappa_3(i) \\ \frac{1}{m!}\left[-\left(t-\varkappa_1(i)\right)^m + 3\left(t-\varkappa_2(i)\right)^m - 3\left(t-\varkappa_3(i)\right)^m\right] & for\ \varkappa_3(i) \le t \le \varkappa_4(i) \\ \frac{1}{m!}\left[-\left(t-\varkappa_1(i)\right)^m + 3\left(t-\varkappa_2(i)\right)^m - 3\left(t-\varkappa_3(i)\right)^m + \left(t-\varkappa_4(i)\right)^m\right] & for\ \varkappa_4(i) \le t \le 1 \end{cases} \tag{4.12}$$

Using Equation (4.10) on Equation (4.9), we get the values of $q_{m,i}(t)'s \quad for \quad i = 3,5,7,9,\cdots, 3p$ which are given by Equation (4.13)

$$q_{m,i}(t) = \sqrt{\frac{3}{2}}\begin{cases} 0 & for \quad 0 \le t \le \varkappa_1(i) \\ \frac{1}{m!}\left(t-\varkappa_1(i)\right)^m & for \quad \varkappa_1(i) \le t \le \varkappa_2(i) \\ \frac{1}{m!}\left[\left(t-\varkappa_1(i)\right)^m - \left(t-\varkappa_2(i)\right)^m\right] & for \quad \varkappa_2(i) \le t \le \varkappa_3(i) \\ \frac{1}{m!}\left[\left(t-\varkappa_1(i)\right)^m - \left(t-\varkappa_2(i)\right)^m - \left(t-\varkappa_3(i)\right)^m\right] & for \quad \varkappa_3(i) \le t \le \varkappa_4(i) \\ \frac{1}{m!}\left[\left(t-\varkappa_1(i)\right)^m - \left(t-\varkappa_2(i)\right)^m - \left(t-\varkappa_3(i)\right)^m + \left(t-\varkappa_4(i)\right)^m\right] & for\ \varkappa_4(i) \le t \le 1 \end{cases} \tag{4.13}$$

4.3 Approximation of Function by Haar scale 3 Wavelets

Theorem 4.3.1: Let $x(t)$ be any square integrable function over the interval $[A, B)$ whose highest order derivative is expressible as a linear combination of Haar wavelet

family as $x^n(t) = \sum_{i=0}^{3p} a_i h_i(t)$. Then all derivatives of x(t) of order less than n are given by

$$x^m(t) = \sum_{i=1}^{3p} a_i q_{n-m,i}(t) + \sum_{\nu=0}^{n-m-1} \frac{(t-A)^\nu}{\nu!} x^{m+\nu}(A) \quad for \quad m = 0,1,2,3 \cdots \cdots \cdots n-2, n-1$$

Proof: We have $x^n(t) = \sum_{i=0}^{3p} a_i h_i(t)$.

Integrating $x^n(t)$ one-time w.r.t t within the limits A to t we get

$$x^{n-1}(t) = \sum_{i=1}^{3p} a_i q_{1,i}(t) + x^{n-1}(A)$$

The theorem is proved by using the principle of mathematical induction on $N (= n - m)$

Take $N = 1 \Rightarrow n - m = 1 \Rightarrow m = n - 1$, by putting $m = n - 1$ we get

$$x^{n-1}(t) = \sum_{i=1}^{3p} a_i q_{1,i}(t) + x^{n-1}(A)$$

which is the same as calculated above. Hence the result is true for N=1

Now assume that the result is true for $N = n - m = k$.

Put $N = k \Rightarrow n - m = k \Rightarrow m = n - k$ in

$$x^{n-k}(t) = \sum_{i=1}^{3p} a_i q_{k,i}(t) + \sum_{\nu=0}^{k-1} \frac{(t-A)^\nu}{\nu!} x^{(n-k)+\nu}(A)$$

To prove the result for $N = k + 1$, integrating the above equation within the limits A to t, we get

$$x^{n-k-1}(t) = \sum_{i=1}^{3p} a_i q_{k+1,i}(t) + \sum_{\nu=0}^{k-1} \frac{(t-A)^{\nu+1}}{(\nu+1)!} x^{(n-k)+\nu}(A) + x^{n-k-1}(A)$$

$$x^{n-k-1}(t) = \sum_{i=1}^{3p} a_i q_{k+1,i}(t) + x^{n-k-1}(A) + \left[\frac{(t-A)^1}{1!} x^{(n-k)}(A) + \frac{(t-A)^2}{2!} x^{(n-k)+1}(A) + \cdots + \frac{(t-A)^k}{k!} x^{(n-k)+(k-1)}(A)\right]$$

$$x^{n-k-1}(t) = \sum_{i=1}^{3p} a_i q_{k+1,i}(t) + \frac{(t-A)^0}{0!} x^{n-(k+1)}(A) + \left[\frac{(t-A)^1}{1!} x^{(n-(k+1))+1}(A) + \frac{(t-A)^2}{2!} x^{(n-(k+1)+2}(A) + \cdots + \frac{(t-A)^k}{k!} x^{(n-(k+1)+k}(A)\right]$$

$$x^{n-(k+1)}(t) = \sum_{i=1}^{3p} a_i q_{k+1,i}(t) + \sum_{\nu=0}^{(k+1)-1} \frac{(t-A)^\nu}{\nu!} x^{(n-(k+1))+\nu}(A)$$

Hence the result is true for $N = n - m = K + 1$. Therefore, the result is true for all the derivatives of x(t). which completes the proof.

Since the members of the family of Haar scale 3 wavelets are orthogonal to each other, thus by using theorem 4.3.2 and the properties of wavelets, any square-integrable function $x(t)$ over the interval [0,1) can be expressed as an infinite series of scale 3 Haar wavelet bases as given in Equation (4.14)

$$x(t) = \sum_{i=0}^{\infty} a_i h_i(t) = a_1 h_i(t) + \sum_{even\ i} a_i \psi^1(3^j t - k) + \sum_{odd\ i} a_i \psi^2(3^j t - k) \tag{4.14}$$

Here $a_i's$ are Haar wavelet coefficients whose values can be calculated as $a_i = \int_0^1 x(t)\, h_i(t) dt$, $i = 1,2,3, \ldots 3p$. In practice, only the finite number of terms are considered, hence considering the first $3p$ terms, where $p = 3^j$, $j = 0,1,2, \ldots$ to approximate the function $x(t)$ we get Equation (4.15)

$$x(t) \approx x_{3p} = \sum_{i=0}^{3p} a_i h_i(t) \tag{4.15}$$

4.4 Convergence Analysis

It has been proved by the Mittal and Pandit [71] that if $x(t)$ is any differentiable function such that $|x'(t)| \leq M\ \forall\ t \in (0,1)$ for some positive real constant M and x(t) is approximated by Haar wavelet family as given below:

$$x_{3p}(t) = \sum_{i=0}^{3p} a_i h_i(t)$$

Then the error bound calculated for Haar wavelet approximation of function $x(t)$ by L_2-norm is given by the Equation (4.16)

$$\left\|x(t) - x_{3p}(t)\right\| \leq \frac{M}{\sqrt{24}}\frac{1}{3^j} = o\left(\frac{1}{p}\right) \tag{4.16}$$

which means if we know the exact value of M then we can get the exact error bound for the approximation. Also, with the increase in the level of resolution (the value of j or p=3^j) error decreased which proves the convergence for approximate solutions to the exact solution. This concept of convergence is also presented by the numerical experiments performed on the following problems.

4.5 Numerical Experiments and Error Analysis

To describe the applicability and effectiveness of the proposed mechanism, eleven linear and nonlinear higher-order boundary value problems have been solved. To check the efficiency of the proposed method L_2 ,L_∞ and absolute errors are calculated which are defined as

$$\text{Absolute error} = |u_{exact}(t_l) - u_{num}(t_l)|$$

$$L_\infty = \max_l |u_{exact}(t_l) - u_{num}(t_l)|$$

$$L_2 = \frac{\sqrt{\sum_{l=1}^{3p} |u_{exact}(t_l) - u_{num}(t_l)|^2}}{\sqrt{\sum_{l=1}^{3p} |u_{exact}(t_l)|^2}}$$

where t_l represents the collocation points of the domain.

Numerical Experiment No. 4.1: - Consider the *eighth order linear* differential equation

$$\frac{d^8x(t)}{dt^8} - x(t) = -8e^t \quad , \quad 0 \leq t \leq 1 \tag{4.17}$$

with the following types of constraints on the solution at the boundary points

$x(0) = 1, x'(0) = 0, x''(0) = -1, x'''(0) = -2, x(1) = 0, x'(1) = -e\,, x''(1) = -2e\,, x'''(1) = -3e$

Analytic solution of the problem is $x(t) = (1-t)e^t$.

The present method is applied to the above problem to test the efficiency of the method and the following solution is obtained:

$x(t) = \sum_{i=1}^{3p} a_i[q_{8,i}(t) - f_1(t)q_{8,i}(1) - f_2(t)q_{7,i}(1) - f_3(t)q_{6,i}(1) - f_4(t)q_{5,i}(1)] - \frac{1}{6}f_1(t) - (e-2)f_2(t) - (2e-3)f_3(t) - (3e-2)f_4(t) - \frac{t^3}{2} - \frac{t^2}{2} + 1$, where

$$f_1(t) = -20t^7 + 70t^6 - 84t^5 + 35t^4 \, , f_2(t) = 10t^7 - 34t^6 + 39t^5 - 15t^4$$

$$f_3(t) = -2t^7 + 6.5t^6 - 7t^5 + 2.5t^4 \, , f_4(t) = \frac{1}{6}t^7 - \frac{1}{2}t^6 + \frac{1}{2}t^5 - \frac{1}{6}t^4,$$

These $a_i's$ are the wavelets coefficients and $q_{j,i}'s$ are the wavelet integrals.

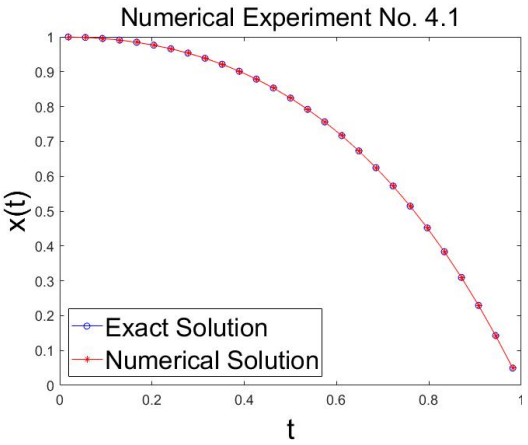

Figure 4.1:Comparison of exact and numerical solution for Numerical Experiment No.4.1

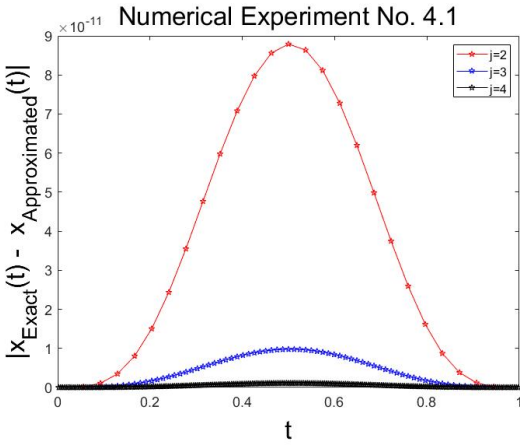

Figure 4.2: Absolute Error at different level of resolution $J = 2,3,4$ in Numerical Experiment No. 4.1

Table 4.1: Exact and Approximated solution by HS3WCM for j=1 for Numerical Experiment No. 4.1

$x(t)$	Exact Solution	Approximated Solution by HS3WCM
0.0556	0.998398425606890	0.998398425605433
0.1667	0.984467010721372	0.984467010648896
0.2778	0.953472569424642	0.953472569105286
0.3889	0.901597042799825	0.901597042162876
0.5000	0.824360635350064	0.824360634559944
0.6111	0.716519011851887	0.716519011198242
0.7222	0.571945470614687	0.571945470278510
0.8333	0.383495981815471	0.383495981737315
0.9444	0.142854690821557	0.142854690819942

The solution is also presented in the form of tables and figures for different collocation points at different levels of resolution for better visibility of results. It is shown in Figure 4.1 and Table 4.1 that the results obtained from the present method are in good

agreement with the exact solution for different values of j (levels of resolution). From Figure 4.2 and Table 4.2, it can be concluded that the errors are reducing by increasing the level of resolution which ensures the convergence of the method. Moreover, L_2 and L_∞ errors at j=1 are 5.60E-10 and 7.90E-10 respectively which are less than error obtained in case of Haar scale 2 wavelet shown in Table 4.3 shows the comparison of the accuracy of results obtained by the present method, Variational Iteration Decomposition Method (VIDM)[96] and optimal Homotopy asymptotic method (OHAM)[97]. It can be concluded from the obtained results, that the present method is providing better results as compared to other methods, which verifies the efficiency and reliability of the method.

Table 4.2: L_2 , L_∞ errors at different level of resolution for Numerical Experiment No.4.1

Level of Resolution (j)	**L_2-error**	**L_2-error**	**L_∞-error**	**L_∞-error**
	Haar scale 2 wavelet	**Haar scale 3 wavelet**	**Haar scale 2 wavelet**	**Haar scale 3 wavelet**
0	1.33E-08	5.40E-09	1.36E-08	7.16E-09
1	2.79E-09	5.60E-10	3.06E-09	7.90E-10
2	7.08E-10	6.23E-11	9.45E-10	8.79E-11
3	1.77E-10	6.92E-12	2.47E-10	9.77E-12
4	4.43E-11	7.69E-13	6.25E-11	1.09E-12
5	1.11E-11	8.54E-14	1.56E-11	1.21E-13
6	2.77E-12	9.52E-15	3.91E-12	1.38E-14

Table 4.3: Comparision of Numerical results at Random collocation Points available in Literature for Numerical Experiment No. 4.1

x(t)	**Exact Solution**	**Approximated Solution**	**HS3WCM(E^*)**	**VIDM(E^*)** [96]	**OHAM(E^*)** [97]
0.1	0.994653826268083	0.994653826215959	5.21E-11	6.71E-08	2.55E-09
0.2	0.977122206528136	0.977122206231891	2.96E-10	1.27E-07	2.84E-09
0.3	0.944901165303202	0.944901165118273	1.85E-10	1.75E-07	3.12E-09
0.4	0.895094818584762	0.895094819504096	9.19E-10	2.06E-07	3.40E-09
0.5	0.824360635350064	0.824360637948572	2.60E-09	2.18E-07	3.67E-09
0.6	0.728847520156204	0.728847523706210	3.55E-09	2.08E-07	3.94E-09
0.7	0.604125812241143	0.604125815143196	2.90E-09	1.78E-07	4.20E-09
0.8	0.445108185698494	0.445108186965076	1.27E-09	1.29E-07	4.45E-09
0.9	0.245960311115695	0.245960311272646	1.57E-10	6.66E-08	4.70E-09

E^* (Absolute Error) =Exact Solution-Approximate Solution

Numerical Experiment No. 4.2 : - Consider the *eighth order linear* differential equation given as:

$$\frac{d^8x(t)}{dt^8}+\frac{d^7x(t)}{dt^7}+\frac{d^6x(t)}{dt^6}+\frac{d^5x(t)}{dt^5}+\frac{d^4x(t)}{dt^4}+\frac{d^3x(t)}{dt^3}+\frac{d^2x(t)}{dt^2}+\frac{dx(t)}{dt}+x(t)= 14\cos t-16\sin t-4tsint \ ,0\le t\le 1 \quad (4.18)$$

with the following types of constraints on the solution at the boundary points $x(0)=0, x'(0)=-1, x''(0)=0, x'''(0)=7, x(1)=0, x'(1)=2sin1\ , x''(1)=4\cos 1+2\sin 1, x'''(1)=6\cos 1-6\sin 1$

Analytic solution of the problem is $x(t)=(t^2-1)\sin t$.

We proposed the following approximate solution of this problem based on the Haar scale 3 wavelet mechanism which satisfies the given boundary conditions

$x(t)=\sum_{i=1}^{3p} a_i[q_{8,i}(t)-f_1(t)q_{8,i}(1)-f_2(t)q_{7,i}(1)-f_3(t)q_{6,i}(1)-f_4(t)q_{5,i}(1)]-\frac{1}{6}f_1(t)+\left(2\sin 1-\frac{5}{2}\right)f_2(t)+(4\cos 1+2\sin 1-7)f_3(t)+(6\cos 1-6\sin 1-7)f_4(t)+\frac{7t^3}{6}-t$, Where

$f_1(t)=-20t^7+70t^6-84t^5+35t^4,\ f_2(t)=10t^7-34t^6+39t^5-15t^4$

$f_3(t)=-2t^7+6.5t^6-7t^5+2.5t^4,\ f_4(t)=\frac{1}{6}t^7-\frac{1}{2}t^6+\frac{1}{2}t^5-\frac{1}{6}t^4$

These $a_i's$ are the wavelets coefficients and $q_{j,i}'s$ are the wavelet integrals.

The obtained solution is compared with the exact solution at the second level of resolutions in Table 4.4 and Figure 4.3. Note that the obtained solution and exact solution are roughly coincided, which explains the high accuracy obtained by the proposed method for a small number of grid points. L_2 and L_∞ errors at j=1 are 1.16E-08, 5.53E-09 respectively which are less than the error obtained in the case of Haar scale 2 wavelets shown in Table 4.5. It can be concluded from Table 4.5 and Figure 4.4 that with the increase in the level of resolution j, the error between the exact solution and obtained solution decreases which ensures the convergence of the proposed solution to the exact solution. In Table 4.6 performance of the proposed method is compared with the Galerkin Method with Septic B-splines[114] and Legendre Galerkin method [99]. We infer that our method is working better than the methods [114] [99] given in Table 2b.

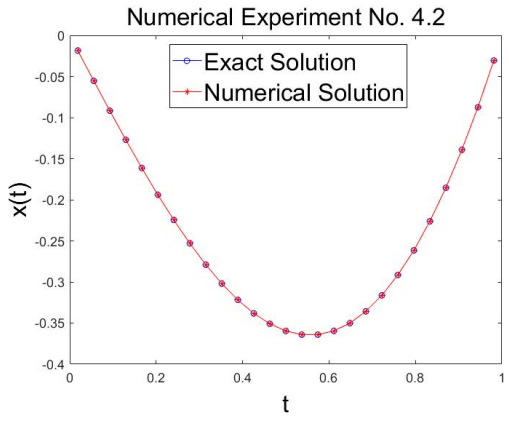

Figure 4.3: Comparison of exact and numerical solution for Numerical Experiment No. 4.2

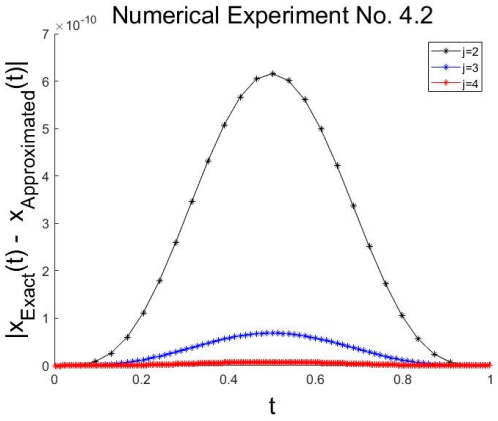

Figure 4.4: Absolute Error at different level of resolution $J = 2,3,4$ in Numerical Experiment No. 4.2

Table 4.4: Exact and Approximated solution by HS3WCM for j=1 for Numerical Experiment No. 4.2

$x(t)$	**Exact Solution**	**Approximated Solution by HS3WCM**
0.0556	-0.055355602430645	-0.055355602419651
0.1667	-0.161287906785265	-0.161287906248417
0.2778	-0.253060393438294	-0.253060391112554
0.3889	-0.321818328942119	-0.321818324390107
0.5000	-0.359569153953152	-0.359569148418721
0.6111	-0.359496601052921	-0.359496596569607
0.7222	-0.316244836086907	-0.316244833830374
0.8333	-0.226165149587678	-0.226165149074205
0.9444	-0.087518515001869	-0.087518514991516

Table 4.5: L_2 and L_∞ errors at different level of resolution for Numerical Experiment No. 4.2

Level of Resolution (j)	L_2**-error**	L_2**-error**	L_∞**-error**	L_∞**-error**
	Haar scale 2 wavelet	**Haar scale 3 wavelet**	**Haar scale 2 wavelet**	**Haar scale 3 wavelet**
0	2.00E-07	1.10E-07	6.89E-08	4.93E-08
1	5.79E-08	1.16E-08	2.14E-08	5.53E-09
2	1.47E-08	1.29E-09	6.60E-09	6.16E-10
3	3.67E-09	1.43E-10	1.73E-09	6.85E-11
4	9.19E-10	1.59E-11	4.37E-10	7.61E-12
5	2.30E-10	1.77E-12	1.10E-10	8.45E-13
6	5.74E-11	1.97E-13	2.74E-11	9.41E-14

Table 4.6: Comparison of Numerical results at Random collocation Points available in Literature for Numerical Experiment No. 4.2

x(t)	Exact	Approximated	HS3WCM(E*)	GMQBS(E*) [114]	LGM(E*) [99]
0.1	-0.098835082480360	-0.098835083008578	5.28E-10	3.80E-07	5.04E-08
0.2	-0.190722557563259	-0.190722561614420	4.05E-09	2.15E-06	5.14E-07
0.3	-0.268923388061819	-0.268923396590150	8.53E-09	5.63E-06	1.56E-10
0.4	-0.327111407539266	-0.327111416381471	8.84E-09	9.75E-06	2.71E-06
0.5	-0.359569153953152	-0.359569157955952	4.00E-09	1.14E-05	3.26E-06
0.6	-0.361371182972823	-0.361371181204998	1.77E-09	1.01E-05	2.82E-06
0.7	-0.328551020491222	-0.328551016592605	3.90E-09	7.27E-06	1.68E-06
0.8	-0.258248192723828	-0.258248190503417	2.22E-09	3.87E-06	5.78E-07
0.9	-0.148832112829222	-0.148832112522090	3.07E-10	1.43E-06	5.88E-08

E^* (Absolute Error) =Exact Solution-Approximate Solution

Numerical Experiment No. 4.3 : - Consider the *eighth order non-linear* differential equation

$$\frac{d^8x(t)}{dt^8} = (x(t))^2e^{-t} \quad , 0 \le t \le 1 \tag{4.19}$$

with the following types of constraints on the solution at the boundary points

$x(0) = 1, x'(0) = 1, x''(0) = 1, x'''(0) = 1, x(1) = e\ , x'(1) = e\ , x''(1) = e\ , x'''(1) = e.$

Analytic solution of the problem is $x(t) = e^t$.

In this problem, non-linearity in the differential equation is tackled by the Quasilinearization technique. By using Quasilinearization technique, above non-linear differential equation is transformed into a sequence of linear differential equations as given in Equation (4.20)

$$\frac{d^8x_{r+1}(t)}{dt^8} - 2e^{-t}x_rx_{r+1} = -x_r^2e^{-t} \quad , \qquad 0 \le t \le 1 \qquad\qquad r = 0,1,2\cdots \tag{4.20}$$

subjected to the boundary conditions

$x_{r+1}(0) = 1, x'_{r+1}(0) = 1, x''_{r+1}(0) = 1, x'''_{r+1}(0) = 1, x_{r+1}(1) = e\ , x'_{r+1}(1) = e\ ,$

$x''_{r+1}(1) = e\ , x'''_{r+1}(1) = e$ where $x_{r+1}(t)$ is the $(r+1)$th approximation for $x(t)$.

Then by applying the present method on the sequence of linear differential equations, we proposed the following solution:

$$x(t) = \sum_{i=1}^{3p} a_i[q_{8,i}(t) - f_1(t)q_{8,i}(1) - f_2(t)q_{7,i}(1) - f_3(t)q_{6,i}(1) - f_4(t)q_{5,i}(1)] + \left(e - \frac{8}{3}\right) f_1(t) + \left(e - \frac{5}{2}\right) f_2(t) + (e-2)f_3(t) + (e-1)f_4(t) + \frac{t^3}{3!} + \frac{t^2}{2!} + t + 1$$

where

$$f_1(t) = -20t^7 + 70t^6 - 84t^5 + 35t^4$$

$$f_2(t) = 10t^7 - 34t^6 + 39t^5 - 15t^4$$

$$f_3(t) = -2t^7 + 6.5t^6 - 7t^5 + 2.5t^4$$

$$f_4(t) = \frac{1}{6}t^7 - \frac{1}{2}t^6 + \frac{1}{2}t^5 - \frac{1}{6}t^4$$

These $a_i's$ are the wavelets coefficients and $q_{j,i}'s$ are the wavelet integrals.

The solution obtained by the present method is explained with the help of tables and figures. Table 4.7 and Figure 4.5 shows the comparison between the exact and obtained solution for the Equation (4.19) at j=1 which explains the high accuracy obtained by the proposed method for a small number of grid points (in this case only 9 grid pts). L_2 and L_∞ errors at j=1 are 2.54E-11, 8.30E-11 respectively which is less than error obtained in case of Haar scale 2 wavelets. Table 4.8 and Figure 4.6 ensures the convergence of the present solution to the exact solution. The performance of the present method is compared with the other methods in Table 4.9 and it can be concluded that the present method is working better than the other methods [100], [101].

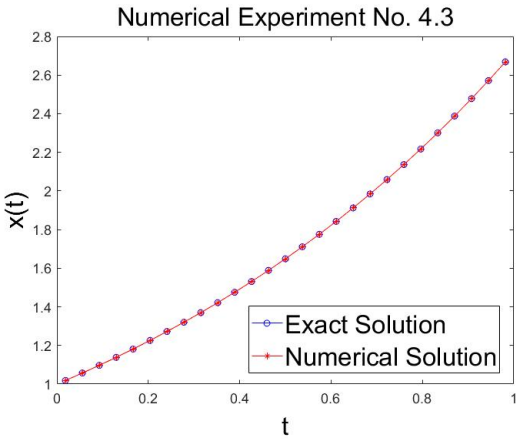

Figure 4.5: Comparison of exact and numerical solution for Numerical Experiment No. 4.3

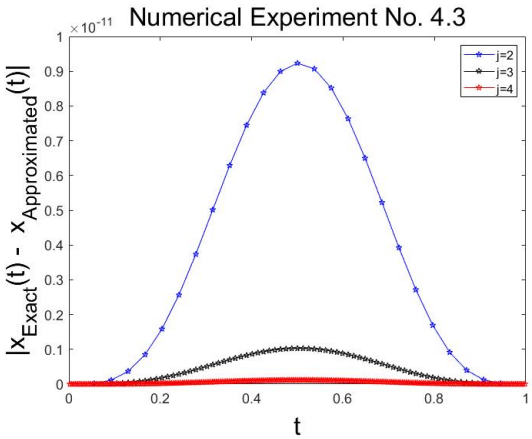

Figure 4.6: Absolute Error at different level of resolution $J = 2,3,4$ in Numerical Experiment No. 4.3

Table 4.7: Exact and Approximated solution by HS3WCM for j=1 for Numerical Experiment No. 4.3

$x(t)$	Exact Solution	Approximated Solution by HS3WCM
0.0556	1.057127744760230	1.057127744760390
0.1667	1.181360412865640	1.181360412873280
0.2778	1.320192788434120	1.320192788467740
0.3889	1.475340615490620	1.475340615557600
0.5000	1.648721270700120	1.648721270783100
0.6111	1.842477459047700	1.842477459116250
0.7222	2.059003694212870	2.059003694248070
0.8333	2.300975890892820	2.300975890900990
0.9444	2.571384434788030	2.571384434788190

Table 4.8: L_2 , L_∞ errors at different level of resolution for Numerical Experiment No.4.3

Level of Resolution (j)	L_2-error	L_2-error	L_∞-error	L_∞-error
	Haar scale 2 wavelet	Haar scale 3 wavelet	Haar scale 2 wavelet	Haar scale 3 wavelet
0	6.31E-10	2.47E-10	1.48E-09	7.50E-10
1	1.27E-10	2.54E-11	3.20E-10	8.30E-11
2	3.22E-11	2.83E-12	9.92E-11	9.23E-12
3	8.05E-12	3.14E-13	2.60E-11	1.03E-12
4	2.01E-12	3.50E-14	6.56E-12	1.14E-13
5	5.03E-13	3.96E-15	1.64E-12	1.33E-14
6	1.26E-13	5.54E-16	4.11E-13	3.11E-15

Table 4.9: Comparision of Numerical results at Random collocation Points available in Literature for Numerical Experiment No. 4.3

x(t)	Exact	Approximated	HS3WCM (E^*)	Reproducing Kernel(E^*) [100]	VIT(E^*) [101]
0.1	1.105170918075640	1.105170918082360	6.72E-12	1.61E-08	1.91E-07
0.2	1.221402758160170	1.221402758200630	4.05E-11	3.07E-08	1.25E-07
0.3	1.349858807576000	1.349858807613920	3.79E-11	4.23E-08	7.25E-08
0.4	1.491824697641270	1.491824697560440	8.08E-11	4.97E-08	4.85E-08
0.5	1.648721270700120	1.648721270427080	2.73E-10	5.23E-08	2.91E-07
0.6	1.822118800390500	1.822118800001710	3.89E-10	4.98E-08	7.80E-08
0.7	2.013752707470470	2.013752707147060	3.23E-10	4.24E-08	1.11E-07
0.8	2.225540928492460	2.225540928350050	1.42E-10	3.08E-08	1.71E-07
0.9	2.459603111156940	2.459603111139210	1.77E-11	1.62E-08	7.93E-08

Numerical Experiment No. 4.4: - Consider the *ninth order linear* differential equation

$$\frac{d^9x(t)}{dt^9} = x(t) - 9e^t \quad , 0 \le t \le 1 \tag{4.21}$$

with the following types of constraints on the solution at the boundary points

$x(0) = 1, x'(0) = 0, x''(0) = -1, x'''(0) = -2, x^{iv}(0) = -3, x(1) = 0, x'(1) = -e$
$x''(1) = -2e\ , x'''(1) = -3e$

Analytic solution of the problem is $x(t) = (1-t)e^t$.
The present method is applied to the linear differential equation (4.21) and we proposed the following solution as

$x(t) = \sum_{i=1}^{3p} a_i[q_{9,i}(t) - f_1(t)q_{9,i}(1) - f_2(t)q_{8,i}(1) - f_3(t)q_{7,i}(1) - f_4(t)q_{6,i}(1)] -$
$\frac{1}{24}f_1(t) + \left(\frac{5}{2} - e\right)f_2(t) + \left(\frac{9}{2} - 2e\right)f_3(t) + (5-3e)f_4(t) - \frac{t^4}{8} - \frac{t^3}{3} - \frac{t^2}{2} + 1$

where

$$f_1(t) = -35t^8 + 120t^6 - 140t^5 + 56,$$

$$f_2(t) = 15t^8 - 50t^7 + 56t^6 - 21t^5,$$

$$f_3(t) = -2.5t^8 + 8t^7 - 8.5t^6 + 3t^5,$$

$$f_4(t) = \frac{1}{6}t^8 - \frac{1}{2}t^7 + \frac{1}{2}t^6 - \frac{1}{6}t^5.$$

These $a_i's$ are the wavelets coefficients and $q_{j,i}'s$ are the wavelet integrals.

Below Figure 4.7 and Table 4.10 shows the numerical solution obtained from the present method at j=1 are in good agreement with the exact solution which explains the high accuracy obtained by the present method for a small number of grid points (in this case only 9 Grid pts). L_2 and L_∞ errors at j=1 are 3.36E-11, 4.65E-11 respectively which are less than error obtained in case of Haar scale 2 wavelets. It can be concluded that the rate of convergence of the Haar scale 3 wavelet is faster than Haar scale 2 wavelets. Table 4.11 and Figure 4.8 ensure the convergence of the proposed solution to the exact solution. The performance of the present method is compared with the other methods and it can be concluded that the present method is working better than the other methods[102][103] given in Table 4.12.

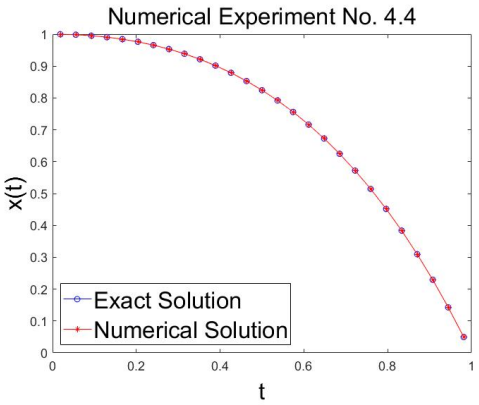

Figure 4.7: Comparison of exact and numerical solution for Numerical Experiment No. 4.4

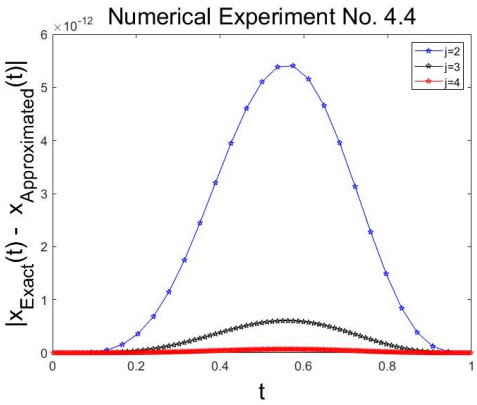

Figure 4.8: Absolute Error at different level of resolution $J = 2,3,4$ in Numerical Experiment No. 4.4

Table 4.10: L_2 , L_∞ errors at different level of resolution for Numerical Experiment No.4.4

Level of Resolution (j)	L_2**-error** **Haar scale 2 wavelet**	L_2**-error** **Haar scale 3 wavelet**	L_∞**-error** **Haar scale 2 wavelet**	L_∞**-error** **Haar scale 3 wavelet**
0	5.32E-10	3.17E-10	5.82E-10	4.20E-10
1	1.73E-10	3.36E-11	2.29E-10	4.65E-11
2	4.26E-11	3.73E-12	6.20E-11	5.41E-12
3	1.06E-11	4.14E-13	1.53E-11	6.03E-13
4	2.65E-12	4.60E-14	3.86E-12	6.71E-14
5	6.64E-13	5.09E-15	9.66E-13	7.55E-15
6	1.66E-13	7.26E-17	2.41E-13	8.11E-17

Table 4.11: Exact and Approximated solution by HS3WCM for j=1 for Numerical Experiment No. 4.4

$x(t)$	**Exact Solution**	**Approximated Solution by HS3WCM**
0.0556	0.998398425606890	0.998398425606881
0.1667	0.984467010721372	0.984467010719958
0.2778	0.953472569424642	0.953472569414279
0.3889	0.901597042799825	0.901597042770934
0.5000	0.824360635350064	0.824360635304049
0.6111	0.716519011851887	0.716519011805412
0.7222	0.571945470614687	0.571945470586460
0.8333	0.383495981815471	0.383495981807899
0.9444	0.142854690821557	0.142854690821380

Table 4.12: Comparision of Numerical results at Random collocation Points available in Literature for Numerical Experiment No. 4.4

x(t)	Exact	Approximated	HS3WCM (E^*)	MVIM(E^*) [102]	SBSCM(E^*) [103]
0.1	0.994653826268083	0.994653826266204	1.88E-12	2.00E-10	1.08E-06
0.2	0.977122206528136	0.977122206495194	3.29E-11	2.00E-10	5.19E-06
0.3	0.944901165303202	0.944901165177828	1.25E-10	2.00E-10	6.13E-06
0.4	0.895094818584762	0.895094818349846	2.35E-10	2.00E-10	1.23E-05
0.5	0.824360635350064	0.824360635081231	2.69E-10	2.00E-10	1.07E-05
0.6	0.728847520156204	0.728847519963689	1.93E-10	6.00E-10	4.91E-06
0.7	0.604125812241143	0.604125812167427	7.37E-11	1.00E-09	9.95E-06
0.8	0.445108185698494	0.445108185693307	5.19E-12	2.00E-09	1.65E-06
0.9	0.245960311115695	0.245960311117830	2.13E-12	3.04E-09	2.00E-06

E^* (Absolute Error) =Exact Solution-Approximate Solution

Numerical Experiment No. 4.5: - Consider the *ninth order non- linear* differential equation

$$\frac{d^9x(t)}{dt^9} - (x(t))^2\frac{dx(t)}{dt} = cos^3t \qquad ,0 \le t \le 1 \tag{4.22}$$

with the following types of constraints on the solution at the boundary points $x(0) = 0, x'(0) = 1, x''(0) = 0, x'''(0) = -1, x'^v(0) = 0, x(1) = \sin 1\ , x'(1) = \cos 1\ , x''(1) = -\sin 1\ , x'''(1) = -\cos 1$

Analytic solution of the problem is $x(t) = \sin t$.

In this problem, non-linearity in the differential equation is tackled by the Quasilinearization technique. By using Quasilinearization technique, given non-linear differential equation is transformed into a sequence of linear differential equations as

$$\frac{d^9x_{r+1}(t)}{dt^9} - 2x_r\,x_r'\,x_{r+1} - x_r^2\,x_{r+1}' + 2x_r^2\,x_r' = cos^3x, 0 \le t \le 1\ , r = 0,1,2\cdots \tag{4.23}$$

subjected to the boundary conditions

$x_{r+1}(0) = 0, x_{r+1}'(0) = 1, x_{r+1}''(0) = 0, x_{r+1}'''(0) = -1, x_{r+1}'^v(0) = 0, x_{r+1}(1) = \sin 1\ , x_{r+1}'(1) = \cos 1\ , x_{r+1}''(1) = -\sin 1\ , x_{r+1}'''(1) = -\cos 1$, where $x_{r+1}(t)$ is the $(r+1)$th approximation for $x(t)$.Then by applying the present method on the sequence of linear differential equations, we proposed the following solution for Equation (4.22) as

$$x(t) = \sum_{i=1}^{3p} a_i[q_{9,i}(t) - f_1(t)q_{9,i}(1) - f_2(t)q_{8,i}(1) - f_3(t)q_{7,i}(1) - f_4(t)q_{6,i}(1)] + \left(\sin 1 - \frac{5}{6}\right) f_1(t) + \left(\cos 1 - \frac{1}{2}\right) f_2(t) + (1 - \sin 1) f_3(t) + (1 - \cos 1) f_4(t) - \frac{t^3}{6} + t$$

Where

$$f_1(t) = -35t^8 + 120t^6 - 140t^5 + 56t^4$$

$$f_2(t) = 15t^8 - 50t^7 + 56t^6 - 21t^5$$

$$f_3(t) = -2.5t^8 + 8t^7 - 8.5t^6 + 3t^5$$

$$f_4(t) = \frac{1}{6}t^8 - \frac{1}{2}t^7 + \frac{1}{2}t^6 - \frac{1}{6}t^5$$

These $a_i's$ are the wavelets coefficients and $q_{j,i}'s$ are the wavelet integrals.

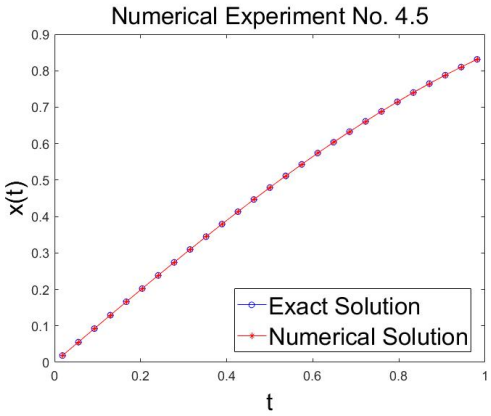

Figure 4.9: Comparison of exact and numerical solution for Numerical Experiment No. 4.5

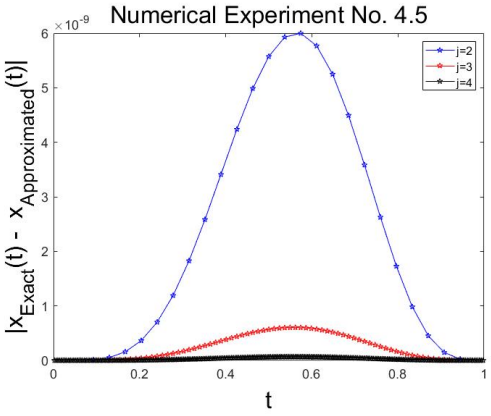

Figure 4.10: Absolute error at different level of resolution $J = 2,3,4$ for Numerical Experiment No. 4.5

Table 4.13: Exact and Approximated solution by HS3WCM for j=1 for Numerical Experiment No. 4.5

$x(t)$	Exact Solution	Approximated Solution by HS3WCM
0.0556	0.055526982004734	0.055526982003702
0.1667	0.165896132693415	0.165896132535308
0.2778	0.274219289210727	0.274219288018338
0.3889	0.379160503917260	0.379160500502594
0.5000	0.479425538604203	0.479425533025153
0.6111	0.573777826311066	0.573777820538742
0.7222	0.661053721884888	0.661053718298351
0.8333	0.740176853196037	0.740176852213119
0.9444	0.810171396017299	0.810171395993874

Table 4.13 and Figure 4.9 shows the comparison between the exact and approximated numerical solution at j=1 for the given problem which explains the high accuracy obtained by the present method for a small number of grid points (in this case only 9 Grid pts). L_2 and L_∞ errors at j=1 are 2.54E-11, 8.43E-11 respectively which are less than error obtained in case of Haar scale 2 wavelets. Table 4.14 and Figure 4.10 ensure the convergence of the proposed solution to the exact solution. The performance of the present method is compared with the other methods [103][104] and it has been found that the present method is working better than the other methods[103][104] given in the Table 4.15.

Table 4.14: L_2 , L_∞ errors at different level of resolution for Numerical Experiment No. 4.5

Level of Resolution (j)	L_2**-error**	L_2**-error**	L_∞**-error**	L_∞**-error**
	Haar scale 2 wavelets	**Haar scale 3 wavelets**	**Haar scale 2 wavelets**	**Haar scale 3 wavelets**
0	6.41E-10	2.17E-10	1.68E-09	7.55E-10
1	1.47E-10	2.54E-11	3.40E-10	8.43E-11
2	3.37E-11	2.93E-12	9.99E-11	9.33E-12
3	8.25E-12	3.34E-13	2.85E-11	1.25E-12
4	2.01E-12	3.85E-14	6.56E-12	1.44E-13
5	5.03E-13	4.75E-15	1.64E-12	1.83E-14
6	1.26E-13	5.93E-16	4.11E-13	3.41E-15

Table 4.15: Comparision of Numerical results at Random collocation Points available in Literature for Numerical Experiment No. 4.5

x(t)	**Exact**	**Approximated**	**HS3WCM (E*)**	**PGM(E*)** [104]	**SBSCM(E*)** [103]
0.1	0.099833416646828	0.099833416630007	1.68E-11	1.86E-07	2.85E-06
0.2	0.198669330795061	0.198669330448275	3.47E-10	7.30E-07	1.35E-06
0.3	0.295520206661340	0.295520205069110	1.59E-09	9.83E-07	4.09E-06
0.4	0.389418342308651	0.389418338575155	3.73E-09	1.22E-06	1.05E-06
0.5	0.479425538604203	0.479425532943724	5.66E-09	8.34E-07	3.45E-05
0.6	0.564642473395035	0.564642467456141	5.94E-09	3.87E-06	3.46E-05
0.7	0.644217687237691	0.644217683060221	4.18E-09	5.66E-06	2.09E-05
0.8	0.717356090899523	0.717356089246222	1.65E-09	4.89E-06	2.01E-05
0.9	0.783326909627483	0.783326909436309	1.91E-10	2.86E-06	3.84E-06

E* (Absolute Error) =Exact Solution-Approximate Solution

Numerical Experiment No. 4.6: - Consider the *tenth order linear* differential equation

$$\frac{d^{10}x(t)}{dt^{10}} = x''(t) - 8e^t \quad , \qquad 0 \le t \le 1 \tag{4.24}$$

with the following types of constraints on the solution at the boundary points

$x(0) = 1, x'(0) = 0, x''(0) = -1, x'''(0) = -2, x^{iv}(0) = -3, ,,$

$x(1) = 0, x'(1) = -e, x''(1) = -2e\ , x'''(1) = -3e, x^{iv}(1) = -4e$

Analytic solution of the problem is $x(t) = (1-t)e^t$.

By applying the Haar Scale 3 wavelet mechanism for the solution of the linear differential equation, we proposed the following solution for the Equation (4.24)

$x(t) = \sum_{i=1}^{3p} a_i[q_{10,i}(t) - f_1(t)q_{10,i}(1) - f_2(t)q_{9,i}(1) - f_3(t)q_{8,i}(1) - f_4(t)q_{7,i}(1) - f_5(t)q_{6,i}(1)] - \frac{1}{24}f_1(t) + \left(\frac{5}{2} - e\right)f_2(t) + \left(\frac{9}{2} - 2e\right)f_3(t) + (5-3e)f_4(t) + (3-4e)f_5(t) - \frac{t^4}{8} - \frac{t^3}{3} - \frac{t^2}{2} + 1$

Where $f_1(t) = 70t^9 - 315t^8 + 540t^7 - 420t^6 + 126t^5$, $f_2(t) = -35x^9 + 155t^8 - 260t^7 + 196t^6 - 56t^5$, $f_3(t) = 7.5\,x^9 - 32.5t^8 + 53t^7 - 38.5t^6 + 10.5t^5$, $f_4(t) = -\frac{5}{6}x^9 + \frac{7}{2}t^8 - \frac{11}{2}t^7 + \frac{23}{6}t^6 - t^5$, $f_5(t) = \frac{1}{24}x^9 - \frac{1}{6}t^8 + \frac{1}{4}t^7 - \frac{1}{6}t^6 + \frac{1}{24}t^5$.

These $a_i's$ are the wavelets coefficients and $q_{j,i}'s$ are the wavelet integrals. Figure 4.11 and Table 4.16 show the comparison between the exact and obtained solution for j=1 which explains the high accuracy obtained by the present method for a small number of grid points (in this case only 9 Grid pts).L_2 and L_∞ errors at j=1 are 1.79E-12, 2.65E-12 respectively which are less than error obtained in case of Haar scale 2 wavelets. Table 4.17 and Figure 4.12 ensure the convergence of the obtained solution (HS3WCM solution) to the exact solution. The performance of the present is compared with the other methods[118], [119] and it has been found that the present method is working better than the other methods given in Table 4.18.

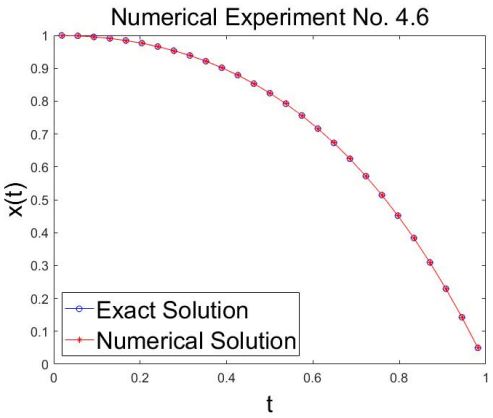

Figure 4.11: Comparison of exact and numerical solution for Numerical Experiment No. 4.6

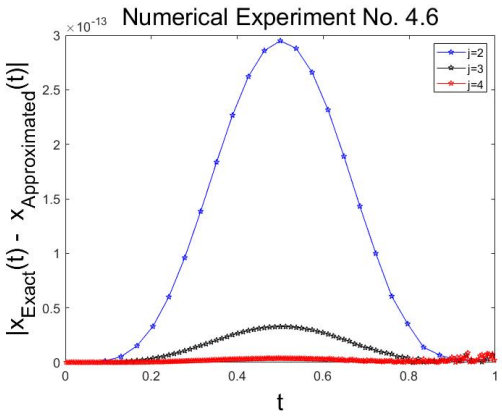

Figure 4.12: Absolute error at different level of resolution $J = 2,3,4$ in Numerical Experiment No. 4.6

Table 4.16: Exact and Approximated solution by HS3WCM for j=1 for Numerical Experiment No. 4.6

x(t)	Exact Solution	Solution by HS3WCM
0.0556	0.998398425606890	0.998398425606891
0.1667	0.984467010721372	0.984467010721508
0.2778	0.953472569424642	0.953472569425507
0.3889	0.901597042799825	0.901597042801862
0.5000	0.824360635350064	0.824360635352717
0.6111	0.716519011851887	0.716519011853969
0.7222	0.571945470614687	0.571945470615589
0.8333	0.383495981815471	0.383495981815614
0.9444	0.142854690821557	0.142854690821560

Table 4.17: L_2 , L_∞ errors at different level of resolution for Numerical Experiment No.4.6

Level of Resolution (j)	L_2-error	L_2-error	L_∞-error	L_∞-error
	Haar scale 2 wavelet	Haar scale 3 wavelet	Haar scale 2 wavelet	Haar scale 3 wavelet
0	3.66E-11	1.51E-11	3.76E-11	2.02E-11
1	8.51E-12	1.79E-12	9.39E-12	2.65E-12
2	2.26E-12	1.98E-13	3.12E-12	2.95E-13
3	5.65E-13	2.21E-14	8.26E-13	3.28E-14
4	1.41E-13	3.20E-15	2.09E-13	8.60E-15
5	3.54E-14	1.87E-15	5.25E-14	9.21E-15
6	9.01E-15	1.91E-15	1.32E-14	1.39E-14

Table 4.18: Comparison of Numerical results at Random collocation Points available in Literature for Numerical Experiment No. 4.6

x(t)	Exact	Approximated	HS3WCM (E^*)	HPM(E^*) [118]	QBSCM(E^*) [119]
0.1	0.994653826268083	0.994653826268138	5.46E-14	1.14E-06	8.82E-06
0.2	0.977122206528136	0.977122206528696	5.60E-13	2.69E-06	8.64E-06
0.3	0.944901165303202	0.944901165303723	5.21E-13	3.70E-06	2.92E-06
0.4	0.895094818584762	0.895094818582427	2.33E-12	4.35E-06	5.96E-07
0.5	0.824360635350064	0.824360635342947	7.12E-12	4.58E-06	6.74E-06
0.6	0.728847520156204	0.728847520146812	9.39E-12	4.36E-06	1.43E-05
0.7	0.604125812241143	0.604125812234420	6.72E-12	3.71E-06	1.27E-05
0.8	0.445108185698494	0.445108185696260	2.23E-12	2.69E-06	8.14E-06
0.9	0.245960311115695	0.245960311115542	1.53E-13	1.42E-06	3.49E-06

E^* (Absolute Error) =Exact Solution-Approximate Solution

Numerical Experiment No. 4.7 : - Consider the *tenth order non-linear* differential equation

$$\frac{d^{10}x(t)}{dt^{10}} = (x(t))^2 e^{-t} \quad , 0 \le t \le 1 \tag{4.25}$$

with the following types of constraints on the solution at the boundary points

$x(0) = 1, x'(0) = 1, x''(0) = 1, x'''(0) = 1, x^{iv}(0) = 1, x^{v}(0) = 1, x(1) = e$,

$x'(1) = e$, $x''(1) = e$, $x'''(1) = e, x^{iv}(1) = e$, $x^{v}(1) = e$

Analytic solution of the problem is $x(t) = e^t$.

Non-linearity in the differential equation is tackled by the Quasilinearization technique. By using Quasilinearization technique given non-linear differential equation is transformed into a sequence of linear differential equations as

$$\frac{d^{10}x_{r+1}(t)}{dt^{10}} = 2x_r x_{r+1} e^{-t} \quad , \quad 0 \le t \le 1 \qquad r = 0,1,2\cdots \tag{4.26}$$

subjected to the boundary conditions

$x_{r+1}(0) = 1, x'_{r+1}(0) = 1, x''_{r+1}(0) = 1, x'''_{r+1}(0) = 1, x^{iv}_{r+1}(0) = 1, x_{r+1}(1) = e$, $x'_{r+1}(1) = e$, $x''_{r+1}(1) = e$, $x'''_{r+1}(1) = e, x^{iv}_{r+1}(0) = e$ where $x_{r+1}(t)$ is the $(r+1)$th approximation for $x(t)$.

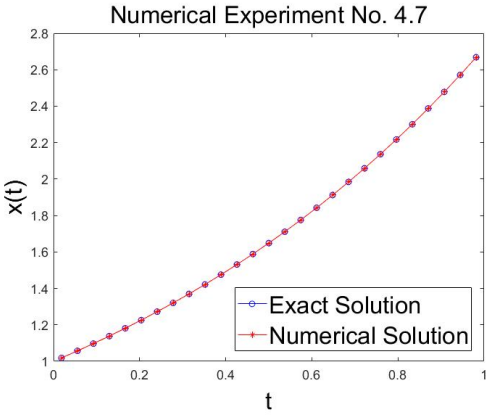

Figure 4.13: Comparison of exact and numerical solution for Numerical Experiment No. 4.7

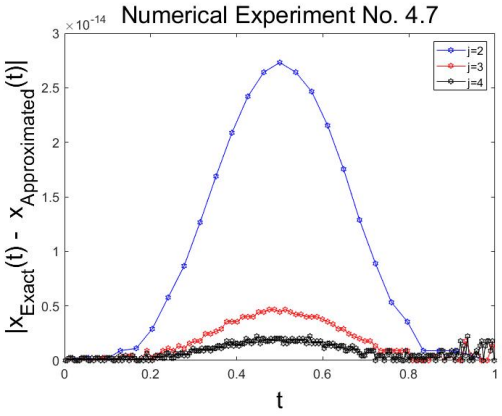

Figure 4.14: Absolute error at different level of resolution $J = 2,3,4$ in Numerical Experiment No. 4.7

By applying the present method on the given linear differential equation, we proposed the following solution

$x(t) = \sum_{i=1}^{3p} a_i[q_{10,i}(t) - f_1(t)q_{10,i}(1) - f_2(t)q_{9,i}(1) - f_3(t)q_{8,i}(1) - f_4(t)q_{7,i}(1) - f_5(t)q_{6,i}(1)] + \left(e - \frac{65}{24}\right) f_1(t) + \left(e - \frac{8}{3}\right) f_2(t) + \left(e - \frac{5}{2}\right) f_3(t) + (e-2) f_4(t) + (e-1) f_5(t) + \frac{t^4}{4!} + \frac{t^3}{3!} + \frac{t^2}{2!} + t + 1$

where $f_1(t) = 70t^9 - 315t^8 + 540t^7 - 420t^6 + 126t^5$, $f_2(t) = -35x^9 + 155t^8 - 260t^7 + 196t^6 - 56t^5$, $f_3(t) = 7.5\,x^9 - 32.5t^8 + 53t^7 - 38.5t^6 + 10.5t^5$, $f_4(t) = -\frac{5}{6}x^9 + \frac{7}{2}t^8 - \frac{11}{2}t^7 + \frac{23}{6}t^6 - t^5$, $f_5(t) = \frac{1}{24}x^9 - \frac{1}{6}t^8 + \frac{1}{4}t^7 - \frac{1}{6}t^6 + \frac{1}{24}t^5$.

These $a_i's$ are the wavelets coefficients and $q_{j,i}'s$ are the wavelet integrals.

Table 4.19: Exact and Approximated solution by HS3WCM for j=1 for Numerical Experiment No. 4.7

x(t)	Exact Solution	Approximated Solution by HS3WCM
0.0556	1.057127744760230	1.057127744760230
0.1667	1.181360412865640	1.181360412865630
0.2778	1.320192788434120	1.320192788434040
0.3889	1.475340615490620	1.475340615490440
0.5000	1.648721270700120	1.648721270699890
0.6111	1.842477459047700	1.842477459047520
0.7222	2.059003694212870	2.059003694212790
0.8333	2.300975890892820	2.300975890892810
0.9444	2.57138443478803	2.57138443478803

Table 4.20: L_2 , L_∞ errors at different level of resolution for Numerical Experiment No. 4.7

Level of Resolution (j)	L_2-error	L_2-error	L_∞-error	L_∞-error
	Haar scale 2 wavelet	Haar scale 3 wavelet	Haar scale 2 wavelet	Haar scale 3 wavelet
0	5.73E-13	1.44E-12	1.75E-12	3.36E-12
1	6.75E-14	3.22E-13	2.32E-13	8.19E-13
2	7.91E-15	8.53E-14	2.73E-14	2.72E-13
3	1.31E-15	2.17E-14	4.66E-15	7.33E-14
4	6.01E-16	5.75E-15	2.22E-15	1.98E-14
5	5.27E-16	1.78E-15	2.22E-15	6.22E-15
6	5.23E-17	8.07E-16	3.55E-16	2.89E-15

Table 4.21: Comparision of Numerical results at Random collocation Points available in Literature for Numerical Experiment No. 4.7

x(t)	Exact	Approximated	HS3WCM	HPM [118]	QBSCM [119]
0.1	1.105170918075640	1.105170918075640	5.77E-15	1.41E-06	1.25E-05
0.2	1.221402758160170	1.221402758160110	6.02E-14	2.69E-06	8.70E-06
0.3	1.349858807576000	1.349858807575920	7.51E-14	3.70E-06	2.15E-06
0.4	1.491824697641270	1.491824697641440	1.73E-13	4.35E-06	1.13E-05
0.5	1.648721270700120	1.648721270700740	6.16E-13	4.58E-06	3.97E-05
0.6	1.822118800390500	1.822118800391350	8.43E-13	4.36E-06	5.40E-05
0.7	2.013752707470470	2.013752707471080	6.12E-13	3.71E-06	6.79E-05
0.8	2.225540928492460	2.225540928492670	2.05E-13	2.69E-06	4.89E-05
0.9	2.459603111156940	2.459603111156960	1.38E-14	1.42E-06	2.00E-05

E^* (Absolute Error) =Exact Solution-Approximate Solution

The proposed solution is compared with the exact solution at different levels of resolutions in Table 4.19 and Figure 4.13. Note that obtained solution and exact solution have roughly coincided which explains the high accuracy obtained by the proposed method for a small number of grid points. L_2 and L_∞ errors at j=1 are 3.22E-13, 8.19E-13 respectively which are less than error obtained in case of Haar scale 2 wavelets shown in Table 4.20. It can be concluded from Table 4.20 and Figure 4.14 that with the increase in the level of resolution j, the error between the exact solution and obtained solution decreases which ensures the convergence of the proposed solution to the exact solution. In Table 4.21, the performance of the proposed method is compared with the Homotopy Perturbation Method [118] and Quintic B-Spline Collocation Method [119]. We infer that our method is working better than the methods [118], [119] given in Table 4.21.

Numerical Experiment No. 4.8 : - Consider the *eleventh order linear* differential equation

$$\frac{d^{(11)}x(t)}{dt} = -11e^t + x(t)\,,\ 0 \le t \le 1 \tag{4.27}$$

with the following types of constraints on the solution at the boundary points

$x(0) = 1, x'(0) = 0, x''(0) = -1, x'''(0) = -2, x^{iv}(0) = -3, x^{v}(0) = -4\,,$

$x(1) = 0, x'(1) = -e\,, x'' = -2e\,, x'''(1) = -3e, x^{iv}(1) = -4e$

Analytic solution of the problem is $x(t) = (1-t)e^t$.

We introduced the following approximate solution for the solution of given differential equation (Equation (4.27)) by applying the Haar Scale 3 wavelet mechanism

$x(t) = \sum_{i=1}^{3p} a_i[q_{11,i}(t) - f_1(t)q_{11,i}(1) - f_2(t)q_{10,i}(1) -$
$f_3(t)q_{9,i}(1) - f_4(t)q_{8,i}(1) - f_5(t)q_{7,i}(1)] - \left(\frac{1}{120}\right)f_1(t) + \left(\frac{8}{3} - e\right)f_2(t) + \left(\frac{31}{6} -$
$2e\right)f_3(t) + (7-3e)f_4(t) + (7-4e)f_5(t) - \frac{t^5}{30} - \frac{t^4}{8} - \frac{t^3}{3} - \frac{t^2}{2} + 1,$

Where $f_1(t) = 126t^{10} - 560t^9 + 945t^8 - 720t^7 + 210t^6$, $f_2(t) = -56t^{10} + 245x^9 - 405t^8 + 300t^7 - 84t^6$, $f_3(t) = 10.5t^{10} - 45\,x^9 + 72.5t^8 - 52t^7 - 14t^6$, $f_4(t) = -t^{10} + \frac{25}{6}x^9 - \frac{13}{2}t^8 + \frac{9}{2}t^7 - \frac{7}{6}t^6 - t^5$, $f_5(t) = \frac{1}{24}x^9 - \frac{1}{6}t^8 + \frac{1}{4}t^7 - \frac{1}{6}t^6 + \frac{1}{24}t^5$. These $a_i's$ are the wavelets coefficients and $q_{j,i}'s$ are the wavelet integrals.

Numerical Experiment No. 4.9 : - Consider the *eleventh order non- linear* differential equation

$$\frac{d^{(11)}x(t)}{dt} + (x(t))^2 = 11(\cos t - \sin t) - t(\cos t + \sin t\,) + t^2(1 - \sin 2t)\ ,\ 0 \le t \le 1 \tag{4.28}$$

with the following types of constraints on the solution at the boundary points

$x(0) = 0, x'(0) = -1, x''(0) = 2, x'''(0) = 3, x^{iv}(0) = -4, x^{v}(0) = -5,$

$x(1) = \sin 1 - \cos 1\,, x'(1) = 2\sin 1\ , x''(1) = 3\cos 1 + \sin 1\,, x'''(1) = 2\cos 1 - 4\sin 1\ , x^{iv}(1) = -5\cos 1 - 3\sin 1$

Analytic solution of the problem is $x(t) = t\,(\sin t - \cos t)$ .The non-linearity in the differential equation is tackled by the quasilinearization technique. By using the quasilinearization technique given non-linear differential equation is transformed into a sequence of linear differential equations as

$$\frac{d^{11}x_{r+1}(t)}{dt^{11}} + 2x_r\ x_{r+1} - x_r^2\ = 11(\cos t - \sin t) - t(\cos t + \sin t\,) + t^2(1 - \sin 2t)\,, \qquad 0 \le t \le 1 \qquad r = 0,1,2\cdots \tag{4.29}$$

subjected to the boundary conditions

$x_{r+1}(0) = 0, x'_{r+1}(0) = -1, x''_{r+1}(0) = 2, x'''_{r+1}(0) = 3, x'^{v}_{r+1}(0) = -4, x^{v}_{r+1}(0) = -5, x_{r+1}(1) = \sin 1 - \cos 1\ , x'_{r+1}(1) = 2\sin 1\ , x''_{r+1}(1) = 3\cos 1 + \sin 1\ , x'''_{r+1}(1) = 2\cos 1 - 4\sin 1\,, x'''_{r+1}(1) = -5\cos 1 - 3\sin 1$ where $x_{r+1}(t)$ is the $(r+1)$th approximation for $x(t)$.

Then by applying the Haar scale 3 wavelet mechanism for the solution of the linear differential equations on the sequence of linear differential equations, we proposed the following solution for the given equation.

$x(t) = \sum_{i=1}^{3p} a_i[q_{11,i}(t) - f_1(t)q_{11,i}(1) - f_2(t)q_{10,i}(1) - f_3(t)q_{9,i}(1) - f_4(t)q_{8,i}(1) - f_5(t)q_{7,i}(1)] + ((\sin 1 - \cos 1) - \frac{7}{24})\,f_1(t) + (2\sin 1 - \frac{13}{8})f_2(t) + \left((3\cos 1 + \sin 1) - \frac{13}{6}\right)f_3(t) + ((2\cos 1 - 4\sin 1) + \frac{7}{2})f_4(t) + (9 - (5\cos 1 + 3\sin 1))f_5(t) - t + \frac{t^2}{2} + \frac{t^3}{3} - \frac{t^4}{8} - \frac{t^5}{30}$,

Where $f_1(t) = 126t^{10} - 560t^9 + 945t^8 - 720t^7 + 210t^6$, $f_2(t) = -56t^{10} + 245x^9 - 405t^8 + 300t^7 - 84t^6$, $f_3(t) = 10.5t^{10} - 45\,x^9 + 72.5t^8 - 52t^7 - 14t^6$, $f_4(t) = -t^{10} + \frac{25}{6}x^9 - \frac{13}{2}t^8 + \frac{9}{2}t^7 - \frac{7}{6}t^6 - t^5$, $f_5(t) = \frac{1}{24}x^9 - \frac{1}{6}t^8 + \frac{1}{4}t^7 - \frac{1}{6}t^6 + \frac{1}{24}t^5$. These $a_i's$ are the wavelets coefficients and $q_{j,i}'s$ are the wavelet integrals.

It can be concluded from Figure 4.15, Figure 4.16, Table 4.22 , and Table 4.23 that the results obtained from the present method are in good agreement with the exact solution. To have more detail of results, absolute error obtained in the present solution is compared with the error obtained in other methods [122]–[124] in Table 4.24 and Table 4.25 and we infer our method provides better accuracy.

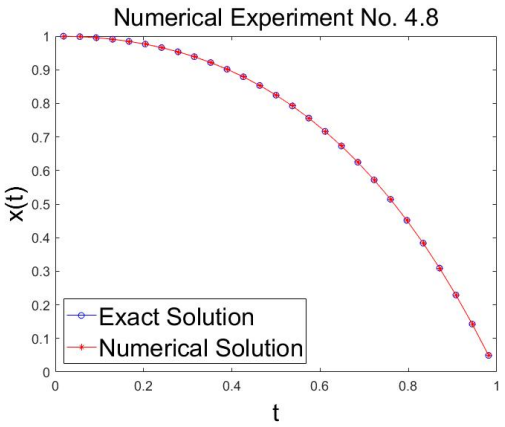

Figure 4.15: Comparison of Exact and Numerical solution for Numerical Experiment No. 4.8

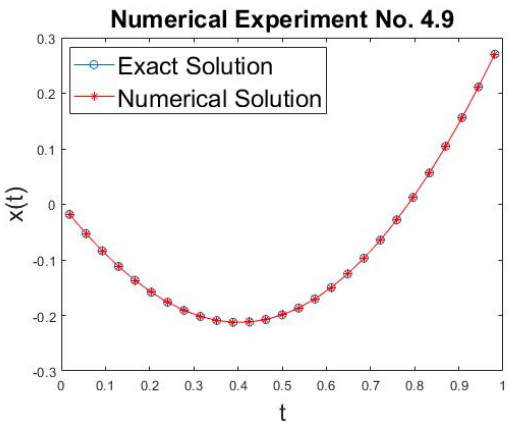

Figure 4.16: Comparison of Exact and Numerical solution for Numerical Experiment No. 4.9

Table 4.22: Exact and Approximated solution by HS3WCM for j=1 for Numerical Experiment No.4.8

x(t)	Exact Solution	Approximated Solution by HS3WCM
0.0556	0.998398425606890	0.998398425606890
0.1667	0.984467010721372	0.984467010721374
0.2778	0.953472569424642	0.953472569424665
0.3889	0.901597042799825	0.901597042799900
0.5000	0.824360635350064	0.824360635350189
0.6111	0.716519011851887	0.716519011852007
0.7222	0.571945470614687	0.571945470614748
0.8333	0.383495981815471	0.383495981815481
0.9444	0.142854690821557	0.142854690821556

Table 4.23: Exact and Approximated solution by HS3WCM for j=1 for Numerical Experiment No. 4.9

x(t)	Exact Solution	Approximated Solution by HS3WCM
0.0556	-0.052385011388556	-0.052385011388556
0.1667	-0.136707849811585	-0.136707849811584
0.2778	-0.190957749800737	-0.190957749800731
0.3889	-0.212399606414346	-0.212399606414325
0.5000	-0.199078511643085	-0.199078511643052
0.6111	-0.149864712744852	-0.149864712744822
0.7222	-0.064483504858708	-0.064483504858693
0.8333	0.056470507594150	0.056470507594154
0.9444	0.211535090710309	0.211535090710311

Table 4.24: Comparison of Numerical results at Random collocation Points available in Literature for Numerical Experiment No. 4.8

x(t)	Exact	Approximated	HS3WCM(E^*)	MADM(E^*) [122]
0.1	0.994653826268083	0.994653826268084	1.44E-15	3.80E-09
0.2	0.977122206528136	0.977122206528185	4.93E-14	4.60E-07
0.3	0.944901165303202	0.944901165303448	2.46E-13	5.30E-06
0.4	0.895094818584762	0.895094818585289	5.27E-13	3.10E-05
0.5	0.824360635350064	0.824360635350693	6.29E-13	1.20E-04
0.6	0.728847520156204	0.728847520156638	4.35E-13	3.60E-04
0.7	0.604125812241143	0.604125812241291	1.48E-13	9.30E-04
0.8	0.445108185698494	0.445108185698504	9.88E-15	2.10E-03
0.9	0.245960311115695	0.245960311115694	1.55E-15	4.30E-03

E^*(Absolute Error) =Exact Solution-Approximate Solution

Table 4.25: Comparision of Numerical results at Random collocation Points available in Literature for Numerical Experiment No. 4.9

x(t)	Exact	Approximated	HS3WCM (E^*)	DTM(E^*)[125]	VIT
0.1	-0.089517074863120	-0.089517074863118	1.67E-15	1.51E-13	1.03E-15
0.2	-0.156279449409236	-0.156279449409184	5.25E-14	5.23E-12	5.34E-14
0.3	-0.197944884739280	-0.197944884739013	2.67E-13	3.07E-11	5.59E-13
0.4	-0.212657060677694	-0.212657060677103	5.91E-13	9.74E-11	3.32E-12
0.5	-0.199078511643085	-0.199078511642340	7.45E-13	3.69E-10	1.48E-11
0.6	-0.156415884908786	-0.156415884908215	5.71E-13	2.00E-09	5.38E-11
0.7	-0.084437150032758	-0.084437150032512	2.46E-13	1.03E-08	1.66E-10
0.8	0.016519505241886	0.016519505241929	4.36E-14	4.39E-08	4.42E-10
0.9	0.145545247221137	0.145545247221138	9.99E-16	1.58E-07	1.04E-09

E^* (Absolute Error) =Exact Solution-Approximate Solution

Numerical Experiment No. 4.10 : - Consider the *twelfth order linear* differential equation

$$\frac{d^{(12)}x(t)}{dt} + tx(t) = -(120 + 23t + t^3)e^t \ , 0 \le t \le 1 \tag{4.30}$$

with the following types of constraints on the solution at the boundary points

$x(0) = 0, x'(0) = 1, x''(0) = 0, x'''(0) = -3, x^{iv}(0) = -8, x^{v}(0) = -15,$

$x(1) = 0, x'(1) = -e\ , x''(1) = -4e\ , x'''(1) = -9e, x^{iv}(1) = -16e\ , x^{v}(1) = -25e.$

Analytic solution of the problem is $x(t) = t(1-t)e^t$.

We proposed the following solution for the Equation (4.30) by applying the present method for the solution of linear differential equation with variable coefficients

$x(t) = \sum_{i=1}^{3p} a_i[q_{12,i}(t) - f_1(t)q_{12,i}(1) - f_2(t)q_{11,i}(1) - f_3(t)q_{10,i}(1) - f_4(t)q_{9,i}(1) - f_5(t)q_{8,i}(1) - f_6(t)q_{7,i}(1)] - \left(\frac{1}{24}\right) f_1(t) + \left(\frac{59}{24} - e\right) f_2(t) + \left(\frac{19}{2} - 4e\right) f_3(t) + \left(\frac{37}{2} - 9e\right) f_4(t) + (23 - 16e) f_5(t) + (15 - 25e) f_6(t) - \frac{t^5}{8} - \frac{t^4}{3} - \frac{t^3}{2} + t$

Where $f_1(t) = -252t^{11} + 1386t^{10} - 3080t^9 + 3465t^8 - 1980t^7 + 462t^6$, $f_2(t) = 126\, t^{11} - 686t^{10} + 1505x^9 - 1665t^8 + 930t^7 - 210t^6$, $f_3(t) = -28t^{11} + \frac{301}{2}t^{10} - 325x^9 + \frac{705}{2}t^8 - 192t^7 - 42t^6$, $f_4(t) = \frac{7}{2}t^{11} - \frac{37}{2}t^{10} + \frac{235}{6}x^9 - \frac{83}{2}t^8 + 22t^7 - \frac{28}{6}t^6$, $f_5(t) = \frac{-1}{4}x^{11} + \frac{31}{24}x^{10} - \frac{8}{3}x^9 + \frac{11}{4}t^8 - \frac{34}{24}t^7 + \frac{7}{24}t^6$

These $a_i's$ are the wavelets coefficients and $q_{j,i}'s$ are the wavelet integrals.

Numerical Experiment No. 4.11: - Consider the *twelfth order non- linear* differential equation

$$\frac{d^{(12)}x(t)}{dt} = 2e^t(x(t))^2 + \frac{d^{(3)}x(t)}{dt}\ , 0 \le t \le 1 \qquad (4.31)$$

with the following types of constraints on the solution at the boundary points

$x(0) = 1, x'(0) = -1, x''(0) = 1, x'''(0) = -1, x^{iv}(0) = 1, x^v(0) = -1\ \ x(1) = e^{-1}, x'(1) = -e^{-1}, x''(1) = e^{-1}, x'''(1) = -e^{-1}, x^{iv}(1) = e^{-1}, x^v(1) = -e^{-1}$

Analytic solution of the problem is $x(t) = e^{-t}$. In this problem, non-linearity in the differential equation is tackled by the quasilinearization technique. By using Quasilinearization technique given non-linear differential equation is transformed into a sequence of linear differential equations as

$$\frac{d^{12}x_{r+1}(t)}{dt^{12}} - \frac{d^{(3)}x_{r+1}(t)}{dt} - 4e^t x_r\ x_{r+1} = -2x_r^2 e^t\ ,\ \ 0 \le t \le 1\ \ , r = 0,1,2\cdots \qquad (4.32)$$

subjected to the boundary conditions

$x_{r+1}(0) = 1, x'_{r+1}(0) = -1, x''_{r+1}(0) = 1, x'''_{r+1}(0) = -1, x^{iv}_{r+1}(0) = 1, x^v_{r+1}(0) = -1, x_{r+1}(1) = e^{-1}, x'_{r+1}(1) = -e^{-1}, x''_{r+1}(1) = e^{-1}, x'''_{r+1}(1) = -e^{-1}, x^{iv}_{r+1}(1) = e^{-1}, x^v_{r+1}(1) = -e^{-1}$ where $x_{r+1}(t)$ is the $(r+1)$th approximation for $x(t)$.

Then by applying the present method for the solution of the linear differential equation on the sequence of linear differential equations as obtained above, we proposed the following solution

$$x(t) = \sum_{i=1}^{3p} a_i[q_{12,i}(t) - f_1(t)q_{12,i}(1) - f_2(t)q_{11,i}(1) - f_3(t)q_{10,i}(1) - f_4(t)q_{9,i}(1) - f_5(t)q_{8,i}(1) - f_6(t)q_{7,i}(1)] + \left(e^{-1} - \frac{44}{120}\right) f_1(t) + \left(\frac{9}{24} - e^{-1}\right) f_2(t) + \left(e^{-1} - \frac{1}{3}\right) f_3(t) + \left(\frac{1}{2} - e^{-1}\right) f_4(t) + e^{-1} f_5(t) + (1 - e^{-1}) f_6(t) - \frac{t^5}{5!} + \frac{t^4}{4!} - \frac{t^3}{3!} + \frac{t^2}{2!} - t + 1$$

Where $f_1(t) = -252t^{11} + 1386t^{10} - 3080t^9 + 3465t^8 - 1980t^7 + 462t^6$, $f_2(t) = 126\,t^{11} - 686t^{10} + 1505x^9 - 1665t^8 + 930t^7 - 210t^6$, $f_3(t) = -28t^{11} + \frac{301}{2}t^{10} - 325x^9 + \frac{705}{2}t^8 - 192t^7 - 42t^6$, $f_4(t) = \frac{7}{2}t^{11} - \frac{37}{2}t^{10} + \frac{235}{6}x^9 - \frac{83}{2}t^8 + 22t^7 - \frac{28}{6}t^6$, $f_5(t) = \frac{-1}{4}x^{11} + \frac{31}{24}x^{10} - \frac{8}{3}x^9 + \frac{11}{4}t^8 - \frac{34}{24}t^7 + \frac{7}{24}t^6$.

These $a_i's$ are the wavelets coefficients and $q_{j,i}'s$ are the wavelet integrals. It can be concluded from Figure 4.17, Figure 4.18, Table 4.26, and Table 4.27 that the results obtained from the present method are roughly coinciding with the exact solution. To have more detail of results, absolute error obtained in the present solution is compared with the error obtained by the other methods [126], [127] given in Table 4.28 and Table 4.29 and we conclude that our method provides better accuracy.

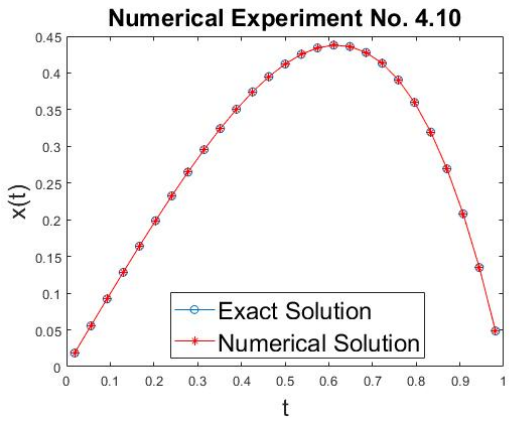

Figure 4.17: Comparison of Exact and Numerical solution for Numerical Experiment No. 4.10

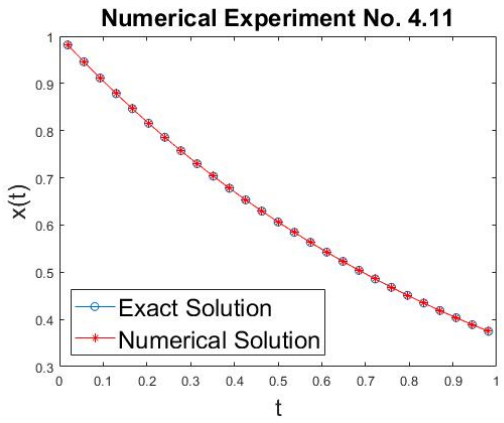

Figure 4.18: Comparison of Exact and Numerical solution for Numerical Experiment No. 4.11

Table 4.26: Exact and Approximated solution by HS3WCM for j=1 for Numerical Experiment No. 4.10

x(t)	Exact Solution	Approximated Solution by HS3WCM
0.0556	0.055466579200383	0.055466579200383
0.1667	0.164077835120229	0.164077835120226
0.2778	0.264853491506845	0.264853491506824
0.3889	0.350621072199932	0.350621072199874
0.5000	0.412180317675032	0.412180317674953
0.6111	0.437872729465042	0.437872729464982
0.7222	0.413071728777274	0.413071728777253
0.8333	0.319579984846226	0.319579984846204
0.9444	0.134918319109249	0.134918319109259

Table 4.27: Exact and Approximated solution by HS3WCM for j=1 for Numerical Experiment No. 4.11

x(t)	Exact Solution	Approximated Solution by HS3WCM
0.0556	0.945959468906765	0.945959468906766
0.1667	0.846481724890614	0.846481724890614
0.2778	0.757465128396966	0.757465128396966
0.3889	0.677809578005450	0.677809578005451
0.5000	0.606530659712633	0.606530659712634
0.6111	0.542747481164222	0.542747481164222
0.7222	0.485671785247712	0.485671785247712
0.8333	0.434598208507078	0.434598208507079
0.9444	0.388895563989223	0.388895563989223

Table 4.28: Comparision of Numerical results at Random collocation Points available in Literature for Numerical Experiment No. 4.10

x(t)	Exact	Approximated	HS3WCM (E^*)	VIT(E^*)[126]	DTM(E^*)[127]
0.1	0.099465382626808	0.099465382626808	4.58E-16	9.52E-13	1.64E-15
0.2	0.195424441305627	0.195424441305619	8.13E-15	1.25E-13	2.08E-13
0.3	0.283470349590961	0.283470349590953	7.77E-15	3.35E-13	3.44E-12
0.4	0.358037927433905	0.358037927433964	5.92E-14	5.38E-13	2.46E-11
0.5	0.412180317675032	0.412180317675209	1.77E-13	8.04E-13	1.10E-10
0.6	0.437308512093722	0.437308512093943	2.21E-13	1.14E-12	3.67E-10
0.7	0.422888068568800	0.422888068568938	1.38E-13	3.93E-13	9.89E-10
0.8	0.356086548558795	0.356086548558830	3.50E-14	1.23E-13	2.28E-09
0.9	0.221364280004126	0.221364280004120	5.47E-15	8.25E-13	4.68E-09

E^*(Absolute Error) =Exact Solution-Approximate Solution

Table 4.29: Comparision of Numerical results at Random collocation Points available in Literature for Numerical Experiment No. 4.11

x(t)	Exact	Approximated	HS3WCM(E^*)	DTM(E^*) [127]	VIT(E^*) [126]
0.1	0.904837418035960	0.904837418035960	1.11E-16	4.11E-15	1.61E-07
0.2	0.818730753077982	0.818730753077982	0.00E+00	1.30E-13	3.07E-07
0.3	0.740818220681718	0.740818220681718	2.22E-16	6.75E-13	4.22E-07
0.4	0.670320046035639	0.670320046035639	7.77E-16	1.53E-12	4.97E-07
0.5	0.606530659712633	0.606530659712633	4.44E-16	1.98E-12	5.22E-07
0.6	0.548811636094027	0.548811636094026	1.11E-16	1.57E-12	4.97E-07
0.7	0.496585303791410	0.496585303791410	1.11E-16	7.17E-13	4.22E-07
0.8	0.449328964117222	0.449328964117222	1.11E-16	1.42E-13	3.07E-07
0.9	0.406569659740599	0.406569659740600	3.33E-16	4.16E-15	1.61E-07

E^*(Absolute Error) =Exact Solution-Approximate Solution

4.6 Conclusion

We have applied the Haar scale 3 wavelet collocation method (HS3WCM) to find the numerical solution of linear and nonlinear HOBVPs. Eleven numerical experiments are performed by considering linear and nonlinear HOBVPs of different orders. L_2 ,L_∞ and absolute errors are calculated for each numerical experiment. It has been observed that as we increase the level of resolution, errors decrease which proves the convergence of HS3WCM solution to the exact solution. High level of accuracy obtained by the proposed method for few grid points (In Numerical Experiment No. 4.11, for two nine grid points, level of accuracy obtained is of 10^{-16}) proves the reliability of this mechanism. The proposed method is equally effective for both linear and nonlinear HOBVPs. The accurateness of the solution is up to the level of 10^{-16} and can be increased by increasing the level of resolution. The performance of the proposed method is compared with the various other methods [4-24] in the numerical experiments and it is found that the proposed method is working better than the other methods. The rapid convergence and high accuracy obtained from the proposed method provides a strong base to extend the application of the method to solve a big class of physical problems governed by ODEs, PDEs, FDEs, and Integral equations. Computational work is fully supportive and compatible with the proposed algorithm.

Chapter 5

Haar Scale 3 Wavelets Based Computational Technique for the investigation of Bagley-Torvik Equations

5.1 Introduction

Fractional calculus is a branch of applied mathematics which emerges as a great tool in explaining the physical and chemical phenomenon with alienate kinetics having microscopic complex behavior. There are fractional differential models which have a non-differentiable but continuous solution such as Weierstrass type functions[1]. These kinds of characteristics are not possible to explain with the help of ordinary or partial differential models. Earlier the field of fractional calculus was purely mathematical without any visible application but in these days, fractional calculus has gained huge importance in the field of science and technology because of its application in the various field like theory of thermo-elasticity[2], viscoelastic fluids[3], dynamics of earthquakes[4], fluid dynamics[5], etc. Bagley-Torvik equation is one of the most important fractional models in the field of viscoelastic fluids. In this model, Bagley and Torvik have studied the motion of a rigid plate immersed into the Newtonian fluid. It is found in the experiment that retarding force is proportional to the fractional derivative of the displacement instead of the velocity. It has been observed during the experiment that the fractional model is superior to the integer-order model for the prediction of characteristics of the same material. But general closed-form solution for fractional Bagley-Torvik equation has yet not been established. Therefore, many researchers are involved in developing the various numerical and semi-analytic schemes for investigating the different phenomena governed by the Bagley-Torvik equation such as Adomian decomposition method [128], Variational iteration method[129], Homotopy analysis method[130], Generalized Taylor collocation method [131], Haar wavelet

method with dilation factor 2[132], Fractional iteration method[133], Bessel collocation method [134], Chebyshev wavelet method [135], Fractional Taylor Method[136], Hybrid functions approximation [137], Gegenbauer Wavelet Method[138], Reproducing kernel [139], Sumudu transformation method [140] etc.

But the study of characteristics of different materials governed by Bagley Torvik equations has yet not been investigated by any of non-dyadic wavelet-based technique. Orthonormal wavelets are one of the modernistic functions which have the capability of dilation and translation. Because of these properties, numerical techniques that involve wavelet bases are showing the qualitative improvement in contrast with other methods. In literature, dyadic wavelets are in preponderance. In 1995, Chui and Lian [115] has developed the Haar scale 3 (non-dyadic) wavelets by using the process of multiresolution analysis. In 2018, Mittal and Pandit have used the Haar scale 3 (non-dyadic) wavelets [71], [141], [142] for solving the various types of differential equations and found that these wavelet bases are equally competent in solving the various types of mathematical models governed by differential equations. Also, it was shown by them that the non-dyadic wavelet has a faster rate of convergence as compared to the Haar scale 2 dyadic wavelets. Moreover, investigation of characteristics of the solution to the Bagley Torvik equation has yet not been done by Haar scale 3 (non-dyadic) wavelet methods. This encourages us to develop a new technique using the Haar scale 3 (non-dyadic) wavelet for analyzing the behavior of systems governed by the Bagley Torvik equation.

The prime purpose of the proposed work is to establish a new computational technique for obtaining the solution of Bagley Torvik equations emerging in the field of fluid dynamics using Haar scale 3 (non-dyadic) wavelet bases as given below

$$\alpha D^2 x(t) + \beta D^{\frac{3}{2}} x(t) + \gamma D^{\frac{1}{2}} x(t) + x(t) = g(t) \tag{5.1}$$

with boundary conditions

$$x(0) = \delta_0 , x(1) = \delta_1 \quad \text{or} \quad x(0) = \delta_2 , x'(1) = \delta_3 \tag{5.2}$$

This chapter follows the sequence of sections as described: In section 2, the basic definitions of fractional calculus are given. In section 3, explicit forms of Haar scale 3 (non-dyadic) parent wavelets with their families and procedure to find their integrals have been explained briefly. Representation of the solution using Haar scale 3 (non-

dyadic) wavelets is explained in section 4. Section 5 explains the method of solution using Haar scale 3 (non-dyadic) wavelets. In section 6, the Argument for the convergence of the technique is given. In section 7, solutions of five different examples of Bagley Torvik equations are produced using the present method to analyze the efficiency and performance of the present method. In section 8, the conclusion drawn from the results and in future research ideas is given.

5.2 Some basic definitions of Fractional calculus

5.2.1 Mittag-Leffler Function

It is an extension of exponential function which has huge importance in the field of fractional calculus. It has two forms of expression as given below

iii. ***One Parameter Mittag-Leffler Function*** [6]for a set of complex numbers and any positive real no α is defined as

$$E_{\alpha} = \sum_{m=0}^{\infty} \frac{z^m}{\Gamma(\alpha m+1)} , \alpha > 0, \alpha \epsilon \mathbb{R} , z \in \mathbb{C} \tag{5.3}$$

iv. ***Two-Parameter Mittag-Leffler Function*** [6] for a set of complex numbers and positive real no's α , β is defined as

$$E_{\alpha,\beta} = \sum_{m=0}^{\infty} \frac{z^m}{\Gamma(\alpha m+\beta)} , \alpha , \beta > 0, \alpha, \beta \epsilon \mathbb{R}, z \in \mathbb{C} \tag{5.4}$$

5.2.2 Riemann-Liouville Fractional Integral Operator [6]

The fractional integral operator defined by the mathematician Riemann-Liouville for the positive real nos. α , a, t over the interval $[a, b]$ is given by

$$_{RL}J_a^{\alpha} f(t) = \frac{1}{\Gamma(\alpha)} \int_a^t f(z)(t-z)^{\alpha-1} dz \tag{5.5}$$

where α denotes the order of derivative and $t \epsilon [a, b]$.

5.2.3 Riemann-Liouville Fractional Differential Operator [6]

The fractional differential operator defined by the mathematician Riemann-Liouville for the positive real nos. α , a, t over the interval $[a, b]$ is given by

$$ {}_{RL}D_a^{\alpha} f(t) = \begin{cases} \frac{1}{\Gamma(m-\alpha)} \frac{d^m}{dt^m} \int_a^t \frac{f(z)}{(t-z)^{\alpha-m+1}} dz \ , m-1 < \alpha < m \in \mathbb{N} \\ \frac{d^m}{dt^m} f(t) \qquad\qquad , \qquad \alpha = m \in \mathbb{N} \end{cases} \tag{5.6} $$

where α denotes the order of derivative and $t\epsilon[a,b]$.

5.2.4 Caputo Fractional Differential Operator [6]

The fractional differential operator defined by the Italian mathematician Caputo for the positive real nos. α , a, t is

$$ {}_{c}D_a^{\alpha} f(t) = \begin{cases} \frac{1}{\Gamma(m-\alpha)} \int_a^t \frac{f^m(z)}{(t-z)^{\alpha-m+1}} dz \ , m-1 < \alpha < m \in \mathbb{N} \\ \frac{d^m}{dt^m} f(t) \qquad\qquad , \qquad \alpha = m \in \mathbb{N} \end{cases} \tag{5.7} $$

where α denotes the order of derivative and $t\epsilon[a,b]$.

5.3 Integrals of Haar scale 3 (non-dyadic) Wavelet

The closed-form expressions for father wavelet, symmetric and antisymmetric mother wavelets for Haar scale 3 (non-dyadic) wavelet family with dilation factor three [71], [115] are given below

Haar scale 3 function

$$ \varphi(t) = \begin{cases} 1 & 0 \le t < 1 \\ 0 & elsewhere \end{cases} \tag{5.8} $$

Haar scale 3 symmetric wavelet function

$$ \psi_1(t) = \frac{1}{\sqrt{2}} \begin{cases} -1 & 0 \le t < \frac{1}{3} \\ 2 & \frac{1}{3} \le t < \frac{2}{3} \\ -1 & \frac{2}{3} \le t < 1 \\ 0 & elsewhere \end{cases} \tag{5.9} $$

Haar scale 3 antisymmetric wavelet function

$$ \psi_2(t) = \sqrt{\frac{3}{2}} \begin{cases} 1 & 0 \le t < \frac{1}{3} \\ 0 & \frac{1}{3} \le t < \frac{2}{3} \\ -1 & \frac{2}{3} \le t < 1 \\ 0 & elsewhere \end{cases} \tag{5.10} $$

The main difference which makes the Haar scale 3 (non-dyadic) wavelets better than the Haar scale 2 dyadic wavelets is that only one mother wavelet is responsible for the construction of whole wavelet family but in case of Haar scale 3 (non-dyadic) wavelets, two mother wavelets with different shapes are responsible for the construction of the whole family. Because of this fact, Haar scale 3 (non-dyadic) wavelets increase the convergence rate of the solution. Wavelets represented by equations (5.9)-(5.10) are the mother wavelets which generate the whole Haar scale 3 (non-dyadic) wavelet family. A multi-resolution analysis is used to get the whole Haar scale 3 (non-dyadic) wavelet family as described below.

5.3.1 Multi-resolution Analysis (MRA)

MRA for space $L_2(R)$ is defined as a sequence of closed subspace $W_j, V_j \subset L_2(R), j \in \mathbb{Z}$ which has the properties as given below

$a)\ \phi(t) \in V_0 \implies \phi(3^j t) \in V_j$

$b)\ \phi(t) \in V_0 \implies \varphi(3^j t - k) \in V_j$

$c)\ \psi^i(t) \in W_0^i, i = 1,2 \implies \psi^i(3^j t) \in W_j^i$

$d)\ \psi^i(t) \in W_0^i, i = 1,2 \implies \psi^i(3^j t - k) \in W_j^i$

$e)\ W_J = W_j^1 \oplus W_j^2 = \oplus W_j^i, i = 1,2$

$f)\ \cdots \subset V_0 \subset V_1 \subset V_2 \subset V_3 \subset V_4 \subset \cdots$

$g)\ \cdots \perp W_0 \perp W_1 \perp W_2 \perp W_3 \perp W_4 \perp \cdots$

$h)\ V_j = V_0 + \sum_{i=0}^{j-1} W_j^1 + \sum_{i=0}^{j-1} W_j^2$

$i)\ \phi(t) \in V_0\ implies\ \phi(\mathrm{t} - \mathrm{k}) \in V_0; k \in \mathbb{Z}$ and it forms Riesz basis in V_0

Now by applying MRA, generalized form of Haar scale 3 (non-dyadic) wavelet family is obtained as follows:

$For\ i = 1$

$$h_i(t) = \varphi(t) = \begin{cases} 1 & 0 \le t < 1 \\ 0 & elsewhere \end{cases} \tag{5.11}$$

$For \quad i = 2,4, \dots 3p-1$

$$h_i(t) = \psi^1\left(3^j t - k\right) = \frac{1}{\sqrt{2}}\begin{cases} -1 & \varkappa_1(i) \le t < \varkappa_2(i) \\ 2 & \varkappa_2(i) \le t < \varkappa_3(i) \\ -1 & \varkappa_3(i) \le t < \varkappa_4(i) \\ 0 & elsewhere \end{cases} \tag{5.12}$$

$For \quad i = 3,6, \dots 3p$

$$h_i(t) = \psi^2\left(3^j t - k\right) = \sqrt{\frac{3}{2}}\begin{cases} 1 & \varkappa_1(i) \le t < \varkappa_2(i) \\ 0 & \varkappa_2(i) \le t < \varkappa_3(i) \\ -1 & \varkappa_3(i) \le t < \varkappa_4(i)' \\ 0 & elsewhere \end{cases} \tag{5.13}$$

where $\varkappa_1(i) = \frac{k}{p}, \varkappa_2(i) = \frac{3k+1}{3p}, \ \varkappa_3(i) = \frac{(3k+2)}{3p}, \ \varkappa_4(i) = \frac{k+1}{p}, \ p = 3^j \ , \ j = 0,1,2, \dots , k = 0,1,2, \dots , p-1$. Here i , j , k respectively represent the wavelet number, level of resolution (dilation), and translation parameters of wavelet family. The values of i $(for\ i > 1)$ can be calculated with the help of j , k by using the following relations $\begin{cases} i - 1 = 3^j + 2k & for\ even\ i \\ i - 2 = 3^j + 2k & for\ odd\ i \end{cases}$.By using this relation for different dilation and translations of $h_2(t), h_3(t)$, we will get the wavelet family as $h_2(t), h_3(t), h_4(t), h_5(t), h_6(t), \dots$ where $h_2(t)$and $h_3(t)$ are also called mother wavelets and rest all the wavelets which we have obtained from mother wavelet are called daughter wavelets.

Now one can easily integrate the equations (5.11)-(5.13) the desired number of times over the interval [A, B) by using Riemann Liouville Integral formula [6] as given below

$$q_{\beta,i}(t) = \frac{1}{\Gamma(\beta)}\int_A^t h_i(x)(t-x)^{\beta-1}dx \qquad \forall \quad 0 \le \beta \le m \,, \quad m = 1,2,3 \dots \dots \ , \qquad i = 1,2,3, \dots \dots 3p \tag{5.14}$$

After evaluating the above integrals $q_{\beta,i}(t)'s \quad for \quad i = 2,4,6,8, \cdots, 3p-1$ are given below $q_{\beta,i}(t) =$

$$\frac{1}{\sqrt{2}}\begin{cases} 0 & for \quad 0 \le t \le \varkappa_1(i) \\ \frac{-1}{\Gamma(\beta+1)}\left(t-\varkappa_1(i)\right)^{\beta} & for \ \varkappa_1(i) \le t \le \varkappa_2(i) \\ \frac{1}{\Gamma(\beta+1)}\left[-\left(t-\varkappa_1(i)\right)^{\beta} + 3\left(t-\varkappa_2(i)\right)^{\beta}\right] & for \quad \varkappa_2(i) \le t \le \varkappa_3(i) \\ \frac{1}{\Gamma(\beta+1)}\left[-\left(t-\varkappa_1(i)\right)^{\beta} + 3\left(t-\varkappa_2(i)\right)^{\beta} - 3\left(t-\varkappa_3(i)\right)^{\beta}\right] & for\ \varkappa_3(i) \le t \le \varkappa_4(i) \\ \frac{1}{\Gamma(\beta+1)}\left[-\left(t-\varkappa_1(i)\right)^{\beta} + 3\left(t-\varkappa_2(i)\right)^{\beta} - 3\left(t-\varkappa_3(i)\right)^{\beta} + \left(t-\varkappa_4(i)\right)^{\beta}\right] & for\ \varkappa_4(i) \le t \le 1 \end{cases} \tag{5.15}$$

$q_{\beta,i}(t)'s \quad for \quad i = 3,5,7,9,\cdots,3p$ are given by $q_{\beta,i}(t) =$

$$\sqrt{\frac{3}{2}}\begin{cases} 0 & for \quad 0 \le t \le \varkappa_1(i) \\ \frac{1}{\Gamma(\beta+1)}\left(t-\varkappa_1(i)\right)^{\beta} & for \quad \varkappa_1(i) \le t \le \varkappa_2(i) \\ \frac{1}{\Gamma(\beta+1)}\left[\left(t-\varkappa_1(i)\right)^{\beta}-\left(t-\varkappa_2(i)\right)^{\beta}\right] & for \quad \varkappa_2(i) \le t \le \varkappa_3(i) \\ \frac{1}{\Gamma(\beta+1)}\left[\left(t-\varkappa_1(i)\right)^{\beta}-\left(t-\varkappa_2(i)\right)^{\beta}-\left(t-\varkappa_3(i)\right)^{\beta}\right] & for \quad \varkappa_3(i) \le t \le \varkappa_4(i) \\ \frac{1}{\Gamma(\beta+1)}\left[\left(t-\varkappa_1(i)\right)^{\beta}-\left(t-\varkappa_2(i)\right)^{\beta}-\left(t-\varkappa_3(i)\right)^{\beta}+\left(t-\varkappa_4(i)\right)^{\beta}\right] & for\ \varkappa_4(i) \le t \le 1 \end{cases} \tag{5.16}$$

$$q_{\beta,i}(t) = \frac{t^{\beta}}{\Gamma(\beta+1)} \qquad for \quad i = 1 \tag{5.17}$$

5.4 Approximation of solution

Using the properties of Haar scale 3 (non-dyadic) wavelets as explained in section 3, any function $x(t) \in L_2(R)$ can be expressed as

$$\begin{aligned} x(t) &= \sum_{i=0}^{\infty} a_i h_i(t) \\ &= a_1 h_1(t) + \sum_{even\ i} a_i \psi^1\left(3^j t - k\right) + \sum_{odd\ i>1} a_i \psi^2\left(3^j t - k\right) \end{aligned} \tag{5.18}$$

Here $a_i's$ are the wavelet coefficients and their values are to be determined by the proposed method. But for computational purposes, one has to consider a finite number of terms. By considering the first $3p$ terms to approximate the function $u(t)$ we get

$$x(t) \approx u_{3p} = \sum_{i=0}^{3p} a_i h_i(t) \ \text{ where } \ p = 3^j, j = 0,1,2,\ldots \tag{5.19}$$

5.5 Method of Solution Based on Haar Scale 3 Wavelets

Consider the Bagley Torvik equation

$$\alpha D^2 x(t) + \beta D^{\frac{3}{2}} x(t) + \gamma D^{\frac{1}{2}} x(t) + \delta x(t) = g(t) \tag{5.20}$$

with initial conditions $x(0) = \delta_2\,, x'(0) = \delta_3$, where $\alpha\,, \beta, \gamma, \delta$ are the arbitrary constants.

Now the solution x(t) for the above equation can be obtained using the following steps

Step1: Approximate the highest order derivative present in the equation (5.20) (i.e. $D^2x(t)$) using the Haar scale 3 (non-dyadic) wavelet bases as

$$D^2x(t) = \sum_{i=0}^{3p} a_i h_i(t) = a_1 h_1(t) + \sum_{even\ i} a_i \psi^1\left(3^j t - k\right) + \sum_{odd\ i>1} a_i \psi^2\left(3^j t - k\right) \tag{5.21}$$

where $a_i's$ for i=0,1, 2…,3p are the Haar scale 3 (non-dyadic) wavelet coefficients

Step 2: By integrating the equation (5.21) within the limits 0 to t, we get

$$x'(t) = \sum_{i=0}^{3p} a_i q_{1,i}(t) + y'(0) = \sum_{i=0}^{3p} a_i q_{1,i}(t) + \delta_3 \tag{5.22}$$

Again, integrating the equation (5.22) within the limits 0 to t, we get

$$x(t) = \sum_{i=0}^{3p} a_i q_{2,i}(t) + \delta_3 t + y(0) = \sum_{i=0}^{3p} a_i q_{2,i}(t) + \delta_3 t + \delta_2 \tag{5.23}$$

Step 3: Differentiate the equation (5.23) using Caputo definition of fractional derivatives we get

$$D^{\frac{1}{2}}x(t) = \sum_{i=0}^{3p} a_i q_{\frac{3}{2},i}(t) + 2\,\delta_3\sqrt{\frac{t}{\pi}} \tag{5.24}$$

$$D^{\frac{3}{2}}x(t) = \sum_{i=0}^{3p} a_i q_{\frac{1}{2},i}(t) + \delta_3 \frac{1}{\sqrt{\pi t}} \tag{5.25}$$

Step 4: Using equations (5.21)-(5.25),Equation (5.20) becomes

$$\alpha \sum_{i=0}^{3p} a_i h_i(t) + \beta\left[\sum_{i=0}^{3p} a_i q_{\frac{1}{2},i}(t) + \delta_3 \frac{1}{\sqrt{\pi t}}\right] + \gamma\left[\sum_{i=0}^{3p} a_i q_{\frac{3}{2},i}(t) + 2\,\delta_3\sqrt{\frac{t}{\pi}}\right] + \delta[\sum_{i=0}^{3p} a_i q_{2,i}(t) + \delta_3 t + \delta_2] = g(t) \tag{5.26}$$

After simplification, we get

$$\sum_{i=0}^{3p} a_i[\alpha h_i(t) + \beta q_{\frac{1}{2},i}(t) + \gamma\, q_{\frac{3}{2},i}(t) + \delta q_{2,i}(t)] = g(t) - \left[\beta\delta_3 \frac{1}{\sqrt{\pi t}} + 2\gamma\delta_3\sqrt{\frac{t}{\pi}} + \delta(\delta_3 t + \delta_2)\right] \tag{5.27}$$

Step 4: After Discretizing the equation (5.27) using the collocation points we get the following matrix system

$$aH = F \tag{5.28}$$

Then using the Thomas algorithm, we obtained the wavelet coefficients $a_i's$. Then by substituting the values of wavelet coefficients $a_i's$ in equation (5.23), we get the non-dyadic wavelet-based solution of Bagley Torvik equations with the given initial conditions. Similarly, by using the above steps we can find the solution of Bagley Torvik equations with other boundary conditions.

5.6 Convergence Analysis

Mittal and Pandit [78] has proved that if $x(t)\,\epsilon L^2(R)$ such that $|x^m(t)| \leq M, \forall\, t\epsilon(0,1)$ where M is any real constant and x(t) is approximated by Haar scale 3 (non-dyadic) family as given below:

$$x_{3p}(t) = \sum_{i=0}^{3p} a_i h_i(t) \tag{5.29}$$

Then the error bound for the solution $x(t)$ using L_2-norm is calculated as

$$\left\|x(t) - x_{3p}(t)\right\| \leq \left(\frac{2}{3}\right)^{2(m-\alpha)} \frac{8\,M^2}{\left(\Gamma(m-\alpha+1)\right)^2}\left(\frac{3^{-2(j+1)(m-\alpha+1)}}{1-3^{-2(m-\alpha)+1}}\right) \tag{5.30}$$

Clearly, the error bound is inversely proportional to the level of resolution which ensures the convergence of approximated solution to exact solution with the increase in the level of resolution j. Moreover, if we know the exact values of $m, \alpha,$ and M, then the maximum value of error bound can also be calculated.

5.7 Error Analysis by Numerical Experiments

To describe the appropriateness of the proposed technique for the Bagley Torvik equations of fractional order, solutions of five different problems obtained by the proposed computational technique have been analyzed and absolute errors are calculated to check the efficiency of the present scheme with the help of following formulas

$$\text{Absolute error} = |x_{exact}(t_l) - x_{num}(t_l)| \tag{5.31}$$

where t_l represents the collocation points of the domain.

Numerical Experiment No. 5.1 : $D^2x + D^{\frac{3}{2}}x + x = t^2 + 4\sqrt{\frac{t}{\pi}} + 2$ under the boundary constraints $x(0) = 0, x(1) = 1$ (5.32)

Exact solution of the problem is $x(t) = t^2$

After applying the method of the solution discussed in section 5.5 the following solution is proposed

$$x(t) = \sum_{i=1}^{3p} a_i[q_{2,i}(t) - tq_{2,i}(1)] + t \tag{5.33}$$

$a_i's$ are the wavelets coefficients which will be obtained by the following procedure and $q_{j,i}'s$ are the wavelet integrals that have been already calculated in section 5.3. After applying the proposed scheme on Equation (5.32), it reduced to the following system

$$\sum_{i=0}^{3p} a_i \left[\sqrt{\pi t}\left(h_i(t) + q_{\frac{1}{2},i}(t) + q_{2,i}(t)\right) - \left(\sqrt{\pi}t^{\frac{3}{2}} + 1\right)q_{2,i}(1)\right] = 4t + 1 + \sqrt{\pi}\left[t^{\frac{5}{2}} - t^{\frac{3}{2}} + 2t^{\frac{1}{2}}\right] \tag{5.34}$$

After discretizing the equation(5.34) using the collocation points we get the following matrix system

$$aH = F$$

After solving the above matrix system, we get the values of $a_i's$.which will be used to find out the solution. Results achieved by the proposed technique are conferred by the graphs and tables for the better visibility of accuracy. Figure 5.1 and Table 5.1 demonstrate the visible agreement in the exact and approximated solutions. In Table 5.1 results achieved by the present technique are compared with other method existing in the recent literature and found it outperform over others methods like Variational Iteration Method (VIM)[129], Homotopy asymptotic method (HAM)[130], Reproducing Kernel Analysis (RKA)[139], which demonstrates the superiority and reliability of the method. Figure 5.2 is depicting the high level of accuracy (which is of order 10^{17}) obtained at the different collocation points.

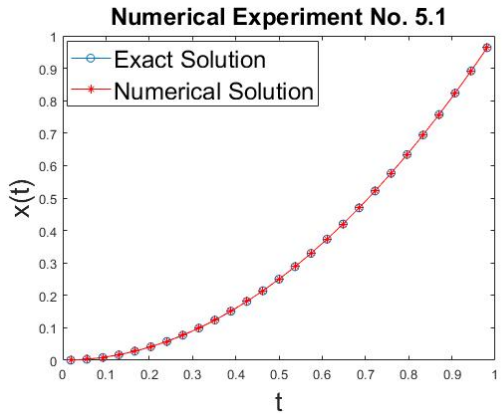

Figure 5.1: Comparison of exact and numerical solution of Numerical Experiment No. 5.1 at the level of resolution J=2

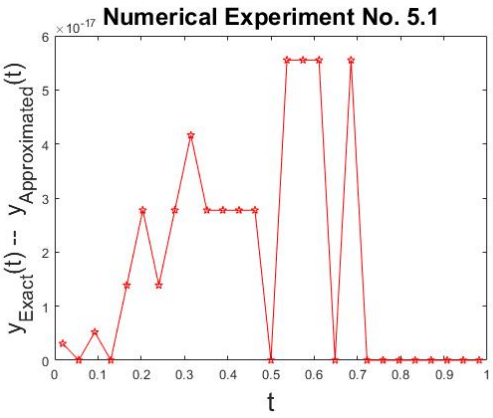

Figure 5.2: Absolute error at the different collocation points considered for the solution of Numerical Experiment No. 5.1

Table 5.1: Comparision of results achieved with other methods in the existing literature for the Numerical Experiment. No. 5.1

t	**Exact Solution**	**Present Method(E*)**	**RKA(E*)**[139]	**VIM(E*)**[129]	**HAM(E*)**[130]
0.1	0.01	6.93889390390723e-18	0	0.5487432e−4	2.3265e-13
0.2	0.04	0	0	0.6312556e−3	1.4385e-11
0.3	0.09	0	0	0.2665571e−2	6.1890e-11
0.4	0.16	2.77555756156289e-17	0	0.7480121e−2	2.2736e-11
0.5	0.25	0	2.77555756156289e-17	0.1679592e−1	1.3680e-10
0.6	0.36	0	5.55111512312578e-17	0.3277307e−1	3.5678e-11
0.7	0.49	5.55111512312578e-17	5.55111512312578e-17	0.5806535e−1	2.6188e-10
0.8	0.64	0	1.11022302545678e-17	0.9588508e−1	4.3416e-10
0.9	0.81	0	1.11022302545678e-17	0.1500768448	1.0816e-10

E*(Absolute Error)

Numerical Experiment No. 5.2 : $D^2x(t) + 0.5\,D^{\frac{1}{2}}x(t) + x(t) = 3 + t^2\left(\frac{1}{\Gamma(2.5)}t^{-0.5} + 1\right)$ w.r.t B. C's $x(0) = 0, x(1) = 2$ (5.35)

Exact solution of the problem is $x(t) = t^2 + 1$.

After applying the method of the solution discussed in section 5.5 the following solution is proposed

$$x(t) = \sum_{i=1}^{3p} a_i[q_{2,i}(t) - tq_{2,i}(1)] + t + 1 \quad (5.36)$$

$a_i's$ are the wavelets coefficients which will be obtained by the following procedure and $q_{j,i}'s$ are the wavelet integrals that have been already calculated in section 5.3.

After applying the proposed technique on the equation no.(5.35). It reduced to the following system

$$\sum_{i=0}^{3p} a_i \left[\left(h_i(t) + \frac{1}{2} q_{\frac{3}{2},i}(t) + q_{2,i}(t) \right) - \left(\frac{t^{\frac{1}{2}}}{\sqrt{\pi}} + t \right) q_{2,i}(1) \right] = t^2 - t + 2 + \left[\frac{4}{3\sqrt{\pi}} t^{\frac{3}{2}} - \frac{1}{\sqrt{\pi}} t^{\frac{1}{2}} \right] \tag{5.37}$$

After discretizing the equation (5.37) using collocation points we get the matrix system.

$$aH = F$$

After solving the above matrix system, we get the vales of $a_i's$.which will be used to find out the solution.

It can be observed from Table 5.2 and Figure 5.3 that the results achieved by the proposed method agree well with the exact solution, which demonstrates the high efficiency of the proposed technique to solve these kinds of problems. Also from Table 5.2, we can conclude that the proposed technique is a strong solver in terms of better accuracy in comparison with the other method [139]. Figure 5.4 is showing the errors at the different colocation points.

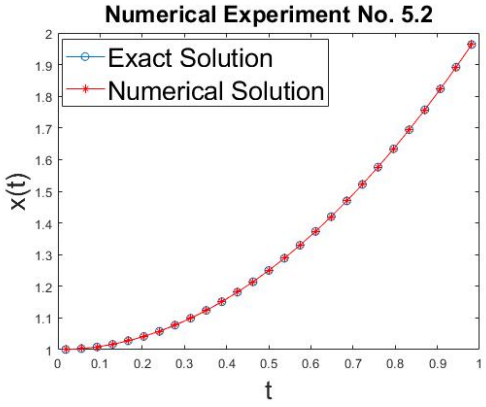

Figure 5.3: Comparison of exact and numerical solution of Numerical Experiment No. 5.2 at the level of resolution J=2

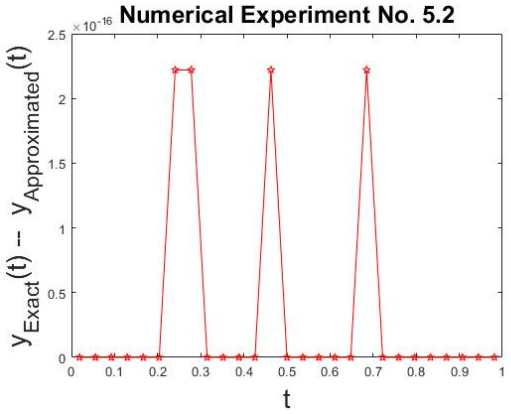

Figure 5.4: Absolute error at the different collocation points considered for the solution of Numerical Experiment No. 5.2

Table 5.2: Comparison of results achieved with other methods in the existing literature for the Numerical Experiment. No. 5.2

t	Exact Solution	Approximated Solution	Present Method(E^*)	RKA(E^*)[139]
0.1	1.01	1.01000000000000000000	0	1.932676241e-12
0.2	1.04	1.04000000000000000000	0	3.161981788e-11
0.3	1.09	1.09000000000000000000	0	3.679907490e-10
0.4	1.16	1.16000000000000000000	0	3.661697390e-09
0.5	1.25	1.25000000000000000000	0	3.300057339e-09
0.6	1.36	1.36000000000000000000	0	2.745960126e-09
0.7	1.49	1.49000000000000022204	2.22044604925031e-16	2.096272045e-10
0.8	1.64	1.64000000000000000000	0	1.404942829e-11
0.9	1.81	1.81000000000000000000	0	7.004619107e-12

E* (Absolute Error)

Numerical Experiment No. 5.3 : Consider the equation $D^2x(t) + D^{\frac{1}{2}}x(t) + x(t) = 2 + t^2\left(\frac{2}{\Gamma(2.5)}t^{-0.5} + 1\right) - t\left(\frac{1}{\Gamma(1.5)}t^{-0.5} + 1\right)$ subjected to the boundary condition $x(0) = 0, x(1) = 0$ (5.38)

Exact solution of the Numerical Experiment is $x(t) = t^2 - t$.

After applying the method of the solution discussed in section 5 the following solution is obtained by the proposed method

$$x(t) = \sum_{i=1}^{3p} a_i[q_{2,i}(t) - tq_{2,i}(1)] \tag{5.39}$$

$a_i's$ are the wavelets coefficients which will be obtained by the procedure discussed above and $q_{j,i}'s$ are the wavelet integrals that have been already calculated in section 5.3. Table 5.3 depicting the performance of the method in contrast with other methods existing in the recent literature. It validates the high efficiency and performance of the method. Getting high accuracy for a small number of grid points makes it a strong solver for these kinds of mathematical models. Figure 5.5 demonstrates that the results achieved with the proposed technique agree well with the exact solution and Figure 5.6 explains the errors in the solution at the different collocation points.

Table 5.3: Comparision of results achieved with other methods in the existing t literature for Numerical Experiment. No. 5.3

t	Exact Solution	Approximated Solution	Present Method (E^*)	RKA(E^*)[139]
0.1	-0.09000	-0.09000000000000000000000000000	0	4.178019042e-12
0.2	-0.16000	-0.16000000000000000027755575615629	-2.77555756156289e-17	6.892891813e-11
0.3	-0.21000	-0.21000000000000000055511151231258	5.55111512312578e-17	8.052572498e-10
0.4	-0.24000	-0.24000000000000000055511151231258	5.55111512312578e-17	8.010652391e-09
0.5	-0.25000	-0.25000000000000000055511151231258	5.55111512312578e-17	7.193844853e-09
0.6	-0.24000	-0.24000000000000000055511151231258	5.55111512312578e-17	5.949374826e-09
0.7	-0.21000	-0.21000000000000000055511151231258	5.55111512312578e-17	4.504783491e-10
0.8	-0.16000	-0.16000000000000000027755575615629	2.77555756156289e-17	2.989430925e-11
0.9	-0.09000	-0.09000000000000000027755575615629	2.77555756156289e-17	1.473612898e-12

E^* (Absolute Error)

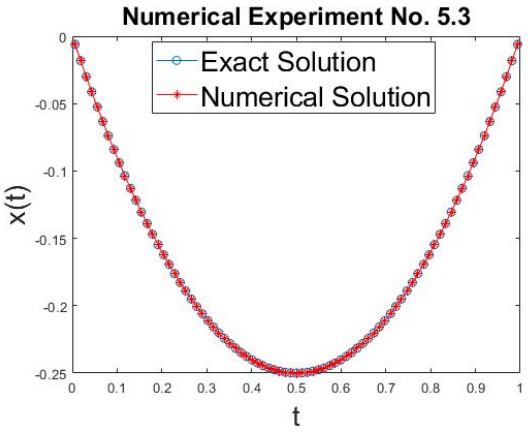

Figure 5.5: Comparison of exact and numerical solution of Numerical Experiment No. 5.3 at the level of resolution J=2

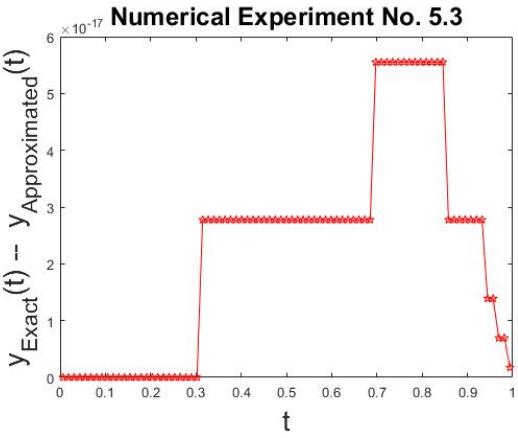

Figure 5.6: Absolute error at the different collocation points considered for the solution of Numerical Experiment No. 5.3

Numerical Experiment No. 5.4 : $D^2x(t) + D^{\frac{3}{2}}x(t) + x(t) = t + \frac{1}{\sqrt{\pi t}} + 1$ subjected the boundary condition $x(0) = 0,\ x'(1) = 1$ (5.40)

to Analytic solution of the problem is $x(t) = t + 1$.

By using the method of the solution discussed in section 5.5, we proposed the following solution for the above equations

$$x(t) = \sum_{i=1}^{3p} a_i q_{2,i}(t) + t + 1 \tag{5.41}$$

$a_i's$ are the wavelets coefficients which will be obtained by the procedure discussed above and $q_{j,i}'s$ are the wavelet integrals that have been already calculated in section 5.3. It is shown in Table 5.4 and Figure 5.8 that the results achieved with the proposed technique are exactly matching with the exact solution with no error. It is also shown in Table 5.4 that the results achieved with the proposed technique are superior to the results obtained by the other methods available in the existing literature. Figure 5.7 explains the high level of agreement between the exact and approximated solution.

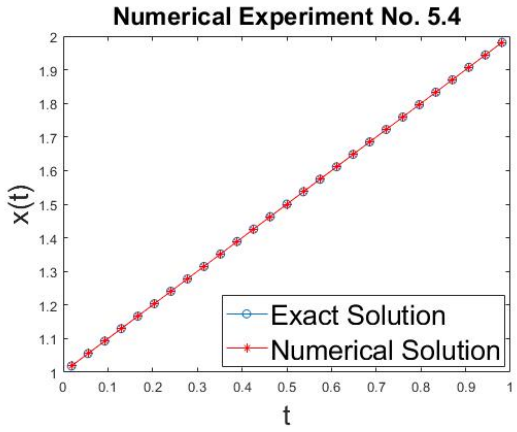

Figure 5.7: Comparison of exact and numerical solution of Numerical Experiment No. 5.4 at the level of resolution J=2

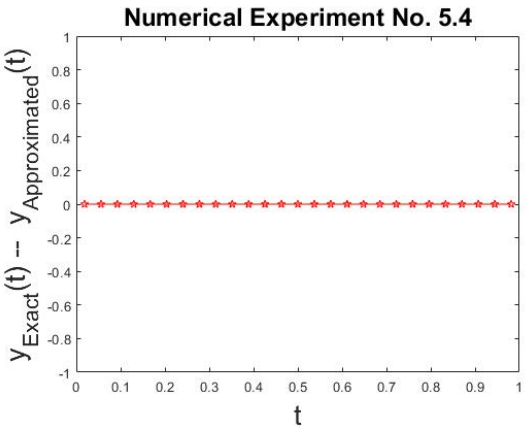

Figure 5.8: Absolute error at the different collocation points considered for the solution of Numerical Experiment No. 5.4

Table 5.4: Comparison of results achieved with other methods in the existing literature for the Numerical Experiment. No. 5.4

t	**Exact Solution**	**Approximated Solution**	**Present Method (E^*)**	**RKA(E^*)**[139]	**BCM(E^*)**[134]
0.1	1.1	1.1	0	0	9.3742e-16
0.2	1.2	1.2	0	0	3.9634e-15
0.3	1.3	1.3	0	0	4.2834e-15
0.4	1.4	1.4	0	0	3.2975e-15
0.5	1.5	1.5	0	0	2.0455e-15
0.6	1.6	1.6	0	2.220446049E-16	1.0277e-15
0.7	1.7	1.7	0	0	3.4773e-16
0.8	1.8	1.8	0	0	6.9289e-17
0.9	1.9	1.9	0	2.220446049E-16	2.3947e-16

E* (Absolute Error)

Numerical Experiment No. 5.5 : $D^{\frac{3}{2}}x(t) + x(t) = t^5 - t^4 + \frac{128}{7\sqrt{\pi}}t^{\frac{7}{2}} - \frac{64}{5\sqrt{\pi}}t^{\frac{5}{2}}$

subjected to the boundary condition $x(0) = 0, x(1) = 0$ (5.42)

Exact solution for this numerical experiment is $x(t) = t^5 - t^4$

Using the method of solution explained in section no 5.5, Following solution is proposed for the numerical experiment no. 5.5

$$x(t) = \sum_{i=1}^{3p} a_i[q_{2,i}(t) - tq_{2,i}(1)] \quad (5.43)$$

$a_i's$ are the wavelets coefficients which will be obtained by the procedure discussed above and $q_{j,i}'s$ are the wavelet integrals that have been already calculated in section 3. Results presented in Figure 5.9 and Figure 5.10 are depicting the performance of the proposed method. It can be observed from these figures that results are roughly matching with the exact solution. Table 5.5 represents the absolute error at the collocation points.

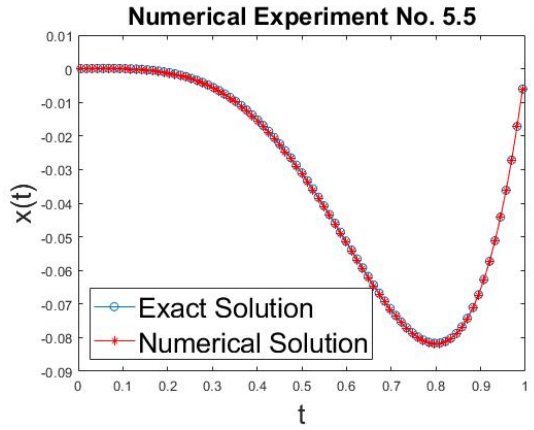

Figure 5.9: Comparison of exact and numerical solution of Numerical Experiment No. 5.5 at the level of resolution J=2

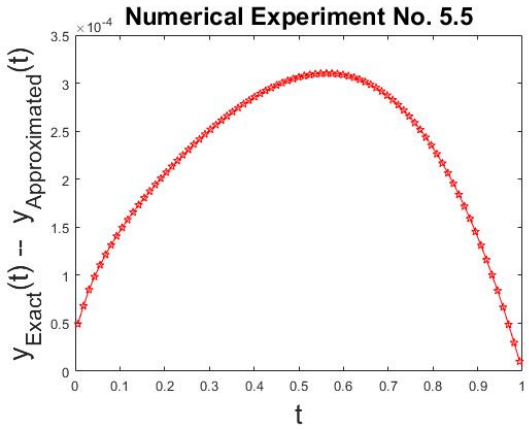

Figure 5.10: Absolute error at the different collocation points in Numerical Experiment No. 5.5

Table 5.5: Comparision of results achieved by the proposed method with the exact solution for the Numerical Experiment. No.5.5

t	Exact Solution	Approximated Solution	Present Method (E^*)
0.00617284	-1.4429480000E-09	4.9171205846E-05	4.92E-05
0.01851852	-1.1542691000E-07	6.7922819931E-05	6.80E-05
0.0308642	-8.7943672400E-07	8.3907873324E-05	8.48E-05
0.04320988	-3.3354066130E-06	9.5100857199E-05	9.84E-05
0.05555556	-8.9967653980E-06	1.0151360079E-04	1.11E-04
0.06790123	-1.9814020830E-05	1.0157260482E-04	1.21E-04
0.08024691	-3.8140343926E-05	9.3243967138E-05	1.31E-04
0.09259259	-6.6697153309E-05	7.3993891171E-05	1.41E-04
0.10493827	-1.0853969954E-04	4.0900842117E-05	1.49E-04
0.11728395	-1.6702264946E-04	-9.2943502120E-06	1.58E-04
0.12962963	-2.4576567051E-04	-8.0140150666E-05	1.66E-04
0.14197531	-3.4861901510E-04	-1.7543265253E-04	1.73E-04
0.15432099	-4.7962910491E-04	-2.9917635750E-04	1.80E-04
0.16666667	-6.4300411523E-04	-4.5554663647E-04	1.87E-04
0.17901235	-8.4307955932E-04	-6.4885316645E-04	1.94E-04
0.19135802	-1.0842838727E-03	-8.8350400114E-04	2.01E-04
0.2037037	-1.3711039977E-03	-1.1639700577E-03	2.07E-04
0.21604938	-1.7080509673E-03	-1.4947498869E-03	2.13E-04
0.22839506	-2.0996254899E-03	-1.8803346416E-03	2.19E-04
0.24074074	-2.5502835338E-03	-2.3251731862E-03	2.25E-04
0.25308642	-3.0644019109E-03	-2.8336373097E-03	2.31E-04
0.2654321	-3.6462438616E-03	-3.4099870140E-03	2.36E-04
0.27777778	-4.2999246389E-03	-4.0583358614E-03	2.42E-04
0.29012346	-5.0293770928E-03	-4.7826163651E-03	2.47E-04
0.30246914	-5.8383172545E-03	-5.5865454139E-03	2.52E-04
0.31481481	-6.7302099212E-03	-6.4735897242E-03	2.57E-04
0.32716049	-7.7082342397E-03	-7.4469313129E-03	2.61E-04
0.33950617	-8.7752492913E-03	-8.5094329872E-03	2.66E-04
0.35185185	-9.9337596759E-03	-9.6636038485E-03	2.70E-04
0.36419753	-1.1185881097E-02	-1.0911564807E-02	2.74E-04
0.37654321	-1.2533305943E-02	-1.2255014107E-02	2.78E-04
0.38888889	-1.3977268878E-02	-1.3695192856E-02	2.82E-04
0.40123457	-1.5518512420E-02	-1.5232850567E-02	2.86E-04
0.41358025	-1.7157252525E-02	-1.6868210697E-02	2.89E-04
0.42592593	-1.8893144178E-02	-1.8600936200E-02	2.92E-04
0.4382716	-2.0725246971E-02	-2.0430095076E-02	2.95E-04
0.45061728	-2.2651990688E-02	-2.2354125925E-02	2.98E-04
0.46296296	-2.4671140892E-02	-2.4370803509E-02	3.00E-04
0.47530864	-2.6779764510E-02	-2.6477204310E-02	3.03E-04
0.48765432	-2.8974195412E-02	-2.8669672090E-02	3.05E-04
0.5	-3.1250000000E-02	-3.0943783462E-02	3.06E-04
0.51234568	-3.3601942792E-02	-3.3294313448E-02	3.08E-04

0.52469136	-3.6023952003E-02	-3.5715201053E-02	3.09E-04
0.53703704	-3.8509085134E-02	-3.8199514831E-02	3.10E-04
0.54938272	-4.1049494554E-02	-4.0739418453E-02	3.10E-04
0.5617284	-4.3636393083E-02	-4.3326136283E-02	3.10E-04
0.57407407	-4.6260019578E-02	-4.5949918942E-02	3.10E-04
0.58641975	-4.8909604518E-02	-4.8600008887E-02	3.10E-04
0.59876543	-5.1573335587E-02	-5.1264605982E-02	3.09E-04
0.61111111	-5.4238323257E-02	-5.3930833072E-02	3.07E-04
0.62345679	-5.6890566377E-02	-5.6584701554E-02	3.06E-04
0.63580247	-5.9514917752E-02	-5.9211076957E-02	3.04E-04
0.64814815	-6.2095049731E-02	-6.1793644516E-02	3.01E-04
0.66049383	-6.4613419790E-02	-6.4314874745E-02	2.99E-04
0.67283951	-6.7051236116E-02	-6.6755989015E-02	2.95E-04
0.68518519	-6.9388423191E-02	-6.9096925131E-02	2.91E-04
0.69753086	-7.1603587380E-02	-7.1316302911E-02	2.87E-04
0.70987654	-7.3673982508E-02	-7.3391389755E-02	2.83E-04
0.72222222	-7.5575475453E-02	-7.5298066235E-02	2.77E-04
0.7345679	-7.7282511722E-02	-7.7010791659E-02	2.72E-04
0.74691358	-7.8768081044E-02	-7.8502569662E-02	2.66E-04
0.75925926	-8.0003682946E-02	-7.9744913774E-02	2.59E-04
0.77160494	-8.0959292343E-02	-8.0707813004E-02	2.51E-04
0.78395062	-8.1603325119E-02	-8.1359697417E-02	2.44E-04
0.7962963	-8.1902603714E-02	-8.1667403713E-02	2.35E-04
0.80864198	-8.1822322707E-02	-8.1596140806E-02	2.26E-04
0.82098765	-8.1326014400E-02	-8.1109455403E-02	2.17E-04
0.83333333	-8.0375514403E-02	-8.0169197584E-02	2.06E-04
0.84567901	-7.8930927218E-02	-7.8735486380E-02	1.95E-04
0.85802469	-7.6950591824E-02	-7.6766675354E-02	1.84E-04
0.87037037	-7.4391047259E-02	-7.4219318181E-02	1.72E-04
0.88271605	-7.1206998208E-02	-7.1048134226E-02	1.59E-04
0.89506173	-6.7351280585E-02	-6.7205974126E-02	1.45E-04
0.90740741	-6.2774827117E-02	-6.2643785369E-02	1.31E-04
0.91975309	-5.7426632931E-02	-5.7310577875E-02	1.16E-04
0.93209877	-5.1253721134E-02	-5.1153389575E-02	1.00E-04
0.94444444	-4.4201108401E-02	-4.4117251993E-02	8.39E-05
0.95679012	-3.6211770559E-02	-3.6145155825E-02	6.66E-05
0.9691358	-2.7226608169E-02	-2.7178016522E-02	4.86E-05
0.98148148	-1.7184412112E-02	-1.7154639868E-02	2.98E-05
0.99382716	-6.0218291745E-03	-6.0116875623E-03	1.01E-05

E^* (Absolute Error)

5.8 Conclusion

After looking at the results of five numerical experiments performed using the proposed technique, we infer that the Bagley-Torvik equation of fractional order can easily be solved by the proposed scheme with less computational cost and high accuracy. For example, in Numerical Experiment no. 1 level of accuracy obtained is or order 10^{-17} for only 9 colocation points in the first iteration. Moreover, the use of common MATLAB subprograms to solve various types of fractions equations, makes it more computer-friendly. Very good accuracy is obtained for a very small number of collocation points and the results achieved are better than or at par with the other methods existing in the recent literature. It makes the proposed scheme a strong solver for these kinds of fractional differential equations. Therefore, by looking at the performance of the method, we conclude that the given method can be extended to solve other sets of fractional differential equations. All the calculations have been performed using MATLAB 7. Computational time taken by each experiment to give solution using MATLAB 7 software installed on system with 4gb ram and intel core i3 processor is 3.546sec, 3.319 sec, 2.410 sec, 3.361 sec, 3.813 sec respectively.

Chapter 6

Haar Scale-3 wavelets and Quasilinearization based Hybrid Technique for the Solution of Coupled Space-Time Fractional- Burgers' Equation

6.1 Introduction

Fractional calculus emerges as a great tool in explaining the physical and chemical phenomenon with alienate kinetics having microscopic complex behavior. There are fractional differential models which have a non-differentiable but continuous solution such as Weierstrass type functions[1]. These kinds of characteristics are not possible to explain with the help of ordinary or partial differential models. Earlier the field of fractional calculus was purely mathematical without any visible application but in these days, fractional calculus has gained huge importance in the field of science and technology because of its application in the various field like theory of thermo-elasticity[2], viscoelastic fluids[3], dynamics of earthquakes[4], fluid dynamics[5], etc. It has also been observed experimentally and from the real-time observation that there are many complex systems in the real world like relaxation in viscoelastic material, pollution diffusion in the surrounding, charge transport in amorphous semiconductors, and many more which show anomalous dynamics. This capability of fractional differential equations of explaining the abnormal dynamic of the system with more efficiency and accuracy has gained huge attention from the scientific community. Many of the important classical differential equations with integer-order has got extensions to the generalized fraction differential equation with an arbitrary order for in-depth study of the corresponding physical model. But the general analytic solution for many fractional differential equations that are non-homogeneous in nature are very difficult

and cumbersome to achieve. Moreover, finding the solution of such equations becomes more challenging when there are nonlinearities in the equations.

Therefore, many researchers are involved in developing the various numerical and semi-analytic schemes for finding solutions to the different problems governed by these differential equations. Some of the fractional differential equations which have been recently studied because of their capability of explaining the real time phenomena's are fractional Black-Scholes equation[143], time-fractional Klein–Gordon equations [144], [145], time-fractional Fisher's equation [146], [147] , fractional Bagley Torvik equation [148], time-fractional Burgers' equation[149], [150] , Fitzhugh–Nagumo fractional differential equation [151], fractional Ginzburg-Landau equation[152], [153], fractional Korteweg-de Vries–Burgers' equation[154], [155], nonlinear fractional order oscillatory Van der Pol system[156], fractional Poisson equation [157],fractional Riccati differential equations [158],fractional Schrodinger equation[159], fractional Sine-Gordon equations[160], fractional Bioheat equations [161] ,time fractional Caudrey-Dodd-Gibbon-Sawada-Kotera equation [162] , Sharma–Tasso–Olver equation[163], Fokker–Planck fractional equation[164], [165], fractional Telegraph equation[166], [167], time-fractional generalized Boussinesq equation[168] , Navier–Stokes time-fractional differential equation [169] ,time-fractional wave equation[170] , two-dimensional fractional Helmholtz equations[171] etc.

Fractional coupled Burgers' equation is also very important in the field of fluid mechanics to study the motion of fluids concentrations under the effect of gravity. It is a mathematical model of time-dependent sedimentation or creaming of different concentrations of two kinds of particles in fluid colloids or suspensions, under the effect of gravity[172]. Burgers' equations are the special case of Navier Stokes' equations and are very much important in the field of science and technology. Researchers are in continuous progress to study the different characteristics of the phenomenon governed by the fractional models by developing the different algorithms to solve time-fractional coupled Burgers' equation such as Fractional Variational iteration method (FVIM)[173], Differential Transformation Method (DTM)[174], Homotopy Perturbation Method (HPM)[175], Coupled Fractional Reduced Differential Transform Method(CFRDTM)[176], Adomian Decomposition Method (ADM) [177], etc. But the

study of characteristics of different concentrations of two kinds of particles governed by fractional coupled Burgers' equation has yet not been investigated by any of the scale 3 Haar wavelet-based technique simultaneously with space and time fraction.

Orthonormal wavelets are one of the modernistic functions which have the capability of dilation and translation. Because of these properties, numerical techniques that involve wavelet bases are showing the qualitative improvement in contrast with other methods. In literature, dyadic wavelets are in preponderance. In 1995, Chui and Lian [115] have developed the Haar scale 3 (non-dyadic) wavelets by using the process of multiresolution analysis. In 2018, Mittal and Pandit have used the scale 3 Haar wavelets [71], [141], [142] for solving the various types of differential equations and found that these wavelet bases are equally competent in solving the various types of mathematical models governed by differential equations. Also, it was shown by them that the Haar scale 3 (non-dyadic) wavelet has a faster rate of convergence as compared to the Haar scale 2 dyadic wavelets. Moreover, investigation of characteristics of the solution to the fractional coupled Burgers' equation has yet not been done by the Scale 3 Haar wavelet methods as far as our knowledge is concerned. This encourages us to develop a new technique using scale 3 Haar wavelet for analyzing the behavior of systems governed by the fractional coupled Burgers' equation.

The prime objective of the proposed work is to provide a new numerical technique for obtaining the solution of space-time fractional-coupled Burgers' Equation (6.1) emerging in the field of fluid dynamics using scale 3 Haar wavelet bases.

$$\begin{cases} \dfrac{\partial^{\alpha} u}{\partial t^{\alpha}} = \dfrac{\partial^2 u}{\partial x^2} - \eta\, u \dfrac{\partial^{\beta} u}{\partial x^{\beta}} - \mu \dfrac{\partial (uv)}{\partial x} \quad , \qquad x \in [\mathrm{a}\,, \mathrm{b}] \quad , t \in [0, T] \\ \dfrac{\partial^{\gamma} v}{\partial t^{\gamma}} = \dfrac{\partial^2 v}{\partial x^2} - \xi\, v \dfrac{\partial^{\delta} v}{\partial x^{\delta}} - \lambda \dfrac{\partial (uv)}{\partial x} \quad , \qquad x \in [\mathrm{a}\,, \mathrm{b}] \quad , t \in [0, T] \end{cases} \tag{6.1}$$

subjected to the boundary constraints given in Equation (6.2)

$$u(a,t) = f_1(t)\ , u(b,t) = f_2(t)\ ,\ v(a,t) = \varphi_1(t)\ \ , v(b,t) = \varphi_2(t) \quad \forall t \in [0, T] \tag{6.2}$$

and with the constraints at the initial value given in Equation (6.3)

$$u(x,0) = h(x) \quad , \qquad v(x,0) = p(x) \qquad \forall \ \ x \in [\mathrm{a}\,, \mathrm{b}] \tag{6.3}$$

$\alpha, \beta, \gamma, \delta$ represents the order of fractional derivatives such that $0 < \alpha, \beta, \gamma, \delta \leq 1$.

Different variations can be observed in the solution space by giving different values to these four parameters $\alpha, \beta, \gamma, \delta$. However, on taking $\alpha = \beta = \gamma = \delta$=1 the fractional-coupled Burgers' equation will respond like a classical coupled Burgers' equation with integer order. η , ξ , μ , λ are arbitrary constants depending upon the system parameter like Peclet number, Reynold number, etc.

This chapter follows the sequence of sections as described: In section 2, explicit forms of scale 3 Haar wavelets with their families and procedure to find their integrals have been explained briefly. Representation of the solution using scale 3 Haar wavelets is explained in section 3. Section 4 explains the method of solution using scale 3 Haar wavelets. In section 5, the convergence of the method is discussed. In section 6, solutions of two different coupled Burgers' fractional equations are produced using the present method to analyze the efficiency and performance of the present method. In section 7, the conclusion drawn from the results and future research ideas are given.

6.2 Scale 3 Haar Wavelets and Its Integrals

The mathematical expressions for father wavelet (Scale 3 Haar function) and mother wavelets for scale 3 Haar wavelet family with dilation factor three [71], [115] are represented by the Equation (6.4),(6.5) and (6.6)

$$h_i(t) = \varphi(t) = \begin{cases} 1 & 0 \le t < 1 \\ 0 & elsewhere \end{cases} \qquad for\ i = 1 \tag{6.4}$$

$$h_i(t) = \psi^1\left(3^j t - k\right) = \frac{1}{\sqrt{2}} \begin{cases} -1 & \varkappa_1(i) \le t < \varkappa_2(i) \\ 2 & \varkappa_2(i) \le t < \varkappa_3(i) \\ -1 & \varkappa_3(i) \le t < \varkappa_4(i) \\ 0 & elsewhere \end{cases}, \qquad for \quad i = 2,4, \dots 3p-1 \tag{6.5}$$

$$h_i(t) = \psi^2\left(3^j t - k\right) = \sqrt{\frac{3}{2}} \begin{cases} 1 & \varkappa_1(i) \le t < \varkappa_2(i) \\ 0 & \varkappa_2(i) \le t < \varkappa_3(i) \\ -1 & \varkappa_3(i) \le t < \varkappa_4(i) \\ 0 & elsewhere \end{cases}, \qquad for \quad i = 3,6, \dots 3p \tag{6.6}$$

where $\varkappa_1(i) = \frac{k}{p}$, $\varkappa_2(i) = \frac{3k+1}{3p}$, $\varkappa_3(i) = \frac{(3k+2)}{3p}$, $\varkappa_4(i) = \frac{k+1}{p}$, $p = 3^j$, $j = 0,1,2, \dots$, $k = 0,1,2, \dots, p-1$. Here i , j , k respectively represent the wavelet number, level of resolution (dilation), and translation parameters of wavelet family. The values of

i ($for\ i > 1$) can be calculated with the help of j, k by using the following relations $i - 1 = 3^j + 2k$ for even values of i and $i - 2 = 3^j + 2k$ for odd values of i. By using this relation for different dilation and translations of $h_2(t), h_3(t)$, we will get the wavelet family as $h_1(t), h_2(t), h_3(t), h_4(t), h_5(t), h_6(t), \ldots$ where $h_2(t)$and $h_3(t)$ are also called mother wavelets and rest all the wavelets which we have obtained from mother wavelets are called daughter wavelets.

The main difference which makes the Haar scale 3 (non-dyadic) wavelets better than the Haar scale 2 dyadic wavelets is that only one mother wavelet is responsible for the construction of whole wavelet family but in case of scale 3 Haar wavelets, two mother wavelets with different shapes are responsible for the construction of the whole family. Because of this fact, scale 3 Haar wavelets increase the convergence rate of the solution. The construction of scale 3 Haar wavelet family is done by using the properties of Multi-resolution analysis which are described below

Now one can easily integrate the Equations (6.4),(6.5) and (6.6) the desired number of times over the interval [A, B) by using Riemann Liouville Integral formula [6] as given in Equation (6.7)

$$q_{\beta,i}(t) = \frac{1}{\Gamma(\beta)} \int_A^t h_i(x)(t-x)^{\beta-1} dx \qquad \forall \quad 0 \le \beta \le m\,, \quad m = 1,2,3 \ldots\ldots\,, \qquad i = 1,2,3, \ldots \ldots 3p \tag{6.7}$$

After evaluating the above integrals for Equation (6.4), we get Equation (6.8)

$$q_{\beta,i}(t) = \frac{t^\beta}{\Gamma(\beta+1)} \qquad for \quad i = 1 \tag{6.8}$$

Using Equation (6.7) on Equation (6.5), we get the values of $q_{\beta,i}(t)'s \ \ for \ \ i = 2,4,6,8, \cdots, 3p-1$ which are given by Equation (6.9)

$$q_{\beta,i}(t) = \frac{1}{\sqrt{2}} \begin{cases} 0 & for \quad 0 \le t \le \varkappa_1(i) \\ \frac{-1}{\Gamma(\beta+1)}\left(t-\varkappa_1(i)\right)^\beta & for \ \ \varkappa_1(i) \le t \le \varkappa_2(i) \\ \frac{1}{\Gamma(\beta+1)}\left[-\left(t-\varkappa_1(i)\right)^\beta + 3\left(t-\varkappa_2(i)\right)^\beta\right] & for \ \ \varkappa_2(i) \le t \le \varkappa_3(i) \\ \frac{1}{\Gamma(\beta+1)}\left[-\left(t-\varkappa_1(i)\right)^\beta + 3\left(t-\varkappa_2(i)\right)^\beta - 3\left(t-\varkappa_3(i)\right)^\beta\right] & for\ \varkappa_3(i) \le t \le \varkappa_4(i) \\ \frac{1}{\Gamma(\beta+1)}\left[-\left(t-\varkappa_1(i)\right)^\beta + 3\left(t-\varkappa_2(i)\right)^\beta - 3\left(t-\varkappa_3(i)\right)^\beta + \left(t-\varkappa_4(i)\right)^\beta\right] & for\ \varkappa_4(i) \le t \le 1 \end{cases} \tag{6.9}$$

Using Equation (6.7) on Equation (6.6), we get the values of $q_{\beta,i}(t)'s \quad for \quad i = 3,5,7,9,\cdots,3p$ which are given by Equation (6.10)

$$q_{\beta,i}(t) =$$

$$\sqrt{\frac{3}{2}}\begin{cases} 0 & for \quad 0 \le t \le \varkappa_1(i) \\ \frac{1}{\Gamma(\beta+1)}\left(t-\varkappa_1(i)\right)^{\beta} & for \quad \varkappa_1(i) \le t \le \varkappa_2(i) \\ \frac{1}{\Gamma(\beta+1)}\left[\left(t-\varkappa_1(i)\right)^{\beta}-\left(t-\varkappa_2(i)\right)^{\beta}\right] & for \quad \varkappa_2(i) \le t \le \varkappa_3(i) \\ \frac{1}{\Gamma(\beta+1)}\left[\left(t-\varkappa_1(i)\right)^{\beta}-\left(t-\varkappa_2(i)\right)^{\beta}-\left(t-\varkappa_3(i)\right)^{\beta}\right] & for \quad \varkappa_3(i) \le t \le \varkappa_4(i) \\ \frac{1}{\Gamma(\beta+1)}\left[\left(t-\varkappa_1(i)\right)^{\beta}-\left(t-\varkappa_2(i)\right)^{\beta}-\left(t-\varkappa_3(i)\right)^{\beta}+\left(t-\varkappa_4(i)\right)^{\beta}\right] & for \ \varkappa_4(i) \le t \le 1 \end{cases} \tag{6.10}$$

6.3 Approximation of Solution

Using the properties of scale 3 Haar wavelets, any function $x(t) \in L_2(R)$ can be expressed an infinite series of scale 3 Haar bases as given in Equation (6.11)

$$u(t) = \sum_{i=0}^{\infty} a_i h_i(t) = a_1 h_1(t) + \sum_{even\ i} a_i \psi^1\left(3^j t - k\right) + \sum_{odd\ i} a_i \psi^2\left(3^j t - k\right) \tag{6.11}$$

Here $a_i's$ are the wavelet coefficients whose values are to be determined by the proposed method. But for computational purposes, one can consider a finite number of terms. By considering the first $3p$ terms to approximate the function $u(t)$ we get Equation (6.12)

$$u(t) \approx u_{3p} = \sum_{i=0}^{3p} a_i h_i(t) \quad \text{where } p = 3^j,\ j = 0,1,2,\ldots \tag{6.12}$$

6.4 Method of Solution

By applying the quasi-linearization technique to linearize the non-linear terms of Equation (6.1), (6.2) and (6.3), we get the equivalent linear expressions given by Equation (6.13),(6.14),(6.15) and (6.16)

$$(uv_x)_{r+1} = u_{r+1}(v_x)_r + u_r(v_x)_{r+1} - u_r(v_x)_r \tag{6.13}$$

$$(vu_x)_{r+1} = v_{r+1}(u_x)_r + v_r(u_x)_{r+1} - v_r(u_x)_r \tag{6.14}$$

$$\left(uu_{\beta}\right)_{r+1} = u_{r+1}\left(u_{\beta}\right)_{r} + u_{r}\left(u_{\beta}\right)_{r+1} - u_{r}\left(u_{\beta}\right)_{r} \tag{6.15}$$

$$(vv_{\delta})_{r+1} = v_{r+1}(v_{\delta})_{r} + v_{r}(v_{\delta})_{r+1} - v_{r}(v_{\delta})_{r} \tag{6.16}$$

using Equations (6.13),(6.14),(6.15) and (6.16), non-linear coupled fractional differential Equations (6.1), (6.2) and (6.3), transformed into a sequence of linear differential equations as given in Equation (6.17) and (6.18)

$$\begin{aligned}\left(\frac{\partial^{\alpha}u}{\partial t^{\alpha}}\right)_{r+1} &= (u_{xx})_{r+1} - \eta\left(u_{r+1}\left(u_{\beta}\right)_{r} + u_{r}\left(u_{\beta}\right)_{r+1} - u_{r}\left(u_{\beta}\right)_{r}\right) \\ &\quad - \mu[(u_{r+1}(v_{x})_{r} + u_{r}(v_{x})_{r+1} - u_{r}(v_{x})_{r}) \\ &\quad + (v_{r+1}(u_{x})_{r} + v_{r}(u_{x})_{r+1} - v_{r}(u_{x})_{r})]\end{aligned} \tag{6.17}$$

$$\begin{aligned}\left(\frac{\partial^{\gamma}v}{\partial t^{\gamma}}\right)_{r+1} &= (u_{xx})_{r+1} - \xi(v_{r+1}(v_{\delta})_{r} + v_{r}(v_{\delta})_{r+1} - v_{r}(v_{\delta})_{r}) \\ &\quad - \lambda[(u_{r+1}(v_{x})_{r} + u_{r}(v_{x})_{r+1} - u_{r}(v_{x})_{r}) \\ &\quad + (v_{r+1}(u_{x})_{r} + v_{r}(u_{x})_{r+1} - v_{r}(u_{x})_{r})]\end{aligned} \tag{6.18}$$

subjected to the boundary constraints given by Equation (6.19)

$$\begin{aligned}&u(a,t_{r+1}) = f_{1}(t_{r+1}) \quad , u(b,t_{r+1}) = f_{2}(t_{r+1}) \ , \ v(a,t_{r+1}) = \varphi_{1}(t_{r+1}) \\ &v(b,t_{r+1}) = \varphi_{2}(t_{r+1})\end{aligned} \tag{6.19}$$

and with the constraints on initial values given by Equation (6.20)

$$\begin{aligned}&u(x,0) = h(x), \ \ v(x,0) = p(x), \ \ \forall \ \mathrm{x} \in [\mathrm{a}\,,\mathrm{b}]\,, \ t_{r+1} \in [0,T] \ \ \text{and} \\ &r = 0,1,2\cdots m-1\end{aligned} \tag{6.20}$$

where t_{r+1} represents $(r+1)$th approximation for t in the process of quasilinearization.

$$\dot{u_{xx}}(x,t) = \sum_{i=1}^{3m} a_{i}h_{i}(x) \tag{6.21}$$

$$\dot{v_{xx}}(x,t) = \sum_{i=1}^{3m} b_{i}h_{i}(x) \tag{6.22}$$

Integrating the Equation (6.21) and (6.22) with respect to t from t_r to t_{r+1} we get

$$u_{xx}(x,t_{r+1}) = (t_{r+1} - t_{r}) \sum_{i=1}^{3m} a_{i}h_{i}(x) + u_{xx}(x,t_{r}) \tag{6.23}$$

$$v_{xx}(x, t_{r+1}) = (t_{r+1} - t_r) \sum_{i=1}^{3m} b_i h_i(x) + v_{xx}(x, t_r) \tag{6.24}$$

Now integrating the Equation (6.23) and (6.24) with respect to x within the limits $0\ to\ x$ we get

$$u_x(x, t_{r+1}) = (t_{r+1} - t_r) \sum_{i=1}^{3m} a_i q_{i,1}(x) + u_x(x, t_r) + \big(u_x(0, t_{r+1}) - u_x(0, t_r)\big) \tag{6.25}$$

$$v_x(x, t_{r+1}) = (t_{r+1} - t_r) \sum_{i=1}^{3m} b_i q_{i,1}(x) + v_x(x, t_r) + \big(v_x(0, t_{r+1}) - v_x(0, t_r)\big) \tag{6.26}$$

again, integrating the Equation (6.25) and (6.26) with respect to x within the limits $0\ to\ x$ we get

$$u(x, t_{r+1}) = (t_{r+1} - t_r) \sum_{i=1}^{3m} a_i q_{i,2}(x) + \big(u(x, t_r) - u(0, t_r)\big) + x\big(u_x(0, t_{r+1}) - u_x(0, t_r)\big) + u(0, t_{r+1}) \tag{6.27}$$

$$v(x, t_{r+1}) = (t_{r+1} - t_r) \sum_{i=1}^{3m} b_i q_{i,2}(x) + \big(v(x, t_r) - v(0, t_r)\big) + x\big(v_x(0, t_{r+1}) - v_x(0, t_r)\big) + v(0, t_{r+1}) \tag{6.28}$$

on substitute the values of unknown quantities $u_x(0, t_{r+1}) - u_x(0, t_r)$, $v_x(0, t_{r+1}) - v_x(0, t_r)$ by evaluating it from the above equations using $x = 1$ in the Equation (6.27) and (6.28), we get

$$u(x, t_{r+1}) = (t_{r+1} - t_r) \sum_{i=1}^{3m} a_i (q_{i,2}(x) - x\, q_{i,2}(1)) + \big(u(x, t_r) - u(0, t_r)\big) + x\big(u(1, t_{r+1}) - u(0, t_{r+1})\big) - x\big(u(1, t_r) - u(0, t_r)\big) + u(0, t_{r+1}) \tag{6.29}$$

$$v(x, t_{r+1}) = (t_{r+1} - t_r) \sum_{i=1}^{3m} b_i (q_{i,2}(x) - x\, q_{i,2}(1)) + \big(v(x, t_r) - v(0, t_r)\big) + x\big(v(1, t_{r+1}) - v(0, t_{r+1})\big) - x\big(v(1, t_r) - v(0, t_r)\big) + v(0, t_{r+1}) \tag{6.30}$$

$$u_x(x, t_{r+1}) = (t_{r+1} - t_r) \sum_{i=1}^{3m} a_i (q_{i,1}(x) - q_{i,2}(1)) + u_x(x, t_r) + \big(u(1, t_{r+1}) - u(0, t_{r+1})\big) - \big(u(1, t_r) - u(0, t_r)\big) \tag{6.31}$$

$$v_x(x,t_{r+1}) = (t_{r+1} - t_r)\sum_{i=1}^{3m} b_i(q_{i,1}(x) - q_{i,2}(1)) + v_x(x,t_r) + \big(v(1,t_{r+1}) - v(0,t_{r+1})\big) - \big(v(1,t_r) - v(0,t_r)\big) \quad (6.32)$$

$$\frac{\partial^\alpha u}{\partial t^\alpha}(x,t_{r+1}) = \frac{(t_{r+1}-t_r)^{1-\alpha}}{\Gamma(2-\alpha)} \sum_{i=1}^{3m} a_i(q_{i,2}(x) - x\, q_{i,2}(1)) + x\, \frac{\partial^\alpha}{\partial t^\alpha}\big(u(1,t_{r+1}) - u(0,t_{r+1})\big) + \frac{\partial^\alpha u}{\partial t^\alpha}(0,t_{r+1}) \quad (6.33)$$

$$\frac{\partial^\beta u}{\partial x^\beta}(x,t_{r+1}) = (t_{r+1} - t_r)\sum_{i=1}^{3m} a_i(q_{i,2-\beta}(x) - \frac{x^\beta}{\Gamma(2-\beta)} q_{i,2}(1)) + \frac{\partial^\beta u}{\partial x^\beta}(x,t_r) + \frac{x^\beta}{\Gamma(2-\beta)}\big[\big(u(1,t_{r+1}) - u(0,t_{r+1})\big) - \big(u(1,t_r) - u(0,t_r)\big)\big] \quad (6.34)$$

$$\frac{\partial^\gamma v}{\partial t^\gamma}(x,t_{r+1}) = \frac{(t_{r+1}-t_r)^{1-\gamma}}{\Gamma(2-\gamma)} \sum_{i=1}^{3m} b_i(q_{i,2}(x) - x\, q_{i,2}(1)) + x\, \frac{\partial^\alpha}{\partial t^\alpha}\big(v(1,t_{r+1}) - v(0,t_{r+1})\big) + \frac{\partial^\alpha v}{\partial t^\alpha}(0,t_{r+1}) \quad (6.35)$$

$$\frac{\partial^\delta v}{\partial x^\delta}(x,t_{r+1}) = (t_{r+1} - t_r)\sum_{i=1}^{3m} a_i(q_{i,2-\delta}(x) - \frac{x^\delta}{\Gamma(2-\delta)} q_{i,2}(1)) + \frac{\partial^\delta v}{\partial x^\delta}(x,t_r) + \frac{x^\delta}{\Gamma(2-\delta)}\big[\big(v(1,t_{r+1}) - v(0,t_{r+1})\big) - \big(v(1,t_r) - v(0,t_r)\big)\big] \quad (6.36)$$

Now using the boundary constraints and discretizing the space variable as $x \to x_l$ where $x_l = \frac{2l-1}{6p}$, $l = 0,1,2,\ldots\ldots 2p$ in the Equations (6.29)-(6.36) and substituting the values obtained in Equation (6.17) and (6.18) the following system of equations(Equation(6.37)) is obtained for different values of r

$$\left.\begin{aligned} a_{1\times 3p}A_{3p\times 3p} + b_{1\times 3p}B_{3p\times 3p} &= C_{1\times 3p} \\ b_{1\times 3p}D_{3p\times 3p} + a_{1\times 3p}E_{3p\times 3p} &= F_{1\times 3p} \end{aligned}\right\} \quad (6.37)$$

where the Equations (6.38) to (6.43) respectively represents the values of A , B, C, D , E and F as

$$A = \left[\frac{(t_{r+1}-t_r)^{1-\alpha}}{\Gamma(2-\alpha)}\Big(q_{i,2}(x_l) - x_l\, q_{i,2}(1)\Big) - (t_{r+1} - t_r)\left\{h_i(x_l) - \eta\left(\big(u_\beta\big)_r\Big(q_{i,2}(x_l) - x_l\, q_{i,2}(1)\Big) + u_r\left(q_{i,2-\beta}(x_l) - \frac{{x_l}^\beta}{\Gamma(2-\beta)}\Big(q_{i,2}(1)\Big)\right)\right) - \mu\left((v_x)_r\Big(q_{i,2}(x_l) - x_l\, q_{i,2}(1)\Big) + v_r\Big(q_{i,1}(x_l) - q_{i,2}(1)\Big)\right)\right\}\right] \quad (6.38)$$

$$B = \Big[\, \mu\,(t_{r+1} - \, t_r\,)\Big((u_x)_r\left(q_{i,2}(x_l) - x_l\, q_{i,2}\,(1)\right) + u_r\left(q_{i,1}(x_l) - q_{i,2}\,(1)\right)\Big)\Big] \tag{6.39}$$

$$\begin{aligned} C = {} & u_{xx}(x_l, t_r) - \eta\,\Big[\big(u_\beta\big)_r\,\Big(\big(u(x_l,t_r) - f_1(t_r)\big) + x_l\big(f_2(t_{r+1}) - \\ & f_1(t_{r+1})\big) - x_l\big(f_2(t_r) - f_1(t_r)\big) + f_1(t_{r+1})\Big) + u_r\,\left(\frac{\partial^\beta u}{\partial x^\beta}(x_l,t_r)\; + \right. \\ & \left.\frac{{x_l}^\beta}{\Gamma(2-\beta)}\Big(\big(f_2(t_{r+1}) - f_1(t_{r+1})\big) - \big(f_2(t_r) - f_1(t_r)\big)\Big)\right) - u_r\big(u_\beta\big)_r\Big] - \\ & \mu\Big[\Big\{(v_x)_r(\,\big(u(x_l,t_r) - f_1(t_r)\big) + x_l\big(f_2(t_{r+1}) - f_1(t_{r+1})\big) - x_l\big(f_2(t_r) - \\ & f_1(t_r)\big) + f_1(t_{r+1}))) + \; u_r\,\Big(\,v_x(x_l,t_r) + \Big(\big(\varphi_2(t_{r+1}) - \varphi_1(t_{r+1})\big)\Big) - \\ & \Big(\big(\varphi_2(t_r) - \varphi_1(t_r)\big)\Big)\,\Big) - u_r(v_x)_r\Big\} + (u_x)_r\Big(\,\big(v(x_l,t_r) - \varphi_1(t_r)\big) + \\ & x_l\Big(\big(\varphi_2(t_{r+1}) - \varphi_1(t_{r+1})\big)\Big) - x_l\Big(\big(\varphi_2(t_r) - \varphi_1(t_r)\big)\Big) + \varphi_1(t_{r+1})\Big) + \\ & v_r\Big(\,u_x(x_l,t_r) + \big(f_2(t_{r+1}) - f_1(t_{r+1})\big) - \Big(\big(\varphi_2(t_r) - \varphi_1(t_r)\big)\Big)\Big) - \\ & v_r(u_x)_r\;\Big] - x_l\;\left(\frac{\partial^\alpha}{\partial t^\alpha}\big(f_2(t) - f_1(t)\big)\right)_{t=t_{r+1}} - \left(\frac{\partial^\alpha f_1(t)}{\partial t^\alpha}\right)_{t=t_{r+1}} \end{aligned} \tag{6.40}$$

$$\begin{aligned} D = {} & \Bigg[\frac{(t_{r+1} - t_r\,)^{1-\gamma}}{\Gamma(2-\gamma)}\Big(q_{i,2}(x_l) - x_l\, q_{i,2}\,(1)\Big) - (t_{r+1} - \, t_r\,)\Big\{h_i(x_l) - \\ & \xi\left((v_\delta)_r\left(q_{i,2}(x_l) - x_l\, q_{i,2}\,(1)\right) + v_r\,\left(q_{i,2-\delta}(x_l) - \frac{{x_l}^\delta}{\Gamma(2-\delta)}\Big(q_{i,2}(1)\Big)\right)\right) - \\ & \lambda\Big((u_x)_r\left(q_{i,2}(x_l) - x_l\, q_{i,2}\,(1)\right) + u_r\left(q_{i,1}(x_l) - q_{i,2}\,(1)\right)\Big)\Big\}\Bigg] \end{aligned} \tag{6.41}$$

$$E = \Big[\, \lambda\,(t_{r+1} - \, t_r\,)\Big((v_x)_r\left(q_{i,2}(x_l) - x_l\, q_{i,2}\,(1)\right) + v_r\left(q_{i,1}(x_l) - q_{i,2}\,(1)\right)\Big)\Big] \tag{6.42}$$

$$
\begin{aligned}
\mathrm{F} = v_{xx}(x_l, t_r) - \xi \Big[(v_\delta)_r \Big(\big(v(x_l, t_r) - \varphi_1(t_r)\big) + x_l \big(\varphi_2(t_{r+1}) - \\
\varphi_1(t_{r+1})\big) - x_l \big(\varphi_2(t_r) - \varphi_1(t_r)\big) + \varphi_1(t_{r+1})\Big) + \; v_r \Big(\frac{\partial^\delta v}{\partial x^\delta}(x_l, t_r) \; + \\
\frac{{x_l}^\delta}{\Gamma(2-\delta)} \Big(\big(\varphi_2(t_{r+1}) - \varphi_1(t_{r+1})\big) - \big(\varphi_2(t_r) - \varphi_1(t_r)\big) \Big) \Big) - v_r (v_\delta)_r \Big] - \\
\lambda \Big[\{ (v_x)_r \big(\big(u(x_l, t_r) - f_1(t_r)\big) + x_l \big(f_2(t_{r+1}) - f_1(t_{r+1})\big) - x_l \big(f_2(t_r) - \\
f_1(t_r)\big) + f_1(t_{r+1})\big) + \; u_r \big(v_x(x_l, t_r) + \big(\varphi_2(t_{r+1}) - \varphi_1(t_{r+1})\big) - \\
\big(\varphi_2(t_r) - \varphi_1(t_r)\big) \big) - u_r (v_x)_r \} + (u_x)_r \Big(\big(v(x_l, t_r) - \varphi_1(t_r)\big) + \\
x_l \big(\varphi_2(t_{r+1}) - \varphi_1(t_{r+1})\big) - x_l \big(\varphi_2(t_r) - \varphi_1(t_r)\big) + \varphi_1(t_{r+1})\Big) + \\
v_r \Big(u_x(x_l, t_r) + \big(f_2(t_{r+1}) - f_1(t_{r+1})\big) - \big(f_2(t_r) - f_1(t_r)\big)\Big) - \\
v_r (u_x)_r \; \Big] - x_l \; \Big(\frac{\partial^\alpha}{\partial t^\alpha} \big(\varphi_2(t) - \varphi_1(t)\big) \Big)_{t=t_{r+1}} - \Big(\frac{\partial^\alpha \varphi_1(t)}{\partial t^\alpha} \Big)_{t=t_{r+1}}
\end{aligned}
\tag{6.43}
$$

The process of the solution starts by taking $r = 0, t_0 = 0$ and the boundary conditions are given in Equation (6.44)

$$
\begin{gathered}
u(x_l, t_r) = u(x_l, 0) = h(x_l), u_x(x_l, t_r) = u_x(x_l, 0) = h_x(x_l), \\
u_{xx}(x_l, t_r) = u_{xx}(x_l, 0) = h_{xx}(x_l) \\
v(x_l, t_r) = v(x_l, 0) = p(x_l), v_x(x_l, t_r) = v_x(x_l, 0) = p_x(x_l), \\
v_{xx}(x_l, t_r) = v_{xx}(x_l, 0) = p_{xx}(x_l)
\end{gathered}
\tag{6.44}
$$

The values of wavelet coefficients can be calculated successively for different values of $r = 0,1,2 \ldots$ by using the Equation (6.45) and (6.46)

$$a_{1\times 3p} = (C - FD^{-1}B) * (A - ED^{-1}B) \tag{6.45}$$

$$b_{1\times 3p} = (C - FE^{-1}A) * (B - DE^{-1}A) \tag{6.46}$$

Then by putting the values of the wavelet coefficient $a_i's \; and \; b_i's$ in the Equation (6.47) and (6.48) one can obtain numerically approximated solution successively for u(x, t) and v(x, t) for r= 0,1,2, 3… as follows

$$
\begin{aligned}
u(x_l, t_{r+1}) = (t_{r+1} - \; t_r) \sum_{i=1}^{3m} a_i (q_{i,2}(x_l) - x_l \, q_{i,2}(1)) + \; \big(u(x_l, t_r) - \\
f_1(t_r)\big) + x_l \big(f_2(t_{r+1}) - f_1(t_{r+1})\big) - x_l \big(f_2(t_r) - f_1(t_r)\big) + f_1(t_{r+1})
\end{aligned}
\tag{6.47}
$$

$$
\begin{aligned}
v(x_l, t_{r+1}) = (t_{r+1} - \; t_r) \sum_{i=1}^{3m} b_i (q_{i,2}(x_l) - x_l \, q_{i,2}(1)) + \; \big(v(x_l, t_r) - \\
\varphi_1(t_r)\big) + x_l \, \big(\varphi_2(t_{r+1}) - \varphi_1(t_{r+1})\big) - x_l \big(\varphi_2(t_r) - \varphi_1(t_r)\big) + \varphi_1(t_{r+1})
\end{aligned}
\tag{6.48}
$$

at various times by using successive iteration for $r = \; 0,1,2,3, \ldots$

6.5 Convergence Analysis

To establish the convergence of the proposed method, we considered the asymptotic extension of Equation (6.47) and (6.48) for a fixed value of $t = t_{r+1}$ and $x = x_l$ as given below

$$u(x,t) = \Delta t * \sum_{i=1}^{\infty} a_i(q_{i,2}(x) - x\, q_{i,2}(1)) + A + Bx \ , Where\ A = u(x_l,t_r) + f_1(t_{r+1}) - f_1(t_r)\ , B = \big(f_2(t_{r+1}) - f_1(t_{r+1})\big) - \big(f_2(t_r) - f_1(t_r)\big) \tag{6.49}$$

$$v(x,t) = \Delta t * \sum_{i=1}^{\infty} b_i(q_{i,2}(x_l) - x\, q_{i,2}(1)) + C + Dx \ , \text{Where } C = \big(v(x_l,t_r) - \varphi_1(t_r)\big) + \varphi_1(t_{r+1})\ , D = \big(\varphi_2(t_{r+1}) - \varphi_1(t_{r+1})\big) - \big(\varphi_2(t_r) - \varphi_1(t_r)\big) \tag{6.50}$$

Now the convergence of the theorem will be proved with the help of the following lemma

Lemma 1: let $u(x) \epsilon L^2(R)$be any square-integrable function such that $|u^m(x)| \leq M, \forall\ x\epsilon(0,1)$ and $D_*^{\alpha}u(x) = \sum_{i=1}^{\infty} a_i h_i(x)$.Then $|a_i| \leq \frac{2\sqrt{2}\,M}{3\Gamma(m-\alpha+1)} \times \frac{1}{3^{j\left(m-\alpha+\frac{1}{2}\right)}}$

Proof: Let $D_*^{\alpha}u(x) = \sum_{i=1}^{\infty} a_i h_i(x)$ be the exact solution and $D_*^{\alpha}u_{3p}(x) = \sum_{i=1}^{3p} a_i h_i(x)$ be the approximated solution

Now the error at the Jth level of resolution can be represented by Equation (6.51) and the value of a_i is given by Equation (6.52)

$$\left\|E_j\right\|^2 = \left\|D_*^{\alpha}u(x) - D_*^{\alpha}u_{3p}(x)\right\|^2 = \left\|\sum_{i=3p+1}^{\infty} a_i h_i(x)\right\|^2 = \left\langle \sum_{i=3p+1}^{\infty} a_i h_i(x)\ , \sum_{i=3p+1}^{\infty} a_i h_i(x) \right\rangle = \int_{-\infty}^{\infty} \sum_{i=3p+1}^{\infty} \sum_{k=3p+1}^{\infty} a_i a_k h_i(x) h_k(x)\, dx = \sum_{i=3p+1}^{\infty} \sum_{k=3p+1}^{\infty} a_i a_k \int_0^1 h_i(x) h_k(x)\, dx = \sum_{i=3p+1}^{\infty} a_i a_i = \sum_{i=3p+1}^{\infty} |a_i|^2 \tag{6.51}$$

$$a_i = 3^{\frac{j}{2}} \int_0^1 h_i(x)\, D_*^{\alpha}u(x)dx = 3^{\frac{j}{2}} \left(\int_0^1 {\psi_i}^1(x)\, D_*^{\alpha}u(x)dx + \int_0^1 {\psi_i}^2(x)\, D_*^{\alpha}u(x)dx \right) = 3^{\frac{j}{2}} \left[\left(\int_{\varkappa_1(i)}^{\varkappa_2(i)} \frac{-1}{\sqrt{2}} D_*^{\alpha}u(x)dx + \right. \right. \tag{6.52}$$

$\int_{\varkappa_2(i)}^{\varkappa_3(i)} \sqrt{2}\, D_*^{\alpha} u(x)dx + \int_{\varkappa_3(i)}^{\varkappa_4(i)} \frac{-1}{\sqrt{2}} D_*^{\alpha} u(x)dx\Big) + \Big(\int_{\varkappa_1(i)}^{\varkappa_2(i)} \frac{\sqrt{3}}{2} D_*^{\alpha} u(x)dx +$

$\int_{\varkappa_3(i)}^{\varkappa_4(i)} \frac{-\sqrt{3}}{2} D_*^{\alpha} u(x)dx\Big)\Big]$

By applying the mean value theorem[178] of integral on Equation (6.52), we get $\varepsilon_1 \in \big(\varkappa_1(i), \varkappa_2(i)\big)$, $\varepsilon_2 \in \big(\varkappa_2(i), \varkappa_3(i)\big)$,$\varepsilon_3 \in \big(\varkappa_3(i), \varkappa_4(i)\big)$ (Equation (6.53)) such that

$$\int_{\varkappa_1(i)}^{\varkappa_2(i)} D_*^{\alpha} u(x)dx = (\varkappa_2(i) - \varkappa_1(i)) D_*^{\alpha} u(\varepsilon_1) = \frac{1}{3p} D_*^{\alpha} u(\varepsilon_1)$$

$$\int_{\varkappa_2(i)}^{\varkappa_3(i)} D_*^{\alpha} u(x)dx = (\varkappa_3(i) - \varkappa_2(i)) D_*^{\alpha} u(\varepsilon_2) = \frac{1}{3p} D_*^{\alpha} u(\varepsilon_2) \tag{6.53}$$

$$\int_{\varkappa_3(i)}^{\varkappa_4(i)} D_*^{\alpha} u(x)dx = (\varkappa_4(i) - \varkappa_3(i)) D_*^{\alpha} u(\varepsilon_3) = \frac{1}{3p} D_*^{\alpha} u(\varepsilon_3)$$

Now using Equation (6.53) ,Equation (6.52) becomes Equation (6.54)

$$a_i = \frac{3^{\frac{j}{2}}}{3p}\left(\left(\frac{\sqrt{3}-1}{\sqrt{2}}\right) D_*^{\alpha} u(\varepsilon_1) + \sqrt{2} D_*^{\alpha} u(\varepsilon_2) - \left(\frac{\sqrt{3}-1}{\sqrt{2}}\right) D_*^{\alpha} u(\varepsilon_3)\right)$$

$$= \frac{3^{\frac{j}{2}}}{3p}\left(\left(\frac{\sqrt{3}-1}{\sqrt{2}}\right) D_*^{\alpha} u(\varepsilon_1) + \sqrt{2} D_*^{\alpha} u(\varepsilon_2) - \left(\frac{\sqrt{3}-1}{\sqrt{2}}\right) D_*^{\alpha} u(\varepsilon_3)\right)$$

$$= 3^{\frac{-j-2}{2}}\left(\left(\frac{\sqrt{3}-1}{\sqrt{2}}\right) D_*^{\alpha} u(\varepsilon_1) + \sqrt{2} D_*^{\alpha} u(\varepsilon_2) - \left(\frac{\sqrt{3}-1}{\sqrt{2}}\right) D_*^{\alpha} u(\varepsilon_3)\right) \tag{6.54}$$

Now by using the Caputo definition of fractional derivatives on Equation (6.54), we get Equation (6.55)

$$a_i = 3^{\frac{-j-2}{2}}\left(\left(\frac{\sqrt{3}-1}{\sqrt{2}}\right)\left(\frac{1}{\Gamma(m-\alpha)}\int_0^{\varepsilon_1} \frac{u^m(z)}{(\varepsilon_1 - z)^{\alpha-m+1}} dz\right) +$$

$$\sqrt{2}\left(\frac{1}{\Gamma(m-\alpha)}\int_0^{\varepsilon_2} \frac{u^m(z)}{(\varepsilon_2 - z)^{\alpha-m+1}} dz\right) - \left(\frac{\sqrt{3}-1}{\sqrt{2}}\right)\left(\frac{1}{\Gamma(m-\alpha)}\int_0^{\varepsilon_3} \frac{u^m(z)}{(\varepsilon_3 - z)^{\alpha-m+1}} dz\right)\Big)$$

$$= \frac{3^{\frac{-j-2}{2}}}{\sqrt{2}\,\Gamma(m-\alpha)}\Big(\big(\sqrt{3}-1\big)\int_0^{\varepsilon_1} \frac{u^m(z)}{(\varepsilon_1 - z)^{\alpha-m+1}} dz - 2\int_{\varepsilon_2}^{0} \frac{u^m(z)}{(\varepsilon_2 - z)^{\alpha-m+1}} dz - \big(\sqrt{3} -$$

$$1\big)\Big(\int_0^{\varepsilon_1} \frac{u^m(z)}{(\varepsilon_3 - z)^{\alpha-m+1}} dz + \int_{\varepsilon_1}^{\varepsilon_3} \frac{u^m(z)}{(\varepsilon_3 - z)^{\alpha-m+1}} dz\Big)\Big) \tag{6.55}$$

$$a_i = \frac{3^{\frac{-j-2}{2}}}{\sqrt{2}\,\Gamma(m-\alpha)}\left(\left(\sqrt{3}-1\right)\left(\int_0^{\varepsilon_1}\frac{u^m(z)}{(\varepsilon_1-z)^{\alpha-m+1}}dz-\int_0^{\varepsilon_1}\frac{u^m(z)}{(\varepsilon_3-z)^{\alpha-m+1}}dz\right)-\right.$$
$$\left.\left(\sqrt{3}-1\right)\left(\int_{\varepsilon_1}^{\varepsilon_3}\frac{u^m(z)}{(\varepsilon_3-z)^{\alpha-m+1}}dz\right)-2\int_{\varepsilon_2}^{0}\frac{u^m(z)}{(\varepsilon_2-z)^{\alpha-m+1}}dz\right)$$

$$|a_i| = \left|\frac{3^{\frac{-j-2}{2}}}{\sqrt{2}\,\Gamma(m-\alpha)}\left(\left(\sqrt{3}-1\right)\left(\int_0^{\varepsilon_1}\frac{u^m(z)}{(\varepsilon_1-z)^{\alpha-m+1}}dz-\int_0^{\varepsilon_1}\frac{u^m(z)}{(\varepsilon_3-z)^{\alpha-m+1}}dz\right)-\right.\right.$$
$$\left.\left.\left(\sqrt{3}-1\right)\left(\int_{\varepsilon_1}^{\varepsilon_3}\frac{u^m(z)}{(\varepsilon_3-z)^{\alpha-m+1}}dz\right)-2\int_{\varepsilon_2}^{0}\frac{u^m(z)}{(\varepsilon_2-z)^{\alpha-m+1}}dz\right)\right| \quad (6.56)$$

$$|a_i| \le \frac{3^{\frac{-j-2}{2}}}{\sqrt{2}\,\Gamma(m-\alpha)}\left[\left(\sqrt{3}-1\right)\left|\int_0^{\varepsilon_1}\frac{u^m(z)}{(\varepsilon_1-z)^{\alpha-m+1}}dz-\int_0^{\varepsilon_1}\frac{u^m(z)}{(\varepsilon_3-z)^{\alpha-m+1}}dz\right|+\right.$$
$$\left.\left(\sqrt{3}-1\right)\left|\int_{\varepsilon_1}^{\varepsilon_3}\frac{u^m(z)}{(\varepsilon_3-z)^{\alpha-m+1}}dz\right|+2\left|\int_{\varepsilon_2}^{0}\frac{u^m(z)}{(\varepsilon_2-z)^{\alpha-m+1}}dz\right|\right] \quad (6.57)$$

$$|a_i| \le \frac{3^{\frac{-j-2}{2}}}{\sqrt{2}\,\Gamma(m-\alpha)}\left[\left(\sqrt{3}-1\right)\int_0^{\varepsilon_1}|u^m(z)|\left[\frac{1}{(\varepsilon_1-z)^{\alpha-m+1}}-\frac{1}{(\varepsilon_3-z)^{\alpha-m+1}}\right]dz+\right.$$
$$\left.\left(\sqrt{3}-1\right)\int_{\varepsilon_1}^{\varepsilon_3}|u^m(z)|\frac{1}{(\varepsilon_3-z)^{\alpha-m+1}}dz+2\int_{\varepsilon_2}^{0}|u^m(z)|\frac{1}{(\varepsilon_2-z)^{\alpha-m+1}}dz\right] \quad (6.58)$$

$$|a_i| \le \frac{3^{\frac{-j-2}{2}}M}{\sqrt{2}\,\Gamma(m-\alpha)}\left[\left(\sqrt{3}-1\right)\int_0^{\varepsilon_1}\left[\frac{1}{(\varepsilon_1-z)^{\alpha-m+1}}-\frac{1}{(\varepsilon_3-z)^{\alpha-m+1}}\right]dz+\right.$$
$$\left.\left(\sqrt{3}-1\right)\int_{\varepsilon_1}^{\varepsilon_3}\frac{1}{(\varepsilon_3-z)^{\alpha-m+1}}dz+2\int_{\varepsilon_2}^{0}\frac{1}{(\varepsilon_2-z)^{\alpha-m+1}}dz\right] \quad (6.59)$$

Taking modulus on both sides of Equation (6.55) and applying the properties of modulus, we get Equation (6.56),(6.57),(6.58),(6.59),(6.60),(6.61) and (6.62)

$$|a_i| \le \frac{3^{\frac{-j-2}{2}}M}{\sqrt{2}\,\Gamma(m-\alpha)}\left[\frac{(\sqrt{3}-1)}{(m-\alpha)}[(\varepsilon_3-\varepsilon_1)^{m-\alpha}-{\varepsilon_3}^{m-\alpha}+{\varepsilon_1}^{m-\alpha}+\right.$$
$$\left.(\varepsilon_3-\varepsilon_1)^{m-\alpha}]-2{\varepsilon_2}^{m-\alpha}\right] \quad (6.60)$$

$m-\alpha > 0, \varepsilon_1 < \varepsilon_3 \Rightarrow {\varepsilon_1}^{m-\alpha} < {\varepsilon_3}^{m-\alpha} \Rightarrow {\varepsilon_1}^{m-\alpha}-{\varepsilon_3}^{m-\alpha} < 0$

$\varepsilon_2 > 0 \Rightarrow -2{\varepsilon_2}^{m-\alpha} < 0$

$\Rightarrow {\varepsilon_1}^{m-\alpha}-{\varepsilon_3}^{m-\alpha}-2{\varepsilon_2}^{m-\alpha} < 0$

$$|a_i| \le \frac{3^{\frac{-j-2}{2}}M}{\sqrt{2}\,\Gamma(m-\alpha)}\left[\frac{(\sqrt{3}-1)}{(m-\alpha)}[2(\varepsilon_3-\varepsilon_1)^{m-\alpha}]\right] < \frac{4.3^{\frac{-j-2}{2}}M}{\sqrt{2}\,\Gamma(m-\alpha+1)}$$

$$= \frac{2\sqrt{2}\,3^{\frac{-j-2}{2}}M}{\Gamma(m-\alpha+1)} \times \frac{1}{3^{j(m-\alpha)}} \tag{6.61}$$

$$|a_i| \le \frac{2\sqrt{2}\,M}{3\Gamma(m-\alpha+1)} \times \frac{1}{3^{j\left(m-\alpha+\frac{1}{2}\right)}} \tag{6.62}$$

Theorem 1: - If $u(x,t)$ represent the exact solution and $u_{3m}\,(x,t)$ represents the Scale 3 Haar wavelet-based approximated solution, then for a fixed value of $t = t_1$

$$\left\|E_j\right\| = \|u(x,t) - u_{3m}\,(x,t)\| \le \frac{4\sqrt{2M}\;K\,|\Delta t|}{\Gamma(m-\alpha+1)}\left(\frac{3^{-j(m-\alpha+\frac{1}{2})}}{1-3^{-\left(m-\alpha-\frac{1}{2}\right)}}\right)$$

Proof. At jth level of resolution, error estimation for the solution is given by

$$\left\|E_j\right\| = \|u(x,t) - u_{3m}\,(x,t)\| = \left|\Delta t * \sum_{i=3m+1}^{\infty} a_i(q_{i,2}(x) - x\,q_{i,2}(1))\right|$$

$$\left\|E_j\right\|^2 = |\Delta t|^2 * \left|\sum_{i=3m+1}^{\infty} a_i(q_{i,2}(x) - x\,q_{i,2}(1))\right|^2 = \left|\int_{-\infty}^{\infty}\langle\sum_{i=3m+1}^{\infty} a_i(q_{i,2}(x) - x\,q_{i,2}(1)) \cdot \sum_{k=3m+1}^{\infty} a_k(q_{k,2}(x) - x\,q_{k,2}(1))\rangle\right|$$

$$\le |\Delta t|^2 * \left|\sum_{i=3m+1}^{\infty}\sum_{k=3m+1}^{\infty}\int_0^1 a_i a_k\,\left(q_{i,2}(x) - xq_{i,2}(1)\right)\left(q_{k,2}(x) - xq_{k,2}(1)\right)dx\right|$$

$$\le |\Delta t|^2 * \left|a_i a_k\,M_{i,k}\right|$$

Where $M_{i,k} = \underset{i,k}{\mathrm{Sup}}\int_0^1 \left(q_{i,2}(x) - xq_{i,2}(1)\right)\left(q_{k,2}(x) - xq_{k,2}(1)\right)dx$

$$\left\|E_j\right\|^2 \le |\Delta t|^2 * \sum_{i=3m+1}^{\infty}\left|a_i(a_{3m}M_{i,3m} + a_{3m+1}M_{i,3m+1} + a_{3m+2}M_{i,3m+2} + a_{3m+3}\,,M_{i,3m+3} + \cdots)\right|$$

$$\le |\Delta t|^2 * \sum_{i=3m+1}^{\infty}\left|a_i M_i(a_{3m} + a_{3m+1} + a_{3m+2} + a_{3m+3}\,, + \cdots)\right| \text{ here} M_i = \underset{i,k}{\mathrm{Sup}}\,M_{i,k}$$

Using the result of Lemma 1 stated in Equation (6.62) in the above equation, we get

$$\left\|E_j\right\|^2 \le \frac{4\sqrt{2}\,K}{\Gamma(m-\alpha+1)}\frac{|\Delta t|^2 3^{-j(m-\alpha+\frac{1}{2})}}{1-3^{-\left(m-\alpha-\frac{1}{2}\right)}}\;\sum_{i=3m+1}^{\infty}|a_i M_i|$$

Take $M = \operatorname{Sup}_i M_i$

$$\left\|E_j\right\|^2 \leq \frac{4\sqrt{2}\ K|\Delta t|^2}{\Gamma(m-\alpha+1)} \frac{M3^{-j(m-\alpha+\frac{1}{2})}}{1-3^{-\left(m-\alpha-\frac{1}{2}\right)}} \sum_{i=3m+1}^{\infty} |a_i|$$

$$= \frac{4\sqrt{2}\ K|\Delta t|^2}{\Gamma(m-\alpha+1)} \frac{M3^{-j(m-\alpha+\frac{1}{2})}}{1-3^{-\left(m-\alpha-\frac{1}{2}\right)}} * \frac{4\sqrt{2}\ K}{\Gamma(m-\alpha+1)} \frac{3^{-j(m-\alpha+\frac{1}{2})}}{1-3^{-\left(m-\alpha-\frac{1}{2}\right)}}$$

$$\left\|E_j\right\| = \frac{4\sqrt{2M}\ K\ |\Delta t|}{\Gamma(m-\alpha+1)} \left(\frac{3^{-j(m-\alpha+\frac{1}{2})}}{1-3^{-\left(m-\alpha-\frac{1}{2}\right)}} \right) \tag{6.63}$$

It is clear from the Equation (6.63) that error bound is inversely proportional to the level of resolution which means that with the increase in the level of resolution, error bound decreases i.e. $j \to \infty \Rightarrow \left\|E_j\right\| \longrightarrow 0$. This proves the convergence of solution u (x, t). Similarly, the convergence of $v(x,t)$ solution can be proved. It ensures the stability of the solutions.

6.6 Results and Discussions Based Upon Numerical Experiments

To describe the appropriateness of the present scheme for fractional coupled Burgers' equation, solutions of two problems obtained by the present scheme have been analyzed and absolute errors are calculated to check the efficiency of the present scheme with the help of following formulas

$$\text{Absolute error} = |u_{exact}(t_l) - u_{num}(t_l)|$$

where t_l represents the collocation points of the domain.

Numerical Experiment No. 6.1: - Consider the following space-time fractional coupled Burgers' equation

$$\begin{cases} \dfrac{\partial^\alpha u}{\partial t^\alpha} = \dfrac{\partial^2 u}{\partial x^2} + 2\,u \dfrac{\partial^\beta u}{\partial x^\beta} - \dfrac{\partial (uv)}{\partial x} \quad , \qquad \text{x} \in [0,1] \quad , t \in [0,T] \\ \dfrac{\partial^\gamma v}{\partial t^\gamma} = \dfrac{\partial^2 v}{\partial x^2} + 2\,v \dfrac{\partial^\delta v}{\partial x^\delta} - \dfrac{\partial (uv)}{\partial x} \quad , \qquad \text{x} \in [0,1] \quad , t \in [0,T] \end{cases} \tag{6.64}$$

Subjected to the boundary conditions given in Equation (6.65)

$$u(0,t) = 0, u(1,t) = e^{-t}\sin 1 \ , \ v(0,t) = 0, v(1,t) = e^{-t}\sin 1 \qquad \forall\ t \in [0,T] \tag{6.65}$$

and with the initial condition given in Equation (6.66)

$$u(x,0) = \sin x \quad , \quad v(x,0) = \sin x \qquad \forall \ \ x \in [0,1] \tag{6.66}$$

The exact solution of the Equation (6.64) subjected to the conditions given in Equation (6.65) and (6.66) $\alpha = \beta = \gamma = \delta = 1$ is

$$u(x,t) = e^{-t} \sin x \qquad , v(x,t) = e^{-t} \sin x \tag{6.67}$$

The numerical solution obtained by applying the given methodology for Equation (6.64) subjected to the conditions given in Equation (6.65) and (6.66) is

$$u(x_l, t_{r+1}) = (t_{r+1} - t_r) \sum_{i=1}^{3m} a_i (q_{i,2}(x_l) - x_l \, q_{i,2}(1)) + \big(u(x_l, t_r) - f_1(t_r)\big) + x_l \big(f_2(t_{r+1}) - f_1(t_{r+1})\big) - x_l \big(f_2(t_r) - f_1(t_r)\big) + f_1(t_{r+1})$$

$$v(x_l, t_{r+1}) = (t_{r+1} - t_r) \sum_{i=1}^{3m} b_i (q_{i,2}(x_l) - x_l \, q_{i,2}(1)) + \big(v(x_l, t_r) - \varphi_1(t_r)\big) + x_l \big(\varphi_2(t_{r+1}) - \varphi_1(t_{r+1})\big) - x_l \big(\varphi_2(t_r) - \varphi_1(t_r)\big) + \varphi_1(t_{r+1})$$

at the various times by using successive iteration for $r = 0,1,2,3,\cdots$. The process of finding the solution in the discrete form starts by taking $r = 0, t_0 = 0$ and $f_1(t_r) = 0, f_2(t_r) = e^{-t_r} \sin 1$, $\varphi_1(t_r) = 0, \varphi_2(t_{r+1}) = e^{-t_r} \sin 1$ for $r = 0, t_0 = 0$ and rest all the values will be obtained using the iterative process.

Results obtained for numerical experiment no. 6.1 are also reported by the way of figures and tables. It can be seen from Figure 1 and Figure 2 that the solution obtained by the proposed method for the case (when $\alpha = \beta = \gamma = \delta = 1$) is in good agreement with the analytical solution available in the literature. Table 1 and Figure 3 shows the absolute errors in the results obtained at the different collocation points for the case $\alpha = \beta = \gamma = \delta = 1$ and it is of order 10^{-5} which assures the efficiency and reliability of the proposed method. In Table 2, results obtained by the present method are compared with another method [176] available in the literature and it is found that the present method outperforms over another method available in the literature. Table 3 is explaining the absolute error in the solution for different values of Δt which illustrate the direct dependence of absolute error on mesh size for time variable. For better visibility contour plots and 2D-solution plots are also given in Figure 4 and Figure 5.

Table 6.1 : Absolute error in numerical results $u(x,t)$ at collocation points for integer order α= β= γ= δ =1 with η= ξ = -2, μ=λ=1 and $\Delta t = 0.1$ in Experiment No.6.1

$x \rightarrow$ $Time(t)$ $\downarrow$	**0.0556**	**0.1667**	**0.2778**	**0.3889**	**0.5**	**0.6111**	**0.7222**	**0.8333**	**0.9444**
0.1	2.30×10^{-5}	5.82×10^{-5}	9.26×10^{-5}	1.24×10^{-4}	1.52×10^{-4}	1.76×10^{-4}	1.97×10^{-4}	2.15×10^{-4}	2.30×10^{-4}
0.2	6.66×10^{-5}	1.69×10^{-4}	2.68×10^{-4}	3.59×10^{-4}	4.39×10^{-4}	5.09×10^{-4}	5.70×10^{-4}	6.22×10^{-4}	6.67×10^{-4}
0.3	1.04×10^{-4}	2.62×10^{-4}	4.16×10^{-4}	5.56×10^{-4}	6.80×10^{-4}	7.88×10^{-4}	8.82×10^{-4}	9.63×10^{-4}	1.03×10^{-3}
0.4	1.30×10^{-4}	3.27×10^{-4}	5.19×10^{-4}	6.93×10^{-4}	8.47×10^{-4}	9.82×10^{-4}	1.10×10^{-3}	1.20×10^{-3}	1.29×10^{-3}
0.5	1.42×10^{-4}	3.57×10^{-4}	5.64×10^{-4}	7.53×10^{-4}	9.20×10^{-4}	1.07×10^{-3}	1.19×10^{-3}	1.30×10^{-3}	1.39×10^{-3}
0.6	1.38×10^{-4}	3.44×10^{-4}	5.44×10^{-4}	7.25×10^{-4}	8.85×10^{-4}	1.03×10^{-3}	1.15×10^{-3}	1.25×10^{-3}	1.34×10^{-3}
0.7	1.17×10^{-4}	2.89×10^{-4}	4.55×10^{-4}	6.06×10^{-4}	7.40×10^{-4}	8.57×10^{-4}	9.58×10^{-4}	1.04×10^{-3}	1.12×10^{-3}
0.8	7.87×10^{-5}	1.94×10^{-4}	3.05×10^{-4}	4.05×10^{-4}	4.94×10^{-4}	5.72×10^{-4}	6.39×10^{-4}	6.97×10^{-4}	7.46×10^{-4}
0.9	2.80×10^{-5}	6.86×10^{-5}	1.08×10^{-4}	1.43×10^{-4}	1.74×10^{-4}	2.02×10^{-4}	2.25×10^{-4}	2.46×10^{-4}	2.63×10^{-4}

Table 6.2: Comparision of Numerical results at Random collocation Points available in Literature for Numerical Experiment. No. 6.1 at integer-order α= β= γ= δ =1 with η= ξ = -2, μ=λ=1 and $\Delta t = 0.1$

Collocation Points (x,t)	**Exact Solution** $u(x,t) = v(x,t) = e^{-t}\sin x$	**Numerical Solution** $u(x,t)$	**Numerical Solution** $v(x,t)$	**Scale 3 Haar wavelet method (Absolute Error)**	**Reduced differential Transform method (Absolute Error)** [176]
(0.1,0.1)	0.090333	0.090329	0.090329	4.09×10^{-6}	1.62×10^{-5}
(0.2,0.2)	0.162657	0.162730	0.162730	7.38×10^{-5}	2.52×10^{-4}
(0.3,0.3)	0.218927	0.219199	0.219199	2.73×10^{-4}	1.24×10^{-3}
(0.4,0.4)	0.261035	0.261596	0.261596	5.61×10^{-4}	3.77×10^{-3}
(0.5,0.5)	0.290786	0.291659	0.291659	8.73×10^{-4}	8.86×10^{-3}
(0.6,0.6)	0.309882	0.311006	0.311006	1.12×10^{-3}	1.76×10^{-2}
(0.7,0.7)	0.319909	0.321135	0.321135	1.23×10^{-3}	3.11×10^{-2}
(0.8,0.8)	0.322329	0.323434	0.323434	1.11×10^{-3}	5.07×10^{-2}
(0.9,0.9)	0.318477	0.319182	0.319182	7.05×10^{-4}	7.71×10^{-2}

Table 6.3: Maximum absolute error in numerical results $u(x,t)$ and $v(x,t)$ at the integer order α= β= γ= δ =1 with η= ξ = -2, μ=λ=1 for different values of Δt .

Δt	$\|E(u)\|_\infty$	$\|E(v)\|_\infty$
0.0100	$1.221420967286724\times 10^{-4}$	$1.221420967286724\times 10^{-4}$
0.0010	$2.218389533070741\times 10^{-6}$	$2.218389533070741\times 10^{-6}$
0.0001	$2.413116217958589\times 10^{-8}$	$2.413116217958589\times 10^{-8}$

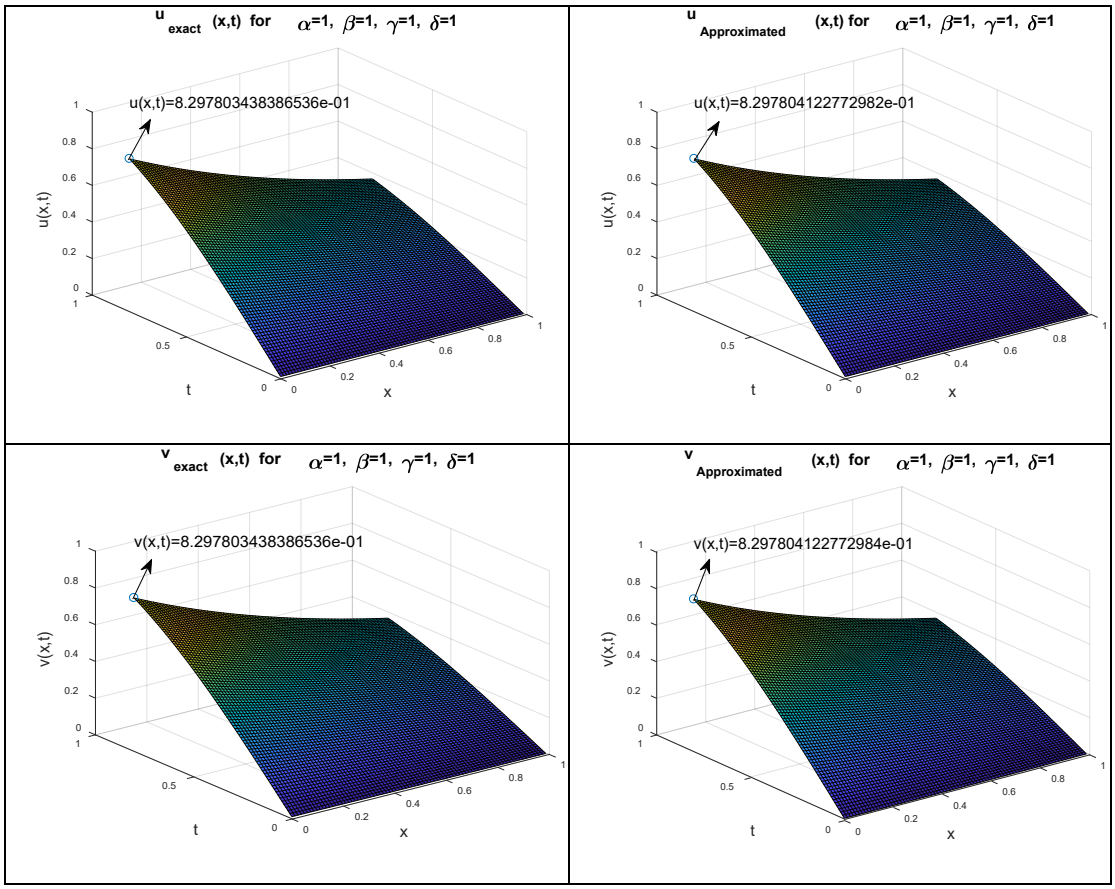

Figure 6.1: 3D Graphical representation of exact and approximated solution of Numerical Experiment No. 6.1 for integer order α= β= γ= δ =1 with η= ξ = -2, μ=λ=1 and Δt = 0.01

The most important fact has been explained by Figure 6 and Figure 7 that when we shift from one classical order derivative (integer-order 0) to another classical order derivative (integer-order 1) in the coupled Burgers' equation the behavior of the solution does not remain the same. Many variations have been observed in the solution space with the variation in the order of time derivative or space derivative which gives a better insight of the microscopic behavior of poly-dispersive sedimentation phenomena of two different types of particle concentration in the fluid.

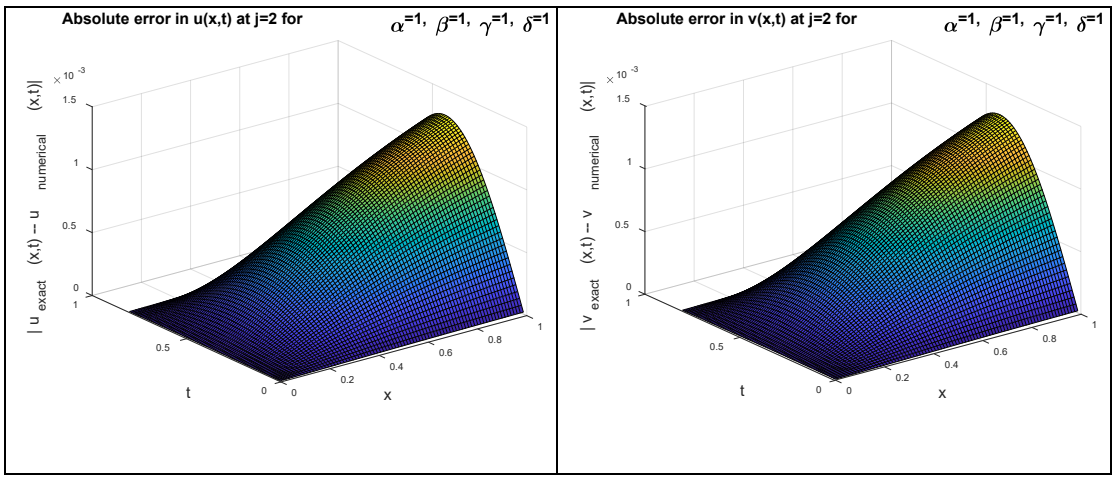

Figure 6.2: Surface plot of absolute error in the solutions u(x,t) and v(x,t) of Numerical Experiment No. 6.1 for j=3 at α= β= γ= δ =1 with η= ξ = -2, μ=λ=1 and Δt = 0.01.

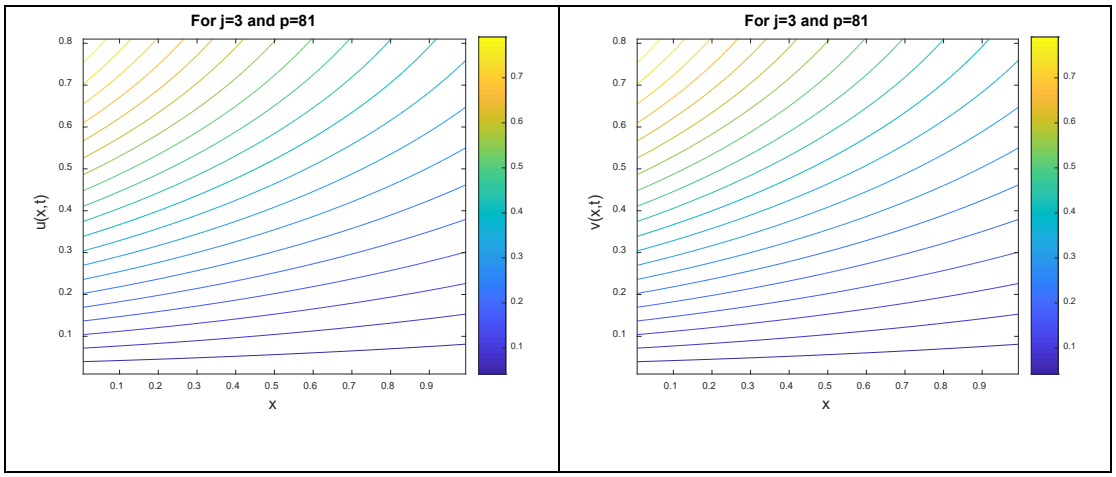

Figure 6.3 :Contour representation of solutions u(x,t) and v(x,t) of Numerical Experiment No. 6.1 at α= β= γ= δ =1 with η= ξ = -2, μ=λ=1 and Δt = 0.01.

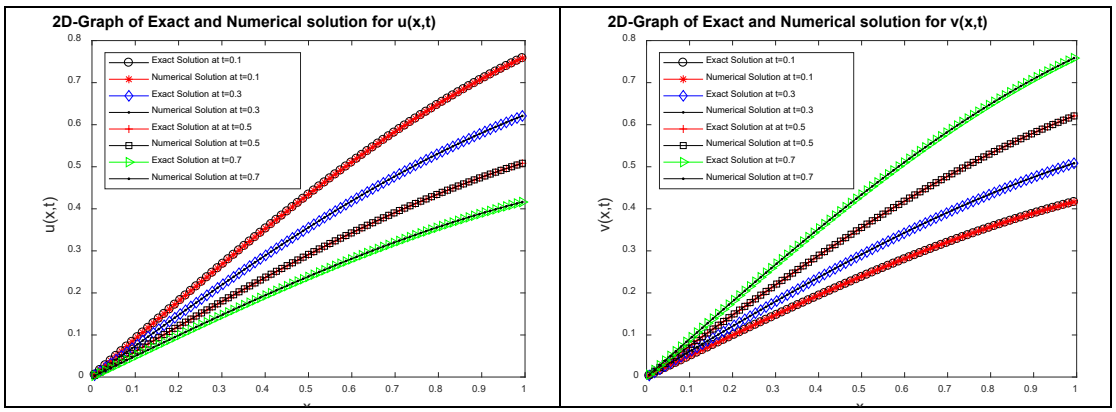

Figure 6.4 :2D-Graphical representation of exact and approximated solutions u(x,t) and v(x,t) of Numerical Experiment No. 6.1 for different values of t at the integer order α= β= γ= δ =1 with η= ξ = -2, μ=λ=1 and Δt = 0.01.

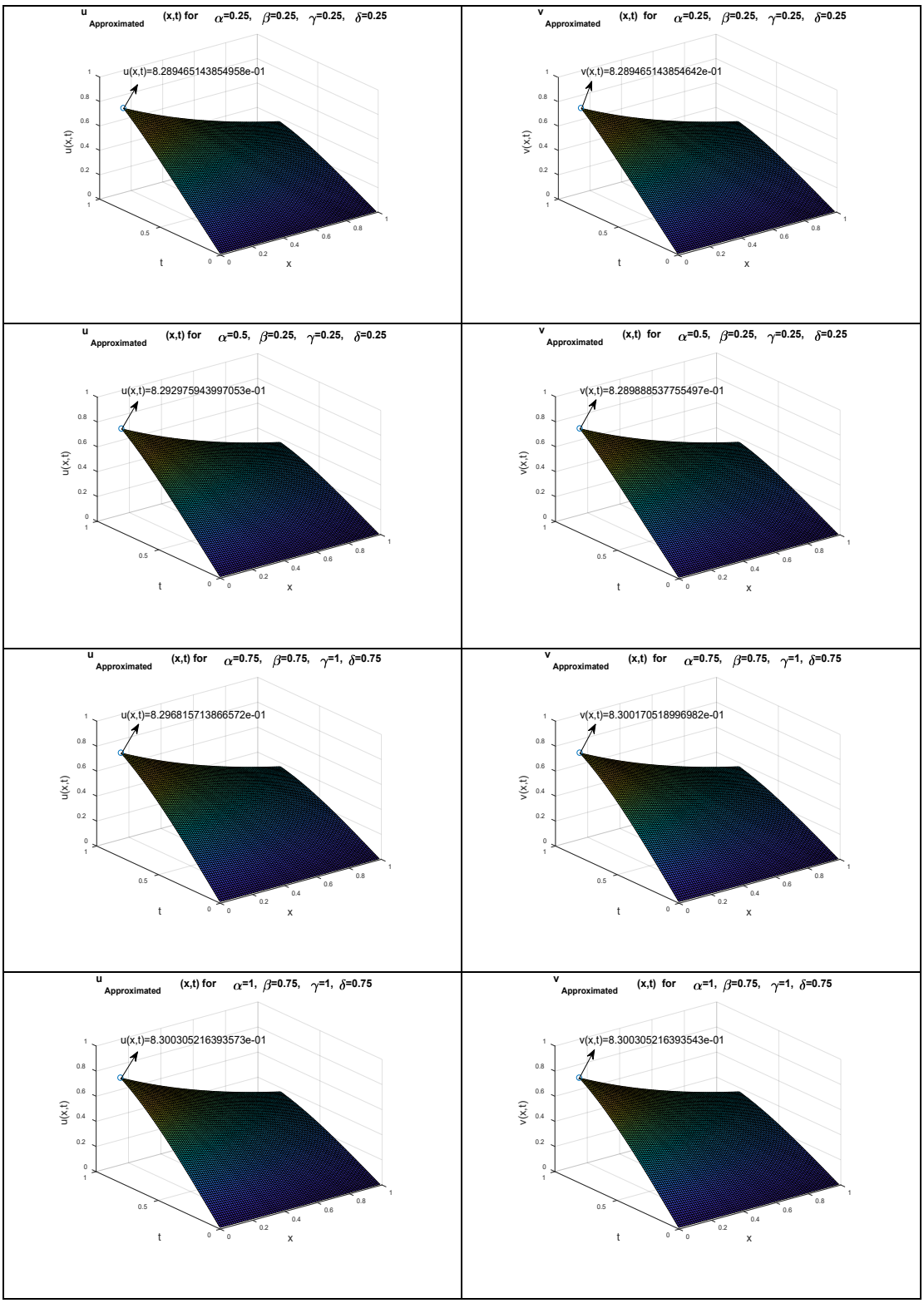

Figure 6.5: Approximate solution of Numerical Experiment No. 6.1 in 3D with different values of α, β, γ, δ ∈ (0,1] for which the solution behaves differently at η= ξ = -2, μ=λ=1 and Δt = 0.01.

Numerical Experiment No. 6.2 : - Consider the following space-time fractional coupled Burgers' equation

$$\begin{cases} \frac{\partial^{\alpha} u}{\partial t^{\alpha}} = \frac{\partial^2 u}{\partial x^2} + 2\,u\frac{\partial^{\beta} u}{\partial x^{\beta}} - \frac{\partial (uv)}{\partial x} \quad , \qquad \text{x} \in [0,1] \quad , t \in [0,T] \\ \frac{\partial^{\gamma} v}{\partial t^{\gamma}} = \frac{\partial^2 v}{\partial x^2} + 2\,v\frac{\partial^{\delta} v}{\partial x^{\delta}} - \frac{\partial (uv)}{\partial x} \quad , \qquad \text{x} \in [0,1] \quad , t \in [0,T] \end{cases} \tag{6.68}$$

Subjected to the boundary conditions given in Equation (6.69)

$$u(0,t) = 0, u(1,t) = 0, v(0,t) = 0, v(1,t) = 0 \qquad \forall \quad t \in [0,T] \tag{6.69}$$

and with the initial condition given in Equation (6.70)

$$u(x,0) = \sin(2\pi x - \pi) \quad , \; v(x,0) = \sin(2\pi x - \pi) \qquad \forall \;\; \text{x} \in [0,1] \tag{6.70}$$

Analytic solution of the Equation (6.68) in special case when $\alpha = \beta = \gamma = \delta = 1$ is

$$u(x,t) = e^{-4\pi^2 t}\sin(2\pi x - \pi) \qquad , \quad v(x,t) = e^{-4\pi^2 t}\sin(2\pi x - \pi) \tag{6.71}$$

The numerical solution obtained by applying the given methodology is

$$u(x_l, t_{r+1}) = (t_{r+1} - \; t_r\,)\sum_{i=1}^{3m} a_i(q_{i,2}(x_l) - x_l\, q_{i,2}(1)) + \big(u(x_l, t_r) - f_1(t_r)\big) + x_l\big(f_2(t_{r+1}) - f_1(t_{r+1})\big) - x_l\big(f_2(t_r) - f_1(t_r)\big) + f_1(t_{r+1})$$

$$v(x_l, t_{r+1}) = (t_{r+1} - \; t_r\,)\sum_{i=1}^{3m} b_i(q_{i,2}(x_l) - x_l\, q_{i,2}(1)) + \big(v(x_l, t_r) - \varphi_1(t_r)\big) + x_l\,\big(\varphi_2(t_{r+1}) - \varphi_1(t_{r+1})\big) - x_l\big(\varphi_2(t_r) - \varphi_1(t_r)\big) + \varphi_1(t_{r+1})$$

at various times by using successive iteration for $r = \; 0,1,2,3,\cdots$. where $f_1(t_r) = 0, f_2(t_r) = 0,\; \varphi_1(t_r) = 0, \varphi_2(t_r) = 0$ for $r = 0, t_0 = 0$ and rest all the values will be obtained using the iterative process.

Table 4 explains the absolute errors in the results obtained by the proposed method for example 2 by considering the domain $x \in [0,1]$ and $\Delta t = 0$ and it is of order 10^{-5} which assures the efficiency and reliability of the proposed method. It can be seen from Figure 8 to Figure 14 that the solution obtained by the proposed method for the case (when $\alpha = \beta = \gamma = \delta = 1$) is in good agreement with the analytical solution available in the literature. Table 5 is explaining the absolute error in the solution for different values of Δt which illustrate the direct dependence of absolute error on mesh size for time variable. It can also be observed from the Figure 13 and Figure 14 that whenever we are changing the values of γ and δ by fixing the values of α, β, we are getting the

change in the solution space of $v(x,t)$ and there is no change in the solution space of $u(x,t)$ and vice versa. It is because of the reason that α, β are orders of the time and space fractional derivatives of $u(x,t)$ respectively and that γ, δ are orders of the time and space fractional derivatives of $u(x,t)$ respectively which explains the importance of fractional models in explaining the microscopic behavior of the phenomenon.

Table 6.4 :Absolute error in numerical results $u(x,t)$ at random collocation points for integer order α= β= γ= δ =1 with η= ξ = -2, μ=λ=1 in Numerical Experiment No.6.2

$x \rightarrow$ / $t \downarrow$	**0.05556**	**0.16667**	**0.27778**	**0.38889**	**0.50000**	**0.61111**	**0.72222**	**0.83333**	**0.94444**
0.1	6.67×10^{-5}	4.35×10^{-5}	3.22×10^{-5}	2.62×10^{-5}	2.25×10^{-5}	1.99×10^{-5}	1.81×10^{-5}	1.67×10^{-5}	1.56×10^{-5}
0.2	1.69×10^{-4}	1.10×10^{-4}	8.17×10^{-5}	6.64×10^{-5}	5.69×10^{-5}	5.05×10^{-5}	4.58×10^{-5}	4.23×10^{-5}	3.95×10^{-5}
0.3	1.92×10^{-4}	1.25×10^{-4}	9.29×10^{-5}	7.55×10^{-5}	6.47×10^{-5}	5.74×10^{-5}	5.21×10^{-5}	4.81×10^{-5}	4.49×10^{-5}
0.4	1.25×10^{-4}	8.18×10^{-5}	6.06×10^{-5}	4.93×10^{-5}	4.22×10^{-5}	3.75×10^{-5}	3.40×10^{-5}	3.14×10^{-5}	2.93×10^{-5}
0.5	2.89×10^{-19}	6.44×10^{-19}	1.05×10^{-18}	1.04×10^{-18}	9.44×10^{-19}	9.33×10^{-19}	1.52×10^{-18}	1.11×10^{-18}	9.49×10^{-19}
0.6	1.25×10^{-4}	8.18×10^{-5}	6.06×10^{-5}	4.93×10^{-5}	4.22×10^{-5}	3.75×10^{-5}	3.40×10^{-5}	3.14×10^{-5}	2.93×10^{-5}
0.7	1.92×10^{-4}	1.25×10^{-4}	9.29×10^{-5}	7.55×10^{-5}	6.47×10^{-5}	5.74×10^{-5}	5.21×10^{-5}	4.81×10^{-5}	4.49×10^{-5}
0.8	1.69×10^{-4}	1.10×10^{-4}	8.17×10^{-5}	6.64×10^{-5}	5.69×10^{-5}	5.05×10^{-5}	4.58×10^{-5}	4.23×10^{-5}	3.95×10^{-5}
0.9	6.67×10^{-5}	4.35×10^{-5}	3.22×10^{-5}	2.62×10^{-5}	2.25×10^{-5}	1.99×10^{-5}	1.81×10^{-5}	1.67×10^{-5}	1.56×10^{-5}

Table 6.5:Maximum absolute error in numerical results u(x,t) and v(x,t) at the integer order α= β= γ= δ =1 with η= ξ = -2, μ=λ=1 for different values of Δt .

Δt	$\|E(u)\|_\infty$	$\|E(v)\|_\infty$
0.0100	$2.09861158048527\times 10^{-4}$	$2.098611580485271\times 10^{-4}$
0.0010	$3.764653977598853\times 10^{-6}$	$3.764653977598853\times 10^{-6}$
0.0001	$6.090606685656975\times 10^{-8}$	$6.090606685656975\times 10^{-8}$

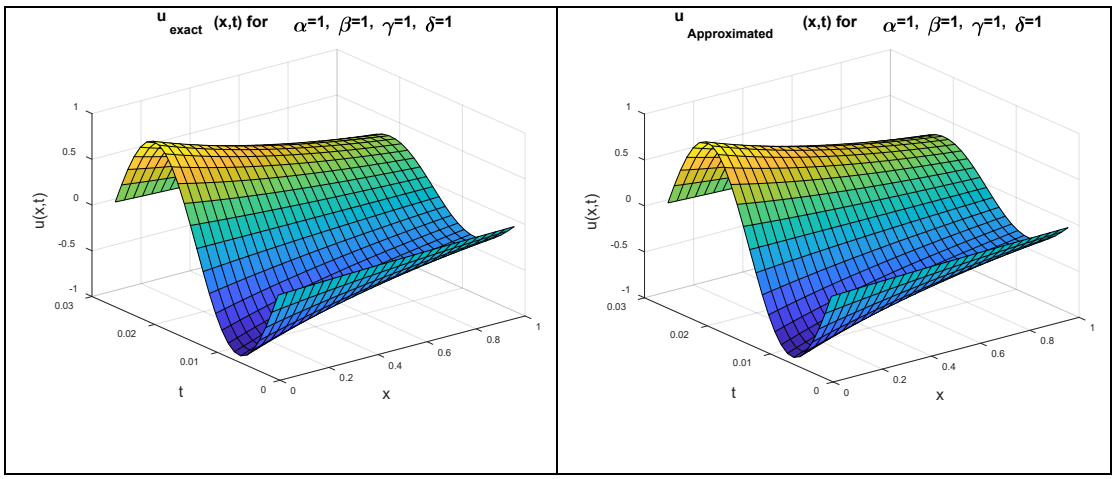

Figure 6.6: 3D Graphical representation of exact and approximated solution u(x,t) of Numerical Experiment No. 6.2 at α= β= γ= δ =1 with η= ξ = -2, μ=λ=1 and Δt = 0.001.

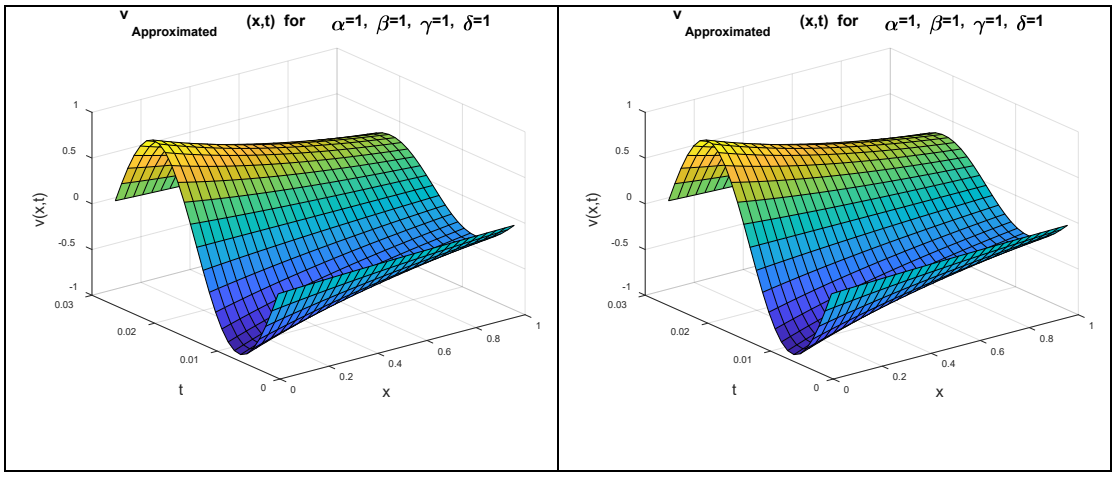

Figure 6.7: 3D Graphical representation of exact and approximated solution v(x,t) of Numerical Experiment No. 6.2 at α= β= γ= δ =1 with η= ξ = -2, μ=λ=1 and Δt = 0.001.

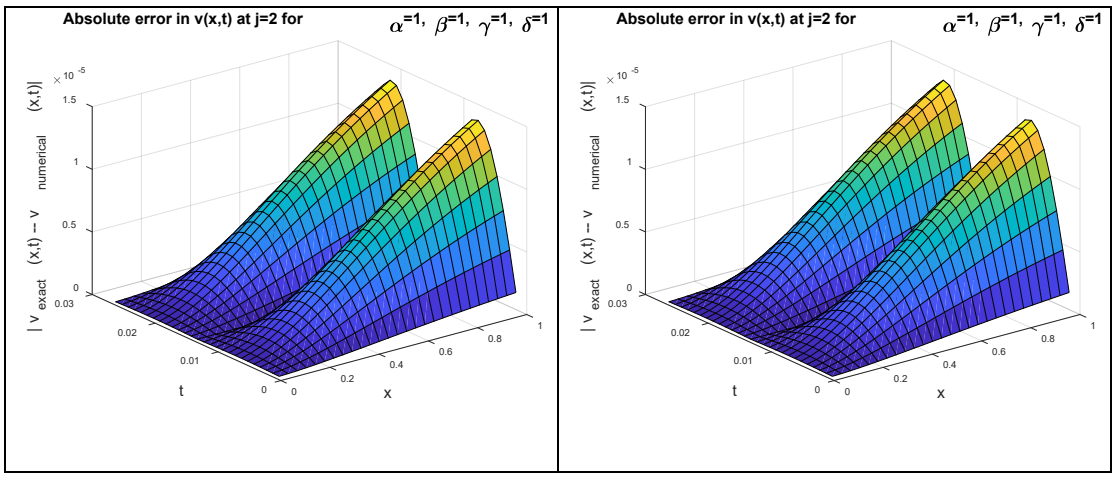

Figure 6.8: Surface plot of absolute error in the solutions u(x,t) and v(x,t) of Numerical Experiment No. 6.2 for j=2 at α= β= γ= δ =1 with η= ξ = -2, μ=λ=1 and Δt = 0.001.

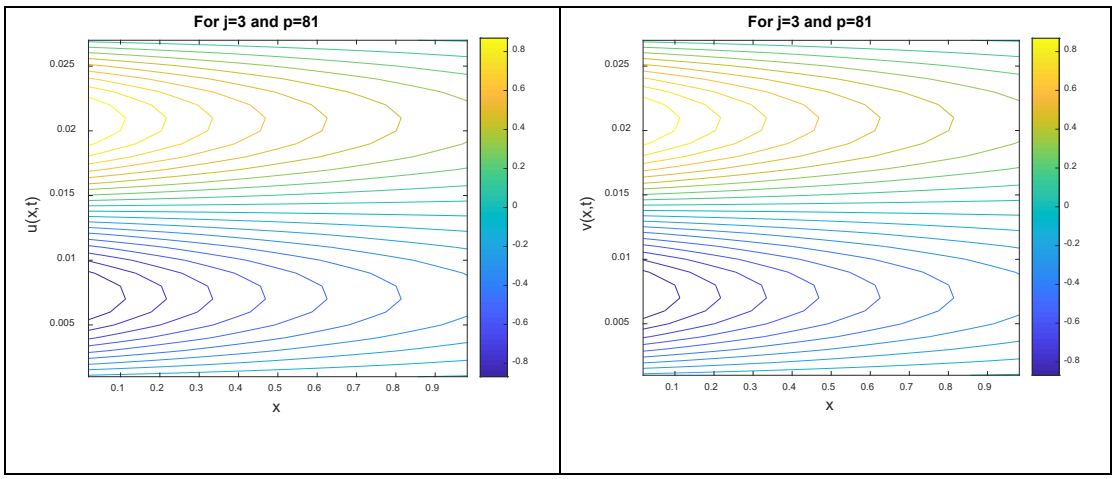

Figure 6.9 :Contour representation of solutions u(x,t) and v(x,t) of Numerical Experiment No. 6.2 at the integer order $\alpha= \beta= \gamma= \delta =1$ with $\eta= \xi = -2$, $\mu=\lambda=1$ and $\Delta t = 0.001$.

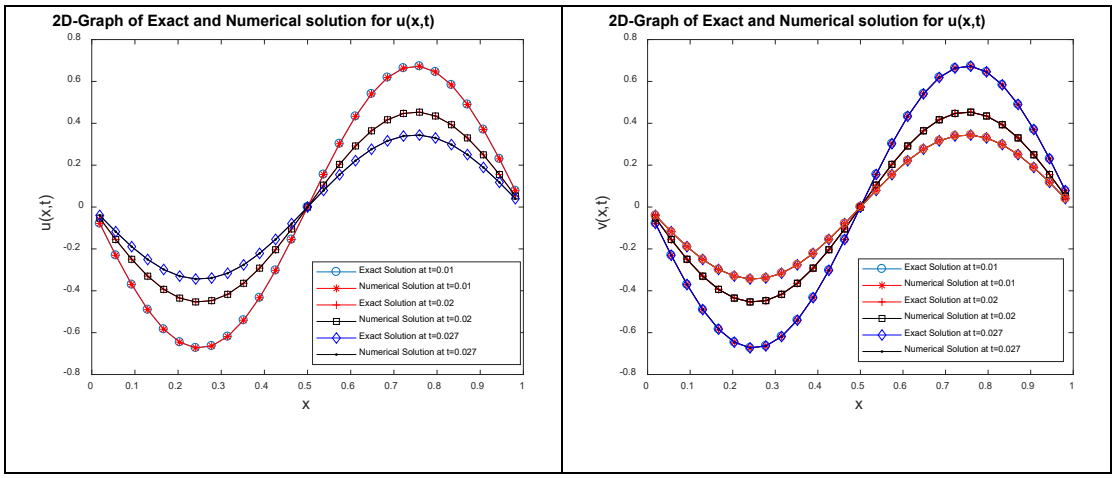

Figure 6.10: 2D-Graphical representation of exact and approximated solutions u(x,t) and v(x,t) of Numerical Experiment No. 6.2 for different values of t at the integer order $\alpha= \beta= \gamma= \delta =1$ with $\eta= \xi = -2$, $\mu=\lambda=1$ and $\Delta t = 0.001$.

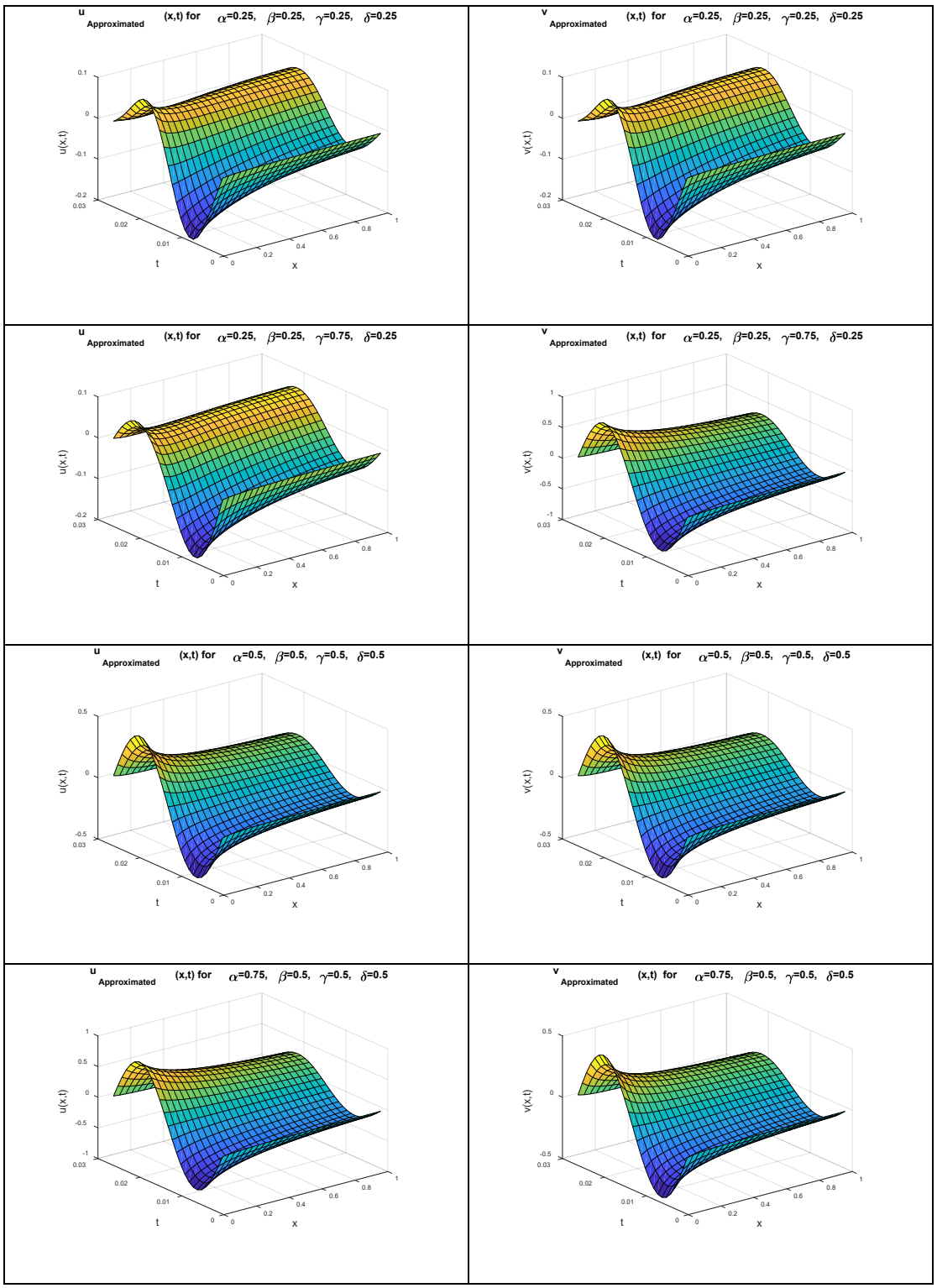

Figure 6.11: Approximate solution of Numerical Experiment No. 6.2 in 3D with different values of α, β, γ, δ ∈ (0,1] for which the solution behaves differently at η= ξ = -2, μ=λ=1 and Δt = 0.001.

6.7 Conclusion

We have developed a scale 3 Haar wavelet-based collocation scheme to find the solution of nonlinear coupled fractional differential equations. Two examples of space-time fractional coupled Burgers' equation with different boundary and initial constraints are considered to prove the reliability and efficiency of the proposed numerical scheme. It has been observed in with the help of MATLAB stimulation and computations that solution is behaving differentially as we vary the order of fractional derivatives in space-time fractional coupled Burgers' equation and giving the accuracy of order 10^{-5} at integer-order derivative (i.e. at $\alpha = \beta = \gamma = \delta$=1) for j=2 which demonstrate the performance of the scheme. The proposed method is compared with another method available in the literature and it is found that the proposed method is working better than the other method. Looking at the performance of the method for the given set of numerical experiments, the proposed method can be extended to explain the behavior of the different phenomenon by solving the system of fractional differential equations governing those phenomena. The proposed method provides an insight into the microscopic behavior of phenomena under study. The given method is also fully supportive and compatible with the ordinary, partial, fractional differential equations and integral equations.

Chapter 7

Two Dimensional Haar Scale 3 Wavelet based solution of Hyperbolic Telegraph Equation.

7.1 Introduction

In this chapter a new numerical technique is developed for obtaining the solution of second-order hyperbolic Telegraph equation of the type given in Equation (7.1), using two-dimensional Haar Scale 3 wavelet bases.

$$\frac{\partial^2 \varphi}{\partial t^2} + 2\alpha \frac{\partial \varphi}{\partial t} + \beta^2 \varphi = \frac{\partial^2 \varphi}{\partial x^2} + g(x,t), \quad (x,t) \in [0,1] \times [0,T] \tag{7.1}$$

under the following types of initial constraints of the type given in Equation (7.2)

$$\varphi(x,0) = \psi_1(x), \quad \frac{\partial \varphi}{\partial t}(x,0) = \psi_2(x) \tag{7.2}$$

and the boundary constraints of the type given in Equation (7.3)

$$\varphi(0,t) = \xi_1(t), \quad t \in [0,T], \quad \varphi(1,t) = \xi_2(t), \quad t \in [0,T] \tag{7.3}$$

where $\alpha > \beta \geq 0$ are known constants, $\psi_1(x), \psi_2(x), \xi_1(t), \xi_2(t), g(x,t)$ are the given functions and $\varphi(x,t)$ is the function whose value is to be determined. When $\alpha > 0, \beta = 0$ then equation represents the damped wave motion equation and when $\alpha > \beta > 0$ then it is named as the Telegraph Equation. These types of equations are emerging in the field of electric signal propagation in cables[179], pulsating blood flow in the arteries[180], 'acoustic wave propagation' in porous media of Darcy-type[181], vibrations in the different structures, walk theory[182], Maxwell viscous fluid parallel flow study[183], etc. Telegraph equation is a special type of hyperbolic equation which is more suitable in modeling the reaction-diffusion as compare to the ordinary diffusion equation for many branches of engineering and sciences. Telegraph equation plays a crucial role in the area of atomic physics and it is considered as one of the fundamental equations of atomic physics. Finding the solution to these types of equations become a

big challenge as there is no established analytic method to solve these kinds of problems. Therefore, many researchers are involved in developing the various numerical and semi-analytic schemes for finding solutions to the different problems governed by telegraph equations. Some of the methods which have been freshly developed and applied to solve the telegraph equations are Septic B-Spline Collocation Method (SBSCM) [184], Cubic B-Spline Quasi-Interpolation Method(CBSQIM)[185], Cubic B-Spline Collocation Method(CBSCM)[186]–[188], Reproducing Kernel Hilbert Space Method(RKHSM)[189], Radial Basis Function Method(RBFM)[190], Dual Reciprocity Boundary Integral Equation Method (DRBIEM)[190], Differential Quadrature Method (DQM)[191], Trigonometric B-Splines Method(TBSM)[187] , Homotopy Analysis Method (HAM)[192],Chebyshev Tau Method(CTM)[193], etc.

But the study of establishing the solution for the Telegraph equation using the Haar scale 3 wavelets has not been attempted in the literature which motivated us to develop a new technique for the solution of these types of equations. Orthonormal wavelets are one of the modernistic functions which have the capability of dilation and translation. Because of these properties, numerical techniques that involve wavelet bases are showing the qualitative improvement in contrast with other methods. In literature, dyadic wavelets are in preponderance. In 1995, Chui and Lian [115] has developed the Haar scale 3 (non-dyadic) wavelets by using the process of multiresolution analysis. In 2018, Mittal and Pandit have used the Haar scale 3 (non-dyadic) wavelets [71], [141], [142], [194] for solving the various types of differential equations and found that these wavelet bases are equally competent in solving the various types of mathematical models governed by differential equations. Also, it was shown by them that the Haar scale 3 wavelet has a faster rate of convergence as compared to the Haar scale 2 dyadic wavelets. This gives us good hope of getting a better solver for these equations by developing a new hybrid technique based upon Haar scale 3 Wavelets for the solution of Telegraph equations.

This chapter follows the sequence of sections as described: In section 2, explicit forms of Haar scale 3 parent wavelets with their families and procedure to find their integrals have been explained briefly. Representation of the solution using Haar scale 3 wavelets is explained in section 3. Section 4 explains the method of solution using Haar scale 3

wavelets. In section 5, solutions of three different Telegraph equation are produced to analyze the competence and performance of the method. In section 6, the conclusion drawn from the results and in future research ideas are given.

7.2 Explicit forms of Haar scale 3 wavelets and their integrals

The mathematical expressions for Haar scale 3 wavelet family [71], [115] are given below

$$h_1(t) = \varphi(t) = \begin{cases} 1 & 0 \le t < 1 \\ 0 & elsewhere \end{cases} \tag{7.4}$$

$$h_i(t) = \psi^1\left(3^j t - k\right) = \frac{1}{\sqrt{2}} \begin{cases} -1 & \varkappa_1(i) \le t < \varkappa_2(i) \\ 2 & \varkappa_2(i) \le t < \varkappa_3(i) \\ -1 & \varkappa_3(i) \le t < \varkappa_4(i) \\ 0 & elsewhere \end{cases}, \quad for \quad i = 2,4, \dots 3p-1 \tag{7.5}$$

$$h_i(t) = \psi^2\left(3^j t - k\right) = \sqrt{\frac{3}{2}} \begin{cases} 1 & \varkappa_1(i) \le t < \varkappa_2(i) \\ 0 & \varkappa_2(i) \le t < \varkappa_3(i) \\ -1 & \varkappa_3(i) \le t < \varkappa_4(i) \\ 0 & elsewhere \end{cases}, \quad for \quad i = 3,6, \dots 3p \tag{7.6}$$

where $\varkappa_1(i) = \frac{k}{p}$, $\varkappa_2(i) = \frac{3k+1}{3p}$, $\varkappa_3(i) = \frac{(3k+2)}{3p}$, $\varkappa_4(i) = \frac{k+1}{p}$, $p = 3^j$, $j = 0,1,2, \dots$, $k = 0,1,2, \dots, p-1$. Here i , j , k respectively represent the wavelet number, level of resolution (dilation), and translation parameters of wavelet family. The values of i $(for\ i > 1)$ can be calculated with the help of j , k by using the following relations $\begin{cases} i - 1 = 3^j + 2k & for\ even\ i \\ i - 2 = 3^j + 2k & for\ odd\ i \end{cases}$.By using this relation for different dilation and translations of $h_2(t), h_3(t)$, we will get the wavelet family where $h_2(t)$ and $h_3(t)$ are also called mother wavelets and rest all the wavelets which we have obtained from mother wavelet are called daughter wavelets.

The main difference which makes the Haar scale 3 (non-dyadic) wavelets better than the Haar scale 2 dyadic wavelets is that only one mother wavelet is responsible for the construction of whole wavelet family but in case of Haar Scale 3 wavelets, two mother wavelets with different shapes are responsible for the construction of the whole family.

Because of this fact, Haar Scale 3 wavelets increase the convergence rate of the solution.

Now one can easily integrate the Equations (7.4)-(7.6)the desired number of times over the interval [A, B) by using the formula as given below

$$q_{m,i}(t) = \int_0^t \int_0^t \int_0^t \cdots\cdots\cdots m\ times \cdots\cdots\cdots \int_0^t h_i(x)(dx)^m = \frac{1}{(m-1)!}\int_0^t (t - x)^{m-1} h_i(x)dx\ ,\quad m = 1,2,3 \ldots\ldots\ldots\ ,\ i = 1,2,3, \ldots\ldots\ldots 3p \tag{7.7}$$

After evaluating the above integrals for Equation (7.4), we get Equation (7.8)

$$q_{\beta,i}(t) = \frac{t^m}{m!} \quad for \quad i = 1 \tag{7.8}$$

Using Equation (7.7) on Equation (7.5), we get the values of $q_{m,i}(t)'s \quad for \quad i = 2,4,6,8,\cdots,3p-1$ which are given by Equation (7.9)

$$q_{m,i}(t) = \frac{1}{\sqrt{2}}\begin{cases} 0 & for \quad 0 \le t \le \varkappa_1(i) \\ \frac{-1}{m!}\left(t-\varkappa_1(i)\right)^m & for \quad \varkappa_1(i) \le t \le \varkappa_2(i) \\ \frac{1}{m!}\left[-\left(t-\varkappa_1(i)\right)^m + 3\left(t-\varkappa_2(i)\right)^m\right] & for \quad \varkappa_2(i) \le t \le \varkappa_3(i) \\ \frac{1}{m!}\left[-\left(t-\varkappa_1(i)\right)^m + 3\left(t-\varkappa_2(i)\right)^m - 3\left(t-\varkappa_3(i)\right)^m\right] & for\ \varkappa_3(i) \le t \le \varkappa_4(i) \\ \frac{1}{m!}\left[-\left(t-\varkappa_1(i)\right)^m + 3\left(t-\varkappa_2(i)\right)^m - 3\left(t-\varkappa_3(i)\right)^m + \left(t-\varkappa_4(i)\right)^m\right] & for\ \varkappa_4(i) \le t \le 1 \end{cases} \tag{7.9}$$

Using Equation (7.7) on Equation (7.6), we get the values of $q_{m,i}(t)'s \quad for \quad i = 3,5,7,9,\cdots,3p$ which are given by Equation (7.10)

$$q_{m,i}(t) = \sqrt{\frac{3}{2}}\begin{cases} 0 & for \quad 0 \le t \le \varkappa_1(i) \\ \frac{1}{m!}\left(t-\varkappa_1(i)\right)^m & for \quad \varkappa_1(i) \le t \le \varkappa_2(i) \\ \frac{1}{m!}\left[\left(t-\varkappa_1(i)\right)^m - \left(t-\varkappa_2(i)\right)^m\right] & for \quad \varkappa_2(i) \le t \le \varkappa_3(i) \\ \frac{1}{m!}\left[\left(t-\varkappa_1(i)\right)^m - \left(t-\varkappa_2(i)\right)^m - \left(t-\varkappa_3(i)\right)^m\right] & for \quad \varkappa_3(i) \le t \le \varkappa_4(i) \\ \frac{1}{m!}\left[\left(t-\varkappa_1(i)\right)^m - \left(t-\varkappa_2(i)\right)^m - \left(t-\varkappa_3(i)\right)^m + \left(t-\varkappa_4(i)\right)^m\right] & for\ \varkappa_4(i) \le t \le 1 \end{cases} \tag{7.10}$$

7.3 Approximation of solution

Using the properties of Haar Scale 3 wavelets as explained in section 3, any function $u(x,t) \in L_2(R)$ can be approximated as

$$u(x,t) = \sum_{i=1}^{\infty}\sum_{l=1}^{\infty} a_{il}\, h_i(x) h_l(t) \tag{7.11}$$

These $a_{il}'s$ will be determined by the proposed method. But for the computational purpose, one can consider a truncated series up to $3p \times 3p$ terms. By considering the $3p \times 3p$ terms to approximate the function $u(x,t)$ we get

$$u(x,t) \approx u_{3p}(x,t) = \sum_{i=1}^{3p}\sum_{l=1}^{3p} a_{il}\, h_i(x) h_l(t) \tag{7.12}$$

where $p = 3^j,\ j, j' = 0,1,2, \ldots$

7.4 Method of Solution

Now space variables are discretized with the help of 'Two dimensional Haar scale 3 wavelets' as explained below

$$\varphi_{xxtt}(x,t) = \sum_{i=1}^{3p}\sum_{l=1}^{3p} a_{i\ell}\, h_i(x)\, h_\ell(t) \tag{7.13}$$

Integrating the Equation (7.13) w.r.t x within the domain 0 to x , we get

$$\varphi_{xtt}(x,t) = \sum_{i=1}^{3p}\sum_{l=1}^{3p} a_{i\ell}\, q_{1,i}(x)\, h_\ell(t) + \varphi_{xtt}(0,t) \tag{7.14}$$

Now by integrating the Equation (7.14) w.r.t x within the domain 0 to 1, the value of $\mathcal{U}_{xtt}(0,t)$ is given by

$$\varphi_{xtt}(0,t) = \big(\varphi_{tt}(1,t) - \varphi_{tt}(0,t)\big) - \sum_{i=1}^{3p}\sum_{l=1}^{3p} a_{i\ell}\, q_{2,i}(1)\, h_\ell(t) \tag{7.15}$$

Using Equation (7.15), Equation (7.14) becomes

$$\begin{aligned}\varphi_{xtt}(x,t) = \sum_{i=1}^{3p}\sum_{l=1}^{3p} a_{i\ell}\Big(q_{1,i}(x) - q_{2,i}(1)\Big)\, h_\ell(t) \\ + \big(\varphi_{tt}(1,t) - \varphi_{tt}(0,t)\big)\end{aligned} \tag{7.16}$$

Again, integrating the Equation (7.16) w.r.t x within the limits we get

$$\varphi_{tt}(x,t) = \sum_{i=1}^{3p}\sum_{l=1}^{3p} a_{i\ell}\big(\, q_{2,i}(x) - \, x\, q_{2,i}(1)\big)\, h_\ell(t) + x\, \varphi_{tt}(1,t) + (1 - x)\, \varphi_{tt}(0,t) \tag{7.17}$$

Taking the limit $0\ to\ t$, integrating the Equation (7.17) w.r.t t and then by applying the boundary conditions, we get Equation (7.18)

$$\varphi_t(x,t) = \sum_{i=1}^{3p}\sum_{l=1}^{3p} a_{i\ell}\big(\, q_{2,i}(x) - \, x\, q_{2,i}(1)\big)\, q_{1,\ell}(t) + x\,(\varphi_t(1,t) - \psi_2(1)) + (1-x)\big(\, \varphi_t(0,t) - \psi_2(0)\big) + \psi_2(x) \tag{7.18}$$

Integrate the Equation (7.18) w.r.t t within the same limit, we get

$$\varphi(x,t) = \sum_{i=1}^{3p}\sum_{l=1}^{3p} a_{i\ell}\Big(\, q_{2,i}(x) - \, x\, q_{2,i}(1)\Big)\, q_{2,\ell}(t) + x\,(\xi_2(t) - \xi_2(0)) - x\, t\, \psi_2(1) + (1-x)\big(\xi_1(t) - \xi_1(0)\big) - (1-x)\, t\psi_2(0) + t\psi_2(x) \tag{7.19}$$

Differentiating the equation (7.19) two times with respect to x ,we get φ_{xx} as given by Equation (7.20)

$$\varphi_{xx}(x,t) = \sum_{i=1}^{3p}\sum_{l=1}^{3p} a_{i\ell}\, h_i(x) q_{2,\ell}(t) + t(\psi_2)_{xx}(x) \tag{7.20}$$

Putting the approximation of φ_{xx} , φ_{tt}, φ_t and φ from Equations (7.17)-(7.20) in Equation (7.1) ,we get Equation (7.21)

$$\begin{aligned} &\textstyle\sum_{i=1}^{3p}\sum_{l=1}^{3p} a_{i\ell}\Big(\, q_{2,i}(x) - \, x\, q_{2,i}(1)\Big)\, h_\ell(t) + x\big(\xi_2(t)\big)_{tt}, \quad + (1 - \\ &x)\big(\xi_1(t)\big)_{tt} + \alpha\, \Big(\textstyle\sum_{i=1}^{3p}\sum_{l=1}^{3p} a_{i\ell}\big(\, q_{2,i}(x) - \, x\, q_{2,i}(1)\big)\, q_{1,\ell}(t) + \\ &x\,(\varphi_t(1,t) - \psi_2(1)) + (1-x)\big(\, \varphi_t(0,t) - \psi_2(0)\big) + \psi_2(x)\Big) + \\ &\beta\Big(\textstyle\sum_{i=1}^{3p}\sum_{l=1}^{3p} a_{i\ell}\Big(\, q_{2,i}(x) - \, x\, q_{2,i}(1)\Big)\, q_{2,\ell}(t) + x\,(\xi_2(t) - \xi_2(0)) - \end{aligned} \tag{7.21}$$

$$x\,t\,\psi_2(1) + (1-x)\big(\xi_1(t) - \xi_1(0)\big) - (1-x)\,t\psi_2(0) + t\psi_2(x)\Big) =$$

$$\sum_{i=1}^{3p}\sum_{l=1}^{3p} a_{i\ell}\, h_i(x) q_{2,\ell}(t) + t(\psi_2)_{xx}(x) + g(x,t)$$

After Simplification Equation (7.21) results into (7.22)

$$\begin{aligned}&\sum_{i=1}^{3p}\sum_{l=1}^{3p} a_{i\ell}\,\Big[\Big(q_{2,i}(x) - x\,q_{2,i}(1)\Big)\,h_\ell(t) + \alpha\Big(\big(q_{2,i}(x) - \\ &x\,q_{2,i}(1)\big)\,q_{1,\ell}(t)\Big) + \beta\Big(\Big(q_{2,i}(x) - x\,q_{2,i}(1)\Big)\,q_{2,\ell}(t)\Big) - \\ &h_i(x)q_{2,\ell}(t)\Big] = g(x,t) + t(\psi_2)_{xx}(x) - \Big(x\big(\xi_2(t)\big)_{tt}, \quad + (1 - \\ &x)\big(\xi_1(t)\big)_{tt}\Big) - \alpha\Big(x\,(\varphi_t(1,t) - \psi_2(1)) + (1-x)\big(\varphi_t(0,t) - \psi_2(0)\big) + \\ &\psi_2(x)\Big) - \beta\Big(x\,(\xi_2(t) - \xi_2(0)) - x\,t\,\psi_2(1) + (1-x)\big(\xi_1(t) - \\ &\xi_1(0)\big) - (1-x)\,t\psi_2(0) + t\psi_2(x)\Big)\end{aligned} \tag{7.22}$$

Now discretizing the variable as $x \to x_r$, $t \to t_s$ where $x_r = \frac{2r-1}{6p}$, $t_s = \frac{2s-1}{6p}$, $r, s = 1,2, \ldots \ldots 3p$ in the Equations (7.22), we get the system of algebraic equations which is given by Equation (7.23)

$$\sum_{i=1}^{3p}\sum_{l=1}^{3p} a_{i\ell}\, R_{i,l,r,s} = F(r,s) \tag{7.23}$$

$$\begin{aligned}\text{Where } R_{i,l,r,s} = &\Big[\Big(q_{2,i}(x_r) - x_r\,q_{2,i}(1)\Big)\,h_\ell(t_s) + \alpha\Big(\big(q_{2,i}(x_r) - \\ &x_r\,q_{2,i}(1)\big)\,q_{1,\ell}(t_s)\Big) + \beta\Big(\Big(q_{2,i}(x_r) - x_r\,q_{2,i}(1)\Big)\,q_{2,\ell}(t_s)\Big) - \\ &h_i(x_r)q_{2,\ell}(t_s)\Big]\end{aligned} \tag{7.24}$$

$$\begin{aligned}F(r,s) = &g(x_r,t_s) + t(\psi_2)_{xx}(x_r) - \Big(x_r\big(\xi_2(t_s)\big)_{tt}, \quad + (1 - \\ &x_r)\big(\xi_1(t_s)\big)_{tt}\Big) - \alpha\Big(x_r\,(\varphi_t(1,t_s) - \psi_2(1)) + (1-x_r)\big(\varphi_t(0,t_s) - \\ &\psi_2(0)\big) + \psi_2(x_r)\Big) - \beta\Big(x_r\,(\xi_2(t_s) - \xi_2(0)) - x_r\,t_s\,\psi_2(1) + \\ &(1-x_r)\big(\xi_1(t_s) - \xi_1(0)\big) - (1-x_r)\,t\psi_2(0) + t_s\psi_2(x_r)\Big)\end{aligned} \tag{7.25}$$

The above system(Equation (7.23)-(7.25)) reduced to the system of algebraic equations and further, it gets reduced to the system of 4D-arrays represented by Equation (7.26)

$$A_{3p\times 3p}R_{3p\times 3p\times 3p\times 3p} = F_{3p\times 3p} \tag{7.26}$$

Further, the above arrays system(Equation (7.26)) is reduced to the following matrix system using the transformations $a_{i\ell} = b_\lambda \ and \ F_{rs} = G_\mu$

$$B_{1\times(3p)^2}S_{(3p)^2\times(3p)^2} = G_{1\times(3p)^2} \tag{7.27}$$

where $\lambda = 3p(i-1)+l$ and $\mu = 3p(r-1)+s$.

The values of b_λ can be calculated successively for different values of $n = 1,2 \ldots$ by solving the above system of equations using the Thomas algorithm via MATLAB Program. Original wavelet coefficients $a_{i\ell}$ can be restored using the above transformation. These coefficients will be used in the equations to determine the final solution of the problem) for different value of t_n for n= 0,1, 2..

7.5 Error analysis with Numerical Experiments

The proposed scheme is tested on some Telegraph equations to judge the competence of the scheme and level of accuracy obtained by the present scheme. $L_2 - error$, $L_\infty - error$ and absolute errors have been calculated for each problem using the present scheme with the help of following formulas

$$\text{Absolute error} = |u_{exact}(x_r,t_s) - u_{num}(x_r,t_s)| \tag{7.28}$$

$$L_\infty = \max_{r,s}|u_{exact}(x_r,t_s) - u_{num}(x_r,t_s)| \tag{7.29}$$

$$L_2 = \frac{\sqrt{\sum_{l=1}^{3p}|u_{exact}(x_r,t_s) - u_{num}(x_r,t_s)|^2}}{\sqrt{\sum_{l=1}^{3p}|u_{exact}(x_r,t_s)|^2}} \tag{7.30}$$

Numerical Experiment No. 7.1 : - Consider the 1D *hyperbolic Telegraph* equation of second order

$$\frac{\partial^2 \varphi}{\partial t^2} + 2\alpha \frac{\partial \varphi}{\partial t} + \beta^2 \varphi = \frac{\partial^2 \varphi}{\partial x^2} + g(x,t), \quad (x,t) \in [0,1] \times [0,T] \quad (7.31)$$

under the following types of initial constraints

$$\varphi(x,0) = e^x, \quad x \in [0,1], \qquad \frac{\partial \varphi}{\partial t}(x,0) = -e^x, \quad x \in [0,1] \quad (7.32)$$

and the boundary constraints

$$\varphi(0,t) = e^{-t}, \quad t \in [0,T], \quad \varphi(1,t) = e^{1-t}, \quad t \in [0,T] \quad (7.33)$$

with $2\alpha = 1$, $\beta = 1$ and $g(x,t) = 0$ and $\varphi(x,t)$ is a function whose value is to be determined.

An existing solution for numerical experiment no. 7.1 is $\varphi(x,t) = e^{x-t}$

We proposed the following numerical solution using the current scheme

$$\varphi(x,t) = \sum_{i=1}^{3p} \sum_{l=1}^{3p} a_{i\ell} \left(q_{2,i}(x) - x\, q_{2,i}(1) \right) q_{2,\ell}(t) + x\,(\xi_2(t) - \xi_2(0)) - x\, t\, \psi_2(1) + (1-x)\left(\xi_1(t) - \xi_1(0)\right) - (1-x)\, t\psi_2(0) + t\psi_2(x)$$

$a_{il}'s$ are the wavelets coefficients which will be obtained by the procedure discussed in section 7.4 and $q_{j,i}'s$ are the wavelet integrals that are already calculated in section 7.3. The particular solution is obtained using the boundary condition on the above equations and presented in the form of tables and figures. Figure 7.1 demonstrates the visible agreement in the exact and approximated solutions. Table 7.2 is depicting the current method performance in comparison with the exact solution existing in the recent literature. We infer that the proposed method is working well. Further, it has been observed from Table 7.1 that the error norm decreases with increase in collocation points which ensures the stability of the proposed numerical scheme. Hence, we can conclude that the proposed technique is a strong solver in terms of good accuracy.

Table 7.1: $\boldsymbol{L_2}$ and $\boldsymbol{L_\infty}$ errors at different value of $\boldsymbol{j}$ for Experiment No.7.1

Level of resolution	$J = 1$	$J = 2$	$J = 3$
L_2-error	4.837014364118279e-05	5.426745837985967e-06	6.036516821232161e-07
L_∞-error	1.151108100422293e-04	1.306821554991622e-05	1.454308205639521e-06

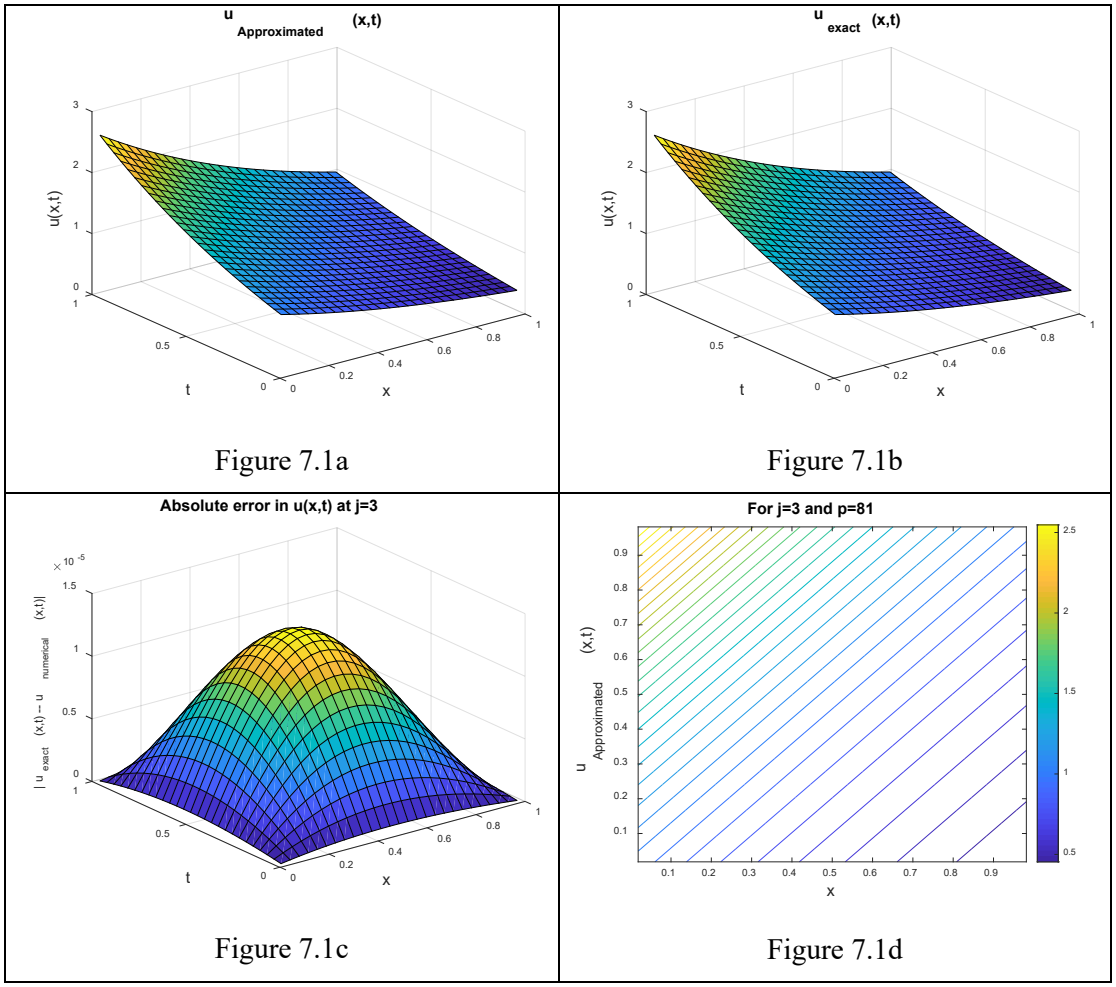

Figure 7.1a

Figure 7.1b

Figure 7.1c

Figure 7.1d

Figure 7.1: Graphical representation of Approximate solution(Figure 7.1a), Exact solution(Figure 7.1b), Absolute error(Figure 7.1c) and contour view of approximate solution(Figure 7.1c) in the Numerical Experiment No.7.1

Table 7.2: Comparison of results achieved for Numerical Experiment No.7.1 with Exact solution

x	***t***	**Approximate Solution**	**Exact solution**	**Absolute error**
0.1	0.1	0.999674	1	3.26E-04
0.2	0.2	0.999229	1	7.71E-04
0.3	0.3	0.999076	1	9.24E-04
0.4	0.4	0.999188	1	8.12E-04
0.5	0.5	0.999310	1	6.90E-04
0.6	0.6	0.999281	1	7.19E-04
0.7	0.7	0.999249	1	7.51E-04
0.8	0.8	0.999416	1	5.84E-04
0.9	0.9	0.999768	1	2.32E-04

Numerical Experiment No. 7.2 : - Consider the 1D *hyperbolic Telegraph* equation of second order

$$\frac{\partial^2 \varphi}{\partial t^2} + 2\alpha \frac{\partial \varphi}{\partial t} + \beta^2 \varphi = \frac{\partial^2 \varphi}{\partial x^2} + g(x,t), \quad (x,t) \in [0,1] \times [0,T] \tag{7.34}$$

under the following types of initial constraints

$$\varphi(x,0) = sinx, \quad \frac{\partial \varphi}{\partial t}(x,0) = -\sin x \quad \forall\, x \in [0,1] \tag{7.35}$$

and the boundary constraints

$$\varphi(0,t) = 0, \;\; \varphi(1,t) = e^{-t}\sin 1\,, \quad t \in [0,T] \tag{7.36}$$

with $\alpha = 2$, $\beta^2 = 2$ and $g(x,t) = 0$ and $\varphi(x,t)$ is the unknown function whose value is to be determined.

An existing solution obtained from the literature for experiment no. 7.2 is $\varphi(x,t) = e^{-t}\sin x$. Results obtained by the proposed scheme has been explained with the help of tables and surface plots. It is very much clear from Figure 2 and Table 7.3 that results achieved with the proposed scheme are roughly coinciding with the analytic solution. The level of accuracy obtained for the solution is of order 10^{-4} which is a noteworthy achievement for these kinds of problems. The solution achieved can further be improved by increasing the number of collocation points. In Table 7.4 error norms obtained by the present scheme are presented in comparison with the exact solution. It has been observed that with the increase in the collocation points (level of resolution), error norms are decreasing which ensures the stability of the proposed scheme. We infer that our scheme is working well.

Table 7.3: Comparison of results achieved for Numerical Experiment No. 7.2 with Exact solution

x	t	Approximate Solution	Exact solution	Absolute error
0.1	0.1	0.089473	0.090333	8.60E-04
0.2	0.2	0.161207	0.162657	1.45E-03
0.3	0.3	0.217964	0.218927	9.63E-04
0.4	0.4	0.260608	0.261035	4.27E-04
0.5	0.5	0.290540	0.290786	2.47E-04
0.6	0.6	0.309681	0.309882	2.02E-04
0.7	0.7	0.319588	0.319909	3.21E-04
0.8	0.8	0.321902	0.322329	4.27E-04
0.9	0.9	0.318267	0.318477	2.10E-04

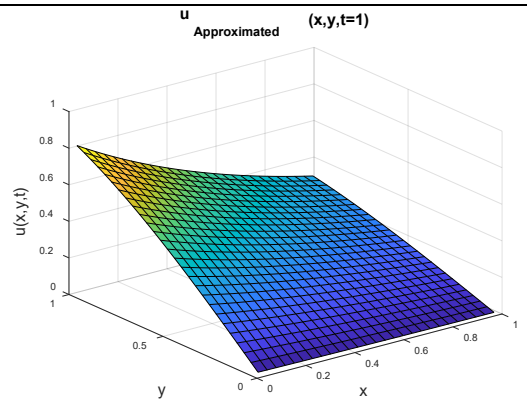

Figure 7.2a

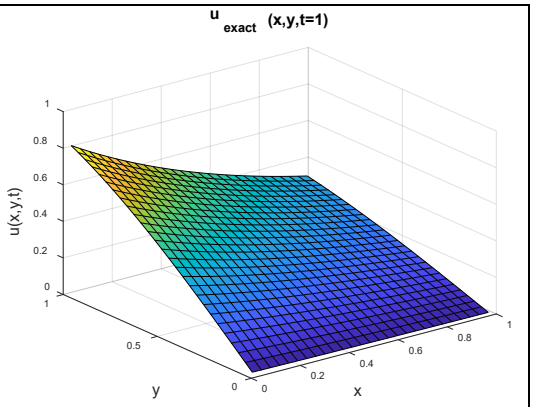

Figure 7.2b

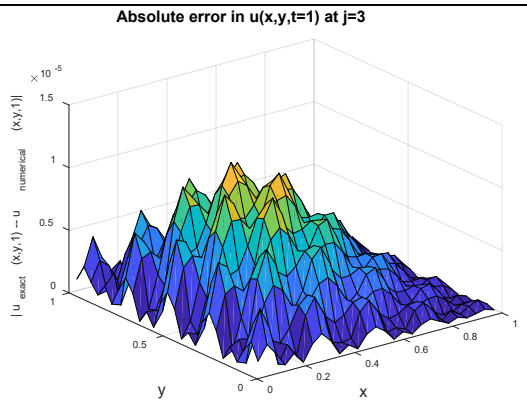

Figure 7.2c

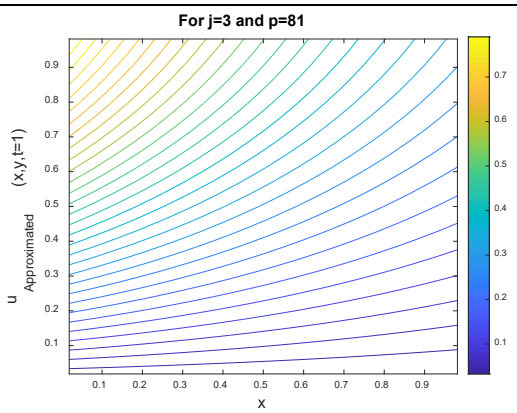

Figure 7.2d

Figure 7.2: Graphical representation of Approximate solution (Figure 7.2a), Exact solution(Figure 7.2b), Absolute error (Figure 7.2c), and contour view of the approx. solution (Figure 7.2d) in the solution of Numerical Experiment no No. 7.2

Table 7.4: $\boldsymbol{L_2}$ and $\boldsymbol{L_\infty}$ errors at different value of $\boldsymbol{j}$ for Numerical Experiment No. 7.2

Level of resolution	$J = 1$	$J = 2$	$J = 3$
L_2-error	2.966139636402692e-04	1.412472863080943e-05	1.508868064851954e-06
L_∞-error	3.086337934932737e-04	1.238748966753134e-05	1.129461926263620e-06

Numerical Experiment No. 7.3: - Consider the 1D *hyperbolic Telegraph* equation of second order

$$\frac{\partial^2 \varphi}{\partial t^2} + 2\alpha \frac{\partial \varphi}{\partial t} + \beta^2 \varphi = \frac{\partial^2 \varphi}{\partial x^2} + g(x,t), \qquad (x,t) \in [0,1] \times [0,T] \tag{7.37}$$

under the following types of initial constraints

$$\varphi(x,0) = x^2, \quad \frac{\partial \varphi}{\partial t}(x,0) = 1 \quad , \; x \in [0,1] \tag{7.38}$$

and the boundary constraints

$$\varphi(0,t) = t\,, \;\; \varphi(1,t) = 1 + t \quad \forall \;\; t \in [0,T] \tag{7.39}$$

with $\alpha = 1$, $\beta = 1$ and $g(x,t) = x^2 + t - 1$ and $\varphi(x,t)$ is the unknown function whose value is to be determined.

The solution obtained from the existing literature for Exp.no.7.3 is $\varphi(x,t) = x^2 + t$.

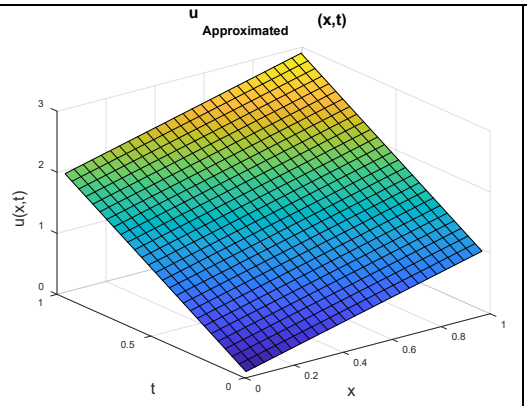

Figure 7.3a

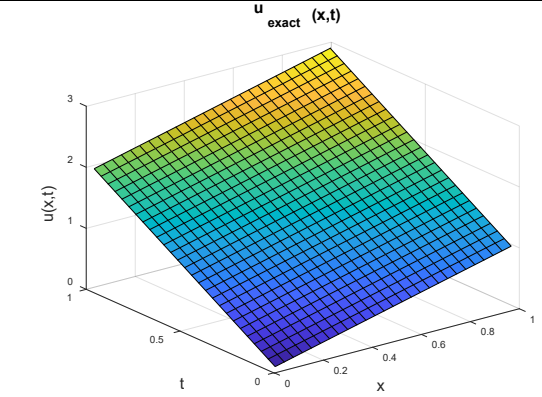

Figure 7.3b

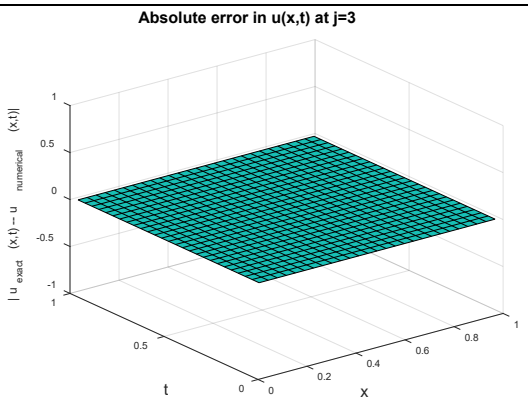

Figure 7.3c

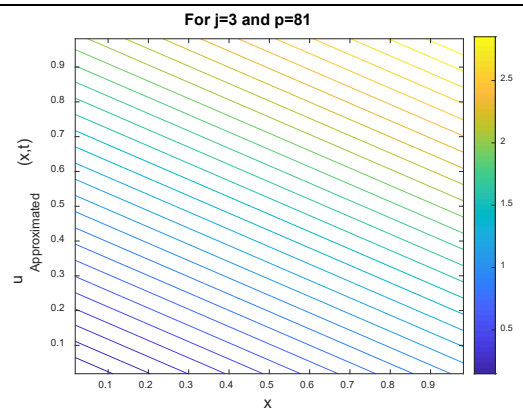

Figure 7.3d

Figure 7.3: Graphical representation of Approximate solution(Figure 7.3a), Exact solution(Figure 7.3b), Absolute error(Figure 7.3c), and contour view of the approx. solution (Figure 7.3d) in the solution of Numerical Experiment No.7.3.

It is shown in Table 7.5 and Figure 7.3 that results achieved with the proposed technique are exactly matching with the exact solution with no error. Figure 7.3 explains the high level of agreement between the exact and approximated solution.

Getting high accuracy for a small number of grid points makes it a strong solver for these kinds of mathematical models.

Table 7.5: Comparison of results achieved for Numerical Experiment No.7.3. with Exact

solution

x	t	Approximate Solution	Exact solution	Absolute error
0.1	0.1	0.3	0.3	0
0.2	0.2	0.6	0.6	0
0.3	0.3	0.9	0.9	0
0.4	0.4	1.2	1.2	0
0.5	0.5	1.5	1.5	0
0.6	0.6	1.8	1.8	0
0.7	0.7	2.1	2.1	0
0.8	0.8	2.4	2.4	0
0.9	0.9	2.7	2.7	0

7.6 Conclusion

After looking at the results of numerical experiments performed on three numerical Experiments with the proposed technique, we infer that 1D- hyperbolic Telegraph equations of second order can easily be solved by the proposed scheme with less computational cost and high accuracy. Level of accuracy obtained is or order 10^{-4} for only 9 colocation points in the first iteration is a noteworthy achievement for these kinds of equations. Moreover, the use of common MATLAB subprograms to solve various types of Telegraph equations, makes it more computer-friendly. Very good accuracy is obtained for a very small number of collocation points makes the proposed scheme a strong solver for these kinds of differential equations. Therefore, by looking at the performance of the method, we conclude that the given method can be extended to solve another set of differential equations. All the calculations have been performed using MATLAB 7 software installed on system with 4gb ram and intel core i3 processor .

Chapter 8

A Hybrid Scheme Based Upon θ −Weighted Differencing and Haar Scale 3 Wavelets for the Approximate Solution of (2+1)-dimensional Partial Differential Equations.

8.1 Introduction

To study the dynamics of any real-time phenomenon happening around us, one of the most accurate approaches is by using a mathematical model of it. It is said that where there is a motion there is a differential equation corresponding to it. Mathematical modeling for a majority of real-time phenomena results in a partial differential equation. Partial differential equations are playing a very important role in predicting the world around us. It can be seen in the literature that the numbers of a phenomenon in science and technology have been studied via linear or non-linear partial differential equations. Most of the partial differential equations do not possess any closed-form solution. Moreover, finding the solution of such equations become more challenging when there are nonlinearities in the equations.

The main purpose of our study is to introduce a new hybrid scheme based upon the θ −weighted differencing and Haar scale 3 (non-dyadic) wavelets for the solution of following types of two-dimensional partial differential equations given in Equation (8.1)

$$\varphi_t - (\Delta\varphi)_t - \alpha\Delta\varphi + \beta\,\nabla\varphi + \gamma\,\nabla.(\varphi\nabla\varphi) + \delta\varphi^2 = \mu\,\nabla.\big(F(\varphi)\big) + f\,(x,y,t), (x,y)\ \in \Omega, t\ >\ 0 \tag{8.1}$$

subjected to initial and boundary constraints are given in Equations (8.2) and (8.3)

$$\varphi(x,y,0) = g(x,y) \qquad \forall\,(x,y) \in\ \Omega \tag{8.2}$$

$$\varphi(x,y,t) = h(x,y,t) \qquad \forall\,(x,y) \in \partial\Omega, \mathrm{t} \in [0,T] \tag{8.3}$$

where Ω is any closed and bounded domain contained in $\mathcal{R}^2$ with smooth or piecewise smooth boundary represented by $\partial\Omega$. $F(\varphi)$ is a non-linear function of φ , $f\,(x,y,t)$, is the source term and α , β , γ, δ, μ are the real constants. In the present study, we will restrict ourselves to the following special cases of the Equation (8.1) under the boundary and initial constraints represented by Equations (8.2) and (8.3).

Case 1: On taking $\alpha = 1$, $\beta = 1$, $\gamma = 0, \delta = 0, \mu = 1$, Equation (8.1) reduced to

$$\varphi_t - (\Delta\varphi)_t - \Delta\varphi + \nabla\varphi = \nabla.\big(F(\varphi)\big) + f\,(x,y,t), (x,y) \in \Omega, t > 0 \tag{8.4}$$

which is known as NBBMB (non-linear Benjamin Bona Mahony Burgers) equation.

Case 2: On taking $\alpha = 0$, $\beta = 0$, $\gamma = -1, \delta = \pi^2, \mu = 0$, Equation (8.1) reduced to

$$\varphi_t - (\Delta\varphi)_t - \nabla.(\varphi\nabla\varphi) + \pi^2\varphi^2 = +f\,(x,y,t), (x,y) \in \Omega, t > 0 \tag{8.5}$$

which is known as a non-linear Sobolev equation.

Case 3: On taking $\alpha = 1$, $\beta = 0$, $\gamma = 0, \delta = 0, \mu = 0$,Equation no.(8.1) reduced to

$$\varphi_t - (\Delta\varphi)_t - \Delta\varphi = f\,(x,y,t), \qquad (x,y) \in \Omega, t > 0 \tag{8.6}$$

which is known as linear Sobolev equation.

Sobolev equations belong to the important class of partial differential equations in which the highest order derivative present in the differential equation contains mixed derivative with respect to time and space. These types of equations have a convincing physical background because of its huge use in Soil moisture migration [195], drainage of liquids through rocks having cracks [196], heat conduction Continuum Mechanics[197], etc. On the same platform, the BBMB equation appeared in the analysis of wave propagation in different mediums like surface waves with a long wavelength in liquids, Acoustic waves in harmonic crystals, Acoustic-gravity waves in incompressible fluids, Hydromagnetic waves in a cold plasma, etc[198]. The extensive appearance of these kinds of equations in the mathematical modeling of different phenomena occurring in science and technology have gained the attention of the scientific community. But the closed form solution of these kinds of equations has yet not been established and even very cumbersome to achieve. Therefore, many

researchers are involved in developing the various numerical and semi-analytic schemes for finding solutions to the different problems governed by these differential equations. Some of the methods which have been recently developed and applied to solve the two-dimensional Sobolev and BBMB equations are Expanded Mixed Finite Element Method (EMFEM)[199], Local Discontinuous Galerkin Method (LDGM)[200], Collocation Spectral Method (CSM)[201], Crank-Nicolson Finite Volume Element Method(CNFVM) [202], Haar Wavelet Method[73], etc.

But the study of establishing the solution for (2+1) dimensional partial differential equations using the Haar scale 3 (non-dyadic) wavelets has not been attempted in the literature which motivated us to develop a new technique for the solution of these types of equations. Orthonormal wavelets are one of the modernistic functions which have the capability of dilation and translation. Because of these properties, numerical techniques that involve wavelet bases are showing the qualitative improvement in contrast with other methods. In literature, dyadic wavelets are in preponderance. In 1995, Chui and Lian [115] has developed the Haar scale 3 (non-dyadic) wavelets by using the process of multiresolution analysis. In 2018, Mittal and Pandit have used the Haar scale 3 (non-dyadic) wavelets [71], [141], [142], [194] for solving the various types of differential equations and found that these wavelet bases are equally competent in solving the various types of mathematical models governed by differential equations. Also, it was shown by them that the Haar scale 3 (non-dyadic) wavelet has a faster rate of convergence as compared to the Haar scale 2 dyadic wavelets. This gives us good hope of getting a better solver for these equations by developing a new hybrid technique based upon θ −Weighted Differencing and Haar scale 3 (non-dyadic) Wavelets for the solution of (2+1) dimensional partial differential equations.

This chapter follows the sequence of sections as described: In section 2, explicit forms of Haar scale 3 (non-dyadic) parent wavelets with their families and procedure to find their integrals have been explained briefly. Representation of the solution using Haar scale 3 (non-dyadic) wavelets is explained in section 3. Section 4 explains the method of solution using Haar scale 3 (non-dyadic) wavelets. In section 5, the convergence of the method is discussed. In section 6, solutions of three different (2+1)-dimensional partial differential Equations are produced using the present method to analyze the

efficiency and performance of the present method. In section 7, the conclusion drawn from the results and in future research ideas is given.

8.2 Explicit forms of Haar scale 3 Wavelets and their integrals

The mathematical expressions for Haar scale 3 (non-dyadic) wavelet family with dilation factor three [71], [115] are given below

$$h_i(t) = \varphi(t) = \begin{cases} 1 & 0 \le t < 1 \\ 0 & elsewhere \end{cases} \qquad for\ i = 1 \tag{8.7}$$

$$h_i(t) = \psi^1(3^j t - k) = \frac{1}{\sqrt{2}} \begin{cases} -1 & \varkappa_1(i) \le t < \varkappa_2(i) \\ 2 & \varkappa_2(i) \le t < \varkappa_3(i) \\ -1 & \varkappa_3(i) \le t < \varkappa_4(i) \\ 0 & elsewhere \end{cases}, \quad for \quad i = 2,4, \dots 3p-1 \tag{8.8}$$

$$h_i(t) = \psi^2(3^j t - k) = \sqrt{\frac{3}{2}} \begin{cases} 1 & \varkappa_1(i) \le t < \varkappa_2(i) \\ 0 & \varkappa_2(i) \le t < \varkappa_3(i) \\ -1 & \varkappa_3(i) \le t < \varkappa_4(i) \\ 0 & elsewhere \end{cases}, \quad for \quad i = 3,6, \dots 3p \tag{8.9}$$

where $\varkappa_1(i) = \frac{k}{p}$, $\varkappa_2(i) = \frac{3k+1}{3p}$, $\varkappa_3(i) = \frac{(3k+2)}{3p}$, $\varkappa_4(i) = \frac{k+1}{p}$, $p = 3^j$, $j = 0,1,2, \dots$, $k = 0,1,2, \dots, p-1$. Here i , j , k respectively represent the wavelet number, level of resolution (dilation), and translation parameters of wavelet family.

The values of $i\ (for\ i > 1)$can be calculated with the help of j , k by using the following relations $\begin{Bmatrix} i - 1 = 3^j + 2k & for\ even\ i \\ i - 2 = 3^j + 2k & for\ odd\ i \end{Bmatrix}$. By using this relation for different dilation and translations of $h_2(t)$, $h_3(t)$, we will get the wavelet family as $h_1(t)$, $h_2(t)$, $h_3(t), h_4(t), h_5(t), h_6(t), \dots$ where $h_2(t)$ and $h_3(t)$ are also called mother wavelets and rest all the wavelets which we have obtained from mother wavelet are called daughter wavelets.

The main difference which makes the Haar scale 3 (non-dyadic) wavelets better than the Haar scale 2 dyadic wavelets is that only one mother wavelet is responsible for the

construction of whole dyadic wavelet family but in case of Haar scale 3 (non-dyadic) wavelets, two mother wavelets with different shapes are responsible for the construction of the whole family. Because of this fact, Haar scale 3 (non-dyadic) wavelets increase the convergence rate of the solution.

Now one can easily integrate the equations (8.7)-(8.9) the desired number of times over the interval [A, B) by using Riemann Liouville Integral formula as given below

$$q_{m,i}(t) = \int_0^t \int_0^t \int_0^t \cdots\cdots m\ times \cdots\cdots \int_0^t h_i(x)(dx)^m = \frac{1}{(m-1)!}\int_0^t (t-x)^{m-1} h_i(x)dx\ ,\quad m = 1,2,3 \ldots\ldots\ldots\ ,\ i = 1,2,3, \ldots\ldots\ldots 3p \tag{8.10}$$

After evaluating the above integrals for Equation (8.7), we get Equation (8.11)

$$q_{\beta,i}(t) = \frac{t^m}{m!} \quad for \quad i = 1 \tag{8.11}$$

Using Equation (8.10) on Equation (8.8), we get the values of $q_{m,i}(t)'s \quad for \quad i = 2,4,6,8,\cdots,3p-1$ which are given by Equation (8.12)

$$q_{m,i}(t) = \frac{1}{\sqrt{2}}\begin{cases} 0 & for \quad 0 \le t \le \varkappa_1(i) \\ \frac{-1}{m!}\left(t-\varkappa_1(i)\right)^m & for \quad \varkappa_1(i) \le t \le \varkappa_2(i) \\ \frac{1}{m!}\left[-\left(t-\varkappa_1(i)\right)^m + 3\left(t-\varkappa_2(i)\right)^m\right] & for \quad \varkappa_2(i) \le t \le \varkappa_3(i) \\ \frac{1}{m!}\left[-\left(t-\varkappa_1(i)\right)^m + 3\left(t-\varkappa_2(i)\right)^m - 3\left(t-\varkappa_3(i)\right)^m\right] & for\ \varkappa_3(i) \le t \le \varkappa_4(i) \\ \frac{1}{m!}\left[-\left(t-\varkappa_1(i)\right)^m + 3\left(t-\varkappa_2(i)\right)^m - 3\left(t-\varkappa_3(i)\right)^m + \left(t-\varkappa_4(i)\right)^m\right] & for\ \varkappa_4(i) \le t \le 1 \end{cases} \tag{8.12}$$

Using Equation (8.10) on Equation (8.9), we get the values of $q_{m,i}(t)'s \quad for \quad i = 3,5,7,9,\cdots,3p$ which are given by Equation (8.13)

$$q_{m,i}(t) = \sqrt{\frac{3}{2}}\begin{cases} 0 & for \quad 0 \le t \le \varkappa_1(i) \\ \frac{1}{m!}\left(t-\varkappa_1(i)\right)^m & for \quad \varkappa_1(i) \le t \le \varkappa_2(i) \\ \frac{1}{m!}\left[\left(t-\varkappa_1(i)\right)^m - \left(t-\varkappa_2(i)\right)^m\right] & for \quad \varkappa_2(i) \le t \le \varkappa_3(i) \\ \frac{1}{m!}\left[\left(t-\varkappa_1(i)\right)^m - \left(t-\varkappa_2(i)\right)^m - \left(t-\varkappa_3(i)\right)^m\right] & for \quad \varkappa_3(i) \le t \le \varkappa_4(i) \\ \frac{1}{m!}\left[\left(t-\varkappa_1(i)\right)^m - \left(t-\varkappa_2(i)\right)^m - \left(t-\varkappa_3(i)\right)^m + \left(t-\varkappa_4(i)\right)^m\right] & for\ \varkappa_4(i) \le t \le 1 \end{cases} \tag{8.13}$$

8.3 Approximation of solution

Using the properties of Haar scale 3 (non-dyadic) wavelets as explained in section 3, any function $x(t) \in L_2(R)$ can be expressed as an infinite series of Haar scale 3 (non-dyadic) wavelet bases as given in Equation (8.14)

$$u(t) = \sum_{i=0}^{\infty} a_i h_i(t)$$
$$= a_1 h_1(t) + \sum_{even\ i} a_i \psi^1(3^j t - k) + \sum_{odd\ i>1} a_i \psi^2(3^j t - k) \quad (8.14)$$

Here $a_i's$ are the wavelet coefficients whose values are to be determined by the proposed method. But for computational purposes, one can consider a finite number of terms. By considering the first $3p$ terms to approximate the function $u(t)$ we get Equation (8.15)

$$u(t) \approx u_{3p} = \sum_{i=0}^{3p} a_i h_i(t) \quad (8.15)$$

where $p = 3^j$, $j = 0,1,2, \ldots$

8.4 Description of Proposed Scheme

This section is used to describe the procedure involved in the proposed scheme for getting the solution to the concerned problems. To make the explanation of the process simple and easy to understand, we are considering the linear case of Equation (8.1) as given by Equation (8.16)

$$\varphi_t - (\Delta\varphi)_t - \Delta\varphi = f\ (x, y, t), \qquad (x, y)\ \in \Omega, t\ >\ 0 \quad (8.16)$$

Using the θ −weighted finite differencing scheme for time discretization, Equation (8.16) becomes

$$(\varphi - \Delta\varphi)_{t=t_{n+1}} - (\varphi - \Delta\varphi)_{t=t_n} = \Delta t \left(\theta\left(\Delta\varphi - f\ (x, y, t)\right)_{t=t_{n+1}} + (1 - \theta)(\Delta\varphi - f\ (x, y, t))_{t=t_n}\right) \quad (8.17)$$

After simplifications Equation (8.17) results in Equation (8.18)

$$\varphi^{n+1} - (1 + \theta\Delta t)\left(\varphi_{xx}^{n+1} + \varphi_{yy}^{n+1}\right) = \varphi^n - (1 - (1 - \theta)\Delta t)\left(\varphi_{xx}^n + \varphi_{yy}^n\right) + (1 - \theta)\Delta t\ f^n + \theta\Delta t\ f^{n+1} \quad (8.18)$$

subjected to initial and boundary constraints given in Equation (8.19)

$$\varphi(x,y,0) = g(x,y) \qquad \forall\,(x,y) \in \Omega,$$
$$\varphi^n(x,y,t) = h(x,y,t_n) \quad \forall\,(x,y) \in \partial\Omega, \mathrm{t} \in [0,T], \quad n = 1,2,3 \ldots \tag{8.19}$$
$$\text{where } \varphi^n = \varphi(x,y,t_n)\,,\ f^n = f(x,y,t_n)\ \,, \Omega = [0.1] \times [0.1]$$

Now space variables are discretized with the help of two dimensional Haar scale 3 (non-dyadic) wavelets as explained below

$$\varphi_{xxyy}^{n+1}(x,y) = \sum_{i=1}^{3p}\sum_{l=1}^{3p} a_{il}^{n+1} h_i(x)\, h_l(y) \tag{8.20}$$

Integrating Equation (8.20) w.r.t x within the domain 0 to x , equation (8.20) leads to

$$\varphi_{xyy}^{n+1}(x,y) = \sum_{i=1}^{3p}\sum_{l=1}^{3p} a_{il}^{n+1} q_{i,1}(x)\, h_l(y) + \varphi_{xyy}^{n+1}(0,y) \tag{8.21}$$

Now by integrating the Equation (8.21) w.r.t x within the domain 0 to 1, the value of $\varphi_{xyy}^{j+1}(0,y)$ is given by

$$\varphi_{xyy}^{n+1}(0,y) = \varphi_{yy}^{n+1}(1,y) - \varphi_{yy}^{n+1}(0,y) - \sum_{i=1}^{3p}\sum_{l=1}^{3p} a_{il}^{n+1} q_{i,2}(1)\, h_l(y) \tag{8.22}$$

Now using Equation(8.22),Equation (8.21) becomes

$$\varphi_{xyy}^{n+1}(x,y) = \sum_{i=1}^{3p}\sum_{l=1}^{3p} a_{il}^{n+1} \left(q_{i,1}(x) - q_{i,2}(1)\right)\, h_l(y) + \varphi_{yy}^{n+1}(1,y) - \varphi_{yy}^{n+1}(0,y) \tag{8.23}$$

Again, integrating the Equation (8.23) w.r.t x within the limits we get

$$\varphi_{yy}^{n+1}(x,y) = \sum_{i=1}^{3p}\sum_{l=1}^{3p} a_{il}^{n+1} \left(q_{i,2}(x) - x\, q_{i,2}(1)\right)\, h_l(y) + x\, \varphi_{yy}^{n+1}(1,y) + (1-x)\varphi_{yy}^{n+1}(0,y) \tag{8.24}$$

Integrate the Equation (8.24) w.r.t y within the limits 0 to y we get

$$\varphi_{y}^{n+1}(x,y) = \textstyle\sum_{i=1}^{3p}\sum_{l=1}^{3p} a_{il}^{n+1} \left(q_{i,2}(x) - x\, q_{i,2}(1)\right) q_{l,1}(y) + x\, \left(\varphi_{y}^{n+1}(1,y) - \varphi_{y}^{n+1}(1,0)\right) + (1-x)\left(\varphi_{y}^{n+1}(0,y) - \varphi_{y}^{n+1}(0,0)\right) + \varphi_{y}^{n+1}(x,0) \tag{8.25}$$

$$\varphi_y^{n+1}(x,0) = \left(\varphi^{n+1}(x,1) - \varphi^{n+1}(x,0)\right) - \sum_{i=1}^{3p}\sum_{l=1}^{3p} a_{il}^{n+1}\left(q_{i,2}(x) - x\, q_{i,2}(1)\right) q_{l,2}(1) - x\left(\varphi^{n+1}(1,1) - \varphi^{n+1}(1,0)\right) + x\varphi^{n+1}(1,0) - (1-x)\left(\varphi^{n+1}(0,1) - \varphi^{n+1}(0,0)\right) + (1-x)\varphi_y^{n+1}(0,0) \tag{8.26}$$

$$\varphi_y^{n+1}(x,y) = \sum_{i=1}^{3p}\sum_{l=1}^{3p} a_{il}^{n+1}\left(q_{i,2}(x) - x\, q_{i,2}(1)\right)\left(q_{l,1}(y) - q_{l,2}(1)\right) + x\ \varphi_y^{n+1}(1,y) + (1-x)\,\varphi_y^{n+1}(0,y) + \left(\varphi^{n+1}(x,1) - \varphi^{n+1}(x,0)\right) - x\left(\varphi^{n+1}(1,1) - \varphi^{n+1}(1,0)\right) - (1-x)\left(\varphi^{n+1}(0,1) - \varphi^{n+1}(0,0)\right) \tag{8.27}$$

Integrate the Equation (8.27) w.r.t y within the limits 0 to y we get Equation (8.28)

$$\varphi^{n+1}(x,y) = \sum_{i=1}^{3p}\sum_{l=1}^{3p} a_{il}^{n+1}\left(q_{i,2}(x) - x\, q_{i,2}(1)\right)\left(q_{l,2}(y) - y q_{l,2}(y)\right) + x\left(\varphi^{n+1}(1,y) - \varphi^{n+1}(1,0)\right) + (1-x)\left(\varphi^{n+1}(0,y) - \varphi^{n+1}(0,0)\right) + y\left(\varphi^{n+1}(x,1) - \varphi^{n+1}(x,0)\right) - xy\left(\varphi^{n+1}(1,1) - \varphi^{n+1}(1,0)\right) - (1-x)y\left(\varphi^{n+1}(0,1) - \varphi^{n+1}(0,0)\right) + \varphi^{n+1}(x,0) \tag{8.28}$$

Similarly, by using the same procedure the expression for φ_{xx}^{j+1}, φ_x^{j+1} can be obtained as given in Equations (8.29) and (8.30).

$$\varphi_{xx}^{n+1}(x,y) = \sum_{i=1}^{3p}\sum_{l=1}^{3p} a_{il}\ h_i(x)\left(q_{l,2}(y) - y\, q_{l,2}(1)\right) + y\,\varphi_{xx}^{n+1}(x,1) + (1-y)\varphi_{xx}^{n+1}(x,0) \tag{8.29}$$

$$\varphi_x^{n+1}(x,y) = \sum_{i=1}^{3p}\sum_{l=1}^{3p} a_{il}^{n+1}\left(q_{i,1}(x) - q_{i,2}(1)\right)\left(q_{l,2}(y) - y\, q_{l,2}(1)\right) + y\ \varphi_x^{n+1}(x,1) + (1-y)\,\varphi_x^{n+1}(x,0) + \left(\varphi^{n+1}(1,y) - \varphi^{n+1}(0,y)\right) - y\left(\varphi^{n+1}(1,1) - \varphi^{n+1}(0,1)\right) - (1-y)\left(\varphi^{n+1}(1,0) - \varphi^{n+1}(0,0)\right) \tag{8.30}$$

Substituting all the above-calculated value in Equation (8.18), it becomes

$$\sum_{i=1}^{3p}\sum_{l=1}^{3p} a_{il}^{n+1}\left(q_{i,2}(x)-x\,q_{i,2}(1)\right)\left(q_{l,1}(y)-q_{l,2}(1)\right)-(1+\theta\Delta t)\Big(\,h_i(x)\left(q_{l,2}(y)-y\,q_{l,2}(1)\right)+\left(q_{i,2}(x)-x\,q_{i,2}(1)\right)\,h_l(y)\Big)=\left(\varphi^{n}-(1-(1-\theta)\Delta t)\left(\varphi_{xx}^{n}+\varphi_{yy}^{n}\right)+(1-\theta)\Delta t\,f^{n}+\theta\Delta t\,f^{n+1}\right)+(1+\theta\Delta t)\Big(y\,\varphi_{xx}^{n+1}(x,1)+(1-y)\varphi_{xx}^{n+1}(x,0)+x\,\varphi_{yy}^{n+1}(1,y)+(1-x)\varphi_{yy}^{n+1}(0,y)\Big)-\left(x\left(\varphi^{n+1}(1,y)-\varphi^{n+1}(1,0)\right)+(1-x)\left(\varphi^{n+1}(0,y)-\varphi^{n+1}(0,0)\right)+y\left(\varphi^{n+1}(x,1)-\varphi^{n+1}(x,0)\right)-xy\left(\varphi^{n+1}(1,1)-\varphi^{n+1}(1,0)\right)-(1-x)y\left(\varphi^{n+1}(0,1)-\varphi^{n+1}(0,0)\right)+\varphi^{n+1}(x,0)\right) \tag{8.31}$$

Now using the boundary constraints and discretizing the space variable as $x \to x_r$, $y \to y_s$ where $x_r=\frac{2r-1}{6p}$, $y_s=\frac{2s-1}{6p}$, $r,s=1,2,\ldots\ldots 3p$ in the equation (8.31) we get the following system of algebraic equations as given in Equation (8.32)

$$\sum_{i=1}^{3p}\sum_{l=1}^{3p} a_{il}^{n+1}\,R_{i,l,r,s}=F(r,s) \tag{8.32}$$

$$R_{i,l,r,s}=\left(q_{i,2}(x_r)-x_r\,q_{i,2}(1)\right)\left(q_{l,1}(y_s)-q_{l,2}(1)\right)-(1+\theta\Delta t)\Big(\,h_i(x_r)\left(q_{l,2}(y_s)-y\,q_{l,2}(1)\right)+\left(q_{i,2}(x_r)-x_r\,q_{i,2}(1)\right)\,h_l(y_s)\Big)\qquad \forall\, i,j \tag{8.33}$$

$$F(r,s)=\left(\varphi^{n}(x_r,y_s)-(1-(1-\theta)\Delta t)\left(\varphi_{xx}^{n}(x_r,y_s)+\varphi_{yy}^{n}(x_r,y_s)\right)+(1-\theta)\Delta t\,f^{n}(x_r,y_s)+\theta\Delta t\,f^{n+1}(x_r,y_s)\right)+(1+\theta\Delta t)\Big(y_s\,\varphi_{xx}^{n+1}(x_r,1)+(1-y_s)\varphi_{xx}^{n+1}(x_r,0)+x\,\varphi_{yy}^{n+1}(1,y_s)+(1-x_r)\varphi_{yy}^{n+1}(0,y_s)\Big)-\left(x_r\left(\varphi^{n+1}(1,y_s)-\varphi^{n+1}(1,0)\right)+(1-x_r)\left(\varphi^{n+1}(0,y_s)-\varphi^{n+1}(0,0)\right)+y_s\left(\varphi^{n+1}(x_r,1)-\varphi^{n+1}(x_r,0)\right)-x_r y_s\left(\varphi^{n+1}(1,1)-\varphi^{n+1}(1,0)\right)-(1-x_r)y_s\left(\varphi^{n+1}(0,1)-\varphi^{n+1}(0,0)\right)+\varphi^{n+1}(x_r,0)\right) \tag{8.34}$$

The above system reduced to the system of algebraic equations (Equation 8.34) and further, it gets reduced to the following system of 4D-arrays (Equation 8.35)

$$A_{3p\times 3p}R_{3p\times 3p\times 3p\times 3p} = F_{3p\times 3p} \tag{8.35}$$

Further, the above 4D-arrays system is reduced to the following 2D-matrix system (Equation (8.35)) using the transformations $a_{il}^{n+1} = b_{\lambda}^{n+1}$ and $F_{rs} = G_{\mu}$

$$B_{1\times(3p)^2}S_{(3p)^2\times(3p)^2} = G_{1\times(3p)^2} \tag{8.36}$$

where $\lambda = 3p(i-1) + l$ and $\mu = 3p(r-1) + s$

Then the values of b_{λ}^{n+1} can be calculated successively for different values of n=1,2… by solving the above system of equation using the Thomas algorithm via MATLAB Program. Original wavelet coefficients a_{il}^{n+1} can be restored using the above transformation. These coefficients will be used in the equations to determine the final solution of the problem) for different value of t_n for n= 0,1, 2..

8.5 Convergence of 2D-Haar Scale 3 Wavelets

In this section, the convergence of 2D-Haar Scale 3 Wavelets for the approximation of two dimentional unknown solution of the problem is discussed with detailed arguments by proving the following theorem

Theorem: If $u(x,y)\ \epsilon\ C^2([0,1]\times[0,1])$ be any square-integrable function such that $\left|\frac{\partial^2 u(x,y)}{\partial x \partial y}\right| \leq M, \forall\ x,y\epsilon[0,1]\times[0,1]$ and $u(x,y) = \sum_{i=1}^{\infty}\sum_{l=1}^{\infty} a_{il}h_i(x)h_l(y)$ .Then

$$\left\|E_{J,J'}\right\|^2 = \left\|u(x,y) - u_{3p,3p'}(x,y)\right\|^2$$
$$\leq \frac{M^2}{26^2}\left(\frac{1}{81}\times\frac{1}{p^3{p'}^3} + \left(\frac{47}{240}\right)\times\frac{1}{p^3} + \left(\frac{47}{240}\right)\times\frac{1}{{p'}^3}\right)$$

where $p = 3^J, J = 0,1,2,\ldots$; $p' = 3^{J'}, J' = 0,1,2,\ldots$ and J , J' are the different level of resolution for the wavelets families of $h_i(x)$, $h_l(y)$ respectively.

Proof: Let $u(x,y) = \sum_{i=1}^{\infty}\sum_{l=1}^{\infty} a_{il}h_i(x)h_l(y)$ be the exact solution and $u_{3p,3p'}(x,y) = \sum_{i=1}^{3p}\sum_{l=1}^{3p'} a_{il}h_i(x)h_l(y)$ be the approximated solution

Now the error in approximating the solution by two dimensional Haar scale 3 (non-dyadic) wavelets is represented by the Equation (8.37)

$$E_{J,J'} = u(x,y) - u_{3p,3p'}(x,y) = \sum_{i=3p+1}^{\infty}\sum_{l=3p'+1}^{\infty} a_{il}h_i(x)h_l(y) + \sum_{i=3p+1}^{\infty}\sum_{l=1}^{3p'} a_{il}h_i(x)h_l(y) + \sum_{i=1}^{3p}\sum_{l=3p'+1}^{\infty} a_{il}h_i(x)h_j(y) = X + Y + Z \quad (8.37)$$

Where the values of X , Y and Z are given by the Equation (8.38)

$$X = \sum_{i=3p+1}^{\infty}\sum_{l=3p'+1}^{\infty} a_{il}h_i(x)h_l(y)\,, Y = \sum_{i=3p+1}^{\infty}\sum_{l=1}^{3p'} a_{il}h_i(x)h_l(y)\ , \quad Z = \sum_{i=1}^{3p}\sum_{l=3p'+1}^{\infty} a_{il}h_i(x)h_l(y) \quad (8.38)$$

$$\left\|E_{J,J'}\right\|^2 = \left\|u(x,y) - u_{3p,3p'}(x,y)\right\|^2 = \|X + Y + Z\,\|^2 = \langle\, X + Y + Z\ , X + Y + Z\rangle = \langle\, X\,, X\rangle + \langle\, Y\,, Y\rangle + \langle Z, Z\,\rangle + 2\langle\, X, Y\rangle + 2\langle\, Y, Z\rangle + 2\langle\, Z, X\rangle \quad (8.39)$$

Now

$$\langle\, X\,, X\rangle = \langle \sum_{i=3p+1}^{\infty}\sum_{l=3p'+1}^{\infty} a_{il}h_i(x)h_l(y)\ , \sum_{i=3p+1}^{\infty}\sum_{l=3p'+1}^{\infty} a_{il}h_i(x)h_l(y)\rangle$$

$$= \int_{-\infty}^{\infty}\int_{-\infty}^{\infty}\left(\sum_{i=3p+1}^{\infty}\sum_{l=3p'+1}^{\infty} a_{il}h_i(x)h_l(y)\right)\left(\sum_{i=3p+1}^{\infty}\sum_{l=3p'+1}^{\infty} a_{il}h_i(x)h_l(y)\right)dx\,dy$$

$$= \sum_{i=3p+1}^{\infty}\sum_{j=3p'+1}^{\infty}\sum_{k=3p+1}^{\infty}\sum_{l=3p'+1}^{\infty} a_{ij}a_{kl}\int_0^1 h_i(x)h_k(x)dx\int_0^1 h_j(y)h_l(y)dy \quad (8.40)$$

Now by using the orthogonal properties of Haar scale 3 (non-dyadic) wavelets on Equation (8.40), we get Equation (8.41)

$$\langle\, X\,, X\rangle = \sum_{i=3p+1}^{\infty}\sum_{l=3p'+1}^{\infty}\left(\frac{1}{3^J}a_{il}\right)\left(\frac{1}{3^{J'}}a_{il}\right) = \frac{1}{3^{J+J'}}\sum_{i=3p+1}^{\infty}\sum_{l=3p'+1}^{\infty} a_{il}^2 \quad (8.41)$$

where J and J'represent the level of resolutions at which solution is approximated

Similarly, by using the procedure discussed in Equation (8.40) and (8.41), we get Equation (8.42)

$$\langle\, Y\,, Y\rangle = \frac{1}{3^{J+J'}}\sum_{i=3p+1}^{\infty}\sum_{l=1}^{3p'} {a_{il}}^2\ ; \qquad \langle\, Z\,, Z\rangle = \frac{1}{3^{J+J'}}\sum_{i=1}^{3p}\sum_{l=3p'+1}^{\infty} {a_{il}}^2$$
$$\langle\, X\,, Y\rangle = \langle\, Y\,, Z\rangle = \langle\, Z, X\rangle = 0 \quad (8.42)$$

Now, Equation (8.39) becomes

$$\left\|E_{J,J'}\right\|^2 = \left(\sum_{i=3p+1}^{\infty}\sum_{l=3p'+1}^{\infty}\frac{1}{3^{J+J'}}a_{il}^2 + \sum_{i=3p+1}^{\infty}\sum_{l=1}^{3p'}\frac{1}{3^{J+J'}}a_{il}^2 + \sum_{i=1}^{3p}\sum_{l=3p'+1}^{\infty}\frac{1}{3^{J+J'}}a_{il}^2\right) \tag{8.43}$$

where a_{ij} is represented by Equation (8.44)

$$a_{ij} = 3^{\frac{J+J'}{2}}\int_0^1\int_0^1 h_i(x)h_l(y)u(x,y)dxdy = 3^{\frac{J}{2}}\int_0^1 h_i(x)\left(3^{\frac{J'}{2}}\int_0^1 h_l(y)\,u(x,y)\,dy\right)dx \tag{8.44}$$

where $h_i(x) = {\psi_i}^1(x) + {\psi_i}^2(x)$, $h_l(y) = {\psi_l}^1(y) + {\psi_l}^2(y)$

$$\int_0^1 h_l(y)\,u(x,y)dy = \int_0^1 {\psi_l}^1(y)\,u(x,y)dy + \int_0^1 {\psi_l}^2(y)\,u(x,y)dy$$
$$= \left(\int_{\varkappa_1(l)}^{\varkappa_2(l)}\frac{-1}{\sqrt{2}}u(x,y)dy + \int_{\varkappa_2(l)}^{\varkappa_3(l)}\sqrt{2}\,u(x,y)dy + \int_{\varkappa_3(l)}^{\varkappa_4(l)}\frac{-1}{\sqrt{2}}u(x,y)dy\right) + \tag{8.45}$$
$$\left(\int_{\varkappa_1(l)}^{\varkappa_2(l)}\frac{\sqrt{3}}{2}u(x,y)dy + \int_{\varkappa_3(l)}^{\varkappa_4(l)}\frac{-\sqrt{3}}{2}u(x,y)dy\right)$$

By applying the mean value theorem of integral on Equation (8.45), we get $\varepsilon_1 \in \left(\varkappa_1(l), \varkappa_2(l)\right)$, $\varepsilon_2 \in \left(\varkappa_2(l), \varkappa_3(l)\right)$, $\varepsilon_3 \in \left(\varkappa_3(l), \varkappa_4(l)\right)$ such that

$$\int_{\varkappa_1(l)}^{\varkappa_2(l)} u(x,y)dy = (\varkappa_2(l) - \varkappa_1(l))u(x,\varepsilon_1) = \frac{1}{3p'}\,u(x,\varepsilon_1)$$

$$\int_{\varkappa_2(l)}^{\varkappa_3(l)} u(x,y)dy = (\varkappa_3(l) - \varkappa_2(l))u(x,\varepsilon_2) = \frac{1}{3p'}\,u(x,\varepsilon_2)$$

$$\int_{\varkappa_3(l)}^{\varkappa_4(l)} u(x,y)dy = (\varkappa_4(l) - \varkappa_3(l))u(x,\varepsilon_3) = \frac{1}{3p'}\,u(x,\varepsilon_3)$$

Now equation (8.45) results into (8.46)

$$\int_0^1 h_l(y)\,u(x,y)dx = \frac{1}{3p'}\left(\left(\frac{\sqrt{3}-1}{\sqrt{2}}\right)u(x,\varepsilon_1) + \sqrt{2}u(x,\varepsilon_2) - \left(\frac{\sqrt{3}+1}{\sqrt{2}}\right)u(x,\varepsilon_3)\right)$$

$$= \frac{1}{3p'}\left(\left(\frac{\sqrt{3}-1}{\sqrt{2}}\right)u(x,\varepsilon_1) + \left(\frac{1+1}{\sqrt{2}}\right)u(x,\varepsilon_2) - \left(\frac{\sqrt{3}+1}{\sqrt{2}}\right)u(x,\varepsilon_3)\right)$$

$$\int_0^1 h_l(y)\,u(x,y)dx = \frac{1}{3p'}\left(\sqrt{\frac{3}{2}}\left(u(x,\varepsilon_1) - u(x,\varepsilon_3)\right) + \frac{1}{\sqrt{2}}\left(u(x,\varepsilon_2) - u(x,\varepsilon_1)\right) + \frac{1}{\sqrt{2}}\left(u(x,\varepsilon_2) - u(x,\varepsilon_3)\right)\right) \tag{8.46}$$

By applying the Lagrange mean value theorem on Equation (8.46), we get $\varepsilon_a \in (\varepsilon_1 , \varepsilon_3) , \varepsilon_b \in (\varepsilon_1, \varepsilon_2), \varepsilon_c \in (\varepsilon_2 , \varepsilon_3)$ such that

$$\int_0^1 h_l(y)\, u(x,y)dx = \frac{1}{3p'}\left(\sqrt{\frac{3}{2}}\,(\varepsilon_1-\varepsilon_3)\frac{\partial u}{\partial y}(x,\varepsilon_a) + \frac{1}{\sqrt{2}}(\varepsilon_2-\varepsilon_1)\frac{\partial u}{\partial y}(x,\varepsilon_b) + \frac{1}{\sqrt{2}}(\varepsilon_2-\varepsilon_3)\frac{\partial u}{\partial y}(x,\varepsilon_c)\right) \tag{8.47}$$

From Equation (8.47), Equation (8.44) becomes

$$a_{ij} = 3^{\frac{J+J'}{2}}\int_0^1 h_i(x)\left(\int_0^1 h_j(y)\, u(x,y)\, dy\right)dx$$

$$= 3^{\frac{J}{2}}\int_0^1 \left({\psi_i}^1(x) + {\psi_i}^2(x)\right)\left(3^{\frac{J'}{2}}\int_0^1 h_j(y)\, u(x,y)\, dy\right)dx$$

$$= \frac{3^{\frac{J+J'}{2}}}{3p'}\int_0^1 \left({\psi_i}^1(x) + {\psi_i}^2(x)\right)\left(\sqrt{\frac{3}{2}}\,(\varepsilon_1-\varepsilon_3)\frac{\partial u}{\partial y}(x,\varepsilon_a) + \frac{1}{\sqrt{2}}(\varepsilon_2-\varepsilon_1)\frac{\partial u}{\partial y}(x,\varepsilon_b) + \frac{1}{\sqrt{2}}(\varepsilon_2-\varepsilon_3)\frac{\partial u}{\partial y}(x,\varepsilon_c)\right)dx$$

$$= \frac{3^{\frac{J+J'}{2}}}{3p'}\left[\left(\sqrt{\frac{3}{2}}\,(\varepsilon_1-\varepsilon_3)\int_0^1 \left({\psi_i}^1(x) + {\psi_i}^2(x)\right)\frac{\partial u}{\partial y}(x,\varepsilon_a)dx + \frac{1}{\sqrt{2}}(\varepsilon_2-\varepsilon_1)\int_0^1 \left({\psi_i}^1(x) + {\psi_i}^2(x)\right)\frac{\partial u}{\partial y}(x,\varepsilon_b)dx + \frac{1}{\sqrt{2}}(\varepsilon_2-\varepsilon_3)\int_0^1 \left({\psi_i}^1(x) + {\psi_i}^2(x)\right)\frac{\partial u}{\partial y}(x,\varepsilon_b)dx\right)\right]$$

Which implies

$$a_{ij} = \frac{3^{\frac{J+J'}{2}}}{3p'}\left(\sqrt{\frac{3}{2}}\,(\varepsilon_1-\varepsilon_3)\left[\left(\int_{\varkappa_1(i)}^{\varkappa_2(i)}\frac{-1}{\sqrt{2}}\frac{\partial u}{\partial y}(x,\varepsilon_a)dx + \int_{\varkappa_2(i)}^{\varkappa_3(i)}\sqrt{2}\frac{\partial u}{\partial y}(x,\varepsilon_a)dx + \int_{\varkappa_3(i)}^{\varkappa_4(i)}\frac{-1}{\sqrt{2}}\frac{\partial u}{\partial y}(x,\varepsilon_a)dx\right) + \left(\int_{\varkappa_1(i)}^{\varkappa_2(i)}\frac{\sqrt{3}}{2}\frac{\partial u}{\partial y}(x,\varepsilon_a)dx + \int_{\varkappa_3(i)}^{\varkappa_4(i)}\frac{-\sqrt{3}}{2}\frac{\partial u}{\partial y}(x,\varepsilon_a)dx\right)\right] + \frac{1}{\sqrt{2}}(\varepsilon_2-\varepsilon_1)\left[\left(\int_{\varkappa_1(i)}^{\varkappa_2(i)}\frac{-1}{\sqrt{2}}\frac{\partial u}{\partial y}(x,\varepsilon_b)dx + \int_{\varkappa_2(i)}^{\varkappa_3(i)}\sqrt{2}\frac{\partial u}{\partial y}(x,\varepsilon_b)dx + \int_{\varkappa_3(i)}^{\varkappa_4(i)}\frac{-1}{\sqrt{2}}\frac{\partial u}{\partial y}(x,\varepsilon_b)dx\right) + \left(\int_{\varkappa_1(i)}^{\varkappa_2(i)}\frac{\sqrt{3}}{2}\frac{\partial u}{\partial y}(x,\varepsilon_b)dx + \int_{\varkappa_3(i)}^{\varkappa_4(i)}\frac{-\sqrt{3}}{2}\frac{\partial u}{\partial y}(x,\varepsilon_b)dx\right)\right] + \frac{1}{\sqrt{2}}(\varepsilon_2-\varepsilon_3)\left[\left(\int_{\varkappa_1(i)}^{\varkappa_2(i)}\frac{-1}{\sqrt{2}}\frac{\partial u}{\partial y}(x,\varepsilon_c)dx + \int_{\varkappa_2(i)}^{\varkappa_3(i)}\sqrt{2}\frac{\partial u}{\partial y}(x,\varepsilon_c)dx + \int_{\varkappa_3(i)}^{\varkappa_4(i)}\frac{-1}{\sqrt{2}}\frac{\partial u}{\partial y}(x,\varepsilon_c)dx\right) + \left(\int_{\varkappa_1(i)}^{\varkappa_2(i)}\frac{\sqrt{3}}{2}\frac{\partial u}{\partial y}(x,\varepsilon_c)dx + \int_{\varkappa_3(i)}^{\varkappa_4(i)}\frac{-\sqrt{3}}{2}\frac{\partial u}{\partial y}(x,\varepsilon_c)dx\right)\right]\right) \tag{8.48}$$

By applying the mean value theorems as applied above, Equation (8.48) becomes

$$a_{ij} = \frac{3^{\frac{J+J'}{2}}}{3p'}\left[\sqrt{\frac{3}{2}}\,(\varepsilon_1-\varepsilon_3)\left(\frac{1}{3p}\left(\sqrt{\frac{3}{2}}\,\left({\varepsilon_{a_1}}'-{\varepsilon_{a_3}}'\right)\frac{\partial^2 u}{\partial x\partial y}(\varepsilon_a',\varepsilon_a)+\right.\right.\right.$$

$$\left.\left.\left.\frac{1}{\sqrt{2}}\left({\varepsilon_{a_2}}'-{\varepsilon_{a_1}}'\right)\frac{\partial^2 u}{\partial x\partial y}(\varepsilon_a'',\varepsilon_a)+\frac{1}{\sqrt{2}}\left({\varepsilon_{a_2}}'-{\varepsilon_{a_3}}'\right)\frac{\partial^2 u}{\partial x\partial y}(\varepsilon_a''',\varepsilon_a\,)\right)\right)+\right.$$

$$\frac{1}{\sqrt{2}}(\varepsilon_2-\varepsilon_1)\left(\frac{1}{3p}\left(\sqrt{\frac{3}{2}}\,\left({\varepsilon_{b_1}}'-{\varepsilon_{b_3}}'\right)\frac{\partial^2 u}{\partial x\partial y}(\varepsilon_b',\varepsilon_b)+\frac{1}{\sqrt{2}}\left({\varepsilon_{b_2}}'-\right.\right.\right.$$

$$\left.\left.\left.{\varepsilon_{b_1}}'\right)\frac{\partial^2 u}{\partial x\partial y}(\varepsilon_b'',\varepsilon_b)+\frac{1}{\sqrt{2}}\left({\varepsilon_{b_2}}'-{\varepsilon_{b_3}}'\right)\frac{\partial^2 u}{\partial x\partial y}(\varepsilon_b''',\varepsilon_b\,)\right)\right)+\frac{1}{\sqrt{2}}(\varepsilon_2-$$

$$\varepsilon_3)\left(\frac{1}{3p}\left(\sqrt{\frac{3}{2}}\,\left({\varepsilon_{c_1}}'-{\varepsilon_{c_3}}'\right)\frac{\partial^2 u}{\partial x\partial y}(\varepsilon_c',\varepsilon_c)+\frac{1}{\sqrt{2}}\left({\varepsilon_{c_2}}'-{\varepsilon_{c_1}}'\right)\frac{\partial^2 u}{\partial x\partial y}(\varepsilon_c'',\varepsilon_c)+\right.\right.$$

$$\left.\left.\frac{1}{\sqrt{2}}\left({\varepsilon_{c_2}}'-{\varepsilon_{c_3}}'\right)\frac{\partial^2 u}{\partial x\partial y}(\varepsilon_c''',\varepsilon_c\,)\right)\right)\Bigg] \qquad (8.49)$$

Where

$${\varepsilon_{a_1}}',{\varepsilon_{b_1}}',{\varepsilon_{c_1}}' \in \left(\varkappa_1(i),\varkappa_2(i)\right),{\varepsilon_{a_2}}',{\varepsilon_{b_2}}',{\varepsilon_{c_2}}' \in \left(\varkappa_2(i),\varkappa_3(i)\right),{\varepsilon_{a_3}}',{\varepsilon_{b_3}}',{\varepsilon_{c_3}}'$$
$$\in \left(\varkappa_3(i),\varkappa_4(i)\right)$$

and

$$\varepsilon_a' \in \left({\varepsilon_{a_1}}',{\varepsilon_{a_3}}'\right),\varepsilon_a'' \in \left({\varepsilon_{a_1}}',{\varepsilon_{a_2}}'\right),\varepsilon_a''' \in \left({\varepsilon_{a_2}}',{\varepsilon_{a_3}}'\right),\ \varepsilon_b' \in \left({\varepsilon_{b_1}}',{\varepsilon_{b_3}}'\right),\varepsilon_a'' \in$$
$$\left({\varepsilon_{b_1}}',{\varepsilon_{b_2}}'\right),\varepsilon_a''' \in \left({\varepsilon_{b_2}}',{\varepsilon_{b_3}}'\right),\ \varepsilon_c' \in \left({\varepsilon_{c_1}}',{\varepsilon_{c_3}}'\right),\varepsilon_c'' \in \left({\varepsilon_{c_1}}',{\varepsilon_{c_2}}'\right),\varepsilon_c''' \in \left({\varepsilon_{c_2}}',{\varepsilon_{c_3}}'\right)$$

Now Equation (8.49) reduced into Equation (8.50)

$$a_{il} \le \frac{3^{\frac{J+J'}{2}}}{3p'}\left[\sqrt{\frac{3}{2}}\left(\frac{-1}{p'}\right)\left(\frac{1}{3p}\right)\left(\sqrt{\frac{3}{2}}\left(\frac{-1}{p}\right)M+\frac{1}{\sqrt{2}}\left(\frac{1}{3p}\right)M+\frac{1}{\sqrt{2}}\left(\frac{-1}{3p}\right)M\right)+\right.$$
$$\frac{1}{\sqrt{2}}\left(\frac{2}{3p'}\right)\left(\frac{1}{3p}\right)\left(\sqrt{\frac{3}{2}}\left(\frac{-1}{p}\right)M+\frac{1}{\sqrt{2}}\left(\frac{1}{3p}\right)M+\frac{1}{\sqrt{2}}\left(\frac{-1}{3p}\right)M\right)+ \qquad (8.50)$$
$$\left.\frac{1}{\sqrt{2}}\left(\frac{-2}{3p'}\right)\left(\frac{1}{3p}\right)\left(\sqrt{\frac{3}{2}}\left(\frac{-1}{p}\right)M+\frac{1}{\sqrt{2}}\left(\frac{1}{3p}\right)M+\frac{1}{\sqrt{2}}\left(\frac{-1}{3p}\right)M\right)\right]$$

After Simplifying Equation (8.50), we get Equation (8.51)

$$a_{il} \le \frac{3^{\frac{J+J'}{2}}}{3p'}\frac{M}{6p'p^2} = \frac{M}{2\times 3^2 \times p'^{\frac{3}{2}}p^{\frac{3}{2}}} \quad \Rightarrow \quad a_{il}^2 \le \frac{M^2}{4\times 3^4 \times p^3 p'^3} \tag{8.51}$$

$$= \frac{M^2}{4\times 3^4 \times 3^{3J}3^{3J'}}$$

Therefore

$$\sum_{i=3p+1}^{\infty}\sum_{l=3p'+1}^{\infty}\frac{1}{3^{J+J'}}a_{il}^2 \le \sum_{i=3p+1}^{\infty}\sum_{l=3p'+1}^{\infty}\frac{1}{3^{J+J'}}\times\frac{M^2}{4\times 3^4\times 3^{3J}3^{3J'}}$$

$$= \sum_{i=3p+1}^{\infty}\sum_{l=3p'+1}^{\infty}\frac{M^2}{4\times 3^{4J+4J'+4}}$$

$$= \frac{M^2}{4}\sum_{i=3p+1}^{\infty}\sum_{l=3p'+1}^{\infty}\frac{1}{3^{4J+4J'+4}} = \frac{M^2}{4}\sum_{i=3^{J+1}+1}^{\infty}3^{-4J-4}\sum_{l=3^{J'+1}+1}^{\infty}3^{-4J'}$$

$$= \frac{M^2}{4}\sum_{i=3^{J+1}+1}^{\infty}3^{-4J-4}\sum_{J'+1}^{\infty}\sum_{l=3^{J'}+1}^{3^{J'+1}}3^{-4J'}$$

$$= \frac{M^2}{4}\sum_{i=3^{J+1}+1}^{\infty}3^{-4J-4}\sum_{J'+1}^{\infty}\left(3^{J'+1}-3^{J'}\right)3^{-4J'} = \frac{M^2}{4}\times\frac{2}{3^4}\sum_{i=3^{J+1}+1}^{\infty}3^{-4J}\sum_{J'+1}^{\infty}3^{-3J'}$$

$$= \frac{M^2}{4}\frac{4}{3^4}\sum_{J+1}^{\infty}3^{-3J}\sum_{J'+1}^{\infty}3^{-3J'}\frac{M^2}{3^4}\times\left(\frac{1}{26}\times\frac{1}{3^{3J}}\right)\times\left(\frac{1}{26}\times\frac{1}{3^{3J}}\right) = \frac{M^2}{3^4\times 26^2}\times\frac{1}{p^3p'^3}$$

$$\sum_{i=3p+1}^{\infty}\sum_{l=3p'+1}^{\infty}\frac{1}{3^{J+J'}}a_{il}^2 \le \frac{M^2}{3^4\times 26^2}\times\frac{1}{p^3p'^3} \tag{8.52}$$

Now consider

$$\sum_{i=3p+1}^{\infty}\sum_{l=1}^{3p'}\frac{1}{3^{J+J'}}a_{il}^2 \le \frac{M^2}{4}\sum_{i=3p+1}^{\infty}\sum_{l=1}^{3p'}\frac{1}{3^{4J+4J'+4}} = \frac{M^2}{4}\sum_{i=3^{J+1}+1}^{\infty}3^{-4J-4}\sum_{l=1}^{3^{J'+1}}3^{-4J'}$$

$$= \frac{M^2}{4} \sum_{i=3^{J+1}+1}^{\infty} 3^{-4J-4} \sum_{0}^{J'} \sum_{l=3^{J'}}^{3^{J'+1}} 3^{-4J'}$$

$$= \frac{M^2}{4} \sum_{i=3^{J+1}+1}^{\infty} 3^{-4J-4} \sum_{0}^{J'} \left(3^{J'+1} - 3^{J'} + 1\right) 3^{-4J'}$$

$$= \frac{M^2}{4} \frac{1}{3^4} \sum_{i=3^{J+1}+1}^{\infty} 3^{-4J} \sum_{0}^{J'} \left(2.3^{-3J'} + 3^{-4J'}\right)$$

$$= \frac{M^2}{4} \frac{2}{3^4} \left(\frac{1}{26} \times \frac{1}{3^{3J}}\right) \left(\frac{54}{26}\left(1 - \frac{1}{3^{3j'+3}}\right) + \frac{81}{80}\left(1 - \frac{1}{3^{4j'+4}}\right)\right)$$

$$\leq \frac{M^2}{4} \frac{2}{3^4} \left(\frac{1}{26} \times \frac{1}{3^{3J}}\right) \left(\frac{1269}{1040}\right) = \frac{M^2}{26^2} \times \left(\frac{47}{240}\right) \times \frac{1}{p^3}$$

$$\sum_{i=3p+1}^{\infty} \sum_{l=1}^{3p'} \frac{1}{3^{J+J'}} a_{il}^2 \leq \frac{M^2}{26^2} \times \left(\frac{47}{240}\right) \times \frac{1}{p^3} \tag{8.53}$$

Similarly proceeding as above, we have

$$\sum_{i=1}^{3p} \sum_{l=3p'+1}^{\infty} \frac{1}{3^{J+J'}} a_{il}^2 \leq \frac{M^2}{26^2} \times \left(\frac{47}{240}\right) \times \frac{1}{p'^3} \tag{8.54}$$

Now using Equations (8.52)-(8.54), Equation (8.43) becomes

$$\left\|E_{J,J'}\right\|^2 = \left(\sum_{i=3p+1}^{\infty} \sum_{l=3p'+1}^{\infty} \frac{1}{3^{J+J'}} a_{il}^2 + \sum_{i=3p+1}^{\infty} \sum_{l=1}^{3p'} \frac{1}{3^{J+J'}} a_{il}^2 + \sum_{i=1}^{3p} \sum_{l=3p'+1}^{\infty} \frac{1}{3^{J+J'}} a_{il}^2 \right)$$

$$\leq \frac{M^2}{3^4 \times 26^2} \times \frac{1}{p^3 p'^3} + \frac{M^2}{26^2} \times \left(\frac{47}{240}\right) \times \frac{1}{p^3} + \frac{M^2}{26^2} \times \left(\frac{47}{240}\right) \times \frac{1}{p'^3}$$

$$\left\|E_{J,J'}\right\|^2 \leq \frac{M^2}{26^2} \left(\frac{1}{81} \times \frac{1}{p^3 p'^3} + \left(\frac{47}{240}\right) \times \frac{1}{p^3} + \left(\frac{47}{240}\right) \times \frac{1}{p'^3} \right) \tag{8.55}$$

For $p \to \infty$, $p' \to \infty$, $\left\|E_{J,J'}\right\| \to 0$ which proves the convergence of the proposed scheme.

8.6 Numerical Experiments and error analysis

To describe the efficiency of the present scheme, some numerical experiments have been conducted on the test problems considering (2+1)-dimensional partial differential equations. L_2 , L_∞ and absolute errors have been calculated to check the level of accuracy of the present scheme with the help of following formulas at a fixed time t

$$\text{Absolute error} = |u_{exact}(x_r, y_s, t) - u_{num}(x_r, y_s, t)| \tag{8.56}$$

$$L_\infty = \max_{r,s} |u_{exact}(x_r, y_s, t) - u_{num}(x_r, y_s, t)| \tag{8.57}$$

$$L_2 = \frac{\sqrt{\sum_{l=1}^{3p} |u_{exact}(x_r, y_s, t) - u_{num}(x_r, y_s, t)|^2}}{\sqrt{\sum_{l=1}^{3p} |u_{exact}(x_r, y_s, t)|^2}} \tag{8.58}$$

Numerical Experiment No. 8.1 : In this Numerical Experiment, we considered the two-dimensional Sobolev equation of the type

$$\varphi_t - (\Delta\varphi)_t - \Delta\varphi = f\ (x, y, t), \qquad (x, y) \in [0,1] \times [0,1], t\ >\ 0 \tag{8.59}$$

with the following boundary and initial constraints

Case I. $(a)\varphi\ (x, y, 0)\ =\ sin(\pi x)\ sin(\pi y)$ $\qquad (x, y) \in [0,1] \times [0,1]$

$(b)\varphi\ (x, y, t) =\ e^{-t} sin(\pi x)\ sin(\pi y)$ $\qquad (x, y) \in\ \partial\Omega, t \in [0, T]$

Source term $f(x, y, t) = -e^{-t} sin(\pi x)\ sin(\pi y)$

Case II. $(a)\varphi\ (x, y, 0)\ = e^{x+y} sin(\pi x)\ sin(\pi y)$ $\qquad (x, y) \in [0,1] \times [0,1]$

$(b)\varphi\ (x, y, t)\ =\ e^{x+y+t}\ sin(\pi x)\ sin(\pi y)$ $\qquad (x, y) \in\ \partial\Omega, t \in [0, T]$

Source term $f(x, y, t) = e^{x+y+t}\big((4\pi^2 - 3)\ sin(\pi x) sin(\pi y) - 4\pi \sin \pi(x + y)\big)$

Case III. $(a)\varphi(x, y, 0)\ = e^{x-y}\ sin(\pi x)\ sin(\pi y)$ $\qquad (x, y) \in [0,1] \times [0,1]$

$(b)\varphi(x, y, t) = e^{x-y-t}\ sin(\pi x)\ sin(\pi y)$ $\qquad (x, y) \in\ \partial\Omega, t \in [0, T]$

Source term $f(x, y, t) = -e^{x-y-t}\ sin(\pi x)\ sin(\pi y)$

Exact solution of Numerical Experiment No. 8.1 for

Case I. $\varphi\ (x, y, t) = e^{-t} sin(\pi x)\ sin(\pi y)$

Case II. $\varphi\ (x, y, t) =\ e^{x+y+t} \sin(\pi x) \sin(\pi y)$

Case III. $\varphi(x, y, t) = e^{x-y-t}\ sin(\pi x)\ sin(\pi y)$

We proposed the following general solution for Numerical Experiment No.8.1 using the proposed scheme

$$\varphi^{n+1}(x,y) = \sum_{i=1}^{3p}\sum_{l=1}^{3p} a_{il}^{n+1}\left(q_{i,2}(x) - x\, q_{i,2}(1)\right)\left(q_{l,2}(y) - y q_{l,2}(y)\right) + x\left(\varphi^{n+1}(1,y) - \varphi^{n+1}(1,0)\right) + (1-x)\left(\varphi^{n+1}(0,y) - \varphi^{n+1}(0,0)\right) + y\left(\varphi^{n+1}(x,1) - \varphi^{n+1}(x,0)\right) - xy\left(\varphi^{n+1}(1,1) - \varphi^{n+1}(1,0)\right) - (1-x)y\left(\varphi^{n+1}(0,1) - \varphi^{n+1}(0,0)\right) + \varphi^{n+1}(x,0)$$

here $\varphi^{n+1}(x,y) = \varphi(x,y,t_{n+1})\ \forall\ (x,y) \in [0,1]\times[0,1], t_{n+1} \in [0,T],\ n = 1,2,3\ldots$,$a_{il}'s$ are the wavelets approximation coefficients and $q_{j,i}'s$ are the integrals of Haar scale 3 (non-dyadic) wavelets.

The particular solution for each case has been obtained using the boundary condition on the Equation (8.59) and presented in the form of tables and figures. It can be seen from Figure 8.1-Figure 8.3 that the results achieved by applying the proposed scheme are in good agreement with the analytic solutions. Table 8.1-Table 8.3 are depicting the performance of the proposed scheme in comparison with the other methods[[73], [203],[204]] existing the recent literature at a different level of resolution. We infer that the proposed method is working better than the other methods[73], [204], and giving the results comparable to the method [203]. Further, it is observed that as we increase the level of resolution j, the error norms decrease which ensures the stability of the proposed numerical scheme. Hence, we can conclude that the proposed technique is a strong solver in terms of better accuracy.

Table 8.1: L_2 , L_∞ errors in the solution at t=1,$\Delta t = 0.01$, $\theta = 0.5$ of Numerical Experiment No. 8.1 for case 1.

J	L_2	L_∞	L_2[204]	L_∞[204]	L_2[73]	L_∞[73]	L_2 [203]	L_∞ [203]
0	4.04E-02	1.49E-02	1.47E-02	6.28 E −02	--	--	2.74 E −02	1.37 E −02
1	5.02E-03	1.84E-03	8.10E-03	2.21 E −02	1.75E−02	7.48E−03	9.30 E −04	4.27 E −04
2	5.72E-04	2.10E-04	2.92E-03	6.49 E −03	8.95E−03	2.15E−03	4.96 E −04	1.46 E −04
3	7.11E-05	2.62E-05	8.01E-04	1.72 E −03	4.01E−03	4.95E−04	9.84 E −05	1.26 E −05

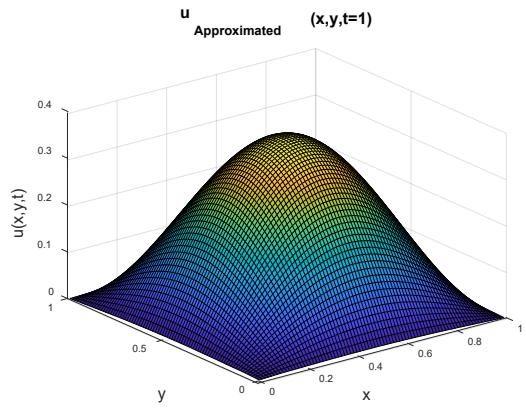

Figure 8.1a

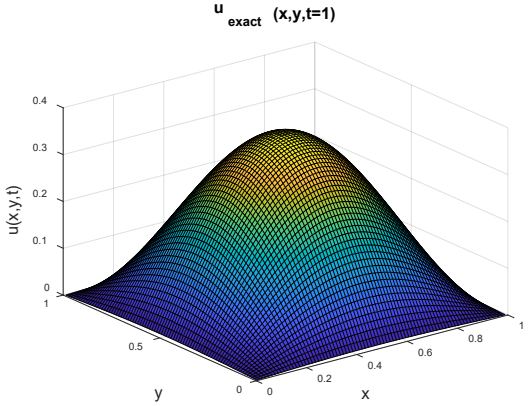

Figure 8.1b

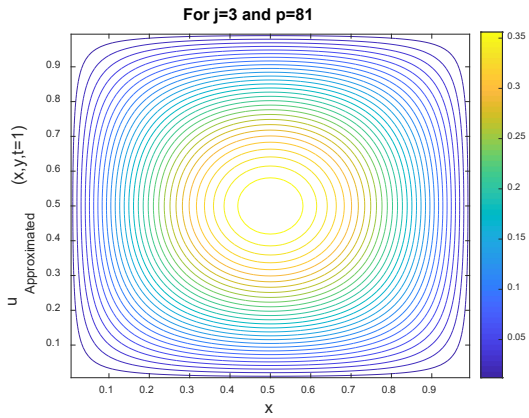

Figure 8.1c

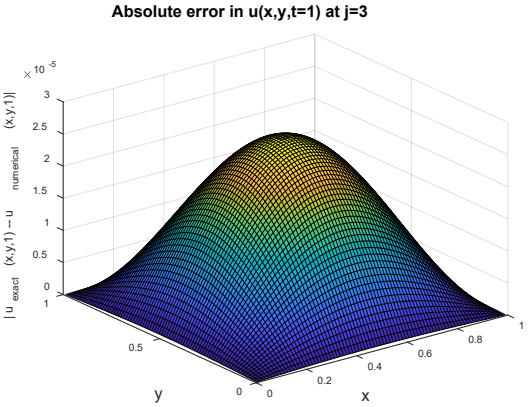

Figure 8.1d

Figure 8.1: Graphical representation of Exact solution(Figure 8.1a), Approximate solution (Figure 8.1b), contour view of the approx. solution (Figure 8.1c) and absolute error(Figure 8.1d) in the solution at t=1, $\Delta t = 0.01$, $\theta = 0.5$ of Numerical Experiment No. 8.1 for case 1.

Table 8.2: L_2 , L_∞ errors in the solution at t=1,$\Delta t = 0.01$, $\theta = 0.5$ of Numerical Experiment No. 8.1 for case 2.

J	L_2	L_∞	L_2[204]	L_∞[204]	L_2[203]	L_∞[203]
0	1.8834E-02	7.6790E-03	6.7382E-01	8.5627E-01	--	--
1	3.0684E-03	1.3353E-03	1.8475E-01	2.7254E-01	6.9125 E −03	3.6864 E −03
2	3.5747E-04	1.5944E-04	4.7550E-02	7.9913E-02	2.0205 E −03	6.1921 E −04
3	4.3790E-05	1.9293E-05	1.1658E-02	2.0915E-02	5.5575 E −04	7.7847 E −05

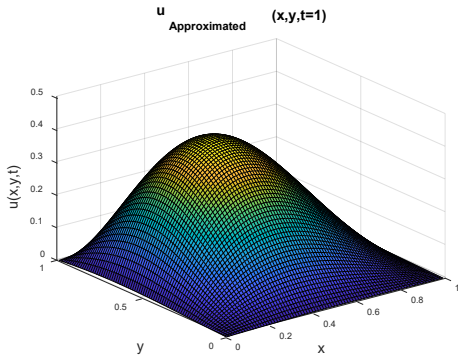

Figure 8.2a

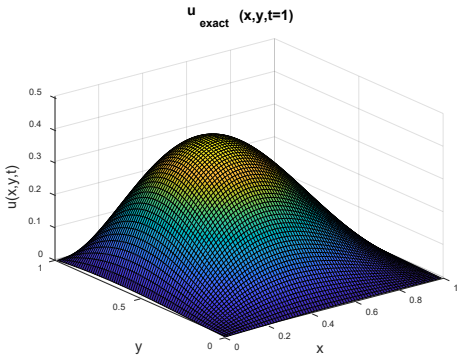

Figure 8.2b

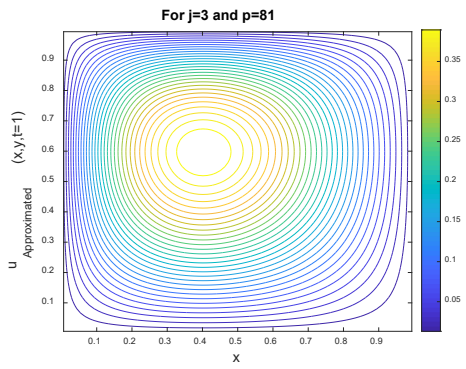

Figure 8.2c

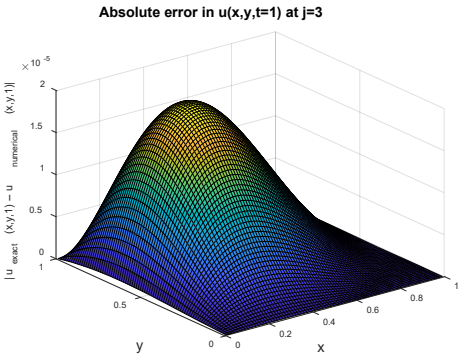

Figure 8.2d

Figure 8.2: Graphical representation of Exact solution (Figure 8.2a), Approximate solution (Figure 8.2b), contour view of the approx. solution (Figure 8.2c) and absolute error(Figure 8.2d) in the solution at t=1, $\Delta t = 0.01$, $\theta = 0.5$ of Numerical Experiment No. 8.1 for case 2.

Table 8.3: L_2 , L_∞ errors in the solution at t=1,$\Delta t = 0.01$, $\theta = 0.5$ of Numerical Experiment No. 8.1 for case 3.

J	L_2	L_∞	L_2[204]	L_∞[204]	L_2 [73]	L_∞ [73]	L_2[203]	L_∞ [203]
0	1.9196 E-02	1.5873 E-01	2.4663 E-03	1.0505 E-02	--	--	1.2031 E −02	8.8937 E −03
1	3.1149 E-03	2.7491 E-02	1.2651 E-03	5.2058 E-03	1.0450 E−02	6.27731 E−03	3.5605 E −04	1.8882 E −04
2	3.5581 E-04	3.2240 E-03	4.2776 E-04	1.6720 E-03	5.9420 E−03	1.7252 E−03	9.4118 E −05	2.9171 E −05
3	3.6585 E-05	3.3583 E-04	1.1685 E-04	4.5449 E-04	2.6154 E−03	3.8947 E−04	2.0569 E −05	3.2249 E −06

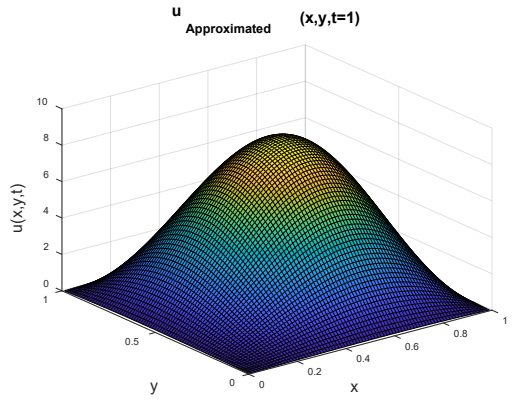

Figure 8.3a

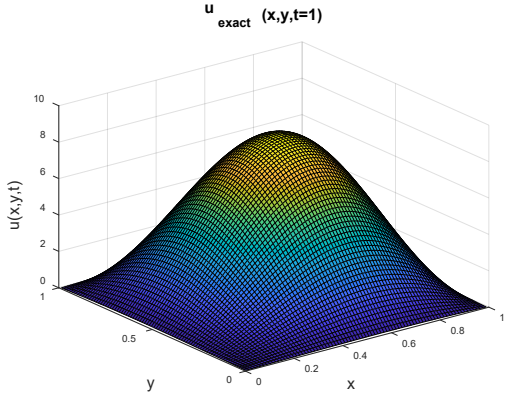

Figure 8.3b

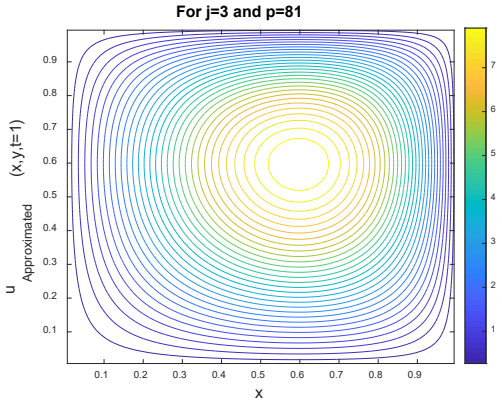

Figure 8.3c

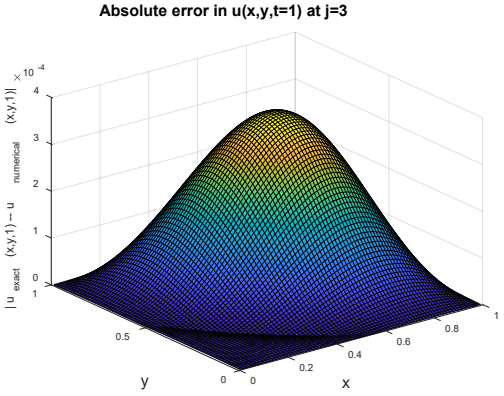

Figure 8.3d

Figure 8.3: Graphical representation of Exact solution (Figure 8.3a), Approximate solution (Figure 8.3b), contour view of the approx. solution (Figure 8.3c) and absolute error (Figure 8.3d) in the solution at t=1, $\Delta t = 0.01$, $\theta = 0.5$ of Numerical Experiment No. 8.1 for case 3.

Numerical Experiment No. 8.2 : In this Numerical Experiment, we considered the two-dimensional non-linear Sobolev equation of the following type

$$\varphi_t - (\Delta\varphi)_t - \nabla.(\varphi\nabla\varphi) + \pi^2\varphi^2 = f\ (x,y,t), (x,y)\ \in \Omega, t\ >\ 0 \qquad (8.60)$$

With the following boundary and initial constraints

$(i)\varphi$ (x, y,0) = sin(πx) sin(πy) $\qquad (x,y) \in [0,1] \times [0,1]$

$(ii)\varphi\ (x,y,t)\ = e^t\ sin(\pi x)\ sin(\pi y) \quad (x,y) \in\ \partial\Omega, \mathrm{t} \in [0,T]$

and the source term

$f\ (x,y,t) = (1+2\pi^2)e^t\ sin(\pi x)sin(\pi y) + 3\pi^2 e^{2t}\ sin^2(\pi x)sin^2(\pi y) -$
$2\pi^2(e^{2t}\ sin^2(\pi x)cos^2(\pi y) + e^{2t}\ cos^2(\pi x)sin^2(\pi y))$

Using the θ −weighted finite differencing scheme for time discretization, the above equation becomes

$\varphi^{n+1} - \left(\varphi_{xx}^{n+1} + \varphi_{yy}^{n+1}\right) - \theta\Delta t\left(\varphi^{n+1}\varphi_{xx}^{n+1} + \varphi^{n+1}\varphi_{yy}^{n+1} + (\varphi_x^2)^{n+1} + \left(\varphi_y^2\right)^{n+1} - \pi^2(\varphi^2)^{n+1}\right) = \varphi^n - \left(\varphi_{xx}^n + \varphi_{yy}^n\right) + (1-\theta)\Delta t(\varphi^n\varphi_{xx}^n + \varphi^n\varphi_{yy}^n + (\varphi_x^2)^n + \left(\varphi_y^2\right)^n - \pi^2(\varphi^2)^n) + (1-\theta)\Delta t f^n + \theta\Delta t\ f^{n+1}$

By applying the quasilinearization technique to linearize the non-linear terms as described below

$(\varphi\varphi_{xx})^{n+1} = \varphi^{n+1}\varphi_{xx}^n + \varphi^n\varphi_{xx}^{n+1} - \varphi^n\varphi_{xx}^n$,

$\left(\varphi\varphi_{yy}\right)^{n+1} = \varphi^{n+1}\varphi_{yy}^n + \varphi^n\varphi_{yy}^{n+1} - \varphi^n\varphi_{yy}^n$

$(\varphi_x^2)^{n+1} = 2\varphi_x^n\varphi_x^{n+1} - (\varphi_x^2)^n$

$\left(\varphi_y^2\right)^{n+1} = 2\varphi_y^n\varphi_y^{n+1} - \left(\varphi_y^2\right)^n$

$(\varphi^2)^{n+1} = 2\varphi^n\varphi^{n+1`} - (\varphi^2)^n$

The equation leads to

$\left(1 - \theta\Delta t\left(\varphi_{xx}^n + \varphi_{yy}^n - 2\pi^2\varphi^n\right)\right)\varphi^{n+1} - (1+\theta\Delta t\ \varphi^n)\left(\varphi_{xx}^{n+1} + \varphi_{yy}^{n+1}\right) - 2\theta\Delta t\left(\varphi_x^n\varphi_x^{n+1} + \varphi_y^n\varphi_y^{n+1}\right) = \varphi^n - \left(\varphi_{xx}^n + \varphi_{yy}^n\right) + (1-2\theta)\Delta t(\varphi^n\varphi_{xx}^n + \varphi^n\varphi_{yy}^n + (\varphi_x^2)^n + \left(\varphi_y^2\right)^n - \pi^2(\varphi^2)^n) + (1-\theta)\Delta t f^n + \theta\Delta t\ f^{n+1}$

Putting the values of φ^{n+1} , φ_{xx}^{n+1} , φ_{yy}^{n+1} , φ_x^{n+1}, φ_y^{n+1} from section 8.4 and using the boundary constraints then discretizing the space variable as $x \to x_r$, $y \to y_s$ where $x_r = \frac{2r-1}{6p}$, $y_s = \frac{2s-1}{6p}$, $r,s = 1,2,\ldots\ldots 3p$ in the above equations we get the following system of algebraic equations

$$\sum_{i=1}^{3p}\sum_{l=1}^{3p} a_{il}^{n+1}\, R_{i,l,r,s} = F(r,s)$$

where

$$R_{i,l,r,s} = \Big(1 - \theta\Delta t\big(\varphi^n_{xx} + \varphi^n_{yy} - 2\pi^2\varphi^n\big)\Big)\Big(q_{i,2}(x) - x\, q_{i,2}(1)\Big)\Big(q_{l,2}(y) - y q_{l,2}(y)\Big) - (1 + \theta\Delta t\, \varphi^n)\ \Big(\ h_i(x_r)\Big(q_{l,2}(y_s) - y\, q_{l,2}(1)\Big) + \Big(q_{i,2}(x_r) - x_r\, q_{i,2}(1)\Big)\ h_l(y_s)\Big) - 2\theta\Delta t\ \Big(\varphi^n_x\Big(q_{i,1}(x) - q_{i,2}(1)\Big)\Big(q_{l,2}(y) - y\, q_{l,2}(1)\Big) + \varphi^n_y\Big(q_{i,2}(x) - x\, q_{i,2}(1)\Big)\Big(q_{l,1}(y) - q_{l,2}(1)\Big)\Big) \qquad \forall\ i,j$$

$$F(r,s) = \Bigg(\varphi^n(x_r,y_s) - \Big(\varphi^n_{xx}(x_r,y_s) + \varphi^n_{yy}(x_r,y_s)\Big) + (1 - 2\theta)\Delta t\Big(\varphi^n(x_r,y_s)\varphi^n_{xx}(x_r,y_s) + \varphi^n(x_r,y_s)\varphi^n_{yy}(x_r,y_s) + \big(\varphi^2_x(x_r,y_s)\big)^n + \Big(\varphi^2_y(x_r,y_s)\Big)^n - \pi^2\big(\varphi^2(x_r,y_s)\big)^n\Big) + (1-\theta)\Delta t f^n(x_r,y_s) + \theta\Delta t\, f^{n+1}(x_r,y_s)\Bigg) - \Big(1 - \theta\Delta t\Big(\varphi^n_{xx}(x_r,y_s) + \varphi^n_{yy}(x_r,y_s) - 2\pi^2\varphi^n(x_r,y_s)\Big)\Big)\Big(x_r\big(\varphi^{n+1}(1,y_s) - \varphi^{n+1}(1,0)\big) + (1-x_r)\big(\varphi^{n+1}(0,y_s) - \varphi^{n+1}(0,0)\big) + y_s\big(\varphi^{n+1}(x_r,1) - \varphi^{n+1}(x_r,0)\big) - x_r y_s\big(\varphi^{n+1}(1,1) - \varphi^{n+1}(1,0)\big) - (1-x_r)y_s\big(\varphi^{n+1}(0,1) - \varphi^{n+1}(0,0)\big) + \varphi^{n+1}(x_r,0)\Big) + \big(1 + \theta\Delta t\ \varphi^n(x_r,y_s)\big)\Big(y_s\ \varphi^{n+1}_{xx}(x_r,1) + (1 - y_s)\varphi^{n+1}_{xx}(x_r,0) + x\ \varphi^{n+1}_{yy}(1,y_s) + (1-x_r)\varphi^{n+1}_{yy}(0,y_s)\Big) + 2\theta\Delta t\big(\varphi^n_x(y_s\ \varphi^{n+1}_x(x_r,1) + (1-y_s)\ \varphi^{n+1}_x(x_r,0) + \big(\varphi^{n+1}(1,y_s) - \varphi^{n+1}(0,y_s)\big) - y_s\big(\varphi^{n+1}(1,1) - \varphi^{n+1}(0,1)\big) - (1-y_s)\big(\varphi^{n+1}(1,0) - \varphi^{n+1}(0,0)\big)\ + \varphi^n_y(x_r\ \varphi^{n+1}_y(1,y_s) + (1-x_r)\ \varphi^{n+1}_y(0,y_s) + \big(\varphi^{n+1}(x_r,1) - \varphi^{n+1}(x_r,0)\big) - x_r\big(\varphi^{n+1}(1,1) - \varphi^{n+1}(1,0)\big) - (1-x_r)\big(\varphi^{n+1}(0,1) - \varphi^{n+1}(0,0)\big)\ \big)$$

The above system reduced to the system of algebraic equations and further, it gets reduced to the following system of 4D-arrays

$$A_{3p\times 3p}R_{3p\times 3p\times 3p\times 3p} = F_{3p\times 3p}$$

Further, the above arrays system is reduced to the following matrix system using the transformations $a^{n+1}_{il} = b^{n+1}_{\lambda}$ *and* $F_{rs} = G_{\mu}$

$$B_{1\times(3p)^2}S_{(3p)^2\times(3p)^2} = G_{1\times(3p)^2}$$

Where $\lambda = 3p(i-1) + l$ and $\mu = 3p(r-1) + s$

Then the values of b_{λ}^{n+1} can be calculated successively for different values of n=1,2… by solving the above system of equation using the Thomas algorithm via MATLAB Program. Original wavelet coefficients a_{il}^{n+1} can be restored by using the above transformation. These coefficients will be used in the equations to determine the final solution of the problem for different value of t_n for n= 0,1, 2..

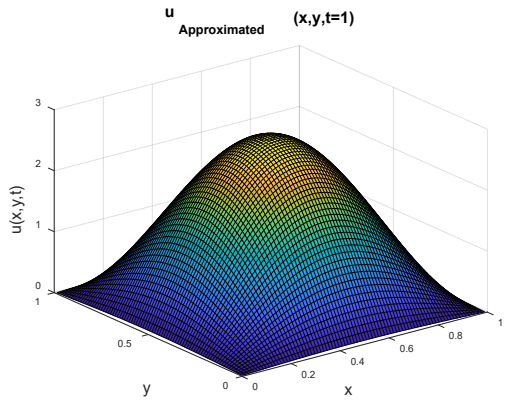

Figure 8.4a

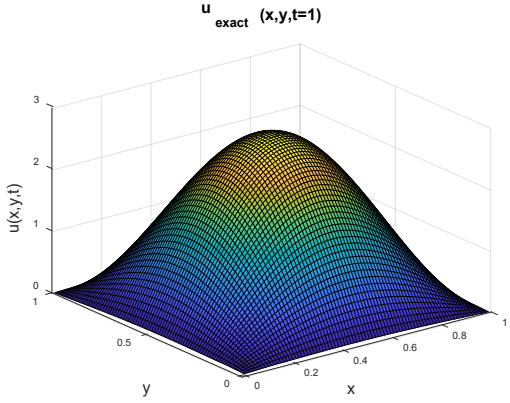

Figure 8.4b

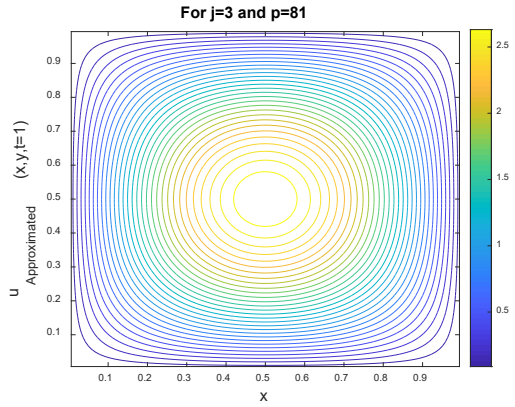

Figure 8.4c

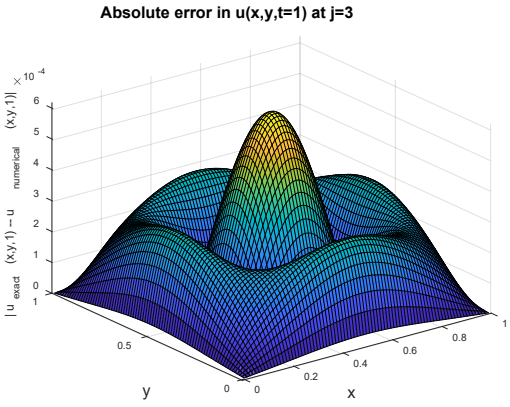

Figure 8.4d

Figure 8.4: Graphical representation of Exact solution (Figure 8.4a), Approximate solution(Figure 8.4b), contour view of the approx. solution (Figure 8.4c) and Absolute error (Figure 8.4d) in the solution at t=1, $\Delta t = 0.01\,, \theta = 0.5$ of Numerical Experiment No. 8.2.

Results obtained by the proposed scheme are explained with the help of tables and surface plots. It is very much clear from Figure 8.4 that results achieved with the proposed scheme are roughly coinciding with the analytic solution. The level of accuracy obtained for the solution is of order 10^{-4} which is a noteworthy achievement

for these kinds of problems. The solution achieved can further be improved by increasing the number of collocation. In Table 8.4 error norms obtained by the present scheme are also compared with the other methods [205][73] at different levels of resolution j and it has been observed that with the increase in the collocation points (level of resolution), error norms are decreasing which ensure the stability of the proposed scheme. We infer that our scheme is working well as compare to the methods [73], [205].

Table 8.4: L_2 , L_∞ errors in the solution at t=1,$\Delta t = 0.001$, $\theta = 1$ of Numerical Experiment No. 8.2.

J	L_2	L_∞	L_2 [73]	L_∞ [73]	L_2 [205]
0	3.8655E-02	1.0441E-01	1.7284E−01	5.8662E−02	3.1576E−02
1	4.7240E-03	1.2236E-02	7.5881E−02	1.3147E−02	7.8313E−03
2	5.0009E-04	9.3648E-04	3.4724E−02	3.0030E−03	1.9572E−03
3	1.7150E-04	6.2176E-04	1.3063E−02	5.5208E−02	-----

Numerical Experiment No. 8.3: In this Numerical Experiment, we considered the two-dimensional non-linear Sobolev equation of the following type

$$\varphi_t - (\Delta\varphi)_t - \Delta\varphi + \nabla\varphi = \nabla.\big(F(\varphi)\big) + f\ (x,y,t), (x,y) \in \Omega, t\ >\ 0$$

With the following boundary and initial constraints

$(i)\varphi\ (x,y,0) = \sin(x+y) \qquad (x,y) \in [0,1] \times [0,1]$

$(ii)\varphi\ (x,y,t)\ =\ t\ sin(x+y) \qquad (x,y) \in\ \partial\Omega, t \in [0,T]$ and

The source terms

$$f(x,y,t) = (3 + 2t - 2t^2\cos(x+y))sin(x+y) + 2\ t\cos\ (x+y)$$

The numerical solution obtained by using the proposed scheme at $t = t_{n+1}$, $n = 0,1,2$ ... is given by

$$\varphi(x,y,t_{n+1}) = \sum_{i=1}^{3p}\sum_{l=1}^{3p} a_{il}^{n+1}\Big(q_{i,2}(x) - x\ q_{i,2}(1)\Big)\Big(q_{l,2}(y) - yq_{l,2}(y)\Big) +$$
$$x\big(\varphi^{n+1}(1,y) - \varphi^{n+1}(1,0)\big) + (1-x)\big(\varphi^{n+1}(0,y) - \varphi^{n+1}(0,0)\big) + y\big(\varphi^{n+1}(x,1) -$$
$$\varphi^{n+1}(x,0)\big) - xy\big(\varphi^{n+1}(1,1) - \varphi^{n+1}(1,0)\big) - (1-x)y\big(\varphi^{n+1}(0,1) - \varphi^{n+1}(0,0)\big) +$$
$$\varphi^{n+1}(x,0)$$

Where the wavelet coefficient a_{il}^{n+1} has been determined will the help of the scheme discussed in section 8.4 and in the Numerical Experiment No. 8.3.

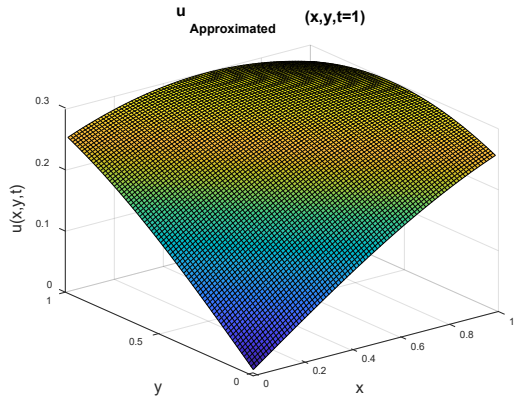

Figure 8.5a

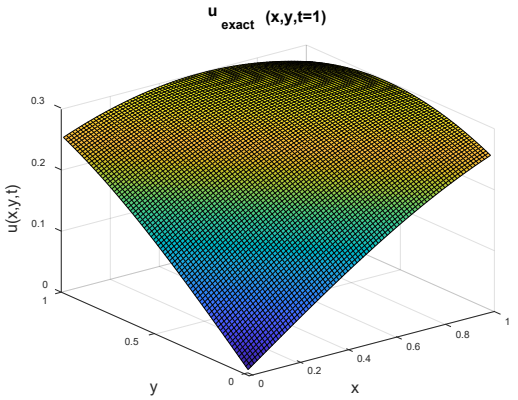

Figure 8.5b

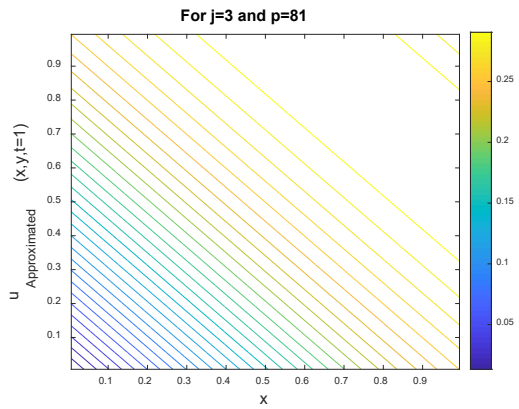

Figure 8.5c

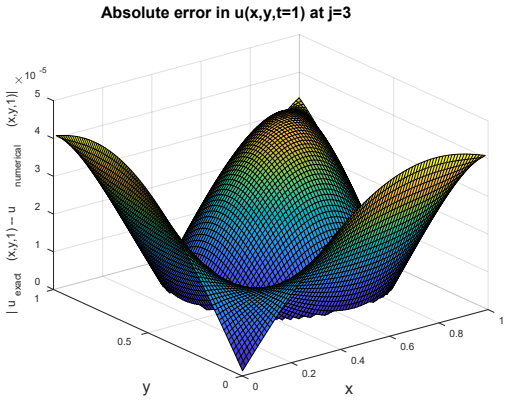

Figure 8.5d

Figure 8.5: Graphical representation of Exact solution (Figure 8.5a), Approximate solution(Figure 8.5b), contour view of the approx. solution (Figure 8.5c) and absolute error (Figure 8.5d) in the solution at t=1, $\Delta t = 0.01$, $\theta = 0.5$ of Numerical Experiment No. 8.3.

The solution for the given problem has been calculated with the help of the proposed scheme and the result achieved have been compared with an exact solution available in the literature. Figure 8.5 is depicting a good agreement in the exact and approximated solutions. Further, L_2 and L_∞ errors have been calculated for different value of t at the level of resolution J=3 and presented in Table 8.5 which demonstrates the efficiency of the proposed scheme. The level of accuracy obtained is of order 10^{-5} for this

problem at J=3 which can be further improved by increasing the level of resolution. Moreover, in Table 8.5 error norms obtained with proposed are also compared with the method [73] and it outperforms over method [73].

Table 8.5: L_2 , L_∞ errors in the solution at the different values of t with $\theta = 0.5$ and J=3 for Numerical Experiment No. 8.3

t	L_2	L_∞	L_2 [73]	L_∞ [73]
0.1	4.9037E-04	7.3137E-05	9.0478E−04	9.7897E−05
0.2	1.6986E-04	5.4437E-05	1.9331E−03	2.0530E−04
0.3	9.1296E-05	4.1336E-05	--	--
0.4	1.2961E-04	7.6725E-05	--	--
0.5	1.8913E-04	1.2210E-04	5.2227E−03	5.6699E−04
0.6	2.4703E-04	1.7748E-04	--	--
0.7	3.0204E-04	2.4279E-04	--	--
0.8	3.5479E-04	3.1806E-04	--	--
0.9	4.0587E-04	4.0327E-04	--	--
1	4.5574E-04	4.9842E-04	8.5980E−03	9.8933E−04

8.7 Conclusion

A new numerical method is developed and implemented on (2+1) dimensional partial differential equations. In the proposed hybrid method θ-weighted differencing scheme is used with the collocation method by considering the two-dimensional Haar scale 3 (non-dyadic) wavelets as the base function. The convergence of the method is proved by establishing the error bound for the proposed method. The proposed method is tested on different linear and nonlinear (2+1) dimensional partial differential equations i.e Sobolev and BBMB (Benjamin–Bona–Mahony–Burgers) Equations and it is found that the scheme outperforms over the other method. Implementation of the proposed scheme is very easy in the computer environment. Similar programming modules can be used to solve the different partial differential equations with little modifications.

Chapter 9
Conclusions and Future Scope

9.1 Conclusions

Most of the physical problems can be modeled in the form of a differential equation for their extensive study. It is exceptionally hard to acquire the analytical solution for most of the differential equations when the differential mathematical model of phenomena carries the nonlinearities, variable coefficients, or a greater number of variables (higher dimensional) in it. This results in the requirement of advanced numerical methods which can be regarded as a strong solver to get an accurate numerical solution for these types of differential equations. Researchers are putting continuous efforts for the improvement of existing methods and the development of new hybrid methods with the aim to develop a strong solver for these kinds of equations. In literature, dyadic wavelets are in preponderance in which dilatation factor runs on the power of 2.

This thesis aims to develop and explore the implementation of Haar Scale 3 (non-dyadic) wavelet-based numerical methods in which the dilatation factor runs on the power of 3. The proposed method is relatively a new idea used to compute the numerical solution of some important higher-order linear and nonlinear boundary value problems, time-dependent partial differential equations., fractional differential equations, and nonlinear system of fractional partial differential equations. In this thesis, we have used Haar Scale 3 and Haar scale 2 wavelets as the main tool with existing numerical techniques such as the Collocation method, Quasilinearization process, and Gauss elimination method to obtain the solution of various linear-nonlinear higher ordered, coupled and fractional differential equations. The condition of convergence of these numerical techniques is derived. Finally, we proposed a new Haar scale 3 (non-dyadic) wavelet-based technique that is more efficient than the classical Haar scale 2 dyadic wavelet-based technique.

Haar scale 3 wavelet basis functions have advantages over the standard Haar scale 2 wavelet basis functions in terms of rate of convergence, accuracy, and efficiency to approximate any function as shown in Table 4.2, 4.5, 4.8 to 4.10, 4.14, 4.17, 4.20 in chapter four. Moreover, the proposed method has given better results as compared to some existing methods in the literature as demonstrated with the help of Table 4.3, 4.6, 4.9 to 4.12, 4.15, 4.18, 4.20, 4.21, 4.24, 4.25, 4.28 in chapter 4, when implemented with collocation and quasilinearization methods. This basis function also reduces the computational complexity in comparison to the finite element method as it is easy to implement with collocation and quasilinearization methods.

The proposed wavelet methods, namely Haar scale 3 (non-dyadic) wavelet collocation method, Haar scale 3 (non-dyadic) wavelet quasilinearization method have proven to be very useful in a large class of problems arising in real-world applications. Due to its inherent features of Haar scale 3 (non-dyadic) wavelets such as computationally cheap, conceptually simple, memory efficient, orthonormality with compact support, this method becomes an improved alternative tool to traditional numerical techniques. In fact, the simplicity, sparsity of non-dyadic wavelet matrices, and solution representation with significantly smaller number of wavelet coefficients increase the speed of convergence of the method. Haar scale 3 (non-dyadic) wavelet-based technique gives a better outcome for less value of the level of resolution. Only a few numbers of collocation points in this technique will lead to the solution and hence reduces the computational cost.

The considered problems in the chapters of thesis arise in mathematical modeling of many physical, chemical and biological phenomena happening in the fields of science and engineering such as viscoelastic flows in fluid dynamics, viscoelastic fluids[3], hydrodynamic and hydromagnetic stability [93], induction motor with two rotor circuits [116], fluid mechanics [172], electric signal propagation in cables[179], pulsate blood flow in the arteries[180], ‘acoustic wave propagation’ in porous media of Darcy-type[181], vibrations in the different structures, walk theory[182], Maxwell viscous fluid parallel flow study[183], Soil moisture migration [195], drainage of liquids through rocks having cracks [196], heat conduction Continuum Mechanics[197], etc in the analysis of wave propagation in different mediums [198].

Although the major findings of the proposed methods are already discussed in the respective preceding chapters, we now summarize some of the advantages of the methods as follows:

1. The proposed method is relatively a new idea used to compute the numerical solution of some important higher-order linear and nonlinear differential equations with the boundary conditions, time-dependent (2+1) dimensional PDEs, FDEs and nonlinear system of FPDEs.
2. Operational matrices of Haar scale 3 (non-dyadic) wavelets and the matrices of integrals of Haar scale 3 (non-dyadic) wavelets are sparse in nature which accelerate computation work involved and creates a very less cost for computation.
3. Non-dyadic Haar wavelet-based methods gives better accuracy as compare to the other existing methods VIDM [96], OHAM [97], GMQBS [117], LGM [99], RKSM [100], VIM [101] , MVID [102], SBSCM [103], PGM [104], HPM [118] , QBSCM [119] , HWCM [120] with dilation factor 2, MADM [121] etc. as shown in the Tables 4.1- Tables 4.29, Table 5.1-Table 5.5,Table 6.2, Table 8.1-Table 8.5 in the different chapter of this thesis.
4. In the context of convergences for the considered equations, rate of convergence of using Haar scale 3 wavelets bases is faster as compare to the Haar scale 2 wavelet basis function
5. While implementing the Haar scale 3 wavelet basis functions with collocation method it is observed that the collocation method is easy to apply with Haar scale 3 wavelets in comparison to other numerical techniques such as finite element methods.
6. Haar scale 3 (non-dyadic) wavelet method is very convenient to solve boundary value problems in ordinary, partial, and fractional differential equations since the boundary conditions will get automatically into the process of the method.
7. Haar scale 3 (non-dyadic) wavelet-based solutions of critical differential equations like fractional Coupled Burgers' equation, linear and non-linear Sobolov, and BBMB equation which are highly complex (2+1) dimensional partial differential equations are obtained with ease.

8. The effectiveness and precision of the proposed method can be seen through the figures given in the different chapters where results obtained with the Scale-3 Haar wavelet and the exact solution available in the literature are lying on one another for a very few numbers of collocations points. The exactness of a solution obtained by the method is up to the degree of 10^{-16} which can be further increased by increasing the number of collocation points as shown in chapter 4.
9. It can be concluded that the Haar scale 3 (non-dyadic) wavelet-based method is more elegant in terms of theory, accuracy, easy implementation on computer system, and small computation cost which provides a better solution in comparison to other classical wavelet methods. One common program can be used as a subprogram for all the problems under consideration which shows the better compatibility of the proposed technique with the computer environment for programming.
10. Haar scale 3 (non-dyadic) wavelets can easily be extended for the higher dimensional and higher-order differential, integral and fractional model using their flexible characteristic.
11. The main limitation with Haar scale 3 wavelet family is that the members of this wavelet family are discontinuous at the partition points. Because of this derivative approach at the initial stage is not applicable. Therefore, one has to adopt the integration procedure to determine the wavelets weight coefficients. Also,computational cost increases with the increase in the level of resolution .
12. Finally, the scale-3 Haar wavelets approach proved to be elegant, effective and have great potential to deal with various types of mathematical models and they are excellent as compare to results available in the literature

9.2 Future Scope

For the physical problems considered in this thesis with single or coupled differential equations, the Haar scale 3 (non-dyadic) wavelet approach is proved to be elegant, effective and has great potential to deal with various types of mathematical models. There are several conceivable ideas which can be concluded from the research work carried out in this thesis, on which someone

interested may focus their upcoming research. Some of them can be summarized as follows:

1. The proposed technique can be extended for the integral equation, integro-differential, and fractional integro-differential equations by using some recent advances in the field of fractional calculus (like Caputo-Fabrizio definitions, Atangana-Baleanu fractional operator). The presented Haar scale 3 (non-dyadic) wavelet methods can also be adapted to find the solution of some new form of linear and nonlinear partial, fractional, and ordinary differential equations.
2. In this thesis, we have used Haar Scale 3 and Haar scale 2 wavelets as the main tool with existing numerical techniques such as Collocation method, Quasilinearization process, and Gauss elimination. But a huge variety of wavelets with different structures and characteristics are existing in the literature like Daubechies, Shannon, Gabor, Legendre, Bernoulli, Hermite, Chebyshev, Spline, Bessel, Laguerre, ultraspherical, Gegenbauer and CAS wavelets, etc . To see the efficiency and accuracy of a numerical technique based on a specific wavelet, a comparative study will be further helpful, motivating, and interesting.
3. While using the Haar scale 3 (non-dyadic) wavelet collocation method, nonlinear problems are linearized by using quasilinearization formula as discussed in the thesis. The proposed technique can also be explored with the other existing technique to handle the non-linearities in equations like the method of lines, Generalized Newton Rapson method, etc.
4. Most of the partial and fractional differential Equations governing the different real-time phenomena solved in this research work are one and two dimensions second order differential equations. The proposed method can be extended to solve higher-order, higher dimensional differential equations appearing in the field engineering and sciences.
5. In this research work, the collocation method is applied with non-dyadic Haar wavelet basis functions. This basis function can also be implemented with other numerical legacy methods and will be compared with numerical techniques or

semi-analytical techniques like the Finite element method, another wavelet technique, etc.

6. In present research work, the convergence of the proposed techniques has been established in the respective chapters. But there are many other venues like stability analysis, statistical analysis (like paired t-test, ANOVA) can also be performed to validate the results obtained from the method.

9.3 List of Publications

1. Numerical solution by Haar wavelet collocation method for a class of higher-order linear and nonlinear boundary value problems. This paper has been published in the Scopus/UGC indexed American journal: AIP-Conference Proceedings with **SJR 0.19**.

Citation:

R. Kumar, H. Kaur, and G. Arora, "Numerical solution by Haar wavelet collocation method for a class of higher-order linear and nonlinear boundary value problems," *AIP Conf. Proc.*, vol. 1860, no. 1, pp. 020038–1–020038–12, 2017); DOI: 10.1063/1.4990337

View online: https://aip.scitation.org/doi/abs/10.1063/1.4990337
Published by the American Institute of Physics

2. A Novel Wavelet Based Hybrid Method for Finding the Solutions of Higher Order Boundary Value Problems. This paper has been published in the SCI/Scopus/UGC indexed Elsevier journal: Ain Shams Engineering Journal with **SJR 0.465** and **Impact factor 3.091** with manuscript no. ASEJ-D-17-00591.

Citation:

G. Arora, R. Kumar, and H. Kaur, "A novel wavelet based hybrid method for finding the solutions of higher-order boundary value problems," *Ain Shams Eng. J.*, vol. 9, no. 4, pp. 3015–3031, Dec. 2018. https://doi.org/10.1016/j.asej.2017.12.006

View online: https://www.sciencedirect.com/science/article/pii/S2090447918300066
Published by Elsevier under the responsibility of Ain Shams University Cairo, Egypt

3. Non-Dyadic Wavelets Based Computational Technique for the investigation of Bagley-Torvik Equations.This paper has been published in the Scopus/UGC indexed journal: "International Journal on Emerging Technologies" with **SJR 0.12** (ISSN No. (Print): 0975-8364, (Online): 2249-3255).

Citation:

H. Kaur, R. Kumar, and G. Arora, "Non-dyadic wavelets based computational technique for the investigation of Bagley-Torvik equations," *Int. J. Emerg. Technol.*, vol. 10, no. 2, pp. 1–14, 2019.

View online: https://www.researchtrend.net/ijet/pdf/1%20IJET-MTH-00048.pdf

4. Scale-3 Haar wavelets and quasilinearization based hybrid technique for the solution of coupled space-time fractional-Burgers. This paper has been published ESCI/Scopus/UGC indexed journal with **SJR 0.16** (ISSN:0128-7680, e-ISSN:2231-8526).

Citation:

G. Arora, R. Kumar, and H. Kaur, "Scale-3 Haar wavelets and quasilinearization based hybrid technique for the solution of coupled space-time fractional-Burgers' equation," *Pertanika J. Sci. Technol.*, vol. 28, no. 2, pp. 579–607, 2020.

View online:
http://www.pertanika.upm.edu.my/Pertanika%20PAPERS/JST%20Vol.%2028%20(2)%20Apr.%202020/10%20JST-1776-2019.pdf

Published by the University Putra Malaysia

5. Haar Scale 3 Wavelet Based Solution of 1D- Hyperbolic Telegraph Equation. This paper has been published UGC indexed journal with ISSN:0971-1260.

Citation:

R. Kumar, "Haar Scale 3 Wavelet Based Solution of 1D- Hyperbolic Telegraph Equation," *Think India J.*, vol. 22, no. 16, pp. 4030–4042, 2019.

Viewonline:
https://journals.eduindex.org/index.php/thinkindia/article/view/17683/12693

Published by Eduindex.

6. Historical Development in Haar Wavelets and Their Application - An Overview. This paper has been published UGC indexed journal with ISSN:2349-5162.

Citation:

R. Kumar, "Historical Development in Haar Wavelets and Their Application - An Overview," *J. Emerg. Technol. Innov. Res.*, vol. 5, no. 11, pp. 1287–1296, 2018.

7. Construction of Non-Dyadic Wavelets Family and their Integral for Multiscale Approximation of Unknown Function. This paper has been published UGC indexed journal with ISSN:2349-5162.

Citation:

R. Kumar, "Construction of Non-Dyadic Wavelets Family and their Integral for Multiscale Approximation of Unknown Function," *J. Emerg. Technol. Innov. Res.*, vol. 5, no. 12, pp. 1–29, 2018.

8. New Scheme for the Solution of (2 + 1)-Dimensional Non-Linear Partial Differential Equations Using 2D-Haar Scale 3 Wavelets and θ − Weighted Differencing. This paper has been published UGC indexed journal with ISSN:2349-5162.

Citation:

R. Kumar, "New Scheme for the Solution of (2 + 1) - Dimensional Non-Linear Partial Differential Equations Using 2D-Haar Scale 3 Wavelets and θ − Weighted Differencing," *J. Emerg. Technol. Innov. Res.*, vol. 6, no. 1, pp. 194–203, 2019.

9. A Hybrid Scheme Based Upon Non-Dyadic Wavelets for the Solution of linear Sobolev Equations. This paper has been published UGC indexed journal with ISSN:2349-5162.

Citation:

R. Kumar, "A Hybrid Scheme Based Upon Non-Dyadic Wavelets for the Solution of linear Sobolev Equations," *J. Emerg. Technol. Innov. Res.*, vol. 6, no. 1, pp. 185–193, 2019.

9.3.1 International/National Conferences Attended

1. An international conference "Recent Advances in fundamental and Applied Science (RAFAS)" was attended on 25-26th November 2016 held at Lovely Professional University and a paper titled "Numerical solution by Haar wavelet collocation method for a class of higher-order linear and nonlinear boundary value problems" was presented (Details of the paper attached).
2. A national conference on "Recent Trends in Numerical Analysis and Computational Techniques" sponsored by DST-SERB, organized by Department of Applied Sciences, DAV Institute of Engineering and Technology, Jalandhar on March 28-29,2017 was attended and a paper titled "A Novel Wavelet-Based Hybrid Method for Finding the Solutions of Higher Order Boundary Value Problems" was presented (Details of the paper attached)
3. An international conference "International Conference on Functional Materials and Simulation Techniques (ICFMST)" jointly organized by the University of Mauritius, Concordia University and Chandigarh University was attended on 7th -8th June 2019 held at Chandigarh University Mohali and a paper titled "Non-Dyadic Wavelets Based Computational Technique for the investigation of Bagley-Torvik Equations" was presented (Details of the paper attached).
4. An international conference "Recent Advances in fundamental and Applied Science (RAFAS)" was attended on 05-06th November 2019 held at Lovely Professional University and a paper titled "Scale-3 Haar wavelets and quasilinearization based hybrid technique for the solution of coupled space-time fractional-Burgers." was presented (Details of the paper attached)

9.4 Proofs of Published Research Papers

Numerical solution by Haar wavelet collocation method for a class of higher order linear and nonlinear boundary value problems

Ratesh Kumar, Harpreet Kaur, and Geeta Arora

Citation: AIP Conference Proceedings **1860**, 020038 (2017); doi: 10.1063/1.4990337
View online: http://dx.doi.org/10.1063/1.4990337
View Table of Contents: http://aip.scitation.org/toc/apc/1860/1
Published by the American Institute of Physics

Numerical Solution by Haar Wavelet Collocation Method for a Class of Higher Order Linear and Nonlinear Boundary Value Problems

Ratesh Kumar[1, b)], Harpreet Kaur[2, a)] and Geeta Arora[1, c)]

[1]*Department of Mathematics, School of Physical Sciences, Lovely Professional University, Phagwara-144411 (Punjab), India*

[2]*Department of Mathematics, Punjab Institute of Technology, Kapurthala,I. K. Gujral Punjab Technical University(Punjab), India*

[a)] Corresponding author: maanh57@gmail.com
[b)] rateshqadian@gmail.com
[c)]geetadma@gmail.com

Abstract. In this paper, Haar wavelet collocation mechanism (HWCM) is developed for obtaining the solution of higher order linear and nonlinear boundary value problems. Mechanism is based on approximation of solution by Haar wavelet family. To tackle the nonlinearity in the problems, Quasilinearization technique is applied. Many examples are considered to prove the successful application of the mechanism developed for getting the highly accurate result. By using the HWCM, an approximate solution for higher order boundary value problems (HOBVPs) are obtained and compared with exact and numerical solutions available in the literature.

Keywords: Haar Wavelet, Quasilinearization, Collocation method and Boundary value problems (65L10)

INTRODUCTION

Higher order boundary value problems (HOBVPs) are getting huge attention from researchers because of the fact that many physical phenomena like hydro dynamic and hydromagnetic stability [1], induction motor with two rotor circuits [2], viscoelastic flows in fluid dynamics etc. are governed by the higher order boundary value problems. Therefore, to find accurate, efficient and simple solution of these problems has achieved the great significance during the last decades. Existence and uniqueness of solution of HOBVPs has been proved by Agarwal in his book [3]. General analytical solution for these kinds of problems has not yet been established. Therefore, researchers are using numerical techniques to find the solutions of HOBVPs. Many numerical mechanisms have been developed in the literature to solve these problems such as Adomian decomposition method (ADM), Variational Iteration Method (VIM), Variational Iteration Decomposition Method (VIDM), Optimal Homotopy asymptotic method (OHAM), Galerkin Method with Quintic B-splines (GMQBS), Legendre Galerkin method (LGM), Reproducing Kernel Space Method (RKSM), Modified Variational Iteration Method (MVID), Sextic B-splines Collocation Method (SBSCM), Petrov-Galerkin Method (PGM), Homotopy Perturbation Method (HPM), Quintic B-Spline Collocation Method (QBSCM) . But many of these methods involve cumbersome calculation process which slows down the rate of convergence and some of these methods are also very sensitive to the initial guess and can fall in the process of infinite iteration for the wrong initial guess and hence can increase the computational cost.

In the past decade wavelet based numerical method has become predominant because of its simple applicability and high accuracy. Wavelet is a small wave which can be manipulated in two ways; one way is translation which means shifting of all points of wavelet in the same direction and for the same distance and other is scaling or dilatation which means stretching or shrinking of original wavelet. Mathematically wavelet can be represented as

$$\psi_{a,b} = \frac{1}{\sqrt{|a|}}\psi\left(\frac{t-b}{a}\right) \quad \ldots (1)$$

Recent Advances in Fundamental and Applied Sciences
AIP Conf. Proc. 1860, 020038-1–020038-12; doi: 10.1063/1.4990337
Published by AIP Publishing. 978-0-7354-1534-8/$30.00

Ain Shams Engineering Journal 9 (2018) 3015–3031

Contents lists available at ScienceDirect

Ain Shams Engineering Journal

journal homepage: www.sciencedirect.com

A novel wavelet based hybrid method for finding the solutions of higher order boundary value problems

Geeta Arora [a], Ratesh Kumar [a,*], Harpreet Kaur [b]

[a] Department of Mathematics, School of Physical Sciences, Lovely Professional University, Phagwara 144411, Punjab, India
[b] Department of Mathematics, I. K. Gujral Punjab Technical University, Kapurthala, Punjab, India

ARTICLE INFO

Article history:
Received 18 September 2017
Revised 9 December 2017
Accepted 31 December 2017
Available online 8 November 2018

Keywords:
Non-dyadic wavelets
Quasi-linearization
Collocation method and boundary value problems (65L10)

ABSTRACT

In this paper, a new wavelet based hybrid method is developed for obtaining the solution of higher order linear and nonlinear boundary value problems. The proposed method is based on approximation of solution by non-dyadic wavelets family with dilation factor 3. Discretization of domain is done by collocation method. The nonlinearities in boundary value problems are tackled by Quasi-linearization technique. Eleven numerical experiments are performed on linear and nonlinear boundary value problems with order ranging from eighth to twelfth to prove the successful application of the proposed method. Also, the obtained solutions are compared with exact and numerical solutions available in the literature to prove the efficiency of the method over other methods.

1. Introduction

Many physical phenomena like hydro dynamic and hydromagnetic stability [1], induction motor with two rotor circuits [2], viscoelastic flows in fluid dynamics etc. are governed by the higher order boundary value problems. Higher order boundary value problems (HOBVPs) have been a major concern for the researchers, especially when these are nonlinear or higher order linear ODE with variable coefficients. Existence and uniqueness of solution for HOBVPs has already been established by Agarwal in his book [3]. But general closed form solution for these kinds of problems has yet not been established. Therefore, researchers are using numerical techniques to find the solutions of HOBVPs. Many numerical mechanisms have been developed by the researchers to solve these problems such as Variational Iteration Decomposition Method (VIDM) [4], Optimal Homotopy Asymptotic Method (OHAM) [5], Galerkin Method with Quintic B-splines (GMQBS) [6], Legendre Galerkin Method (LGM) [7], Reproducing Kernel Space Method (RKSM) [8], Variational Iteration Method (VIM) [9], Modified Variational Iteration Method (MVID) [10], Sextic B-splines Collocation Method (SBSCM) [11], Petrov-Galerkin Method (PGM) [12], Homotopy Perturbation Method (HPM) [13], Quintic B-Spline Collocation Method (QBSCM) [14], Haar Wavelet Colocation Method (HWCM) [15] with dilation factor 2, Modified Adomian Decomposition Method (MADM) [16] etc.

Wavelet based numerical techniques are one of the latest techniques in mathematical theory of approximation which are in considerable qualitative progress in comparison with other methods. Majority of the work has been done by using dyadic wavelets. Till date no literature is available for the use of non-dyadic wavelets in finding the solution of higher order boundary value problems. The existence of non-dyadic wavelets have been proved by Chui and Lian [17] in 1995 in the study of construction of wavelets. This motivates and inspires us to use non-dyadic wavelet with collocation method for the solution of HOBVPs. In the present study, a new wavelet based hybrid method is developed by using non-dyadic wavelet with collocation method.

The main objective of our work is to establish a non-dyadic Haar wavelet based collocation technique for numerical solution of linear and nonlinear HOBVPs emerging in many physical phenomena. To test the efficiency and accuracy of the method, we consider the general HOBVPs of the type

$$x^n(t) = f\left(t, x, x', x'' \cdots x^{n-1}\right) \quad a \le t \le b \tag{1.1}$$

with the following types of constraints on the solution at the boundary points

* Corresponding author.
E-mail address: ratesh.11755@lpu.co.in (R. Kumar).
Peer review under responsibility of Ain Shams University.

Production and hosting by Elsevier

https://doi.org/10.1016/j.asej.2017.12.006
2090-4479/

International Journal on Emerging Technologies 10(2a): 14-26(2019)

ISSN No. (Print): 0975-8364
ISSN No. (Online): 2249-3255

Non-Dyadic Wavelets Based Computational Technique for the investigation of Bagley-Torvik Equations

Harpreet Kaur[1], Ratesh Kumar[2] and Geeta Arora[2]
[1]Department of Mathematics, I.K. Gujral Punjab Technical University, Kapurthala, India
[2]Department of Mathematics, Lovely Professional University, Phagwara, India

(Corresponding author: Ratesh Kumar, rateshqadian@gmail.com)
(Received 02 April 2019, Revised 01 June 2019 Accepted 08 June 2019)
(Published by Research Trend, Website: www.researchtrend.net)

ABSTRACT: The aim of proposed study is to develop a new hybrid method using the non-dyadic wavelets for the investigation of Bagley-Torvik Equation. Non-dyadic wavelets are used to estimate the solution by series approximation. To handle the fractional derivatives and integrals in the problem, Caputo sense definition of derivatives and Riemann-Liouville definitions of integrals are used. Numerical solution has been produces for five different fractional Bagley-Torvik Equations to establish the competency of the proposed method.

Keywords: Non-dyadic wavelets, Bagley-Torvik Equation, Caputo derivatives, Quasi-linearization, Fractional differential equations (65L10)

I. INTRODUCTION

Fractional calculus is a branch of applied mathematics which emerges as a great tool in explaining the physical and chemical phenomenon with alienate kinetics having microscopic complex behavior. There are fractional differential models which have a non-differentiable but continuous solution such as Weierstrass type functions [1]. These kinds of characteristics are not possible to explain with the help of ordinary or partial differential models. Earlier the field of fractional calculus was purely mathematical without any visible application but in these days, fractional calculus has gained a huge importance in the field of science and technology because of its application in the various field like theory of thermo-elasticity [2], viscoelastic fluids [3], dynamics of earthquakes [4], fluid dynamics [5] etc. Bagley-Torvik equation is one of the most important fractional model in the field of viscoelastic fluids. In this model, Bagley and Torvik has studied the motion of rigid plate immersed into the Newtonian fluid. It is found in the experiment that retarding force are proportional to the fractional derivative of the displacement instead of the velocity. It has been observed during the experiment that fractional model is superior than the integer order model for the prediction of characteristics of the same material. But general closed-form solution for fractional Bagley-Torvik equation has yet not been established. Therefore, many researchers are involved in developing the various numerical and semi-analytic schemes for investigating the different phenomena governed by the Bagley-Torvik equation such as Adomian decomposition method [6], Variational iteration method [7], Homotopy analysis method[8], Generalized Taylor collocation method [9], Haar wavelet method with dailation factor 2[10], Fractional iteration method [11], Bessel collocation method [12], Chebyshev wavelet method [13], Fractional Taylor Method [14], Hybrid functions approximation [15], Gegenbauer Wavelet Method [16], Reproducing kernel algorithm [17], Sumudu transformation method [18] etc.

But the study of characteristics of different materials governed by Bagley Torvik equations has yet not been investigated by non-dyadic wavelet-based technique. Wavelets are one of the modernistic orthonormal functions which have a capability of dilation and translation. Because of these properties, numerical techniques which involve wavelets bases are showing the qualitative improvement in contrast with other methods. In literature, dyadic wavelets are in preponderance. In 1995, Chui and Lian [19] has developed the non-dyadic wavelets by using the process of multire solution analysis. In 2018, Mittal and Pandit have used the non-dyadic wavelets [20]–[22] for solving the various types of differential equations and found that these wavelet bases are equally competent in solving the various types of mathematical models governed by differential equations. Also, it was shown by them that the non-dyadic wavelet has a faster rate of convergence as compared to the dyadic wavelets. Moreover, investigation of characteristics of the solution to the Bagley Torvik equation has yet not been done by non-dyadic wavelet methods. This encourages us to develop a new technique using non-dyadic wavelet for analyzing the behavior of systems governed by the Bagley Torvik equation.

The prime purpose of proposed work is to establish a new computational technique for obtaining the solution of following types of Bagley Torvik equations emerging in the field of fluid dynamics using non-dyadic wavelet bases.

$$\begin{cases} \alpha D^2 x(t) + \beta D^{\frac{3}{2}} x(t) + \gamma D^{\frac{1}{2}} x(t) + x(t) = g(t) \\ with \\ boundary\ conditions \\ x(0) = \delta_0 , x(1) = \delta_1 \\ or \\ x(0) = \delta_2 , x'(1) = \delta_3 \end{cases} \quad (1)$$

Pertanika J. Sci. & Technol. 28 (2): 579 - 607 (2020)

PERTANIKA JOURNALS

SCIENCE & TECHNOLOGY

Journal homepage: http://www.pertanika.upm.edu.my/

Scale-3 Haar Wavelets and Quasilinearization based Hybrid Technique for the Solution of Coupled Space-Time Fractional - Burgers' Equation

Geeta Arora[1], Ratesh Kumar[1]* and Harpreet Kaur[2]

[1]*Department of Mathematics, Lovely Professional University, Punjab, India*
[2]*Department of Mathematics, I.K. Gujral Punjab Technical University, Punjab, India*

ABSTRACT

The aim of this study is to develop a hybrid method using scale 3 Haar wavelets for obtaining the solution of coupled space-time fractional Burgers' equation. Scale 3 Haar wavelets were used to estimate the solution by series approximation. Caputo and Riemann-Liouville definitions were used to handle the fractional derivatives and integrals in the problem. A quasi-linearization technique was implemented to handle the nonlinearity in the problems. Two examples of coupled space-time fractional Burgers' equations were studied to analyze the performance of the proposed technique.

Keywords: Caputo derivatives, fractional coupled Burgers' Equation, Quasi-linearization, Riemann-Liouville integration, scale 3 Haar wavelets

INTRODUCTION

Fractional calculus emerges as a great tool in explaining the physical and chemical phenomenon with alienate kinetics having microscopic complex behavior. There are fractional differential models which have a non-differentiable but continuous solution such as Weierstrass type functions (Zahle & Ziezold, 1996). These kinds of characteristics are not possible to explain with the help of ordinary or partial differential models. Earlier the field of fractional calculus was purely mathematical without any visible application but in these days, fractional calculus has gained a huge importance in the field of science and technology because of its application in the various field like theory of thermo-elasticity (Povstenko, 2009), viscoelastic fluids (Tripathi et al., 2010), dynamics of earthquakes (Lopes et al., 2013) and fluid dynamics (Momani & Odibat, 2006a). It

ARTICLE INFO

Article history:
Received: 15 September 2019
Accepted: 02 January 2020
Published: 15 April 2020

E-mail addresses:
geetadma@gmail.com (Geeta Arora)
rateshqadian@gmail.com (Ratesh Kumar)
maanh52@gmail.com (Harpreet Kaur)
* Corresponding author

ISSN: 0128-7680
e-ISSN: 2231-8526

THINK INDIA JOURNAL

ISSN: 0971-1260
Vol-22-Issue-16-August-2019

Haar (Scale 3) Wavelet Based Solution of 1D- Hyperbolic Telegraph Equation.

Ratesh Kumar

ratesh.11755@lpu.co.in

School of Chemical Engineering and Physical Sciences

Lovely Faculty of Technology and Sciences

Lovely Professional University, Phagwara-144411, Punjab, India

Abstract. The main focus of the current work is to introduce the new numerical technique based upon theHaar scale 3 wavelets for the solution of 1D- hyperbolic telegraph equation. In this scheme,spatial discretization is done by scale 3 Haar wavelets. The collocation method is used with Haar scale 3 wavelets to convert 1D- hyperbolic telegraph equation into the system of algebraic equations which are further solved with the help of Thomas algorithm. The proposed scheme is tested on four different equations of above said types to establish the competency of the proposed scheme.

Keywords: Scale 3 Haar wavelets,1D- hyperbolic telegraph equation, Partial differential Equations (65L10)

1. Introduction

The prime objective of current work is to provide new numerical technique for obtaining the solution of second order hyperbolic Telegraph equation of the following type, using two-dimensional Haar Scale 3 wavelet bases.

$$\frac{\partial^2\varphi}{\partial t^2} + 2\alpha\frac{\partial\varphi}{\partial t} + \beta^2\varphi = \frac{\partial^2\varphi}{\partial x^2} + g(x,t), (x,t) \in [0,1] \times [0,T] \tag{1.1}$$

under the following types of initial constraints

$$\varphi(x,0) = \psi_1(x)$$

$$\frac{\partial\varphi}{\partial t}(x,0) = \psi_2(x)$$

and the boundary constraints

$$\varphi(0,t) = \xi_1(t), \quad t \in [0,T]$$

$$\varphi(1,t) = \xi_2(t), \quad t \in [0,T]$$

Where $\alpha > \beta \geq 0$ are known constants, $\psi_1(x), \psi_2(x), \xi_1(t), \xi_2(t), g(x,t)$ are the given functions and $\varphi(x,t)$ is the function whose value is to be determined. When $\alpha > 0, \beta = 0$ then equation represents the damped wave motion equation and when $\alpha > \beta > 0$ then it isnamed asthe telegraph Equation. These types of equations emerging in the fieldof electric signal propagation in cables[1], pulsate blood flow in the arteries[2], 'acoustic wave propagation' in porous media of Darcy-type[3], vibrations in the different structures,

Historical Development in Haar Wavelets and Their Application - An Overview

Ratesh Kumar

School of Chemical Engineering and Physical Sciences,

Lovely Professional University, Punjab.

Abstract: - In this paper, basic idea of wavelets, its connection with Fourier expansion and advantages of wavelet expansion over Fourier expansion is reviewed. Further the idea of removing Gibb's phenomena over Fourier phenomena is also discussed. The discrete wavelet transform is very much useful in solving the various problems in the field of science and technology. Therefore, these transformations have attained very good prestige of being very effective individually and by getting hybrid with other established techniques in solving the many of the real time problems. One of the oldest and mathematically most simple as compared with other wavelets which owes its origin to 1910 is the Haar wavelet. This review aims to provide the fantastic application of Haar wavelets in solving the various problem of science and technology. In current article some computational and mathematical capabilities of Haar wavelets and diverse applications in various field have been reviewed. Some future scope in the direction of developing the new hybrid method for solving the various advance problems have also been discussed.

Introduction

The decomposition, synthesis and analysis of functions, in various function spaces, is one of the most useful activities of mathematics, mathematical physics and lastly of Data/signal processing in engineering. It is one of the most intensively studied topics in mathematics since the beginning of 19th century. The bold declaration of Fourier (Pinsky, (2002)), about expressing any periodic function in the form of trigonometric series kept the entire scientific community on alert for nearly two centuries-especially in establishing convergence, uniform

convergence etc of Fourier Series. In this process one finds blossoming of rich topics like Lebesgue integral, functions of striking theories in Banach space, Hilbert space etc.

A function has power series representation if it is smooth and gives its local structure accurately. Fourier series of functions with classical orthogonal functions is useful for the global analysis of functions. These can be used for representing functions with no smoothness properties but they are inefficient for analysing the detail behaviour of a function near a point. A pure Fourier basis diagonalizes translation invariant linear operators. We look for a basis (of function spaces) that is well localized in frequency and nearly diagonalizes the operator i.e. their matrix entries decay rapidly away from the diagonal. Also, it is desirable a basis to be well localized in space for effective local analysis. What is missing is a method for analysing the local irregular behaviour of functions that aren't smooth and this is where wavelets come into play. Wavelet is a small impulsive function which can be operated in two ways; one way is translation w.r.t the initial condition

Construction of Non-Dyadic Wavelets Family and their Integral for Multiscale Approximation of Unknown Function

Ratesh Kumar

School of Chemical Engineering and Physical Sciences

Lovely Faculty of Technology and Sciences

Lovely Professional University, Phagwara-144411, Punjab, India

Abstract

The main focus of the current work is to construct a compactly supported non-dyadic orthonormal wavelet family with scale factor 3. Orthonormal wavelet families are very much helpful in solving the various problems arises in the field of science and technology. For the construction of non-dyadic wavelet family, multi-resolution analysis (MRA) technique is used on trivial Haar scale 3 type function given by C.K Chui. Integrals of members of non-dyadic wavelet family have been calculated for their usein multiscale approximation of unknown function running in various types differential or integral equation. Matrices of Haar Scale 3 wavelets and their integrals have constructed for their use in solving the various types of differential and integral equations. Two numerical experiments have been conducted to test the efficiency of the given wavelet family in approximating the unknown function.

1 Haar Scale 3 Wavelets Family

Let us Consider any two arbitrary integers $\mathcal{A}$, $\mathcal{B}$ such that $\mathcal{B} > A$. let J be the maximum level of resolution to be considered for phenomena under study. Define new quantities $M, j, k. p$ such that $M = 3^J, p = 3^j$, $j = 0,1,2, \dots J$, $k = 0,1,2, \dots, p-1$, where j denotes the level of resolution and $k$the translation in wavelets. Now divide the interval $[\mathcal{A}, \mathcal{B})$ into $3M$ uniform subinterval of equal length $\Delta t = \frac{\mathcal{B}-\mathcal{A}}{3M}$. When J=0, $\mathcal{A} = 0$ and $\mathcal{B} = 1$ then we have the following members in Haar Scale 3 wavelet family[1] (Haar Scale 3 wavelet family).

$$h_1(t) = \psi^0(t) = \begin{cases} 1 & 0 \le t < 1 \\ 0 & elsewhere \end{cases} \qquad (1.1)$$

$$h_2(t) = \psi^1(t) = \frac{1}{\sqrt{2}} \begin{cases} -1 & 0 \le t < \frac{1}{3} \\ 2 & \frac{1}{3} \le t < \frac{2}{3} \\ -1 & \frac{2}{3} \le t < 1 \\ 0 & elsewhere \end{cases} \qquad (1.2)$$

A Hybrid Scheme Based Upon Non-Dyadic Wavelets for the Solution of linear Sobolev Equations

Ratesh Kumar

School of Chemical Engineering and Physical Sciences

Lovely Faculty of Technology and Sciences

Lovely Professional University, Phagwara-144411, Punjab, India

Abstract. The current work aims to introduce a hybrid technique based upon the θ −weighted differencing and non-dyadic wavelets for the solution of (2+1)-dimensional linear Sobolev Equations etc. In the scheme, time discretization is done by the θ −weighted finite differencing scheme and spatial discretization is done by Non-dyadic wavelets. The proposed scheme is tested on five different linear and nonlinear equations of above said types to establish the competency of the proposed scheme.

Keywords: Non-dyadic wavelets, Theta weighted finite difference, Quasilinearization, Partial differential Equations (65L10)

1 Introduction

Sobolev equations belong to the important class of partial differential equations in which the highest order derivative present in the differential equation contains mixed derivative. with respect to time and space. These types of equations have a convincing physical background because of its huge use in Soil moisture migration [1], drainage of liquids through rocks having cracks [2], heat conduction Continuum Mechanics[3], etc. The extensive appearance of these kinds of equations in the mathematical modelling of different phenomena occurring in science and technology have gained the attention of the scientific community. But the analytic solutions Sobolev equations are very cumbersome to achieve. Therefore, many researchers are involved in developing the various numerical and semi-analytic schemes for finding solutions to the different problems governed by these differential equations. Some of the methods which have been recently developed and applied to solve the two-dimensional Sobolev and BBMB equations are Expanded Mixed Finite Element Method (EMFEM)[4] , Local Discontinuous Galerkin Method (LDGM)[5], Collocation Spectral Method (CSM)[6], Crank-Nicolson Finite Volume Element Method(CNFVM) [7], Haar Wavelet Method[8].

But the study of establishing the solution for (2+1) dimensional partial differential equations using the non-dyadic wavelets has not been attempted in the literature which motivated us to develop a new technique for the solution of these types of equations. Wavelets are one of the modernistic orthonormal functions which have a capability of dilation and translation. Because of these properties, numerical techniques which involve wavelets bases are showing the qualitative improvement in contrast with other methods. In literature, dyadic wavelets are in preponderance. In 1995, Chui and Lian [9] has developed the non-dyadic wavelets by using the process of multiresolution analysis. In 2018, Mittal and Pandit have used the non-dyadic wavelets [10]–[13] for solving the various types of differential equations and found that these wavelet bases are equally competent in solving the various types of mathematical models governed by differential equations. Also, it was shown by them that the non-dyadic wavelet has a faster rate of convergence as compared to the dyadic wavelets. This gives us good hope of getting a better solver for these equations by developing a new hybrid technique based upon θ −Weighted Differencing and Non-Dyadic Wavelets for the solution of (2+1) dimensional partial differential equations.

The manuscript follows the sequence of sections as described: In section 2, explicit forms of non-dyadic parent wavelets with their families and procedure to find their integrals have been explained briefly. Representation of the solution using non-dyadic wavelets is explained in section 3. Section 4 explains the method of solution using non-dyadic wavelets. In section 5, the convergence of the method is discussed. In

New Scheme for the Solution of (2+1)-Dimensional Non-Linear Partial Differential Equations Using 2D-Haar Scale 3 Wavelets and θ −Weighted Differencing

Ratesh Kumar

School of Chemical Engineering and Physical Sciences

Lovely Faculty of Technology and Sciences

Lovely Professional University, Phagwara-144411, Punjab, India

Abstract. Current article proposes a hybrid technique based upon the θ −weighted differencing and Haar scale 3 wavelets for the solution of (2+1)-dimensional non-linear partial differential equations such as Sobolev and BBMB (Benjamin–Bona–Mahony–Burgers) Equations etc. In this scheme, time discretization is done by the θ −weighted finite differencing scheme and spatial discretization is done by 2D-Haar scale 3 wavelets. The quasilinearization process is used wherever we encountered with the non-linearity in the equations. The proposed scheme is tested on some nonlinear equations of above said types to establish the competency of the proposed scheme.

Keywords: Haar scale 3 wavelets, Theta weighted finite difference, Quasilinearization, Partial differential Equations (65L10)

1 Introduction

To study the dynamics of any real-time phenomenon happening around us, one of the most accurate approaches is by using a mathematical model of it. It is said that where there is a motion there is a differential equation corresponding to it. Mathematical modelling for a majority of real-time phenomena's results into a partial differential equation. Partial differential equations are playing a very important role in predicting the world around us. It can be seen in the literature that the numbers of phenomenon in science and technology have been studies via non-linear partial differential equations. Most of the non-linear partial differential equations do not possess any closed-form solution. Moreover, finding the solution of such equations becomes more challenging when there is a nonlinearity in the higher dimensional equation.

The main purpose of our study is to introduce a new hybrid scheme based upon the θ −weighted differencing and Haar scale 3 wavelets for the solution of following types of three-dimensional non-linear partial differential equations

$$\varphi_t - (\Delta\varphi)_t - \alpha\Delta\varphi + \beta\,\nabla\varphi + \gamma\,\nabla.(\varphi\nabla\varphi) + \delta\varphi^2 = \mu\,\nabla.\big(F(\varphi)\big) + f\,(x,y,t), (x,y) \in \Omega, t > 0 \quad (1.1)$$

subjected to initial and boundary constraints

$$\varphi(x,y,0) = g(x,y) \qquad \forall\,(x,y) \in \Omega \quad (1.2)$$

$$\varphi(x,y,t) = h(x,y,t) \qquad \forall\,(x,y) \in \partial\Omega, \mathrm{t} \in [0,T] \quad (1.3)$$

where Ω is any closed and bounded domain contained in $\mathcal{R}^2$ with smooth or piecewise smooth boundary represented by $\partial\Omega$. $F(\varphi)$ is a non-linear function of φ , $f\,(x,y,t)$, is the source term and α , β , γ, δ, μ are the real constants. In the present study, we will restrict ourselves to the following special cases of the equation no. (1.1) under the boundary and initial constraints represented by equations (1.2)-(1.3).

Case 1: On taking $\alpha = 1$, $\beta = 1$, $\gamma = 0, \delta = 0, \mu = 1$, Equation no. (1.1) reduced to

$$\varphi_t - (\Delta\varphi)_t - \Delta\varphi + \nabla\varphi = \nabla.\big(F(\varphi)\big) + f\,(x,y,t), (x,y) \in \Omega, t > 0 \quad (1.4)$$

which is known as NBBMB (non-linear Benjamin Bona Mahony Burgers) equation.

References

[1] M. Zahle and H. Ziezold, “Fractional derivatives of Weierstrass-type functions,” *J. Comput. Appl. Math.*, vol. 76, no. 1–2, pp. 265–275, 1996.

[2] Y. Z. Povstenko, “Thermoelasticity that uses fractional heat conduction equation,” *J. Math. Sci.*, vol. 162, no. 2, pp. 296–305, 2009, doi: 10.1007/s10958-009-9636-3.

[3] D. Tripathi, S. K. Pandey, and S. Das, “Peristaltic flow of viscoelastic fluid with fractional Maxwell model through a channel,” *Appl. Math. Comput.*, vol. 215, no. 10, pp. 3645–3654, 2010, doi: 10.1016/j.amc.2009.11.002.

[4] A. M. Lopes, J. A. Tenreiro Machado, C. M. A. Pinto, and A. M. S. F. Galhano, “Fractional dynamics and MDS visualization of earthquake phenomena,” *Comput. Math. with Appl.*, vol. 66, no. 5, pp. 647–658, 2013, doi: 10.1016/j.camwa.2013.02.003.

[5] S. Momani and Z. Odibat, “Analytical approach to linear fractional partial differential equations arising in fluid mechanics,” *Phys. Lett. Sect. A Gen. At. Solid State Phys.*, vol. 355, no. 4–5, pp. 271–279, 2006, doi: 10.1016/j.physleta.2006.02.048.

[6] S. Das, *Functional Fractional Calculus*, Second. Berlin Heidelberg: Springer-Verlag, 2011.

[7] M. Abdelouahab and N. Hamri, “The Grunwald–Letnikov Fractional-Order Derivative with Fixed Memory Length,” *Mediterr. J. Math.*, vol. 13, no. 2, pp. 557–572, 2016, doi: 10.1007/s00009-015-0525-3.

[8] A. Haar, “Zur theorie der orthogonalen funktionen systeme,” *Math. Ann.*, vol. 69, no. 3, pp. 331–371, 1910, doi: 10.1007/BF01456326.

[9] S. G. Mallat, “Multiresolution approximations and wavelet orthonormal bases for approximating L2(R) functions,” *Trans. Am. Math. Soc.*, vol. 315, no. 1, pp.

69–87, 1989, doi: 10.1090/S0002-9947-1989-1008470-5.

[10] Meyer Y, “Orthonormal wavelets. In: Combers JM, Grossmann A, Tachamitchian P (eds) Wavelets, time-frequency methods and phase space.” Springer-Verlag, Berlin, 1989.

[11] I. Daubechies, “Orthonormal bases of compactly supported wavelets,” *Commun. Pure Appl. Math.*, vol. 41, no. 7, pp. 909–996, 1988, doi: 10.1002/cpa.3160410705.

[12] I. Daubechies, “Ten Lectures of Wavelets,” *CBMS-NSF Regional Conference Series in Applied Mathematics*. Springer-Verlag, Berlin, 1992, doi: http://dx.doi.org/10.1137/1.9781611970104.

[13] V. Mishra and Sabina, “Wavelet Galerkin solutions of ordinary differential equations,” *Int. J. Math. Anal.*, vol. 5, no. 9–12, pp. 407–424, 2011.

[14] N. Truong and S. Gilbert, *Wavelets and Filter Banks*. Wellesley Cambridge Press , USA, 1996.

[15] C. F. Chen and C. H. Hsiao, “Haar wavelet method for solving lumped and distributed-parameter systems,” *IEE Proc. - Control Theory Appl.*, vol. 144, no. 1, p. 87, 1997, doi: 10.1049/ip-cta:19970702.

[16] Ü. Lepik, “Application of Wavelet Transform Techniques To Vibration Studies,” *Proc. Est. Acad. Sci. Phys. Math*, vol. 50, no. 3, pp. 155–168, 2001.

[17] Ü. Lepik and E. Tamme, “Numerical solution of differential equations using Haar wavelets,” *Dyn. Syst. Appl. Proc.*, vol. Proceeding, no. July, pp. 494–507, 2004.

[18] Ü. Lepik, “Numerical solution of differential equations using Haar wavelets,” *Math. Comput. Simul.*, vol. 68, no. 2, pp. 127–143, 2005, doi: 10.1016/j.matcom.2004.10.005.

[19] Ü. Lepik, “Numerical solution of evolution equations by the Haar wavelet method,” *Appl. Math. Comput.*, vol. 185, no. 1, pp. 695–704, 2007, doi: 10.1016/j.amc.2006.07.077.

[20] Ü. Lepik, “Application of the Haar wavelet transform to solving integral and differential equations,” *Proc. Est. Acad. Sci. Phys. Math*, vol. 56, no. 1, pp. 28–46, 2007, doi: 10.1117/12.736416.

[21] Ü. Lepik and E. Tamme, “Solution of nonlinear Fredholm integral equations via the Haar wavelet method,” *Proc. Est. Acad. Sci. Phys. Math.*, vol. 56, no. 1, pp. 17–27, 2007.

[22] Ü. Lepik, “Solving integral and differential equations by the aid of non-uniform Haar wavelets,” *Appl. Math. Comput.*, vol. 198, no. 1, pp. 326–332, 2008, doi: 10.1016/j.amc.2007.08.036.

[23] P. Chang and P. Piau, “Haar Wavelet Matrices Designation in Numerical Solution of Ordinary Differential Equations,” *IAENG Int. J. Appl. Math.*, vol. 38, no. 3, pp. 164–168, 2008.

[24] Ü. Lepik, “Solving fractional integral equations by the Haar wavelet method,” *Appl. Math. Comput.*, vol. 214, no. 2, pp. 468–478, 2009, doi: 10.1016/j.amc.2009.04.015.

[25] E. Babolian and A. Shahsavaran, “Numerical solution of nonlinear Fredholm integral equations of the second kind using Haar wavelets,” *J. Comput. Appl. Math.*, vol. 225, no. 1, pp. 87–95, 2009, doi: 10.1016/j.cam.2008.07.003.

[26] G. Hariharan and K. Kannan, “Haar wavelet method for solving some nonlinear Parabolic equations,” *J. Math. Chem.*, vol. 48, no. 4, pp. 1044–1061, 2010, doi: 10.1007/s10910-010-9724-0.

[27] G. Hariharan, “Solving Finite Length Beam Equation by the Haar Wavelet Method,” *Int. J.*, vol. 9, no. 1, pp. 27–34, 2010, doi: 10.5120/1349-1819.

[28] G. Hariharan, “Haar Wavelet Method for Solving the Klein-Gordon and the Sine-Gordon Equations,” *Int. J. Nonlinear Sci.*, vol. 11, no. 2, pp. 180–189, 2011.

[29] Ü. Lepik, “Exploring vibrations of cracked beams by the Haar wavelet method,” *Est. J. Eng.*, vol. 17, no. 3, pp. 271–284, 2011, doi: 10.3176/eng.2012.1.05.

[30] V. Mishra, H. Kaur, and R. C. Mittal, “Haar Wavelet Algorithm for Solving Certain,” *Int. J. Appl. Math Mech*, vol. 8, no. 6, pp. 69–82, 2011.

[31] Ü. Lepik, “Solving PDEs with the aid of two-dimensional Haar wavelets,” *Comput. Math. with Appl.*, vol. 61, no. 7, pp. 1873–1879, 2011, doi: 10.1016/j.camwa.2011.02.016.

[32] N. Berwal, D. Panchal, and C. . L. . Parihar, “Solution of Wave-Like Equation Based on Haar Wavelet,” *LE Math.*, vol. 67, no. II, pp. 157–167, 2012, doi: 10.4418/2012.67.2.12.

[33] G. Hariharan, “Wavelet method for a class of fractional Klein-Gordon equations,” *J. Comput. Nonlinear Dyn.*, vol. 8, no. 2, pp. 1–6, 2013, doi: 10.1115/1.4006837.

[34] S. Sekar and C. Jaisankar, “Numerical Solution for The Integro-Differential Equations Using Single Term Haar Wavelet Series Method,” *Int. J. Math. Arch.*, vol. 4, no. 11, pp. 97–103, 2013.

[35] N. Berwal, D. Panchal, and C. L. Parihar, “Numerical solution of series L−C−R equation based on Haar wavelet,” *Ital. J. pure Appl. Math.*, vol. 30, pp. 157–166, 2013.

[36] H. Kaur, V. Mishra, and R. C. Mittal, “Numerical Solution of a Laminar Viscous Flow Boundary Layer Equation Using Uniform Haar Wavelet Quasi-linearization Method,” *World Acad. Sci. Eng. Technol.*, vol. 79, no. 5, pp. 1682–1687, 2013.

[37] U. Saeed and M. U. Rehman, “Haar wavelet operational matrix method for fractional oscillation equations,” *Int. J. Math. Math. Sci.*, vol. 2014, no. August, pp. 1–9, 2014, doi: 10.1155/2014/174819.

[38] U. Saeed and M. U. Rehman, “Assessment of Haar Wavelet-Quasilinearization Technique in Heat Convection-Radiation Equations,” *Appl. Comput. Intell. Soft Comput.*, vol. 2014, no. 1, pp. 1–5, 2014, doi: 10.1155/2014/454231.

[39] R. C. Mittal, H. Kaur, and V. Mishra, “Haar wavelet-based numerical

investigation of coupled viscous Burgers' equation," *Int. J. Comput. Math.*, vol. 92, no. 8, pp. 1643–1659, 2014, doi: 10.1080/00207160.2014.957688.

[40] Asmita C. Patel & V. H. Pradhan, "Wavelet Galerkin Scheme for Nonlinear Partial Differential Equations," *Int. J. Res. Applied, Nat. Soc. Sci.*, vol. 2, no. 8, pp. 69–78, 2014.

[41] S. Arora, Y. S. Brar, and S. Kumar, "Haar Wavelet Matrices for the Numerical Solutions of Differential Equations," *Int. J. Comput. Appl.*, vol. 97, no. 18, pp. 33–36, 2014.

[42] H. M. Osama, S. F. Fadhel, and A. M. Zaid, "Numerical Solution of Fractional Variational Problems Using Direct Haar Wavelet Method," *Int. J. Innov. Res. Sci. Eng. Technol.*, vol. 3, no. 5, pp. 1–9, 2014.

[43] S. S. Ray, "Two reliable approaches involving Haar wavelet method and Optimal Homotopy Asymptotic method for the solution of fractional Fisher type equation," *J. Phys. Conf. Ser.*, vol. 574, p. 012131, 2015, doi: 10.1088/1742-6596/574/1/012131.

[44] Ö. Oruç, F. Bulut, and A. Esen, "A Haar wavelet-finite difference hybrid method for the numerical solution of the modified Burgers' equation," *J. Math. Chem.*, vol. 53, no. 7, pp. 1592–1607, 2015, doi: 10.1007/s10910-015-0507-5.

[45] M. Kumar and S. Pandit, "An efficient algorithm based on Haar wavelets for numerical simulation of Fokker-Planck equations with constants and variable coefficients," *Int. J. Numer. Methods Heat Fluid Flow*, vol. 25, no. 1, pp. 41–56, 2015, doi: 10.1108/HFF-03-2014-0084.

[46] S. C. Shiralashetti and A. B. Deshi, "An efficient Haar wavelet collocation method for the numerical solution of multi-term fractional differential equations," *Nonlinear Dyn.*, vol. 83, no. 1–2, pp. 293–303, 2016, doi: 10.1007/s11071-015-2326-4.

[47] M. Fallahpour, M. Khodabin, and K. Maleknejad, "Approximation solution of two-dimensional linear stochastic Volterra integral equation by applying the Haar wavelet," *Int. J. Math. Model. Comput.*, vol. 5, no. 4, pp. 361–372, 2015.

[48] S. C. Shiralashetti, A. B. Deshi, and P. B. Mutalik Desai, “Haar wavelet collocation method for the numerical solution of singular initial value problems,” *Ain Shams Eng. J.*, vol. 1, pp. 4–11, 2015, doi: 10.1016/j.asej.2015.06.006.

[49] I. Singh, S. Arora, and S. Kumar, “Numerical Solution Of Wave Equation Using Haar Wavelet,” *Int. J. Pure Appl. Math.*, vol. 98, no. 4, pp. 457–469, 2015, doi: 10.12732/ijpam.v98i4.4.

[50] S. C. Shiralashetti, M. H. Kantli, and A. B. Deshi, “Haar wavelet based numerical solution of nonlinear differential equations arising in fluid dynamics,” *Int. J. Comput. Mater. Sci. Eng.*, vol. 05, no. 02, p. 1650010, 2016, doi: 10.1142/S204768411650010X.

[51] S. C. Shiralashetti, L. M. Angadi, A. B. Deshi, and M. H. Kantli, “Haar wavelet method for the numerical solution of Klein–Gordan equations,” *Asian-European J. Math.*, vol. 09, no. 01, pp. 1650012(1–14), 2016, doi: 10.1142/S1793557116500121.

[52] F. A. Shah, R. Abass, and L. Debnath, “Numerical Solution of Fractional Differential Equations Using Haar Wavelet Operational Matrix Method,” *Int. J. Appl. Comput. Math.*, vol. 1, pp. 1–23, 2016, doi: 10.1007/s40819-016-0246-8.

[53] A. C. Patel and V. H. Pradhan, “Numerical solution of one dimensional contaminant transport equation with variable coefficient (temporal) by using Haar wavelet,” *Glob. J. Pure Appl. Math.*, vol. 12, no. 2, pp. 1283–1292, 2016.

[54] Ö. Oruç, F. Bulut, and A. Esen, “Numerical Solutions of Regularized Long Wave Equation By Haar Wavelet Method,” *Mediterr. J. Math.*, vol. 13, no. 5, pp. 3235–3253, 2016, doi: 10.1007/s00009-016-0682-z.

[55] H. Kaur and S. M. Kang, “Haar Wavelets Based Time Discretization Technique for Solving Nonlinear Partial Differential Equations,” *Int. J. Pure Apllied Math.*, vol. 108, no. 1, pp. 63–78, 2016, doi: 10.12732/ijpam.v108i1.8.

[56] S. C. Shiralashetti, L. M. Angadi, M. H. Kantli, and A. B. Deshi, “Numerical solution of parabolic partial differential equations using adaptive gird Haar wavelet collocation method,” *Asian-European J. Math.*, vol. 10, no. 1, pp. 1–11,

2016, doi: 10.1142/S1793557117500267.

[57] S. Foadian, R. Pourgholi, S. H. Tabasi, and J. Damirchi, “The inverse solution of the coupled nonlinear reaction–diffusion equations by the Haar wavelets,” *Int. J. Comput. Math.*, vol. 96, no. 1, pp. 105–125, 2019, doi: 10.1080/00207160.2017.1417593.

[58] B. Prakash, A. Setia, and D. Alapatt, “Numerical solution of nonlinear fractional SEIR epidemic model by using Haar wavelets,” *J. Comput. Sci.*, vol. 22, pp. 109–118, 2017, doi: 10.1016/j.jocs.2017.09.001.

[59] M. Erfanian, M. Gachpazan, and H. Beiglo, “A new sequential approach for solving the integro-differential equation via Haar wavelet bases,” *Comput. Math. Math. Phys.*, vol. 57, no. 2, pp. 297–305, 2017, doi: 10.1134/S096554251702004X.

[60] S. Arbabi, A. Nazari, and M. T. Darvishi, “A two-dimensional Haar wavelets method for solving systems of PDEs,” *Appl. Math. Comput.*, vol. 292, pp. 33–46, 2017, doi: 10.1016/j.amc.2016.07.032.

[61] F. A. Shah and R. Abass, “An operational Haar wavelet collocation method for solving singularly perturbed boundary-value problems,” *SeMA J.*, vol. 74, no. 4, pp. 457–474, 2017, doi: 10.1007/s40324-016-0094-9.

[62] U. Saeed, “Haar adomian method for the solution of fractional nonlinear Lane-Emden type equations arising in astrophysics,” *Taiwan. J. Math.*, vol. 21, no. 5, pp. 1175–1192, 2017, doi: 10.11650/tjm/7969.

[63] S. C. Shiralashetti, R. A. Mundewadi, S. S. Naregal, and B. Veeresh, “Haar Wavelet Collocation Method for the Numerical Solution of Nonlinear Volterra-Fredholm-Hammerstein Integral Equations,” *Glob. J. Pure Appl. Math.*, vol. 13, no. 2, pp. 463–474, 2017.

[64] R. A. Mundewadi and B. A. Mundewadi, “Hermite Wavelet Collocation Method for the Numerical Solution of Integral and Integro - Differential Equations,” *Int. J. Math. Trends Technol.*, vol. 53, no. 3, pp. 215–231, 2018, doi: 10.14445/22315373/ijmtt-v53p527.

[65] I. Aziz, Siraj-ul-Islam, and M. Asif, “Haar wavelet collocation method for three-dimensional elliptic partial differential equations,” *Comput. Math. with Appl.*, vol. 73, no. 9, pp. 2023–2034, 2017, doi: 10.1016/j.camwa.2017.02.034.

[66] Z. Avazzadeh and M. Heydari, “Haar wavelet method for solving nonlinear age-structured population models,” *Int. J. Biomath.*, vol. 10, no. 8, pp. 1–21, 2017, doi: 10.1142/S1793524517501145.

[67] U. Saeed, “Haar wavelet operational matrix method for system of fractional nonlinear differential equations,” *Int. J. Wavelets, Multiresolution Inf. Process.*, vol. 15, no. 5, pp. 1–16, 2017, doi: 10.1142/S0219691317500436.

[68] R. Jiwari, V. Kumar, R. Karan, and A. S. Alshomrani, “Haar wavelet quasilinearization approach for MHD Falkner-Skan flow over permeable wall via Lie group method,” *Int. J. Numer. Methods Heat Fluid Flow*, vol. 27, no. 6, pp. 1332–1350, 2017, doi: 10.1108/HFF-04-2016-0145.

[69] R. Singh, H. Gargyand, and A. Garg, “Haar wavelet quasilinearization technique for doubly singular boundary value problems,” *arXiv Prepr. arXiv1711.10682*, pp. 1–20, 2017, [Online]. Available: http://arxiv.org/abs/1711.10682.

[70] S. Pandit, R. Jiwari, K. Bedi, and M. E. Koksal, “Haar wavelets operational matrix based algorithm for computational modelling of hyperbolic type wave equations,” *Eng. Comput.*, vol. 34, no. 8, pp. 2793–2814, 2017, doi: 10.1108/EC-10-2016-0364.

[71] R. C. Mittal and S. Pandit, “Sensitivity Analysis of Shock Wave Burgers ’ Equation via a Novel Algorithm Based on scale-3 Haar Wavelets,” *Int. J. Comput. Math.*, vol. 95, no. 3, pp. 601–625, 2017, doi: 10.1080/00207160.2017.1293820.

[72] S. Pandit, M. Kumar, R. N. Mohapatra, and A. Ali, “Shock Waves Analysis of Planar and Non Planar Nonlinear Burgers ’ Equation using Scale-2 Haar Wavelets,” *Int. J. Numer. Methods Heat Fluid Flow*, vol. 27, no. 8, pp. 1814–1850, 2017, doi: https:// doi.org/10.1108/HFF-05-2016-0188.

[73] S. Haq, A. Ghafoor, M. Hussain, and S. Arifeen, “Numerical solutions of two

dimensional Sobolev and generalized Benjamin – Bona – Mahony – Burgers equations via Haar wavelets," *Comput. Math. with Appl.*, vol. 77, no. 2, pp. 565–575, 2018, doi: 10.1016/j.camwa.2018.09.058.

[74] M. Ahsan, Siraj-ul-Islam, and I. Hussain, "Haar wavelets multi-resolution collocation analysis of unsteady inverse heat problems," *Inverse Probl. Sci. Eng.*, vol. 27, no. 11, pp. 1498–1520, 2019, doi: 10.1080/17415977.2018.1481405.

[75] M. Kirs, K. Karjust, I. Aziz, E. Õunapuu, and E. Tungel, "Free vibration analysis of a functionally graded material beam: evaluation of the Haar wavelet method," *Proc. Est. Acad. Sci.*, vol. 67, no. 1, p. 1, 2018, doi: 10.3176/proc.2017.4.01.

[76] I. Singh and S. Kumar, "Haar Wavelet Methods for Numerical Solutions of Harry Dym (HD), BBM Burger ' s and 2 D Diffusion Equations," *Bull. Brazilian Math. Soc. New Ser.*, vol. 49, no. 2, pp. 313–338, 2018, doi: 10.1007/s00574-017-0055-7.

[77] J. Majak, M. Pohlak, K. Karjust, M. Eerme, J. Kurnitski, and B. S. Shvartsman, "New higher order Haar wavelet method: Application to FGM structures," *Compos. Struct.*, vol. 201, pp. 72–78, 2018, doi: 10.1016/j.compstruct.2018.06.013.

[78] R. C. Mittal and S. Pandit, "Quasilinearized Scale-3 Haar wavelets-based algorithm for numerical simulation of fractional dynamical systems," *Eng. Comput. (Swansea, Wales)*, vol. 35, no. 5, pp. 1907–1931, 2018, doi: 10.1108/EC-09-2017-0347.

[79] O. Baghani, "A correction to 'Rationalized Haar wavelet bases to approximate solution of nonlinear Fredholm integral equations with error analysis [Applied Mathematics and Computation 265 (2015) 304–312],'" *Appl. Math. Comput.*, vol. 352, pp. 249–257, 2019, doi: 10.1016/j.amc.2019.01.033.

[80] S. Saleem, I. Aziz, and M. Z. Hussain, "A simple algorithm for numerical solution of nonlinear parabolic partial differential equations," *Eng. Comput.*, 2019, doi: 10.1007/s00366-019-00796-z.

[81] Ö. Oruç, A. Esen, and F. Bulut, “A Haar wavelet approximation for two-dimensional time fractional reaction–subdiffusion equation,” *Eng. Comput.*, vol. 35, no. 1, pp. 75–86, 2019, doi: 10.1007/s00366-018-0584-8.

[82] M. Ahsan, I. Ahmad, M. Ahmad, and I. Hussian, “A numerical Haar wavelet-finite difference hybrid method for linear and non-linear Schrödinger equation,” *Math. Comput. Simul.*, vol. 165, pp. 13–25, 2019, doi: 10.1016/j.matcom.2019.02.011.

[83] A. Mohammadi, N. Aghazadeh, and S. Rezapour, “Haar wavelet collocation method for solving singular and nonlinear fractional time-dependent Emden–Fowler equations with initial and boundary conditions,” *Math. Sci.*, vol. 13, no. 3, pp. 255–265, 2019, doi: 10.1007/s40096-019-00295-8.

[84] A. Kaushik, G. Gupta, M. Sharma, and V. Gupta, “A Wavelet Based Rationalized Approach for the Numerical Solution of Differential and Integral Equations,” *Differ. Equations Dyn. Syst.*, vol. 27, no. 1–3, pp. 181–202, 2019, doi: 10.1007/s12591-017-0393-3.

[85] R. C. Mittal and S. Pandit, “New Scale-3 Haar Wavelets Algorithm for Numerical Simulation of Second Order Ordinary Differential Equations,” *Proc. Natl. Acad. Sci. India Sect. A - Phys. Sci.*, vol. 89, no. 4, pp. 799–808, 2019, doi: 10.1007/s40010-018-0538-y.

[86] I. Awana and F. A.Shah, “An efficient Haar wavelet collocation method for solving Pennes Bioheat Transfer Model,” *Acta Univ. Apulensis*, vol. 2019, no. 60, pp. 75–89, 2019, doi: 10.17114/j.aua.2019.60.06.

[87] M. Ratas and A. Salupere, “Application of higher order haar wavelet method for solving nonlinear evolution equations,” *Math. Model. Anal.*, vol. 25, no. 2, pp. 271–288, 2020, doi: 10.3846/mma.2020.11112.

[88] N. Pervaiz and I. Aziz, “Haar wavelet approximation for the solution of cubic nonlinear Schrodinger equations,” *Phys. A Stat. Mech. its Appl.*, vol. 545, 2020, doi: 10.1016/j.physa.2019.123738.

[89] A. Kumar, M. S. Hashmi, A. Q. Ansari, and S. Arzykulov, “Haar wavelet based

algorithm for solution of second order electromagnetic problems in time and space domains," *J. Electromagn. Waves Appl.*, vol. 34, no. 3, pp. 362–374, 2020, doi: 10.1080/09205071.2020.1713225.

[90] G. Ahmadnezhad, N. Aghazadeh, and S. Rezapour, "Haar wavelet iteration method for solving time fractional Fisher's equation Ghader," *Comput. Methods Differ. Equations*, pp. 1–18, 2020, doi: 10.22034/cmde.2020.31527.1475.

[91] R. Singh, V. Guleria, and M. Singh, "Haar wavelet quasilinearization method for numerical solution of Emden–Fowler type equations," *Math. Comput. Simul.*, vol. 174, pp. 123–133, 2020, doi: 10.1016/j.matcom.2020.02.004.

[92] S. Foadian, R. Pourgholi, S. H. Tabasi, and H. Zeidabadi, "Solving an inverse problem for a generalized time-delayed burgers-fisher equation by Haar wavelet method," *J. Appl. Anal. Comput.*, vol. 10, no. 2, pp. 391–410, 2020, doi: 10.11948/20170028.

[93] S. Chandrasekhar, *Hydrodynamic and Hydromagnetic Stability*, First. New York: Dover Publications, 1981.

[94] G. Richards and P.R.R. Sarma, "Reduced Order Models for Induction Motors With Two Rotor Circuits," *IEEE Trans. Energy Convers.*, vol. 9, no. 4, pp. 673–678, 1994.

[95] R. . Agarwal, *Boundary Value Problems for Higher Order Differential Equations*, First. Singapore: World Scientific, 1986.

[96] M. A. Noor and S. T. Mohyud-Din, "Variational Iteration Decomposition Method for Solving Eighth-Order Boundary Value Problems," *Differ. Equations Nonlinear Mech.*, vol. 2007, no. 2, pp. 1–16, 2007, doi: 10.1155/2007/19529.

[97] S. Haq, M. Idrees, and S. Islam, "Application of optimal Homotopy asymptotic method to eighth order initial and boundary value problems," *Int. J. Appl. Math. Comput.*, vol. 2, no. 4, pp. 73–80, 2010.

[98] S. Ballem and K. N. S. Kasi Viswanadham, "Numerical solution of sixth order boundary value problems by Galerkin method with quartic B-splines,"

Internatioanl J. Comput. Appl., vol. 89, no. 15, pp. 7–13, 2014, doi: 10.1007/978-981-13-1903-7_58.

[99] Z. Elahi, G. Akram, and S. S. Siddiqi, "Numerical solution for solving special eighth-order linear boundary value problems using Legendre Galerkin method," *Math. Sci.*, vol. 10, no. 4, pp. 201–209, 2016, doi: 10.1007/s40096-016-0194-9.

[100] G. Akram and H. U. Rehman, "Numerical solution of eighth order boundary value problems in reproducing Kernel space," *Numer. Algorithms*, vol. 62, no. 3, pp. 527–540, 2013, doi: 10.1007/s11075-012-9608-4.

[101] J.-H. He, "The variational iteration method for eighth-order initial-boundary value problems," *Phys. Scr.*, vol. 76, no. 6, pp. 680–682, 2007, doi: 10.1088/0031-8949/76/6/016.

[102] S. T. Mohyud-din and A. Yildirim, "Solutions of Tenth and Ninth-order Boundary Value Problems by Modified Variational Iteration Method," *Appl. Appl. Math.*, vol. 5, no. 1, pp. 11–25, 2010.

[103] S. M. Reddy, "Collocation Method for Ninth Order Boundary Value Problems by Using Sextic B-splines," *Int. Res. J. Eng. Technol.*, vol. 3, no. 9, pp. 781–785, 2016.

[104] K. N. S. Kasi Viswanadham and S. M. Reddy, "Numerical Solution of Ninth Order Boundary Value Problems by Petrov-Galerkin Method with Quintic B-splines as Basis Functions and Septic B-splines as Weight Functions," *Procedia Eng.*, vol. 127, no. 09, pp. 1227–1234, 2015, doi: 10.1016/j.proeng.2015.11.470.

[105] Siraj-ul-Islam, I. Aziz, and B. Šarler, "The numerical solution of second-order boundary-value problems by collocation method with the Haar wavelets," *Math. Comput. Model.*, vol. 52, no. 9–10, pp. 1577–1590, 2010, doi: 10.1016/j.mcm.2010.06.023.

[106] Fazal-i-Haq, I. Hussain, and A. Ali, "A Haar Wavelets Based Numerical Method for Third-order Boundary and Initial Value Problems," *Eng. Technol.*, vol. 13, no. 10, pp. 2244–2251, 2011.

[107] Fazal-i-Haq and A. Ali, “Numerical Solution of Fourth Order Boundary-Value Problems Using Haar Wavelets,” *Appl. Math. Sci.*, vol. 5, no. 63, pp. 3131–3146, 2011.

[108] Fazal-i-Haq, A. Ali, and I. Hussain, “Solution of sixth-order boundary-value problems by collocation method using Haar wavelets,” *Int. J. Phys. Sci.*, vol. 7, no. 43, pp. 5729–5735, 2012, doi: 10.5897/IJPS11.696.

[109] A. P. Reddy and C. Sateesha, “Application of Haar Wavelet Collocation Method to Solve the Fifth Order Ordinary Differential Equations,” *Int. J. Math. Arch.*, vol. 7, no. 8, pp. 53–62, 2016.

[110] A. Reddy, S. Manjula, C. Sateesha, and N. Bujurke, “Haar Wavelet Approach for the Solution of Seventh Order Ordinary Differential Equations,” *Math. Model. Eng. Probl.*, vol. 3, no. 2, pp. 108–114, 2016, doi: 10.18280/mmep.030212.

[111] R. E. Bellman and R. E. Kalaba, *Quasilinearization and Nonlinear Boundary-Value Problems*, vol. 8, no. 3. American Elsevier Publishing Company, 1966.

[112] H. Kaur, R. . Mittal, and V. Mishra, “Haar Wavelet Quasilinearization Approach for Solving Nonlinear Boundary Value Problems,” *Am. J. Comput. Math.*, vol. 01, no. 03, pp. 176–182, 2011, doi: 10.4236/ajcm.2011.13020.

[113] E. Babolian and A. Shahsavaran, “Numerical solution of nonlinear Fredholm integral equations of the second kind using Haar wavelets,” *J. Comput. Appl. Math.*, vol. 225, no. 1, pp. 87–95, 2009, doi: 10.1016/j.cam.2008.07.003.

[114] S. Ballem and K. N. S. K. Viswanadham, “Numerical Solution of Eighth Order Boundary Value Problems by Galerkin Method with Septic B-splines,” *Procedia Eng.*, vol. 127, pp. 1370–1377, 2015, doi: 10.1016/j.proeng.2015.11.496.

[115] C.-K. Chui and J.-A. Lian, “Construction of Compactly Supported Symmetric and Antisymmetric Orthonormal Wavelets with Scale 3,” *Appl. Comput. Harmon. Anal.*, vol. 2, no. 1, pp. 21–51, 1995.

[116] G. Richards and P. Sarma, “Reduced order models for induction motors with two

rotor circuits," *IEEE Trans. Energy Convers.*, vol. 9, no. 4, pp. 673–678, 1994.

[117] S. M. Reddy, "Numerical Solution of Eighth Order Boundary Value Problems by Petrov- Galerkin Method with Quintic B-splines as basic functions and Septic B-Splines as weight functions," *Int. J. Eng. Comput. Sci.*, vol. 5, no. 09, pp. 17902–17908, 2016, doi: 10.18535/ijecs/v5i9.19.

[118] S. T. Mohyud-din and A. Yildirim, "Solution of Tenth and Ninth-Order Boundary Value Problems by Homotopy Perturbation Method," *J. Korean Soc. Ind. Appl. Math.*, vol. 14, no. 1, pp. 17–27, 2010.

[119] K. N.S.Kasi Viswanadham and Y. Showri Raju, "Quintic B-Spline Collocation Method for Tenth Order Boundary Value Problems," *Int. J. Comput. Appl.*, vol. 51, no. 15, pp. 7–13, 2012, doi: 10.5120/8116-1735.

[120] R. Kumar, H. Kaur, and G. Arora, "Numerical solution by Haar wavelet collocation method for a class of higher order linear and nonlinear boundary value problems," *AIP Conf. Proc.*, vol. 1860, no. 1, pp. 020038–1–020038–12, 2017, doi: 10.1063/1.4990337.

[121] H. Patel and R. Meher, "Modified Adomian Decomposition Method for Solving Eleventh-order Initial and Boundary Value Problems," *Br. J. Math. Comput. Sci.*, vol. 8, no. 2, pp. 134–146, 2015, doi: 10.9734/BJMCS/2015/16155.

[122] R. Meher and H.-S. Patel, "Modified Adomian Decomposition Method for Solving Eleventh-order Initial and Boundary Value Problems," *Br. J. Math. Comput. Sci.*, vol. 8, no. 2, pp. 134–146, 2015, doi: 10.9734/BJMCS/2015/16155.

[123] Siraj-Ul-Islam, B. Šarler, I. Aziz, and Fazal-I-Haq, "Haar wavelet collocation method for the numerical solution of boundary layer fluid flow problems," *Int. J. Therm. Sci.*, vol. 50, no. 5, pp. 686–697, 2011, doi: 10.1016/j.ijthermalsci.2010.11.017.

[124] Shahid S.Siddiqi, G. Akram, and I. Zulfiqar, "Solution of Eleventh Order Boundary Value Problems Using Variational Iteration Technique," *Eur. J. Sci. Res.*, vol. 30, no. 4, pp. 505–525, 2009.

[125] A. Hussain, S. T. Mohyud-din, and A. Yildirim, “A Comparison of Numerical Solutions of Eleventh Order Two-point Boundary Value Problems,” vol. 7, no. 3, pp. 181–189, 2012.

[126] A. S. V. Ravi Kanth and K. Aruna, “Variational iteration method for twelfth-order boundary-value problems,” *Comput. Math. with Appl.*, vol. 58, no. 11–12, pp. 2360–2364, 2009, doi: 10.1016/j.camwa.2009.03.025.

[127] S. U. Islam, S. Haq, and J. Ali, “Numerical solution of special 12th-order boundary value problems using differential transform method,” *Commun. Nonlinear Sci. Numer. Simul.*, vol. 14, no. 4, pp. 1132–1138, 2009, doi: 10.1016/j.cnsns.2008.02.012.

[128] S. S. Ray and R. K. Bera, “Analytical solution of the Bagley Torvik equation by Adomian decomposition method,” *Appl. Math. Comput.*, vol. 168, no. 1, pp. 398–410, 2005, doi: 10.1016/j.amc.2004.09.006.

[129] A. Ghorbani and A. Alavi, “Application of He’s variational iteration method to solve semidifferential equations of n th order,” *Math. Probl. Eng.*, vol. 2008, pp. 1–9, 2008, doi: 10.1155/2008/627983.

[130] H. H. Fadravi, H. saber. Nik, and R.Buzhabadi, “Homotopy Analysis Method Based on Optimal Value of the Convergence Control Parameter for Solving Semi-Differential Equations,” *J. Math. Ext.*, vol. 5, no. 2, pp. 105–121, 2011.

[131] Y. Çenesiz, Y. Keskin, and A. Kurnaz, “The solution of the Bagley-Torvik equation with the generalized Taylor collocation method,” *J. Franklin Inst.*, vol. 347, no. 2, pp. 452–466, 2010, doi: 10.1016/j.jfranklin.2009.10.007.

[132] S. Saha Ray, “On Haar wavelet operational matrix of general order and its application for the numerical solution of fractional Bagley Torvik equation,” *Appl. Math. Comput.*, vol. 218, no. 9, pp. 5239–5248, 2012, doi: 10.1016/j.amc.2011.11.007.

[133] T. Mekkaoui and Z. Hammouch, “Approximate analytical solutions to the Bagley-Torvik equation by the fractional iteration method,” *Ann. Univ. Craiova, Math. Comput. Sci. Ser.*, vol. 39, no. 2, pp. 251–256, 2012.

[134] S. Yuzbasi, “Numerical solution of the Bagley-Torvik equation by the Bessel collocation method,” *Math. Methods Appl. Sci.*, vol. 36, no. 3, pp. 300–312, 2013, doi: 10.1002/mma.2588.

[135] F. Mohammadi, “Numerical solution of Bagley-Torvik equation using Chebyshev wavelet operational matrix of fractional derivative,” *Int. J. Adv. Appl. Math. Mech.*, vol. 2, no. 1, pp. 83–91, 2014.

[136] V. S. Krishnasamy and M. Razzaghi, “The Numerical Solution of the Bagley–Torvik Equation With Fractional Taylor Method,” *J. Comput. Nonlinear Dyn.*, vol. 11, no. 5, 2016, doi: 10.1115/1.4032390.

[137] S. Mashayekhi and M. Razzaghi, “Numerical solution of the fractional Bagley-Torvik equation by using hybrid functions approximation,” *Math. Methods Appl. Sci.*, vol. 39, no. 3, pp. 353–365, 2016, doi: 10.1002/mma.3486.

[138] H. M. Srivastava, F. A. Shah, and R. Abass, “An Application of the Gegenbauer Wavelet Method for the Numerical Solution of the Fractional Bagley-Torvik Equation,” *Russ. J. Math. Phys.*, vol. 26, no. 1, pp. 77–93, 2019, doi: 10.1134/S1061920819010096.

[139] O. Abu Arqub and B. Maayah, “Solutions of Bagley–Torvik and Painlevé equations of fractional order using iterative reproducing kernel algorithm with error estimates,” *Neural Comput. Appl.*, vol. 29, no. 5, pp. 1465–1479, 2018, doi: 10.1007/s00521-016-2484-4.

[140] R. M. Jena and S. Chakraverty, “Analytical solution of Bagley-Torvik equations using Sumudu transformation method,” *SN Appl. Sci.*, vol. 1, no. 3, pp. 1–6, 2019, doi: 10.1007/s42452-019-0259-0.

[141] R. C. Mittal and S. Pandit, “Quasilinearized Scale-3 Haar wavelets-based algorithm for numerical simulation of fractional dynamical systems,” *Eng. Comput.*, vol. 35, no. 5, pp. 1907–1931, 2018, doi: https:// doi.org/10.1108/EC-09-2017-0347.

[142] R. C. Mittal and S. Pandit, “New Scale-3 Haar Wavelets Algorithm for Numerical Simulation of Second Order Ordinary Differential Equations,” *Proc.*

Natl. Acad. Sci. India Sect. A Phys. Sci., vol. 89, no. 4, pp. 799–808, 2019, doi: https://doi.org/10.1007/s40010-018-0538-y.

[143] J.-S. Duan, L. Lu, L. Chen, and Y.-L. An, "Fractional model and solution for the Black-Scholes equation," *Math. Methods Appl. Sci.*, vol. 41, no. 2, pp. 697–704, Oct. 2017, doi: 10.1002/mma.4638.

[144] M. Inc, A. Yusuf, A. Isa Aliyu, and D. Baleanu, "Time-fractional Cahn–Allen and time-fractional Klein–Gordon equations: Lie symmetry analysis, explicit solutions and convergence analysis," *Phys. A Stat. Mech. its Appl.*, vol. 493, no. 1, pp. 94–106, 2018, doi: 10.1016/j.physa.2017.10.010.

[145] K. Hosseini, P. Mayeli, and R. Ansari, "Bright and singular soliton solutions of the conformable time-fractional Klein–Gordon equations with different nonlinearities," *Waves in Random and Complex Media*, vol. 28, no. 3, pp. 426–434, 2018, doi: 10.1080/17455030.2017.1362133.

[146] X. Zhang, Y. He, L. Wei, B. Tang, and S. Wang, "A fully discrete local discontinuous Galerkin method for one-dimensional time-fractional Fisher ' s equation," *Int. J. Comput. Math.*, vol. 91, no. 9, pp. 2021–2038, 2014, doi: 10.1080/00207160.2013.866233.

[147] A. Atangana, "On the new fractional derivative and application to nonlinear Fisher ' s reaction – diffusion equation," *Appl. Math. Comput.*, vol. 273, pp. 948–956, 2016, doi: 10.1016/j.amc.2015.10.021.

[148] S. S. Ray, "On Haar wavelet operational matrix of general order and its application for the numerical solution of fractional Bagley Torvik equation," *Appl. Math. Comput.*, vol. 218, pp. 5239–5248, 2012, doi: 10.1016/j.amc.2011.11.007.

[149] N. A. Khan, A. Ara, and A. Mahmood, "Numerical solutions of time-fractional Burgers equations: A comparison between generalized differential transformation technique and homotopy perturbation method," *Int. J. Numer. Methods Heat Fluid Flow*, vol. 22, no. 2, pp. 175–193, 2012, doi: 10.1108/09615531211199818.

[150] M. Inc, “The approximate and exact solutions of the space- and time-fractional Burgers equations with initial conditions by variational iteration method,” *J. Math. Anal. Appl.*, vol. 345, no. 1, pp. 476–484, 2008, doi: 10.1016/j.jmaa.2008.04.007.

[151] D. Kumar, J. Singh, and D. Baleanu, “A new numerical algorithm for fractional Fitzhugh–Nagumo equation arising in transmission of nerve impulses,” *Nonlinear Dyn.*, vol. 91, no. 1, pp. 307–317, 2018, doi: 10.1007/s11071-017-3870-x.

[152] T. Shen, J. Xin, and J. Huang, “Time-space fractional stochastic Ginzburg-Landau equation driven by Gaussian white noise,” *Stoch. Anal. Appl.*, vol. 36, no. 1, pp. 103–113, 2018, doi: 10.1080/07362994.2017.1372783.

[153] A. Mohebbi, “Fast and high-order numerical algorithms for the solution of multidimensional nonlinear fractional Ginzburg-Landau equation,” *Eur. Phys. J. Plus*, vol. 133, no. 2, pp. 1–13, 2018, doi: 10.1140/epjp/i2018-11846-x.

[154] Q. Wang, “Numerical solutions for fractional KdV – Burgers equation by Adomian decomposition method,” *Appl. Math. Comput.*, vol. 182, no. 2006, pp. 1048–1055, 2006, doi: 10.1016/j.amc.2006.05.004.

[155] Z. Odibat and S. Momani, “The variational iteration method: An efficient scheme for handling fractional partial differential equations in fluid mechanics,” *Comput. Math. with Appl.*, vol. 58, no. 11, pp. 2199–2208, 2009, doi: 10.1016/j.camwa.2009.03.009.

[156] S. S. Ray and A. Patra, “Haar wavelet operational methods for the numerical solutions of fractional order nonlinear oscillatory Van der Pol system,” *Appl. Math. Comput.*, vol. 220, pp. 659–667, 2013, doi: 10.1016/j.amc.2013.07.036.

[157] M. H. Heydari, M. R. Hooshmandasl, F. M. Maalek Ghaini, and F. Fereidouni, “Two-dimensional Legendre wavelets for solving fractional Poisson equation with Dirichlet boundary conditions,” *Eng. Anal. Bound. Elem.*, vol. 37, no. 11, pp. 1331–1338, 2013, doi: 10.1016/j.enganabound.2013.07.002.

[158] S. Momani and N. Shawagfeh, “Decomposition method for solving fractional

Riccati differential equations," *Appl. Math. Comput.*, vol. 182, no. 2006, pp. 1083–1092, 2006, doi: 10.1016/j.amc.2006.05.008.

[159] F. D. M. Bezerra, A. N. Carvalho, T. Dlotko, and M. J. D. Nascimento, "Fractional Schrödinger equation; solvability and connection with classical Schrödinger equation," *J. Math. Anal. Appl.*, vol. 457, no. 1, pp. 336–360, 2018, doi: 10.1016/j.jmaa.2017.08.014.

[160] H. Karayer, D. Demirhan, and F. Buyukkilic, "Solutions of local fractional sine-Gordon equations," *Waves in Random and Complex Media*, vol. 5030, pp. 1–9, 2018, doi: 10.1080/17455030.2018.1425572.

[161] J. Singh, P. K. Gupta, and K. N. Rai, "Solution of fractional bioheat equations by finite difference method and HPM," *Math. Comput. Model.*, vol. 54, no. 9–10, pp. 2316–2325, 2011, doi: 10.1016/j.mcm.2011.05.040.

[162] D. Baleanu, M. Inc, A. Yusuf, and A. I. Aliyu, "Lie symmetry analysis, exact solutions and conservation laws for the time fractional Caudrey–Dodd–Gibbon–Sawada–Kotera equation," *Commun. Nonlinear Sci. Numer. Simul.*, vol. 59, pp. 222–234, 2018, doi: 10.1016/j.cnsns.2017.11.015.

[163] R. Roy, M. A. Akbar, and A. M. Wazwaz, "Exact wave solutions for the nonlinear time fractional Sharma–Tasso–Olver equation and the fractional Klein–Gordon equation in mathematical physics," *Opt. Quantum Electron.*, vol. 50, no. 1, pp. 1–19, 2018, doi: 10.1007/s11082-017-1296-9.

[164] A. M. S. Mahdy and G. M. A. Marai, "Numerical Solution for the time-fractional Fokker-Planck equation Using Fractional Power Series Method and The shifted Chebyshev polynomials of the third kind," *Int. J. Appl. Eng. Res.*, vol. 13, no. 1, pp. 366–374, 2018.

[165] H. Zhang, X. Jiang, and X. Yang, "A time-space spectral method for the time-space fractional Fokker–Planck equation and its inverse problem," *Appl. Math. Comput.*, vol. 320, pp. 302–318, 2018, doi: 10.1016/j.amc.2017.09.040.

[166] A. M. Tawfik, H. Fichtner, R. Schlickeiser, and A. Elhanbaly, "Analytical solutions of the space–time fractional Telegraph and advection–diffusion

equations," *Phys. A Stat. Mech. its Appl.*, vol. 491, pp. 810–819, 2018, doi: 10.1016/j.physa.2017.09.105.

[167] S. Momani, "Analytic and approximate solutions of the space- and time-fractional telegraph equations," *Appl. Math. Comput.*, vol. 170, no. 2005, pp. 1126–1134, 2005, doi: 10.1016/j.amc.2005.01.009.

[168] C. Lu, C. Fu, and H. Yang, "Time-fractional generalized Boussinesq equation for Rossby solitary waves with dissipation effect in stratified fluid and conservation laws as well as exact solutions R," *Appl. Math. Comput.*, vol. 327, pp. 104–116, 2018, doi: 10.1016/j.amc.2018.01.018.

[169] S. Momani and Z. Odibat, "Analytical solution of a time-fractional Navier-Stokes equation by Adomian decomposition method," *Appl. Math. Comput.*, vol. 177, no. 2, pp. 488–494, 2006, doi: 10.1016/j.amc.2005.11.025.

[170] Z. M. Odibat and S. Momani, "Approximate solutions for boundary value problems of time-fractional wave equation," vol. 181, pp. 767–774, 2006, doi: 10.1016/j.amc.2006.02.004.

[171] S. Abuasad, K. Moaddy, and I. Hashim, "Analytical treatment of two-dimensional fractional Helmholtz equations," *J. King Saud Univ. - Sci.*, vol. 31, no. 4, pp. 659–666, 2019, doi: 10.1016/j.jksus.2018.02.002.

[172] S. E. Esipov, "Coupled Burgers equations: A model of polydispersive sedimentation," *Phys. Rev. E*, vol. 52, no. 4, pp. 3711–3718, 1995, doi: 10.1103/PhysRevE.52.3711.

[173] A. Prakash, M. Kumar, and K. K. Sharma, "Numerical method for solving fractional coupled Burgers equations," *Appl. Math. Comput.*, vol. 260, no. 2015, pp. 314–320, 2015, doi: 10.1016/j.amc.2015.03.037.

[174] J. Liu and G. Hou, "Numerical solutions of the space- and time-fractional coupled Burgers equations by generalized differential transform method," *Appl. Math. Comput.*, vol. 217, no. 16, pp. 7001–7008, 2011, doi: 10.1016/j.amc.2011.01.111.

[175] A. Yildirim and A. Kelleci, “Homotopy perturbation method for numerical solutions of coupled Burgers equations with time-and space-fractional derivatives,” *Int. J. Numer. Methods Heat Fluid Flow*, vol. 20, no. 8, pp. 897–909, 2010, doi: 10.1108/09615531011081423.

[176] S. S. Ray, “Numerical solutions of (1 + 1) dimensional time fractional coupled Burger equations using new coupled fractional reduced differential transform method,” *Int. J. Comput. Sci. Math.*, vol. 4, no. 1, pp. 1–15, 2013.

[177] Y. Chen and H.-L. An, “Numerical solutions of coupled Burgers equations with time- and space-fractional derivatives,” *Appl. Math. Comput.*, vol. 200, no. 2008, pp. 87–95, 2008, doi: 10.1016/j.amc.2007.10.050.

[178] P. K. Sahoo and T. Riedel, *Mean Value Theorems and Functional Equations*. Singapore, 1998.

[179] P. M. Jordan and A. Puri, “Digital signal propagation in dispersive media,” *J. Appl. Phys.*, vol. 85, no. 3, pp. 1273–1282, 1999, doi: 10.1063/1.369258.

[180] R. K. Mohanty, “New unconditionally stable difference schemes for the solution of multi-dimensional telegraphic equations,” *Int. J. Comput. Math.*, vol. 86, no. 12, pp. 2061–2071, 2009, doi: 10.1080/00207160801965271.

[181] H. Pascal, “Pressure wave propagation in a fluid flowing through a porous medium and problems related to interpretation of Stoneley’s wave attenuation in acoustical well logging,” *Int. J. Eng. Sci.*, vol. 24, no. 9, pp. 1553–1570, 1986, doi: 10.1016/0020-7225(86)90163-1.

[182] J. Banasiak and J. R. Mika, “Singularly perturbed telegraph equations with applications in the random walk theory,” *J. Appl. Math. Stoch. Anal.*, vol. 11, no. 1, pp. 9–28, 1998, doi: 10.1155/S1048953398000021.

[183] H. D. B. Hamburg, “Non-Newtonian Fluid Mechanics,” *J. Nonnewton. Fluid Mech.*, vol. 4, no. 4, p. 373, 1979, doi: 10.1016/0377-0257(79)80009-9.

[184] M. Dosti and A. Nazemi, “Septic B-spline collocation method for solving one-dimensional hyperbolic telegraph equation,” *World Acad. Sci. Eng. Technol.*,

vol. 80, no. 8, pp. 1085–1089, 2011.

[185] M. Dosti and A. Nazemi, “Solving one-dimensional hyperbolic telegraph equation using cubic B-spline quasi-interpolation,” *World Acad. Sci. Eng. Technol.*, vol. 52, no. 4, pp. 4–24, 2011.

[186] R. C. Mittal and R. Bhatia, “Numerical solution of second order one dimensional hyperbolic telegraph equation by cubic B-spline collocation method,” *Appl. Math. Comput.*, vol. 220, no. 2013, pp. 496–506, 2013, doi: 10.1016/j.amc.2013.05.081.

[187] T. Nazir, M. Abbas, and M. Yaseen, “Numerical solution of second-order hyperbolic telegraph equation via new cubic trigonometric B-splines approach,” *Cogent Math.*, vol. 4, no. 1, pp. 1–17, 2017, doi: 10.1080/23311835.2017.1382061.

[188] S. Sharifi and J. Rashidinia, “Numerical solution of hyperbolic telegraph equation by cubic B-spline collocation method,” *Appl. Math. Comput.*, vol. 281, no. 2016, pp. 28–38, 2016, doi: 10.1016/j.amc.2016.01.049.

[189] M. Inc, A. Akgül, and A. Kiliçman, “Numerical solutions of the second-order one-dimensional telegraph equation based on reproducing kernel hilbert space method,” *Abstr. Appl. Anal.*, vol. 2013, pp. 1–13, 2013, doi: 10.1155/2013/768963.

[190] M. Dehghan and A. Ghesmati, “Solution of the second-order one-dimensional hyperbolic telegraph equation by using the dual reciprocity boundary integral equation (DRBIE) method,” *Eng. Anal. Bound. Elem.*, vol. 34, no. 1, pp. 51–59, 2010, doi: 10.1016/j.enganabound.2009.07.002.

[191] R. Jiwari, S. Pandit, and R. C. Mittal, “A Differential Quadrature Algorithm for the Numerical Solution of the Second-Order One Dimensional Hyperbolic Telegraph Equation,” *Int. J. Nonlinear Sci.*, vol. 13, no. 3, pp. 259–266, 2012.

[192] B. Raftari, H. Khosravi, and A. Yildirim, “Homotopy analysis method for the one-dimensional hyperbolic telegraph equation with initial conditions,” *Int. J. Numer. Methods Heat Fluid Flow*, vol. 23, no. 2, pp. 355–372, 2013, doi:

10.1108/09615531311293515.

[193] A. Saadatmandi and M. Dehghan, “Numerical Solution of Hyperbolic Telegraph Equation Using the Chebyshev Tau Method,” *Numer. Methods Partial Differ. Equ.*, vol. 26, no. 1, pp. 239–252, 2010, doi: 10.1002/num.20442.

[194] G. Arora, R. Kumar, and H. Kaur, “A novel wavelet based hybrid method for finding the solutions of higher order boundary value problems,” *Ain Shams Eng. J.*, vol. 9, no. 4, pp. 3015–3031, 2018, doi: 10.1016/j.asej.2017.12.006.

[195] T. W. TING, “Certain Non-steady Flows of Second-order Fluids,” *Arch. Ration. Mech. Anal.*, vol. 14, no. 1, pp. 1–26, 1963.

[196] G. . Barenblatt, I. . Zheltov, and I. . Kochina, “Basic Concepts in The Theory Of Seepage Of Homogeneous Liquids In Fissured Rocks [Strata],” *J. Appl. Math. Mech.*, vol. 24, no. 5, pp. 1286–1303, 1960.

[197] T. W. Ting, “A Cooling Process According to Two-Temperature Theory of Heat Conduction,” *J. Math. Anal. Appl.*, vol. 45, no. 1, pp. 23–31, 1974.

[198] S. Abbasbandy and A. Shirzadi, “The first integral method for modified Benjamin-Bona-Mahony equation,” *Commun. Nonlinear Sci. Numer. Simul.*, vol. 15, no. 7, pp. 1759–1764, 2010, doi: 10.1016/j.cnsns.2009.08.003.

[199] N. Li, P. Lin, and F. Gao, “An expanded mixed finite element method for two-dimensional Sobolev equations,” *J. Comput. Appl. Math.*, vol. 348, pp. 342–355, 2018, doi: 10.1016/j.cam.2018.08.041.

[200] D. Zhao and Q. Zhang, “Local Discontinuous Galerkin Methods with Generalized Alternating Numerical Fluxes for Two-dimensional Linear Sobolev Equation,” *J. Sci. Comput.*, vol. 78, no. 3, pp. 1660–1690, 2019, doi: 10.1007/s10915-018-0819-2.

[201] S. Jin and Z. Luo, “A collocation spectral method for two-dimensional Sobolev equations,” *Bound. Value Probl.*, vol. 2018, no. 1, pp. 1–13, 2018, doi: 10.1186/s13661-018-1004-0.

[202] Z. Luo, “A Crank-Nicolson finite volume element method for two-dimensional

Sobolev equations," *J. Inequalities Appl.*, vol. 2016, no. 1, p. 188, 2016, doi: 10.1186/s13660-016-1131-z.

[203] Ö. Oruç, "A computational method based on Hermite wavelets for two-dimensional Sobolev and regularized long wave equations in fluids," *Numer. Methods Partial Differ. Equ.*, vol. 34, no. 5, pp. 1693–1715, 2018, doi: 10.1002/num.22232.

[204] F. Gao and X. Wang, "A modified weak galerkin finite element method for sobolev equation," *J. Comput. Math.*, vol. 33, no. 3, pp. 307–322, 2015, doi: 10.4208/jcm.1502-m4509.

[205] S. He, H. Li, and Y. Liu, "Time discontinuous Galerkin space-time finite element method for nonlinear Sobolev equations," *Front. Math. China*, vol. 8, no. 4, pp. 825–836, 2013, doi: 10.1007/s11464-013-0307-9.